

ISSN 1512-1127

საქართველოს გეოფიზიკური საზოგადოების
ჟურნალი

სერია ა. დედამიწის ფიზიკა

**JOURNAL
OF THE GEORGIAN GEOPHYSICAL SOCIETY**

Issue A. Physics of Solid Earth

ტომი 17ა 2014

vol. 17A 2014

ISSN 1512-1127

საქართველოს გეოფიზიკური საზოგადოების
ჟურნალი

სერია ა. დედამიწის ფიზიკა

**JOURNAL
OF THE GEORGIAN GEOPHYSICAL SOCIETY**

Issue A. Physics of Solid Earth

ტომი 17A 2014

vol. 17A 2014

საქართველოს გეოფიზიკური საზოგადოების ჟურნალი

მთავარი რედაქტორი: თ. ჭელიძე

სერიის ა. ფიზიკური მკვლევების შიშობა

ა სერიის სარედაქციო კოლეგია

ა. კორძაძე (მთ. რედაქტორის მოადგილე), კ. ქართველიშვილი (სერიის რედაქტორი), ვ. აბაშიძე, ა. ამირანაშვილი (მდივანი), თ. ჭელიძე, ნ. გლონტი, ა. გველესიანი (სერიის რედაქტორის მოადგილე), გ. გუგუნავა, თ. მაჭარაშვილი, კ. ეფტაქსიასი (საბერძენეთი), ა. გოგინაშვილი (მექსიკა), ნ. ვარამაშვილი, გ. ჯაში, ი. გეგენი (საფრანგეთი), ი. ჩშაუ (გერმანია), ვ. სტაროსტენკო (უკრაინა), ჯ. ქირია, ლ. დარახველიძე

სერიის შინაარსი:

ჟურნალი (ა) მოიცავს მყარი დედამიწის ფიზიკის ყველა მიმართულებას. გამოქვეყნებულ იქნება: კვლევითი წერილები, მიმოხილვები, მოკლე ინფორმაციები, დისკუსიები, წიგნების მიმოხილვები, განცხადებები.

ЖУРНАЛ ГРУЗИНСКОГО ГЕОФИЗИЧЕСКОГО ОБЩЕСТВА

Главный редактор: Т. Челидзе

Серия А. Физика Твердой Земли

Редакционная коллегия серии А:

А. Кордзадзе (зам. главного редактора), К. З. Картвелишвили (редактор серии), В.Г. Абашидзе, А.Г. Амиранашвили (секретарь), Т.Л. Челидзе, Н. Глонти, А.И. Гвелесиани (зам. редактора серии), Г.Е. Гугунава, Т. Мачарашвили, К. Эфтаксиас (Греция), А.Гогичайшвили (Мексика), Н. Варамашвили, Г.Г. Джаши, И. Геген (Франция), И. Чшау (Германия), В. Старостенко (Украина), Дж. Кириа, Л. Даракхвелидзе.

Содержание журнала:

Журнал (А) Грузинского геофизического общества охватывает все направления физики твердой Земли. В журнале будут опубликованы научные статьи, обзоры, краткие информации, дискуссии, обзоры книг, объявления.

JOURNAL OF THE GEORGIAN GEOPHYSICAL SOCIETY

Editor-in-Chief: T. Chelidze

Issue A. Physics of Solid Earth

Editorial board:

A. Kordzadze (Associate Editors), K. Kartvelishvili (Issue Editor), V. Abashidze, A. Amiranashvili (secretary), T. Chelidze, N. Ghlonti, A. Gvelesiani (Vice-Editor of Issue), G. Gugunava, T. Matcharashvili, K. Eftaxias (Greece), A. Gogichaishvili (Mexico), N. Varamashvili, G. Jashi, Y. Gueguen (France), J. Zschau (Germany), V. Starostenko (Ukraine), J. Kiria, L. Darakhvelidze.

Scope of the Journal:

The Journal (A) is devoted to all branches of the Physics of Solid Earth. Types of contributions are: research papers, reviews, short communications, discussions, book reviews, and announcements.

მისამართი:

საქართველო, 0160, თბილისი, ალექსიძის ქ. 1, მ. ნოდიას გეოფიზიკის ინსტიტუტი
ტელ.: 233-28-67; Fax; (995 32 2332867); e-mail: tamaz.chelidze@gmail.com; akordzadze@yahoo.com; avto_amiranashvili@hotmail.com

გამოქვეყნების განრიგი და ხელმოწერა

სერია (ა) გამოიცემა წელიწადში ერთხელ. ხელმოწერის ფასია (უცხოელი ხელმომწერისათვის) 30 დოლარი, საქართველოში – 10 ლარი, ხელმოწერის მოთხოვნა უნდა გაიგზავნოს რედაქციის მისამართით. შესაძლებელია ონლაინ წვდომა: <http://openjournals.gela.org.ge/index.php/GGS/index>

Адрес:

Грузия, 0160, Тбилиси, ул. Алексидзе, 1. Институт геофизики им. М. З. Нодиа
Тел: 33-28-67; 94-35-91; Fax: (99532) 332867; e-mail: tamaz.chelidze@gmail.com; akordzadze@yahoo.com; avto_amiranashvili@hotmail.com

Порядок издания и условия подписи:

Том серии (А) издается по одному номеру в год. Подписная цена 30 долларов США, включая стоимость пересылки. Заявка о подписке высылается в адрес редакции. Возможен онлайн доступ <http://openjournals.gela.org.ge/index.php/GGS/index>

Address:

M. Nodia Institute of Geophysics, 1 Alexidze Str., 0160 Tbilisi, Georgia
Tel.: 233-28-67; Fax: (99532) 332867; e-mail: tamaz.chelidze@gmail.com; akordzadze@yahoo.com; avto_amiranashvili@hotmail.com

Publication schedule and subscription information:

One volume of issue (A) per year is scheduled to be published. The subscription price is 30 \$, including postage.

Subscription orders should be sent to editor's address. Online access is possible: <http://openjournals.gela.org.ge/index.php/GGS/index>

M9 Tohoku earthquake response in Georgia – possible local tremors and hydroseismic effects

T. Chelidze¹, I. Shengelia², N. Zhukova¹, T. Matcharashvili^{1,2}, G. Melikadze¹,
G. Kobzev¹

1. M. Nodia Institute of Geophysics at Iv. Javakhishvili Tbilisi State University Alexidze str. 0160, Tbilisi, Georgia, tamaz.chelidze@gmail.com
2. Ilia State University

Abstract

Presently, there are a lot of observations on the significant impact of strong remote earthquakes on underground water and local seismicity regime (so called nonvolcanic or dynamical tremors). On the other side, teleseismic wave trains give rise to several hydraulic effects in boreholes, namely water level oscillations, which mimic seismograms (hydroseismograms). Both these effects are closely related to each other as one of main factors reducing local strength of rocks is the pore pressure of fluids.

Some evidence of possible dynamic triggering from great Tohoku (M9) earthquake has been obtained recently in the West Caucasus. Besides tremors, clear identical anomalies on the large part of territory of Georgia from Borjomi to Kobuleti in the borehole water levels has been observed at passing S- and Love-Rayleigh teleseismic waves of Tohoku earthquake. We presume that coincidence of possible tremor signal with water level anomaly (oscillation) makes much more reliable event classification as a triggered one. We also report a new observation on water level oscillations during passage of multiple surface Rayleigh waves.

1. Introduction.

Presently, there are a lot of observations on the significant impact of strong remote earthquakes on underground water regime and triggered local seismicity (so called nonvolcanic or dynamical tremors). The stresses imparted by teleseismic wave trains according to assessments are 10^5 times smaller than confining stresses at the depth, where dynamical tremors are generated. Many of such results still are subject of intense scientific discussions due to the weakness of wave trains from remote earthquakes, but nevertheless are quite logical in the light of undisputable strong nonlinearity of processes underlying seismicity: the tremors are generated due to a nonlinear effect of super-sensitivity to a weak impact. On the other side, teleseismic wave trains give rise to several hydraulic effects in boreholes, namely water level oscillations, which mimic seismograms (hydroseismograms). Both these effects, seismo-hydraulic and triggered tremors are closely related to each other as one of main factors reducing local strength of rocks is the pore pressure of fluids: this is the scope of relatively new direction, so called hydroseismology. Thus we presume that coincidence of possible tremor signal with water level anomaly (oscillation) makes much more reliable triggered seismic event classification.

The stresses imparted by teleseismic wave trains according to assessments are 10^5 times smaller than confining stresses at the depth, where the tremors are generated (Hill and Prejean, 2009; Prejean and Hill, 2009). Our laboratory data on stick-slip confirm reality of triggering and synchronization under weak mechanical forcing (Chelidze et al, 2010). According to (Brodsky et al, 2003; Wang, C.-Y., Manga, 2010; Zhang and Huang, 2011) the dynamically triggered tremors (DTT) can be related to the fluid pore pressure change due to passage of wave trains from remote strong earthquakes; that is why we carried out integrated analysis of seismic and WL data. Good correlation of WL signals with offsets of strongest teleseismic waves (S , L , R) should be some validation of hypothesis that perturbations in filtered seismic records of remote earthquakes (EQs) are indeed DTT events.

There are fundamental questions which have to be answered in order to make the domain of dynamically triggered seismicity useful instrument of earth crust physics. It is not clear why dynamic triggering (DT) is not observed everywhere (Parsons et al, 2014), why it is observed mainly in some specified tectonic zones (extensional, hydrothermal areas), why the same dynamical forcing results in different response in similar tectonic zones, how ubiquitous is the phenomenon, is there a coupling of DT and water level change in boreholes, how DT can be related to the stress state in the depth, where the DT is forming, etc.

2. Local possible tremors triggered by Tohoku earthquake in Georgia

The dynamic triggering due to the great Tohoku M 9 earthquake (2011), Japan was observed in local seismicity all around the globe (Gonzalez-Huizar et al. 2010; Obara and Matsuzawa, 2013). The main characteristic of DT events are peak dynamic values of stress (T_p) or strain (ε_p); for shear waves $T_p \approx G (u_p/v_s)$ and $\varepsilon_p \approx u_p/v_s$; here G is the shear modulus, u_p is particle' peak velocity and v_s is velocity of the shear wave. Analysis of the field data gives values of T_p from 0.01MPa to 1MPa (ε_p from 0.03 to 3 microstrain). We assume that such large scatter is due to the impact of another important factor, namely, the local (site) strength of earth material, which is highly heterogeneous. Thus what matters is not the absolute value of T_p or ε_p , but the difference between local stress and local strength or resistance to failure (Chelidze and Matcharashvili, 2013, 2014). This is why in some areas high T_p do not trigger local seismicity and, on contrary, some areas manifest DT even at low peak stresses (Hill, Prejean, 2009;). One of main factors reducing local strength is the pore pressure of fluids, which is the scope of relatively new direction, so called hydroseismology (Costain and Bollinger, 2010).

We presume that Tohoku EQ could also trigger local seismic events in Georgia (Caucasus), which is a continental collision area, separated from Japan by 7800 km. The teleseismic waves' phases onsets at Tbilisi and Oni seismic stations (s/s) for the main shock are as following (UTC/GMT): p - 05 57 41, S - 06 07 26; Love - 06 18 00, Rayleigh - 06 21 30. Though it is accepted that extensional tectonics and presence of hydrothermal sources favors dynamical triggering of local tremors (Prejean and Hill, 2009), the latest analysis shows that weak "seismicity rate significantly increases immediately after (~45 min) M7 mainshocks in all tectonic settings and ranges" (Parsons et al, 2014).

Band pass (0.5-20 Hz) filtered records at two broadband seismic stations (s/s) located in Oni (South slope of Greater Caucasus) and Tbilisi (valley of river Kura), separated by the distance 130 km, as well as in Azerbaijan (Altiagach station ATG) were analyzed. The digital records were processed using SEISMOTOOL program (Chelidze et al, 2014) as well as by standard procedure (Chao et al, 2012) are shown in Fig.1. The sequence of triggered events is quite similar at seismic stations of the region.

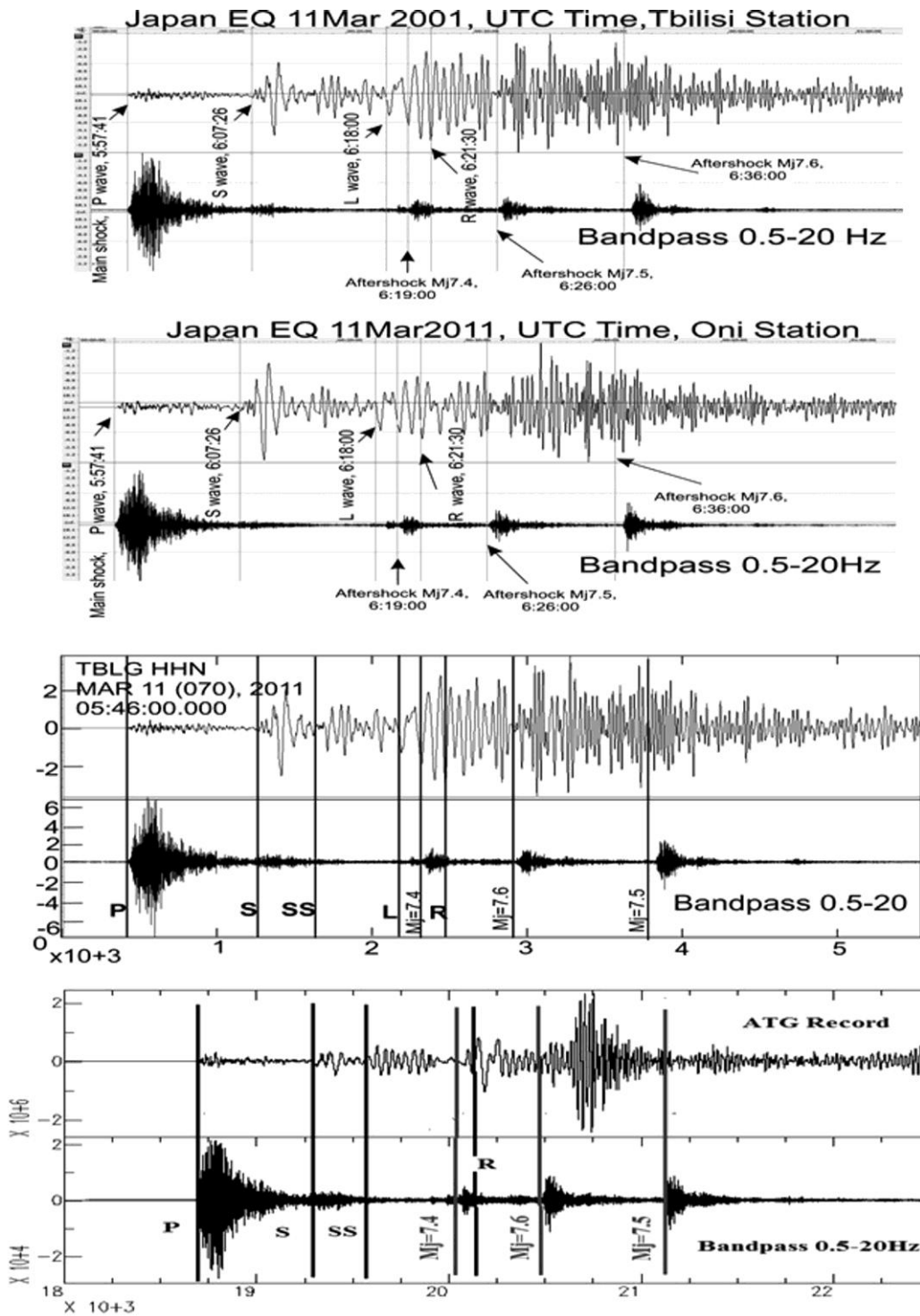


Fig. 1. a, b, c, d. Broadband record of M 9 Tohoku EQ, Japan (11.03.2011) wave train NS-component (upper channel) and the same high-pass band (0.5-20 Hz) filtered record (lower channel). Phases of seismic waves from the mainshock and arrival times of *p*-waves of strong aftershocks are marked by vertical lines. (a) at Tbilisi s/s; (b) the same for Oni s/s; in (a) and (b) the original records were processed using the SEISMOTOOL program (Chelidze et al, 2014). (c) at Tbilisi s/s (NS-component); (d) Z-component at Altiagach s/s (ATG), Azerbaijan. In (c) and (d) original EQ records (upper channels) were filtered by high-pass band 0.5-20 Hz filter (lower channel) using standard filtering procedure (Chao et al, 2012).

The strongest event in the filtered signal coincides with the arrival of *p*-waves. The source of the strong seismic signal at *p*-wave arrival time in the bandpass 0.5-20 Hz filtered record (Fig. 1) is ambiguous: maybe it is a processing artifact caused by the specific range of filter as the burst practically vanishes at 5-20 Hz bandpass filtering. Thus in the following analysis we ignore *p*-wave effect (see section 4). Nevertheless, we still prefer to use bandpass filter 0.5-20 Hz as the DTT corresponding to *S*, *L* and *R*- waves as well as signals from strong aftershocks can be clearly distinguished in the filtered record.

As the seismic network in Caucasus is not dense and high quality the standard approach to tremors' identification (Chao et al, 2012, 2013; Peng et al, 2010) is not effective here. We suggest the proxy method for discrimination of tremors generated by remote EQ that can be used even at one station; of course this does not allow calculation of location, depth and other details. Our approach is an analog of Reasenbergs' spatial β -parameter (Reasenbergs, 1985) in the temporal domain. We used the following criteria for presumed tremor discrimination:

i. Deviation by 3 sigma (3 times standard deviation) from the background seismic record scanned for several hours before EQ - this is considered as a lower threshold of presumed tremor signal. An additional condition is that the oscillation amplitudes of tremors should exceed ± 0.05 of the maximal amplitude of the considered EQ (Fig.1, b, c) or ± 0.25 for EQ record in db (Fig 1 a, b) or the corresponding value in counts /bit during 5 s (500 counts).. In case of Tohoku EQ this criterion corresponds to (2500 counts/bit) for amplitudes during 500 counts.

ii. 3 sigma deviation lasts at least 5 s (500 counts)

The number of such "tremors" increased 4-6 times in both Tbilisi and Oni stations during the first several hours after Tohoku EQ and cumulative curve increases drastically during passage of teleseisms (Fig. 2). Of course the strong aftershocks also can contribute to the statistics and the problem needs thorough consideration. According to USGS data Tohoku EQ from 05.46 11 March 2011 (local UTC) produces 112 aftershocks in the range M4.7-M7.9, which is much more than number of presumable tremors in Oni s/s, which equals 29. The onsets of 13 "tremor" signals coincide with the arrivals of *p*-waves of M6 and stronger aftershocks. The cause of other "tremor" signals is not clear as there were so many aftershocks that their *p*-wave arrival time coincidence with tremor signals can be quite accidental (for example such accidental coincidence was found for aftershock of M4.9, but we know that the isolated events of such magnitude from Japan do not cause tremor-like signals). So we can presume that at least half of "tremors" in Fig. 2 can be of local genesis, but still the significant increment in number of possible tremors remains. Still, in future the problem of discrimination of local tremors' signals from aftershocks should be analyzed in detail to avoid wrong interpretation (<http://earthquake.usgs.gov/earthquakes/seqs/usc0001xgp.php>).

As the pure seismological information is not enough to recognize local tremors in following we try to involve into interpretation process local hydroseismic data because simultaneous appearance of local tremor-like signal and local WL oscillations during passage of wave trains from remote EQ especially when there are not strong aftershock's can be an solid argument for tremor identification (Brodsky et al, 2003).

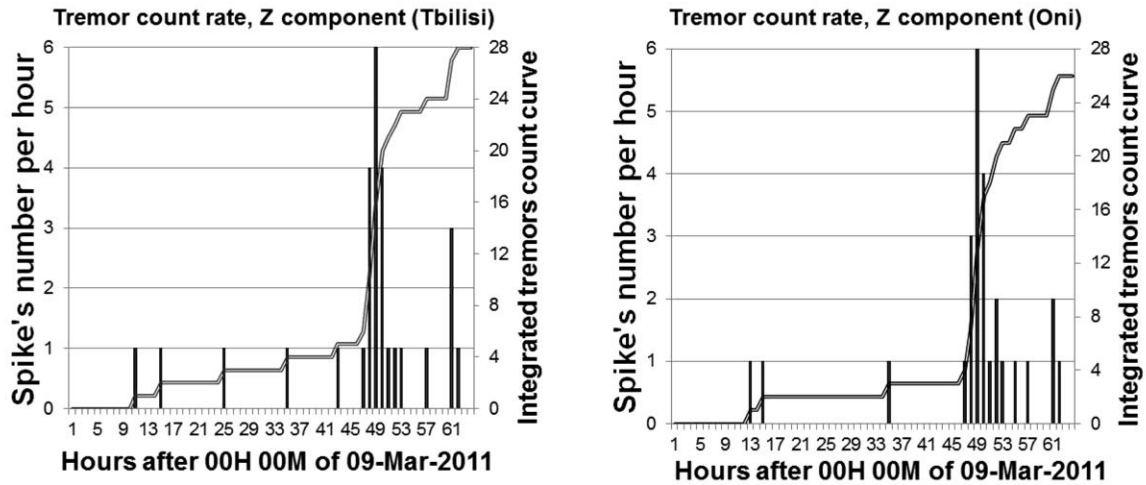


Fig. 2. Tremors' rate (number of presumable local events per hour) and cumulative curve of tremors before, during and after Tohoku event. Tohoku EQ p-wave arrival time is marked by the arrow.

3. Seismohydraulic effects in Georgia related to Tohoku EQ

Our next task was to compare the possible tremor signals with anomalies in water levels (WL) in deep wells' network in Georgia (Fig.3), operated by the M. Nodia Institute of Geophysics. Regular monitoring by this network is going on for several decades.

It was important to find WL anomalous changes and compare them with teleseismic waves' phases as well as to assess pressure and stress changes of correlated seismic and WL signals: according to Brodsky et al (2003) the tremors can be triggered by fluid pore pressure change during teleseismic wave passage. Generally (Wang et al, 2009; Zhang, Huang, 2011; Wang, Manga, 2010), WL respond to the EQ wave trains' impact depends on the distance of the well to the ruptured fault: i. Very close to the fault intensive shaking may increase opening of fractures, i.e.it cause rock dilatation and consequently, WL dropdown; ii. Outside this zone, but still very close to the fault shaking can consolidate loose sediments causing sudden upraise of WL; iii. In the intermediate field both positive and negative signs of sustained WL change are observed, which are explained by permeability changes;



Fig. 3. Network of WL borehole stations in Georgia

iv. Lastly, in the far field (which is our case) mainly correlated with seismic wave oscillations of WL are observed (hydroseismograms), sometimes accompanied with sustained WL change. As the seismic impact is instantaneous, it is expected that pore water has no time to flow, which in turn means that the WL response is undrained (Wang, Manga, 2010).

WL monitoring network in Georgia includes the following deep wells: Kobuleti, Borjomi, Axalkalaki, Marneuli, Lagodekhi, Ajameti and Oni (Table 1, Fig.3).

Table 1. Locations and depths of wells in Georgia

Location	Depth of well, meters	Location	Depth of well, meters
Kobuleti	2000	Akhalkalaki	1400
Marneuli	3505	Ajameti	1339
Borjomi70	1339	Lagodekhi	800
Borjomi Park (borehole is located on the top of the fault).	30	Oni	255

The sampling rate at all these wells is 1/min (except Oni, where the sample rate is 1/10 min). Measurements are sensors MPX5010 (resolution 1% of the scale) recorded by datalogger XR5 SE-M remotely by modem Siemens MC-35i using program LogXR; datalogger can acquire WL data for 30 days at the 1/min sampling rate. The range of WL measurements by this equipment is 0-100 cm.

Below (Fig.4) we show water level respond to a series of Japan earthquakes 11 March 2011 with following *p*-wave arrival times of the main shock and aftershocks: a) M 9; time - 05: 57; b) Mw7.4, time - 06.19; c) Mw =7.9, time – 06: 26; d) Mw =7.7, time – 06: 36. The oscillations due to the EQ impact last for 24-12 hours in various wells.

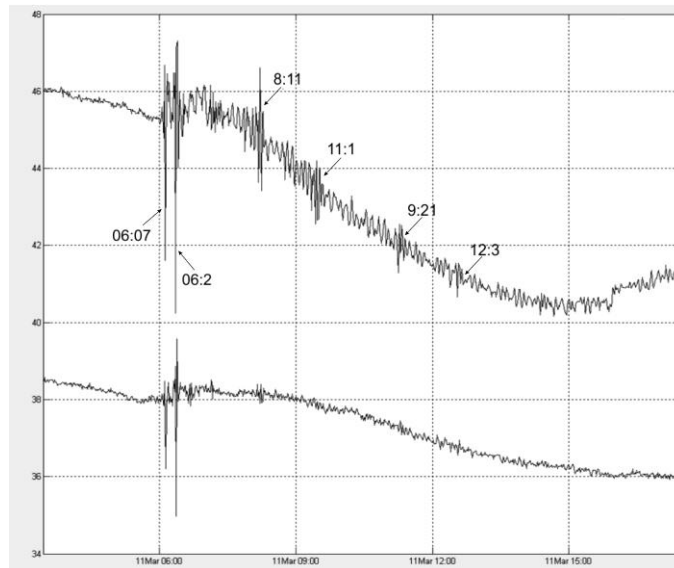


Fig.4. Water Level change in Kobuleti (top), Borjomi Park (middle) and Marneuli (bottom) boreholes before and during Japan M9 earthquake, 11 March 2011 in conventional units (1/min sample rate): compressed 24 hour record.

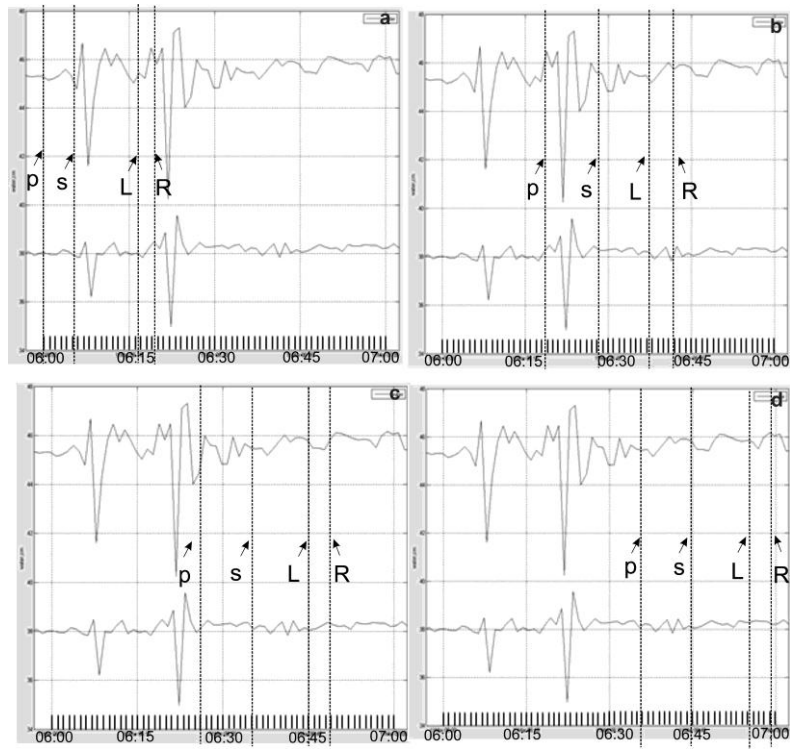


Fig.5 a, b, c, d. Water Level change in Kobuleti BorjomiPark (top) and (bottom) before and during first 30 minutes of Japan M9 earthquake, 11 March 2011 in conventional units (1/min sample rate), aftershocks and seismic phases; expanded records. On (a, b, c, d) the dashed lines mark onsets of the teleseismic p, S, Love and Rayleigh waves generated by the main shock Mw9 (a), and aftershocks Mw7.4 (b), Mw7.9 (c), Mw7.7, (d) correspondingly. The best correlation between teleseismic wave phases and pattern of strong WL signals is for the main shock (Fig. 5a). The most important phases of strong aftershocks (S, L, R) pass to late to cause major WL signals (Figs. 5 b, c, d).

It was interesting to know whether the wells recording oscillations due to seismic waves respond also to earth tides. In Fig.6 the two-weeks' record of WL in Kobuleti well is presented: upper figure shows original record and lower one – the same record after elimination of atmospheric pressure effect. It is evident that Tohoku EQ oscillations are superimposed on the tidal variations and that both responses are of almost the same amplitude – several (5-6) cm.

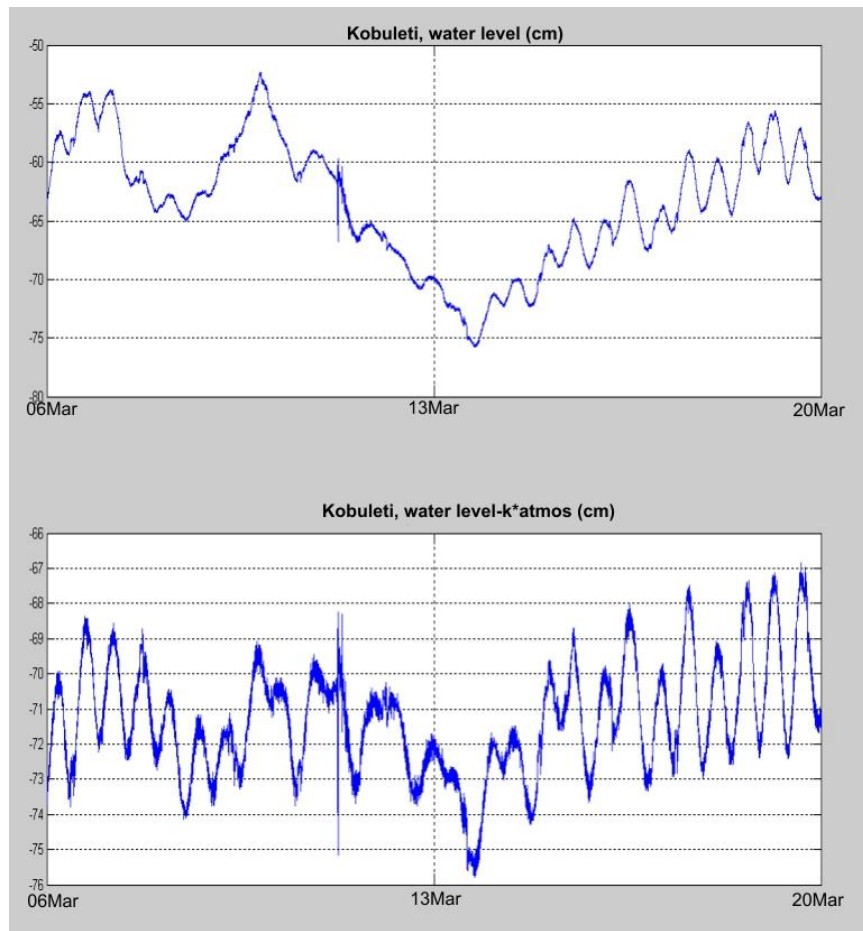


Fig. 6. WL record at Kobuleti borehole 06-20 March 2011: (a) original record of WL, absolute values, cm; (b) WL after removal of atmospheric pressure effect in reduced units; note well-marked tidal variations.

As the WL values in different wells change in a very wide range in order to show their reactions on the same plot, the signals from the i -th borehole (WL_i) are plotted in conventional units, namely, they are shifted along y-axis according to the expression: $(WL_i) = WL_o - [\min(WL_i)] + \text{offset}$; where WL_o is the observed WL, $[\min(WL_i)]$ is a minimum WL in borehole for the year 2011 and the offset is a constant, needed to fit WL curves into the same plot. For example, on the Figs (4, 5) the value of $[\min(WL_1)]$ for Kobuleti is -106 cm, the value of offset = 0; for Borjomi $[\min(WL_2)]$ is - 523 cm; offset - 6 cm. Reduced water level value obtained after this manipulation is shown on vertical axes of Figs. 4,5.

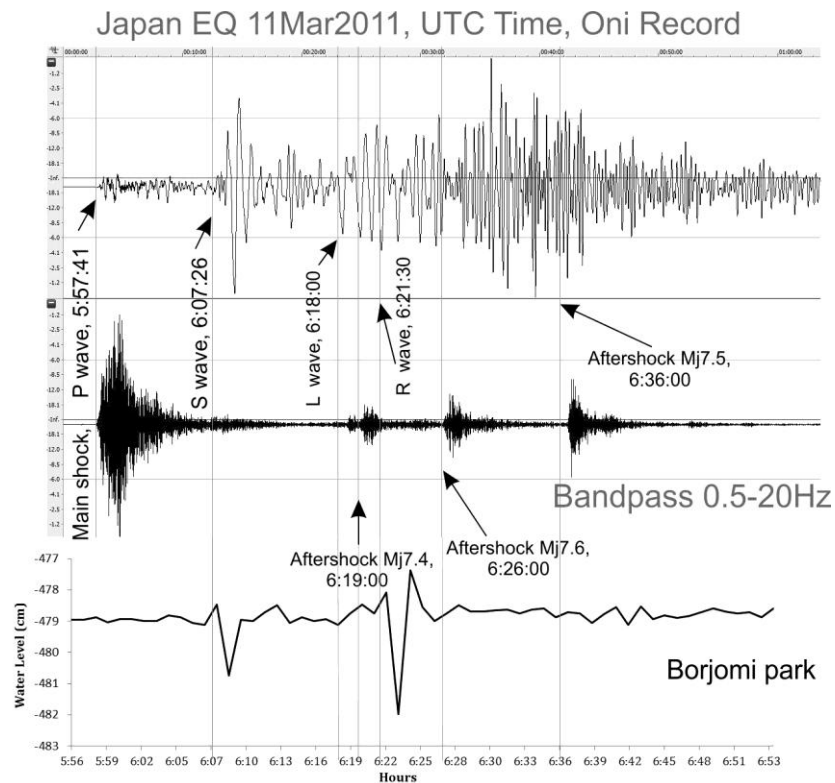


Fig. 7. The integrated plot of seismic and WL events in Georgia during Tohoku event. It is evident that the first strong WL perturbation at 06.07 correlates definitely with S-wave offset; no aftershocks are recorded at that time. The second strongest WL event between 06:19 and 06:22 coincides with both onset of L/R waves' package (06:18-06:21) and aftershock $M_j7.4$ at (06:19). Note, however, that the foreshock of Tohoku event (2011-03-09) of the same magnitude ($M_j7.3$) as well as stronger aftershock at 06.36 do not produce any characteristic WL oscillations; thus the most probable explanation of WL effect at 06:19 is the passage of L/R waves.

WL signals from the Tohoku events are fixed in Kobuleti, Borjomi Park, (Figs. 4, 5, 6), Marneuli and Oni boreholes.

Figs. 5, 6 demonstrate a striking similarity of hydraulic responses to passage of some phases of teleseismic waves from Tohoku event in areas separated by 300 km: namely, to S-wave and to summary impact of Love and Rayleigh waves (as the sampling rate was 1/m, it is impossible to separate reaction to L and R waves). Besides phases of the main shock, the strong aftershocks of Tohoku EQ also can affect WL; the first strong ($M_j7.4$) aftershock reach Tbilisi 11 March 2011 on 06:19. Note, however, that the foreshock of Tohoku event (2011-03-09) of the same magnitude ($M_j7.3$) as well as even stronger aftershocks at 06.26 ($M_j7.6$) and 06.36 ($M_j7.5$) do not produce any characteristic WL oscillations. Thus the most probable explanation of WL effect at 06:19 is the passage of the main shock generated L+R waves. Further, the best correlation between teleseismic wave phases and pattern of strong WL signals is for the main shock (Fig. 5a). The most important phases of strong aftershocks (S, L, R) pass too late to cause major WL signals (Figs. 5 b, c, d). We can conclude that there is good coincidence between teleseismic S waves onsets, some local tremor signals and hydroseismic anomalies. At the same time we cannot affirm that all seismic signal in the filtered record are definitely local tremors – some of them are most probably p-waves of strong aftershocks (Fig.7).

Finally, we conclude that teleseismic S and L+R waves of Tohoku EQ excite significant and quite identical WL anomalies on the whole territory of Georgia. In principle this means that corresponding

pore pressure changes can excite DTT though the existing data do not allow making decisive conclusions.

3. Spectrum of WL oscillations following Tohoku EQ and mantle surface waves.

It is evident that after Tohoku EQ water level undergoes characteristic oscillations, which decay in a dozen of hours (Fig. 4). The spectrum of WL oscillations for 10th and 11th March is shown in Fig. 8.

After Tohoku EQ in the spectrum of WL oscillations appear several spikes around frequencies $2.5 \cdot 10^{-3}$; $4.0 \cdot 10^{-3}$; $4.9 \cdot 10^{-3}$; $6.2 \cdot 10^{-3}$; $7.2 \cdot 10^{-3}$ Hz. Highest frequencies seem to be harmonics of the first mode ($2.5 \cdot 10^{-3}$ Hz) with a multiplier approximately 1.3. The intensity of harmonics is especially high during the first 30 min after EQ. The reverberations are absent in the spectrum for the 10th March (Fig.8a, black curve). The spectrogram of the same WL record also shows intensive signals around above frequencies (Fig. 8b). The observed reverberations in WL hardly can be explained by the excitation of so called Krauklis waves which propagate back and forth along fluid-filled fractures of the aquifer, emitting periodic seismic signal (Tary et al, 2014). The frequency of Krauklis wave depends on the fracture width, shear modulus of the solid, fluid density and the ratio of shear and longitudinal waves: in order to be in the observed range, the system should contain unrealistically long and thin cracks.

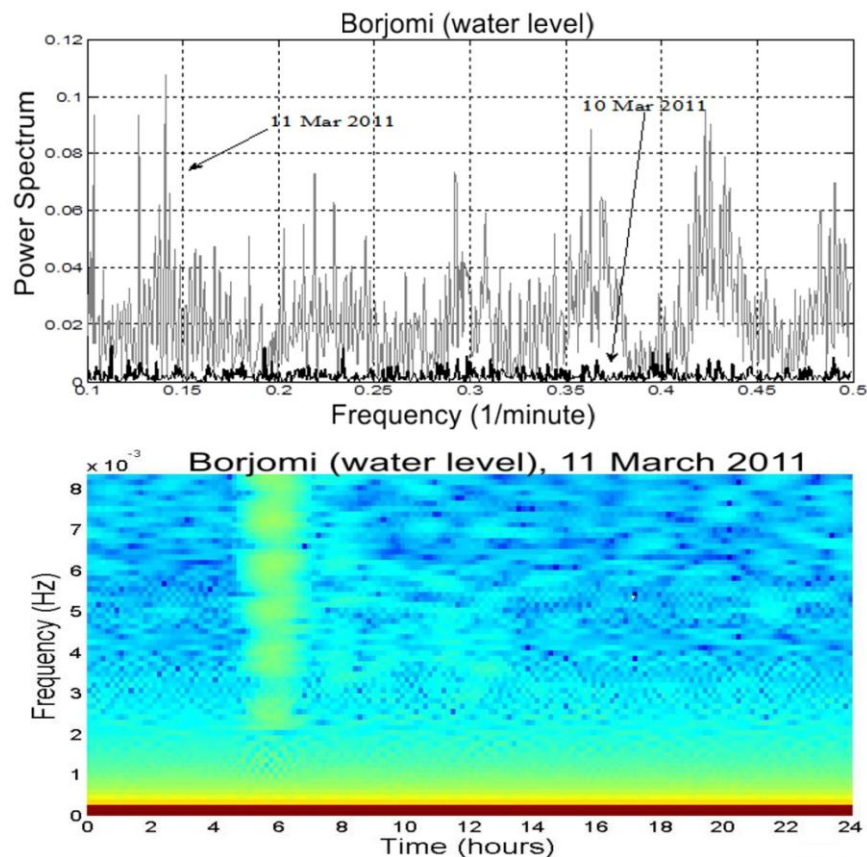


Fig.8. Spectrum (a) and spectrogram (b) of WL oscillations in Borjomi borehole before, during and after Tohoku EQ. The black curve in (a) is a background spectrum calculated for 10 March and grey curve - for 11 March. The last one shows several strong spikes at (central) frequencies $2.5 \cdot 10^{-3}$; $4.0 \cdot 10^{-3}$; $4.9 \cdot 10^{-3}$; $6.2 \cdot 10^{-3}$; $7.5 \cdot 10^{-3}$ Hz (periods 2-7 min), which are visible in the spectrogram (b) also and probably correspond to Rayleigh waves R1-R5.

The observed reverberations in WL hardly can be explained by the excitation of so called Kraukis waves which propagate back and forth along fluid-filled fractures of the aquifer, emitting periodic seismic signal (Tary et al, 2014). The frequency of Krauklis wave depends on the fracture width, shear modulus of the solid, fluid density and the ratio of shear and longitudinal waves and is of the order of tens of Hz in typical aquifers: in order to be in the observed low-frequency range (Fig. 8), the system should contain unrealistically long and thin cracks.

The most probable explanation of WL oscillations with periods 2-7 min is the impact of mantle surface waves (Love and Rayleigh), which can excite seismic signals with periods up to about 500 s (Bormann, 2012), which fits to the observed WL oscillations' frequencies: 410^{-3} to R5; $4.9 \cdot 10^{-3}$ to R4; $6.2 \cdot 10^{-3}$ to R3 and $7.5 \cdot 10^{-3}$ Hz to R2 (Figs. 4, 8). These WL oscillation frequencies are compared to frequencies of Rayleigh waves in Table 2.

Table 2. Comparison of periods in WL oscillations with periods of multiple Rayleigh phases

Rayleigh phases	Periods of Rayleigh phases, s	Periods in WL oscillations, s
R2	110	133
R3	155	161
R4	185	200
R5	220	250

Taking into account wide distribution of observed WL oscillation periods (Fig.8 a, b), the dominant WL periods are close enough to these of Rayleigh phases.

We can conclude that our interpretation on coupling of WL events with multiple surface R-wave phases is confirmed by both good coincidence of WL signals and R-waves arrival times as well as by closeness of their frequencies' ranges.

4. Fusion of seismic and WL effects in Georgia related to Tohoku EQ

In the Table 3 the seismological and WL information on the Toholu EQ impact in Georgia is summed. Here and in the Table 3 $\Delta(WL)_{mR}$ and $\Delta(WL)_{mG}$ are the maximal WL signal (peak-to-peak amplitude of oscillations) for R-group waves and L/G-group waves correspondingly, cm; ΔP_{mG} and ΔP_{mR} are the maximal water pressure change during L/G-waves and R-wave passage, KPa; v_S , v_G and v_R are correspondingly the velocities of S, L/G and R waves in cm/s; $\Delta\sigma_G$ and $\Delta\sigma_R$ are the dynamic stress changes for L/G waves and R waves correspondingly, KPa; ΔL_S , ΔL_L and ΔL_R are accordingly displacements due to S, L/G and R waves in cm; χ is the amplification factor of seismic waves in the well calculated as the amplitude of water level oscillations in meters $\Delta(WL)_m$ to the particle velocity in the seismic waves v (or its proxy Peak Ground Velocity - PGV), $\chi = \Delta(WL)_m/v$ in units m/(m/s) (Brodsky et al, 2003).

Love/Rayleigh phases induce maximal WL displacement (peak-to-peak amplitude), which vary from 4 cm in Borjomi to 10 cm in Oni. The hydraulic effect (displacement) is

4-10 times larger than seismic L or R wave displacement. In order to estimate dynamic stress (Chao, Peng et al, 2011) we measure the peak ground velocity for the Love and Rayleigh waves in the instrument-corrected NS and vertical component seismograms, respectively (Table 3). Then we calculate the corresponding dynamic stress ($\Delta\sigma$) based on equation: $\Delta\sigma = G (du/dt) /v$, where G is the average shear rigidity of crust - 35 GPa, v - phase velocities accordingly 4.0 and 3.5 km/s for Love and Rayleigh waves, (du/dt) is a Peak Ground Velocity (PGV) respectively. Measured PGV for Love and Rayleigh waves are 0.09 and 0.1cm/sec, respectively. So the corresponding dynamic stress is about 10

KPa. These data allow calculating the amplification factor χ , which turns to be of the order of 80 ± 10 m/(m/s). Interestingly, the calculation of the similar factor for tidal response χ_t results very low amplification value: $\chi_t \approx 3 \cdot 10^{-6}$ m/(m/s) due to a low velocity of deformation.

The different WL responses in different boreholes to practically the same mechanical impact (11 KPa) is explained by the difference in aquifers' transmissivity/storage: large amplitudes of WL are favored by a high transmissivity/low storativity (Wang, Manga, 2010; Brodsky et al, 2003).

Table 3. Seismic and hydraulic reactions to Tohoku (M9) EQ in Georgia

Site name	$\Delta(WL)_{mR}$, cm	ΔP_{mR} KPa	v_s cm/s	ΔL_s cm	v_L cm/s	ΔL_L , cm	v_R cm/s	ΔL_R , cm	$\Delta \sigma_G$ $\Delta \sigma_R$ KPa	χ m/(m/s)
Kobuleti	8	0.8	0.1	1	0.09	1.4	0.11	1.2	11	80
BorjomiPark	4	0.4	0.1	1	0.09	1.4	0.11	1.2	11	89
Oni	10	1	0.1	1	0.09	1.4	0.11	1.2	11	73

Generally, earlier it was accepted that the main impact on WL should cause Rayleigh wave as it provokes volume change. The strong enough response of WL to S- and Love waves passage was considered less probable as these wave does not lead to volumetric strain. Nevertheless recent observations document WL coherent oscillations with S- and Love waves (Wang, Manga, 2010). Our data also confirm strong impact of S-wave on WL in Georgia boreholes (Figs. 5, 6).

There is also very interesting detail on the WL plot for Borjomi well (Fig.4, trace for Z-component): clear delayed WL perturbations are registered at the following times: 08:11, 09:21, 11:14 and 12:33, which cannot be associated with aftershocks.

The possible explanation of these anomalies is the passage of late teleseismic phases, namely multiple surface waves circling the Earth: according to Peng et al (2011) they also trigger seismic events. The most effective in delayed triggering of microearthquakes are the first three groups of multiple surface waves (G1-R1, G2-R2, etc). Indeed, analysis of seismograms shows that exactly at the above mentioned times of WL perturbations arrive multiple surface waves R2 (08.10), R3 (09.21), R4 (11.13) and R5 (12.30), which travelled correspondingly 289, 431, 649 and 791 degrees (Bormann, 2012). Thus, we show that multiple surface R waves can generate not only local microseismicity, but also significant WL signals.

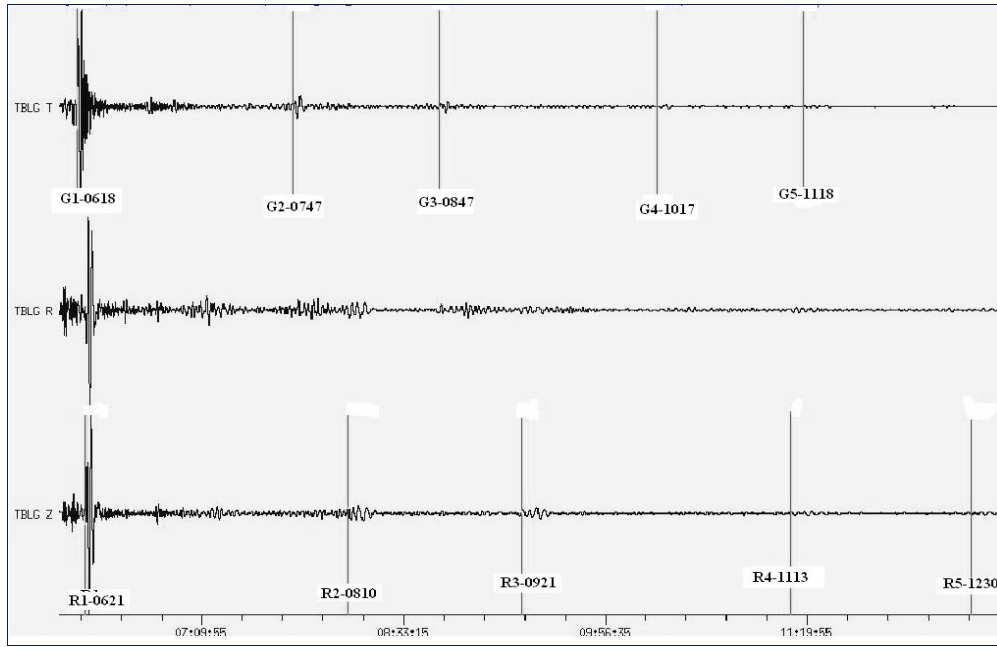


Fig.9. Seismogram with arrivals of multiple surface G and R waves at Tbilisi s/s.

On the other hand WL does not respond to the arrival of Love waves (G1, G2 etc – compare Figs.4, 9). Thus the WL signals, recorded at 08:11, 9:21, 11:14 and 12:33 are definitely triggered by passing multiple surface R-waves (Fig.4, 9). Table 4 summarizes corresponding seismic and WL data.

Table.4. Seismic and hydraulic response to the multiple surface waves (R2, R3, R4, R5 and G2, G3, G4, G5) of Tohoku, M9, EQ in Kobuleti, Georgia.

Site name	$\Delta(WL)_{mR}$ cm	ΔP_{mR} KPa	$\Delta(WL)_{mG}$ cm	ΔP_{mG} KPa	v_G cm/s	$\Delta\sigma_G$ KPa	v_R cm/s	$\Delta\sigma_R$ KPa	χ m/(m/s)
Kobuleti	3.20	0.32	-	-	G2 – 0.030	3.0	R2 - 0.020	2.0	160
	1.65	0.17	-	-	G3 – 0.015	1.5	R3 - 0.018	1.5	90
	1.26	0.13	-	-	G4 – 0.007	0.7	R4 - 0.008	0.7	160
	0.90	0.09	-	-	G5 – 0.003	0.3	R5 - 0.006	0.5	150

We can conclude that though the stress change imparted by multiple surface waves of both G and R-groups are comparable (Table 4), the WL responds strongly only to R-waves impact. This result is in agreement with the statement that for WL change porous space should consolidate or dilate; Rayleigh waves give rise to volumetric strain what satisfies this model (Wang, Manga, 2010). S and L waves have not volumetric component and accordingly they should not affect WL, but the recent data (Wang, Manga, 2010; Hill et al, 2013; Wang et al, 2009) as well as our results show that S and SS waves also significantly change WL. The mechanisms suggested for explanation of the latter observation include anisotropic poroelastic effect (Brodsky et al, 2003), permeability enhancement of fractured rocks due to

removal of blocking elements by oscillating fluid (Wang, Manga, 2010) or just strong anisotropy/heterogeneity of aquifer rocks, which can add volumetric component to a shear displacement; such effect is absent in isotropic homogeneous material.

Thus our new observation obtained by integrated analysis of seismic and water level records (hydroseismograms) document, for the first time, that multiple surface R waves generate not only local microseismicity (Peng et al, 2011), but also significant synchronous WL signals (unlike less efficient multiple surface G waves), see Figs. 4 and 8 (Chelidze et al, 2014).

Conclusions

The great Tohoku earthquake provokes significant local seismic and hydraulic events in Georgia triggered by passage of teleseismic wave trains, mainly by S and Love-Rayleigh waves. Some seismic triggered events are masked by offsets of strong aftershocks of Tohoku earthquake. Thus in future the problem of discrimination of local tremors' signals from aftershocks should be analyzed in detail to avoid wrong interpretation.

Comparison of WL anomalies with seismic waves' phases can help to discriminate triggered events from aftershock signals. The strong hydraulic events with amplitude 8-10 cm, correlated with passage of S- and L-R waves are caused by mechanical displacement of the order of 1 cm, i.e WL response to displacement is amplified 8-10 times due to mechanical stress change 11 KPa. It should be noted that the WL response at wells separated by hundreds of km are practically identical. Besides WL response to the first arrivals of S and Love-Rayleigh phases, there are some clear delayed WL perturbations, which document for the first time that passage of multiple surface Rayleigh waves: R2, R3, R4, R5 imparting dynamic stresses of the order of 0.5-2 KPa, also can affect WL regime. The amplification factor for S and L+R waves is of the order of 80.

Though teleseismic S and L+R waves of Tohoku EQ excite significant and quite identical WL anomalies on the whole territory of Georgia, which means that corresponding pore pressure changes can excite DTT the obtained data do not allow making decisive conclusions related to generation of local tremors by this event.

Further development of sensitive devices, dense networks and processing methods will develop a new avenue in seismology, which can be defined as DT microseismology and which will study systematically small earthquakes and tremors, especially events, triggered and synchronized by remote strong earthquakes (magnitudes 7-8). These events at present are ignored by routine seismological processing and are not included in traditional catalogues. At the same time, DT microseismic events contain very important information on geodynamical processes and can give clues to understanding fine mechanism of nonlinear seismic process and may be, even contribute to the problem of earthquake forecast.

Acknowledgments

The authors express their gratitude to the Rustaveli National Science Foundation of Georgia (Project FR/567/9-140/12) for the financial support.

References.

- Bormann, P. (Ed.) (2012). *New Manual of Seismological Observatory Practice* (NMSOP-2), IASPEI, GFZ German Research Centre for Geosciences, Potsdam; <http://nmsop.gfz-potsdam.de>;
- Brodsky, E., Roeloffs, E., Woodcock, D., Gall, I., and Manga, M. (2003). A mechanism for sustained groundwater pressure changes induced by distant earthquakes. *J. Geophys. Res.* 108, B8, 2390, doi:10.1029/2002JB002321,
- Chao, K., Z. Peng, C. Wu, C.-C. Tang, and C.-H. Lin (2012). Remote triggering of non-volcanic tremor around Taiwan, *Geophys. J. Int.* 188, no. 1, 301–324, doi: 10.1111/j.1365-246X.2011.05261.x.
- Chao, K., Peng Z. Gonzalez-Huizar, H., Aiken, Ch., Enescu, B., Kao, H., Velasco, A., Obara, K. and Matsuzawa, T. (2013), A global Search for triggered tremor following the 2011 Mw9.0 Tohoku earthquake. *Bull. Seis. Soc. America*, 103, 1551-1571, doi: 10.1785/0120120171
- [Chelidze, T.](#), [Matcharashvili, T.](#), [Lursmanashvili, O.](#), [Varamashvili, N.](#), [Zhukova, N.](#) and Meparidze, E. (2010). [Triggering and Synchronization of Stick-Slip: Experiments on Spring-Slider System](#). In: *Synchronization and Triggering: from Fracture to Earthquake Processes*. Eds. [V.de Rubeis](#), [Z. Czechowski](#), [R. Teisseyre](#), pp.123-164.
- T. Chelidze and T. Matcharashvili. (2013). Triggering and Synchronization of Seismicity: Laboratory and Field Data - a Review. In: *Earthquakes – Triggers, Environmental Impact and Potential Hazards*. (Ed. K. Konstantinou), Nova Science Pub. Pp. 165- 231.
- T. Chelidze and T. Matcharashvili, (2014). Dynamical Patterns in Seismology. In: *Recurrence Quantification Analysis: Theory and best practices*. (Eds. C.Webber and N.Marwan). Springer Cham Heidelberg, pp. 291-335.
- Chelidze, T., Zhukova, N., Matcharashvili, T. 2014. SEISMOTOOL – an easy way to see, listen, analyze seismograms. *Seismol. Res. Letters.* 85, 889-895.
- T. Chelidze, I. Shengelia, N. Zhukova, T. Matcharashvili, G. Melikadze, G. Kobzev. (2014). Coupling of Multiple Rayleigh Waves and Water Level Signals during 2011 Great Tohoku Earthquake observed in Georgia, Caucasus, *Bull. of the Georgian National Academy of Sciences.* v. 8, no. 2, 76- 79.
- Costain, J. and Bollinger, J. (2010). Review: Research results in Hydroseismicity from 1987 to 2009. *Bull. Seismol. Soc. Am.* 100, 1841-1858, doi: 10.1785/0120090288.
- Gonzalez-Huizar, H., Velasco, A., Peng, Zh. and Castro, R. (2012). Remote triggered seismicity caused by the 2011, M9.0 Tohoku-Oki, Japan earthquake. *Geophys. Res. Letters.*39, L10302, doi: 10.1029/2012GL051015.
- Hill, D. and Prejean, S. (2009). Dynamic triggering. In: *Earthquake Seismology*. Ed. H. Kanamori. Elsevier. pp. 257-293.
- Hill, D., Peng Zh., Shelly, D., and Ch. Aiken. (2013). S-Wave Triggering of Tremor beneath the Parkfield, California, Section of the San Andreas Fault by the 2011 Tohoku, Japan, Earthquake: Observations and Theory. *Bull. Seis. Soc. America*, 103, 1541–1550.
- Obara, K. and Matsuzawa, T. (2013). A Global Search for Triggered Tremor Following the 2011 Mw 9.0 Tohoku Earthquake. *Bull. Seismol. Soc. Am.*, **103**, 1551–1571.
- Parsons, T., Segou, M., Marzocchi, W., (2014). The global aftershock zone. *Tectonophysics.* 18, 1–3.
- Peng, Z., Wu, C. and Aiken C. (2011). Delayed triggering of microearthquakes by multiple surface waves circling the Earth, *Geophys. Res. Lett.*, 38, L04306, doi:10.1029/2010GL046373.
- Prejean, S. and Hill, D. (2009). Dynamic triggering of earthquakes. In: *Encyclopedia of Complexity and Systems Science*, R. A. Meyers (Ed.), Springer, pp. 2600-2621.
- Reasenberg, P. (1985). Second-order moment of central California seismicity, 1969-1982. *J. Geophys. Res.*, 90, 5479-5495.
- Tary, J. B., van der Baan, M. and Eaton, D. W. (2014). Interpretation of resonance frequencies recorded during hydraulic fracturing treatments. *J. Geophys. Res. Solid Earth*, 119. doi:10.1002/2013JB010904. doi:10.1002/2013JB010904.

Wang, C.-Y., Chia, Y., Wang, P.-L., Dreger, D. (2009). Role of S waves and Love waves in coseismic permeability enhancement. *Geoph. Res. Lett.* 36, L09404, doi:10.1029/2009GL037330.
Wang, C.-Y., Manga, M. (2010). *Earthquakes and Water*. Springer-Verlag Berlin Heidelberg.
Zhang, Y. and Huang, F. (2011). Mechanism of Different Coseismic Water-Level Changes in Wells with similar Epicentral Distances in Intermediate Field. *Bull. Seis. Soc. America*, 101, 1531-1541.

Отклик на землетрясение Тохоку М9 в Грузии – локальные треморы и гидросейсмические эффекты

Тамаз Челидзе¹, Ия Шенгелия², Наталья Жукова¹, Темур Мачарашвили^{1,2},
Георгий Меликадзе¹, Геннадий Кобзев¹

1. Институт Геофизики им. М. Нодиа;
2. 2. Университет им. Ильи Чавчавадзе

Резюме

В настоящее время имеется много данных о значительном влиянии сильных удаленных землетрясений на режимы подземных вод и локальной сейсмичности (т.н. невулканические или динамические треморы). Оба эти эффекта часто тесно связаны друг с другом, ибо одним из главных факторов, снижающим локальную прочность пород является поровое давление флюидов.

Некоторые свидетельства в пользу динамического триггерирования локальных треморов сильнейшим землетрясением Тохоку (М9) были получены недавно на Западном Кавказе. Кроме треморов, выявлены ясные аномалии в уровнях вод в скважинах при прохождении телесейсмических S-L-R волн, идентичные на всей территории Грузии от Боржоми до Кобулет. Мы полагаем, что совпадение предполагаемого сигнала от тремора с аномалией (осцилляцией) в уровнях вод в скважинах делает более надежной классификацию локального сейсмического сигнала как триггерированного явления. Обнаружены, видимо, впервые, заметные осцилляции в уровнях вод в скважинах при прохождении кратных поверхностных волн Релея.

დიდი ტოჰოკუს მიწისძვრის (M9) გამოძახილი საქართველოში - ლოკალური ტრემორები და ჰიდროსეისმური ეფექტები

თამაზ ჭელიძე¹, ია შენგელია², ნატალია ჟუკოვა¹, თემურ მაქარაშვილი^{1,2},
გიორგი მელიქაძე¹, გენადი კობზევი¹

1. მ.ნოდიას გეოფიზიკის ინსტიტუტი;
2. ილიას უნივერსიტეტი

ბოლო დროს მიღებულ იქნა ზოგიერთი მტკიცებულება იმისა, რომ უძლიერესმა (M9) ტოჰოკუს მიწისძვრამ დასავლეთ კავკასიაში გამოიწვია ადგილობრივი ტრემორების დინამიკური ტრიგერირება. გარდა ტრემორებისა აღმოჩენილია მკვეთრი ანომალიები

ჭაბურღილებში წყლის დონეებში, რომლებიც გამოწვეულია ტოპოკუს მიწისძვრით აღძრული S-L-R ტელესეისმური ტალღებით და რომლებიც იდენტურია საქართველოს მთელს ტერიტორიაზე ბორჯომიდან ქობულეთამდე. ჩვენ მიგვაჩნია, რომ შესაძლო ტრემორისა და წყლის დონის ანომალიის (ოსცილაციის) სინქრონული გამოჩენა მეტსანდობას ანიჭებს ლოკალური სეისმური სიგნალის კლასიფიკაციას როგორც ტრიგერირებულ ტრემორს. პირველად იქნა დაკვირვებული ჭაბურღილებში წყლის დონის მნიშვნელოვანი ოსცილაციები რელის ზედაპირული ჯერადი ტალღების გავრცელების დროს.

Acoustic pulses detecting methods in granular media

Nodar Varamashvili, Tamaz Chelidze, Zurab Chelidze

*M. Nodia Institute of Geophysics of Ivane Javakhishvili Tbilisi State University,
1, Alexidze Str., 380093 Tbilisi, Georgia*

Abstract

The prevention of loss to life and property due to natural calamities is viewed very seriously in many countries of the world. There are many uncertainties in the forecasting of when a movement in a landslide will occur. Acoustic emission (AE) is a natural phenomenon that occurs when a solid subjected to stress experiences non-elastic deformation – fracturing or stick-slip. Acoustic emissions carry information about location, intensity and mechanisms of deformation occurring in a material. The aim of our research is attempt to construct a sensitive acoustic emission registrator. One of the goals of our experiment is optimization of equipment to use them in the field and work for development of a landslides' acoustic early warning system.

Introduction

For many countries around the world landslides are one the most severe of all natural disasters, with large humanitarian and economic losses. The earth surface is not static but dynamic system and landforms change over time as a result of weathering and surface processes (i.e., erosion, sediment transport and deposition). The fast mass-movement has a potential to cause significant harm to population and civil engineering projects. Landslides are important natural geomorphic agents that shape mountainous areas and redistribute sediment (Sidle And Ochiai, 2006). Large-scale experiments and field observations show that the landslide may reveal a slow steady slip, episodic stick-slip or sudden acceleration.

Problem description

Landslides are sources of considerable hazards for human life, economy and infrastructure in mountainous areas, such as Georgia. This is why understanding of properties, statistics, and dynamics of this process in order to reveal its physical nature, to predict landslides or to decrease mass movement risk is an important scientific and practical problem.

Landslides occur in hills/mountains in response to a wide variety of terrain conditions and triggering processes like heavy rainstorms, earthquakes, floods and unsafe developmental activities. With growing population, urbanization and human interventions in terms of developmental activities over unstable slopes, landslides pose increasing risk to human lives, buildings, structures, infrastructures and environment (**Anderson and Holcombe, 2013**). Changing climatic conditions manifested in the form of global warming, glacial melting, erratic and uneven rains, extreme temperature conditions etc. are also extending these risks to even unexpected areas. Large scale deforestation along with faulty management has led to increased vulnerability to landslides.



Fig.1. The landslide in Dariali Gorge in northern Georgia, on the Greater Caucasus range 17 May 2014. It severed the road connecting Georgia and Russia causing large economic losses and several deaths

Acoustic emissions (AE) is a natural phenomenon that occurs when a solid is subjected to large enough stress. This external stress, causes fracturing or stick-slip on various scale and a sudden release of sound waves resulting in acoustic/microseismic activity, which can be detected by transducers. AE are transient, high-frequency, elastic waves' bursts generated by the rapid release of stored elastic energy. In brittle materials like rocks, crack formation and crack propagation generate AE. In granular materials, frictional sliding and rolling are sources of AE. Another source of AE in the nature is the breaking of roots.

Acoustic emissions carry information about location, intensity, and deformation mechanisms occurring in a material. It is a non-invasive method and gives real-time information on what is happening during deformation. In rock mechanics, AE monitoring has been successfully used to identify various stages of the failure process, such as crack initiation, crack growth, and crack propagation prior to global failure.

Traditional methods of monitoring slope movements have included surface surveying and sub-surface instrumentation techniques. However, many of these methods lack the sensitivity to detect deformation at low pre-failure strain rates. Over 40 years research has been conducted on the use of AE to monitor soil movements. Interesting work has been carried by Chelidze et al., (2012) out. The most notable contributions in terms of field of AE monitoring were provided by Koerner *et al.* (1981) and Dixon *et al.* (2003).

Detecting AE generated by a developing shear surface within a slope is not an easy task. As AE propagates through soil, it suffers from a loss of signal amplitude: attenuation is high in soil because it is a particulate (granular) medium and energy is lost as AE travels across boundaries from one particle to another. The use of a waveguide to provide a path of low attenuation from the source of the AE (within a soil slope) to the sensor (usually situated above ground surface) has become a standard practice in AE research. The presence of a waveguide, typically a metal pipe inserted within an unstable slope, also greatly increases the monitoring ability of the AE sensor.

Dixon *et al.* (1996) outlined two generic types of waveguides; passive and active. A passive waveguide does not introduce additional sources of AE, and thus all detected AE is assumed to

originate from the surrounding soil slope. In comparison, the active waveguide uses an annulus of high AE-responsive backfill material around the waveguide. As the slope deforms the waveguide, AE is assumed to originate from the backfill only.

Kousteni (2002) showed that gravel emitted higher levels of AE than sand.

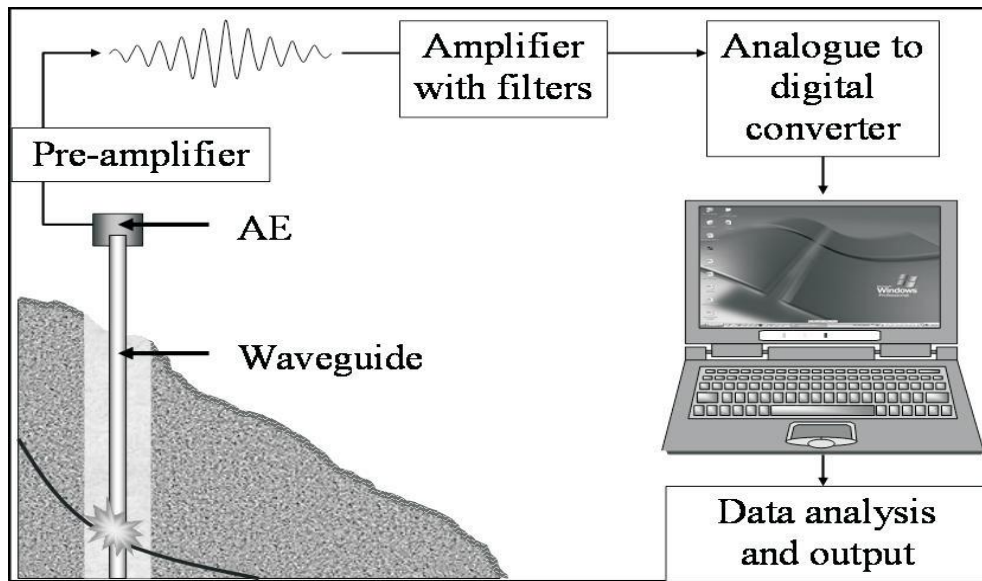


Fig. 2. Components of an AE monitoring system (Dixon et al., 2003)

Figure 2 shows a schematic representation of a typical AE instrumentation system. AE originating from the deformation of a backfill within the active waveguide propagates along a steel waveguide to a piezoelectric sensor secured to the top of the metal waveguide. The AE signal is then amplified by a preamplifier and an amplifier to enable the signal to travel down the lengths of cable without being subsequently affected by background or electrical noise. Finally the AE is converted to a digital signal for subsequent analysis and manipulation using real time data acquisition software.

Experimental setup

The main goal of our study is registration and monitoring of landslide slow motion (creep) by recording the acoustic emission. For this goal we early developed the special equipment (Varamashvili et al., 2013), by which occurred landslide modeling process and registration occurred during this acoustic emissions. The goal of acoustic monitoring is to record acoustic signals generated by preliminary displacement of geologic formations before activation of the fast phase of landslides

The similar technique based on the recording of the acoustics generated by displacement in the gravel coating around acoustic sensor was earlier developed by Loughborough University team, but it demands drilling of relatively deep borehole down to the sliding surface. This procedure is quite expensive. Our objective was to develop a cost-effective version of the mentioned method. The idea is to use two sensitive acoustic probes grounded on different depths, one on the depth of several meters and other close to the day surface. The former probe is the basic and the role of latter one is to distinguish signals of surface origin, which in this case are considered as noise.

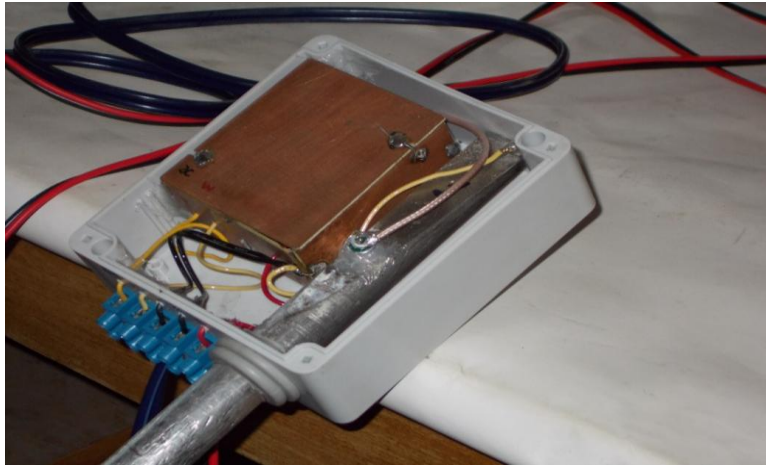


Fig.3. Acoustic sensors

The probes are constructed from thick-wall stainless steel tube (Fig.3) containing acoustic sensor. The length can be chosen according to the depth of investigation by screwing additional sections to the tube containing basic sensor. The length of these sections is 1.5 m; the maximal depth of probe is of the order of 4 m.

The diameter of the tubes is 20 mm and the thickness of the walls is 2 mm. In order to transfer surface acoustic wave without significant loss the contact of sections is performed with maximal accuracy. This ensures strong contact between sections and minimizes acoustic energy losses.

The upper part of the basic probe is manufactured as a cylinder rod with an inclined cut. The precise finish of the cut surface guarantees good contact of acoustic sensor with probe tube. Investigation of various types of acoustic sensors in laboratory led to conclusion that for the frequency range of interest, i.e. frequencies generated by displacements in the gravel coating (5-25 KHz) the best solution is the capacity capsule-microphone, glued with his sensitive membrane side to the surface of the upper end of the probe.

Electronic module consists of low-noise amplifier, buffer amplifiers of output for signal wavetrains and precision peak-integrator and DC voltage output for recording in the data logger. The integrator fixes in its memory the maximal value of obtained signal and after this the signal decays by the rate 5% per minute. Fixing on data logger the readings with the sampling rate 1 per minute allow obtaining the necessary information on the variation of acoustic noise in the time domain. This method allows saving the power, what is important in field conditions. There are two outputs for fixing signal in two different ways. Signal output 1 allows obtaining acoustic waveform recording by application of high quality ADC. It is also possible to record acoustic signals in the real-time regime, when signal from the output 1 is transferred to the USB recording oscilloscope with the input ADC module capable to record acoustic signals up to the frequency 100 KHz. The signal from output 2 can be recorded simultaneously by another channel of the same USB oscilloscope with input set to DC regime.

Registration of acoustic pulses occurring at small shifting of the landslide soil was produced by the acoustic sensor, which was attached to the USB oscilloscope (Fig.4), with which after using special processing software information is sent to computer.

The goal of our experiment the increase in sensitivity of the acoustic sensor by changing its mechanical parts. For this goal plastic small volume was filled with gravel (Fig.4a). At its center was placed aluminum stem with small cross-section, on which was fixed electronic block of the acoustic sensor. In one experiment on an aluminum rod was fixed aluminum radiator (Fig4b), which increases the useful area of the sensor and therefore, in our opinion, its sensitivity. In a second experiment, nothing was fixed to the aluminum rod.

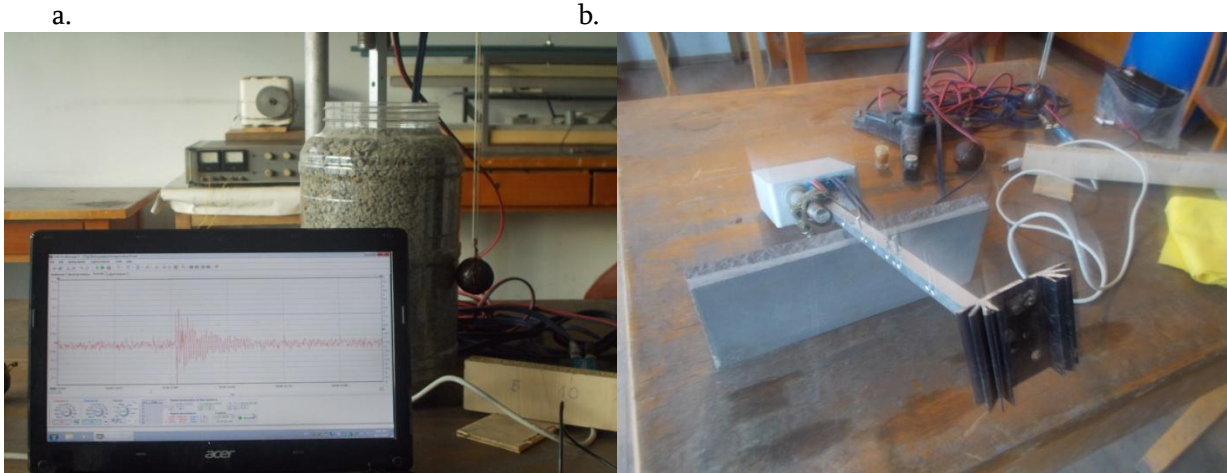


Fig.4. a) experimental equipment, b) acoustic sensor with fixed aluminum rod and radiator for increasing sensitivity

On the gravel-filled, plastic container made mechanical impact from the outside, using a pendulum, and recorded an acoustic signal by the sensitive sensor or conventional acoustic sensor. Pendulum used to effect could be measured (Fig.4). Mass of the pendulum $m \approx 175 \text{ g}$, length of $l \approx 50 \text{ cm}$. Pendulum collision with the upper plate was realized from different distances: 10, 15, 20 and 25 cm.

It is interesting to calculate force the pendulum is acting on the plate. The magnitude of this force will be different for different collision distances. It is necessary to carry out the following calculations:

We need to calculate

1. What height the pendulum reaches at various deviations from the initial position
2. Corresponding potential energy
3. Speed at collision of the pendulum weight with a plate
4. The value of impact momentum (pulse) which the pendulum passes to the plate (about a half of the full pulse)
5. Finally, knowing the duration of the collision it is possible to calculate the force

At 10 cm deviation the pendulum rises to a height of $h \approx 2 \cdot 10^{-2} \text{ m}$, corresponding potential energy equals $E_p = mgh$. pendulum speed at collision with a plate $v = \sqrt{2gh} \approx 0.63 \frac{\text{m}}{\text{s}}$, the value of pulse which the pendulum delivers to the plate $p \approx 0.11 \text{ kg} \cdot \frac{\text{m}}{\text{s}}$. From analysis we conclude that the pendulum-equipment interaction duration time is $t \approx 0.125 \text{ s}$. Accordingly, the impact force is: $F = \frac{p}{t} \approx 0.88 \text{ N}$

Table1. Gradations of the pendulum deviations and corresponding forcing values on the container

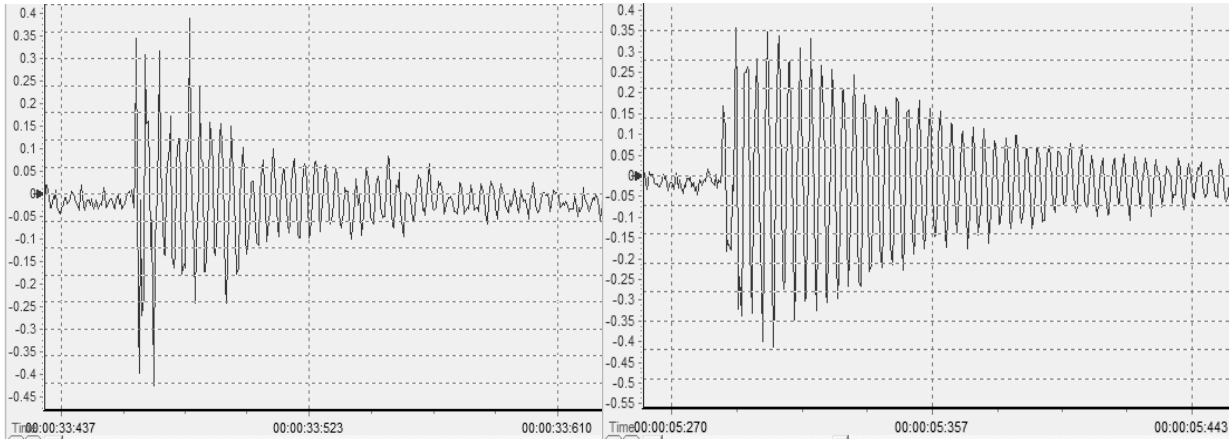
Deviation cm	10	15	20	25
Heigh, m	$2 \cdot 10^{-2}$	$4,5 \cdot 10^{-2}$	$0,8 \cdot 10^{-1}$	$1,25 \cdot 10^{-1}$
Pendulum forcing, N	0.88	1.33	1.77	2.21

Results analysis

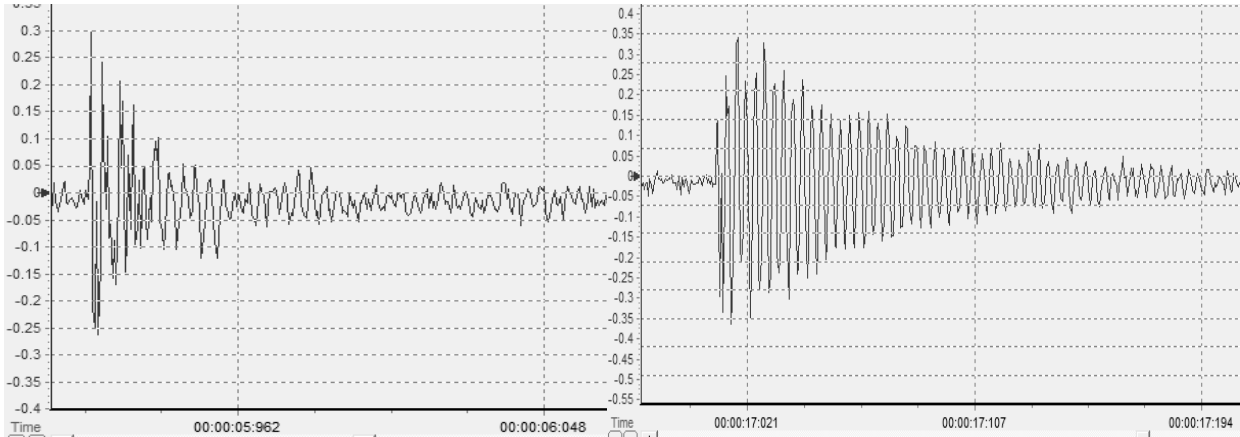
Experimental equipment is described above (Fig.4). Records of acoustic signal waveform using USB oscilloscope;

a.1.

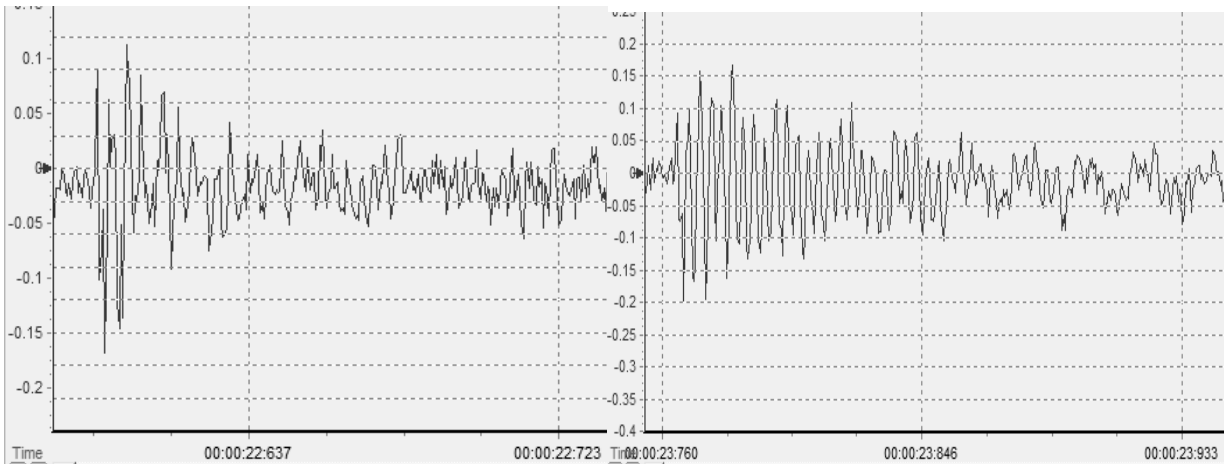
2.



b.



c.



d.

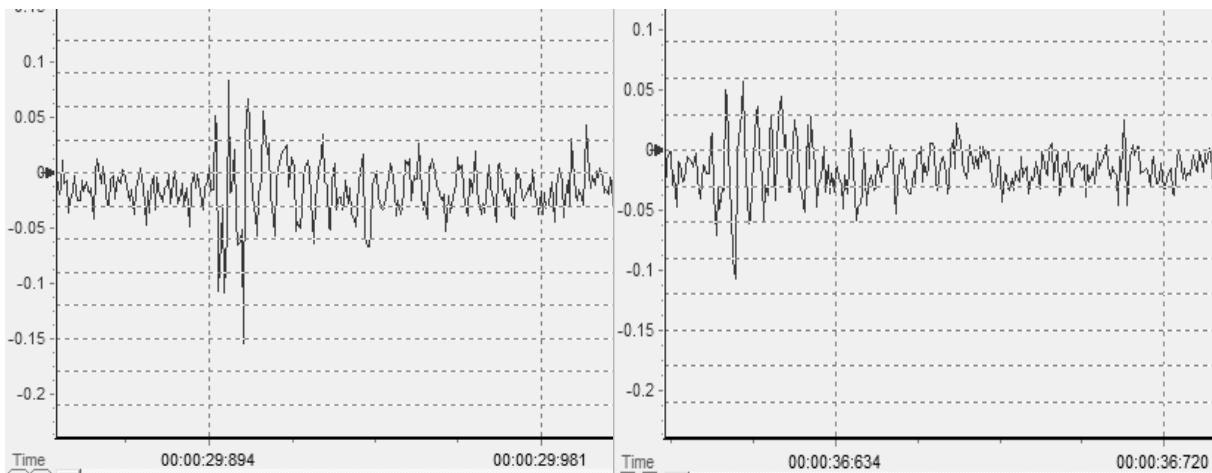


Fig.5. Recording acoustic pulses encountered in collisions on a plastic container from different distances: 1 column-sensitive sensor, 2 column-conventional sensor, a) Pendulum deviation of 25 cm, b) deviation of 20 cm, c) deviation of 15 cm, d) deviation of 10 cm; x-axis is time in sec, y-axis is the acoustic signal intensity in volts.

As can be seen from Fig5, the difference of sensitive and conventional sensor records is not significant. Especially for the large deviation of the pendulum. By small (10 cm) deviation (case d) the amplitude of the sensitive sensor records is larger than normal sensor records. This may be due to the fact that by the strong collision a pendulum with a plastic container sensor begins to vibrate, which causes a change in the amplitude and spectrum of the acoustic signal recording. For weak pendulum collisions vibrate not occur and there is a registration occurred acoustic emissions. At this time of great importance to the sensor receiving surface area and its orientation with respect to the acoustic emission source. A series of experiments are planned to look for a sensitive sensor for optimum shape. Our guess is that in this direction, it is possible to develop monitoring and early warning acoustic system for revealing landslide incipient slipping.

Refereces

- [1] Anderson, M. G. and Holcombe, E. Community-Based Landslide Risk Reduction, The World Bank, Washington, DC, 2013
- [2] Chelidze, T., Varamashvili, N. and Chelidze, Z., Acoustic early warning telemetric system of catastrophic debris flows in mountainous areas, Journal of the Georgian Geophysical Society, Issue A, vol.15A, 2012, 35-42
- [3] Dixon, N. Kavanagh, J. and Hill, R. Monitoring landslide activity and hazard by acoustic emission. Journal of the Geological Society of China, Vol.39, No. 4, 1996, 437-464
- [4] Dixon, N., Hill, R. and Kavanagh, J. Acoustic emission monitoring of slope instability: Development of an active wave guide system. Institution of Civil Engineers Geotechnical Engineering Journal, 156, 2, 2003, 83-95
- [5] Koerner, R.M. McCabe, W. M. and Lord, A. E., Acoustic emission behavior and monitoring of soils. Proceedings of the First Synopsis on Acoustic Emission in Soils, 1981, 93-141
- [6] Kousteni, A., Investigation of Acoustic Emission Waveguide Systems for Detecting Slope Instability. PhD Thesis, The Nottingham Trent University, 2002

- [7] Sidle, R.C. and Ochiai H., Landslides-Processes, Prediction, and Land Use, AGU, Washington, DC, 2006
- [8] Spriggs, M. and Dixon, N. The Instrumentation of Landslides Using Acoustic Emission, Geotechnical News, September, 2005, 27-31.
- [9] Varamashvili, N., Chelidze, T., and Chelidze, Z., Acoustic pulses generated by landslide activation: laboratory modeling, Journal of Georgian Geophysical Society, Issue (A), Physics of Solid Earth, 2013

მარცვლოვან გარემოში აკუსტიკური იმპულსების დეტექტირების მეთოდები

ნოდარ ვარამაშვილი, თამაზ ჭელიძე, ზურაბ ჭელიძე

რეზიუმე

სტიქიური უბედურებების შედეგად მსხვერპლისა და ზარალის თავიდან ასაცილებლად პრევენციული ზომები სერიოზულად განიხილება მსოფლიოს ბევრ ქვეყანაში. არსებობს ბევრი გაურკვევლობა მეწყრის დასრიალების დროის პროგნოზირებაში. აკუსტიკური ემისია არის ბუნებრივი მოვლენა, რომელიც ხდება, როდესაც მყარი სხეული იმყოფება დამაბულობის ქვეშ. აკუსტიკური ემისია ატარებს ინფორმაციას სხეულში მიმდინარე დეფორმაციის მექანიზმის, ადგილმდებარეობის და ინტენსივობის შესახებ. ჩვენი კვლევის მიზანია მაქსიმალურად მგრძნობიარე აკუსტიკური იმპულსის რეგისტრატორის კონსტრუირების მცდელობა. ჩვენი ექსპერიმენტების ერთ-ერთი მიზანია აპარატურის ოპტიმიზაცია რათა მოვახერხოთ მისი გადატანა სავსე პირობებში და ვიმუშაოთ მეწყრის დასრიალების წინასწარი შეტყობინების აკუსტიკური სისტემის შექმნაზე.

Методы детектирования акустических импульсов в сыпучих средах

Нодар Варамашвили, Тамаз Челидзе, Зураб Челидзе

Резюме

Предотвращение потери жизни и имущества в результате стихийных бедствий в настоящее время рассматривается очень серьезно во многих странах мира. Есть много неопределенности в оценке момента, когда произойдет движение оползня. Акустическая эмиссия является естественным явлением, которое происходит, когда твердое тело подвергается деформации. Акустическая эмиссия несет информацию о локализации, интенсивности и механизме деформации, происходящей в материале. Цель нашего исследования попытка конструирования чувствительного регистратора акустической эмиссии. Одна из целей нашего эксперимента, оптимизация оборудования для использования его в полевых условиях и создание акустической системы раннего оповещения активизации оползня.

Arnold's tongues at electromagnetic and mechanical synchronization of stick-slip

T. Chelidze, E. Mepharidze, D. Tephnadze
M. Nodia Institute of Geophysics, 1, Alexidze str. 0171, Tbilisi, Georgia

Abstract

Synchronization phenomena are encountered in various fields, from mechanics to biological and social processes. Thus it is only natural that synchronization is observed in many geophysical fields, as the Earth is embedded in the oscillating field of different origin with extremely wide range of frequencies, from seconds to months and years. These large-scale natural processes can be modeled in laboratory. In the paper, the results of laboratory experiments on the mechanical and electromagnetic synchronization of mechanical instability (slip) of a slider-spring system are presented. Slip events were recorded as acoustic emission bursts. The data allow delineating approximately of the synchronization regions (Arnold's tongues) in the plot of forcing intensity versus forcing frequency for both mechanical and electromagnetic synchronization.

Introduction

Synchronization is encountered in various fields, from mechanics to biological and economical processes (Pikovsky et al., 2003). Thus it is only natural that synchronization phenomena are observed in many geophysical fields, as the Earth is embedded in the oscillating field of different origin with extremely wide range of frequencies, from seconds to months and years. For example there are a lot of (disputable) observations that seismic activity is coupled with the action of such weak oscillating fields as Earth tides, solar activity, atmospheric pressure, electromagnetic pulses (storms), seasonal variations, and reservoir exploitation. The intensity of stress, invoked by these superimposed periodical mechanical or electromagnetic (EM) oscillations is as a rule much smaller (of the order of 0.1-1 bar) than that of the main driving force – tectonic stress (Prejean and Hill, 2009). Nevertheless, finally, this weak interaction may invoke the phenomenon of synchronization, at least, the so called phase synchronization – PS (Rosenblum et al., 1996; 1997). It is evident that these phenomena cannot be understood in the framework of traditional linear approach and that such high sensitivity to weak impact imply essentially nonlinear interactions (Kantz and Schreiber, 1997).

Experimental set up.

Experimental set up in synchronization experiments represents a system of two horizontally oriented plates of the same roughly finished basalt. The supporting and the slipping basalt blocks were saw-cut and roughly finished. The height of surface protuberances was in the range of 0.1-0.2 mm.

A constant pulling force F_p of the order of 10 N was applied to the upper (sliding) plate; in addition, the same plate was subjected to periodic mechanical or electric perturbations (forcing) with variable frequency (from 10 to 120 Hz) and amplitude (from 0 to 1000 V in case of EM forcing or applying from 0 to 5 V to mechanical vibrator in case of mechanical forcing). Mechanical pull from both these forcing were much weaker compared to the pulling force of the spring; the electric field was normal to the sliding plane.



Fig.1. The scheme of laboratory installation for studying stick-slip synchronization.

Slip events in synchronization experiments were registered as acoustic bursts by the sound card of PC. The scheme of installation is presented in Fig. 1. Details of the setup and technique are given in (Chelidze et al., 2002; Chelidze and Lursmanashvili, 2003; Chelidze and Varamashvili, 2010). In order to pick phases of AE signals' relative to forcing phase onsets more precisely, a special package was developed for reducing the level of ambient noise (Zhukova et al., 2013): the result is shown in Fig.2.

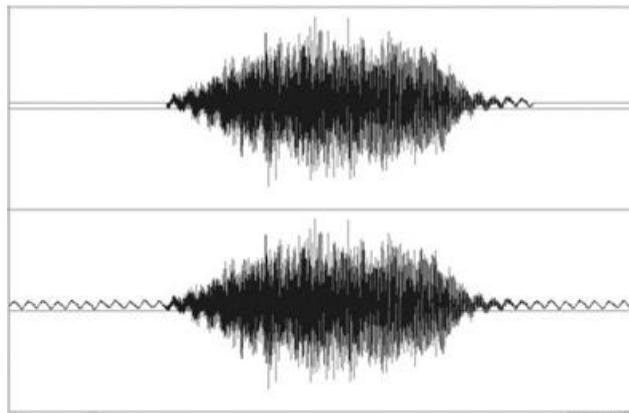


Fig. 2. Filtered (up) and original unfiltered (down) records of AE signal during stick-slip.

Synchronization parameters.

Synchronization of oscillating autonomous system of natural frequency ω_0 by forcing frequency ω results in modification of systems' natural frequency ω_0 to the so called observed frequency Ω .

In our experiments the following parameters were varied: i) the stiffness of the spring, K_s ; ii) the frequency, f of superimposed periodical perturbation; iii) the amplitude of the external excitation or forcing (here voltage V_a is applied to electrodes in case of electromagnetic forcing or voltage V applied to mechanical vibrator in case of mechanical forcing); iv) the velocity of drag, v_d ; v) the normal (nominal) stress σ_n .

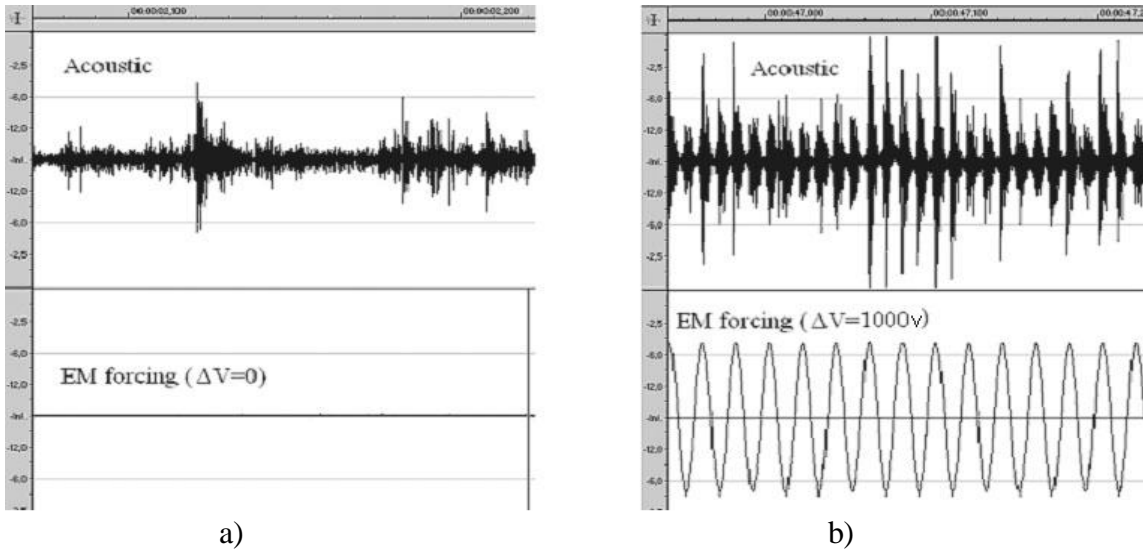


Fig. 3. The upper traces record AE signals generated by slips; the lower channel records EM forcing; a) – non synchronized and b) - synchronized (expanded) stick-slip process. The vertical axis shows the intensity of signal in dB and horizontal axis shows the time.

Synchronization at electromagnetic forcing - Arnold's tongue.

The example of synchronized and non-synchronized stick-slip at electromagnetic (EM) forcing are shown in Fig. 3.

Synchronization was observed only at some definite sets of parameters (K_s , f , V_a). The “phase diagram” for variables f , and V_a or so-called Arnold's tongue (see Pikovsky et al., 2003) is presented in the Fig. 4.

The minimum forcing intensity needed for a strong synchronization corresponds to the forcing frequencies 60-80 Hz.

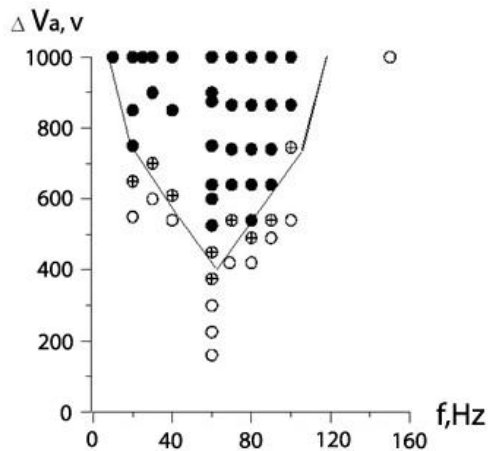


Fig. 4. Stick-slip synchronization area (Arnold's tongue) for various intensities (V_a) and frequencies (f) of the external periodic EM forcing. Filled circles – strong, circles with crosses – intermittent and empty circles – absence of synchronization.

Synchronization affects not only waiting times, but also frequency-energy distribution. Decrease of contribution of extreme events at synchronization is confirmed by calculation of the coefficient of variation CV (CV=standard deviation/mean). As it is shown in Fig.5, the extent of the deviation from the mean value of released AE power calculated for consecutive sliding windows, decreases at synchronization. That means that synchronization limits the energy release associated with individual AE events (quantization effect).

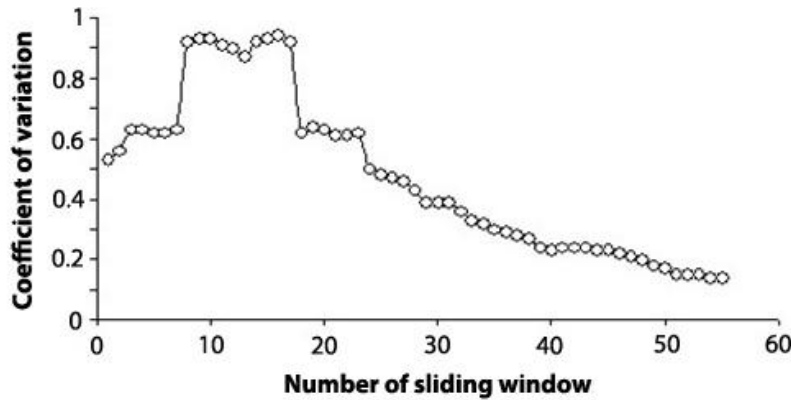


Fig. 5. Coefficient of variation of power of acoustic emission time series at increased external forcing for 500 data length sliding window with 50 data shift. The first 20 windows correspond to no or very weak forcing; windows from 50 to 56 correspond to maximal forcing.

Synchronization by mechanical forcing.

Relatively weak mechanical periodic perturbations also imposes some ordering on the slip, namely a phase synchronization. Mechanical forcing was realized by the vibrator “CB-5” for normal directed forcing and by “CB-20” for tangential directed forcing. The intensity of mechanical vibration was regulated by the voltage applied to the vibrator.

In our experiments with mechanical forcing as a rule the high order phase synchronization was observed, namely, the triggered slip occurred only after several tens of forcing periods. High-order synchronization (HOS) means that the forcing (ω) and observed (Ω) frequencies in the system are related to each other by some winding ratio ($n \div m$) that is $n\omega = m\Omega$ (Chelidze et al., 2010a, 2010b). The winding ratio $n \div m$ at mechanical forcing was in the range 80:1 to 200:1, depending on the experimental conditions.

The experiments with mechanical forcing were carried out at following parameters: the stiffness of the spring, $K_s = 78.4$ N/m, 235.2 N/m and 1705.2 N/m; the voltage at vibrator was 0.5 V, 1 V, 1.5 V, 2 V, 3 V; the frequency of forcing was varied in the range 10-120 Hz (Chelidze et al., 2005; 2013).

In order to assess the strength of phase synchronization phase differences between the phase of periodic forcing signal and the onset of AE burst was picked out and the plots of probability density functions (PDF) of number of AE signals at certain phases of forcing (in bins of period) were constructed (Figs. 6- 12).

Figs. 6 - 12 shows PDF-s obtained for spring stiffnesses 78.4 N/m, 235.2 N/m, 1705.2 N/m and forcing frequencies 10 Hz, 20 Hz 50 Hz, 80 Hz and 120 Hz at various intensities of forcing (frequency of sensor was 20 Hz).

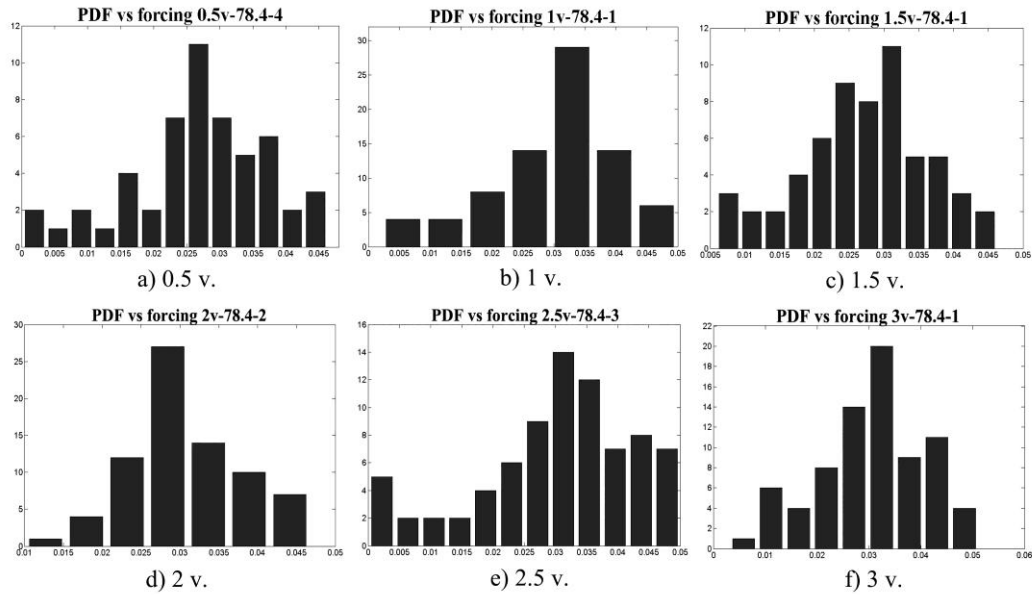


Fig. 6. PDF of number of AE signals at certain phases of forcing (in bins of period) for the stiffness of the spring $K_s = 78.4$ N/m and forcing frequency 20 Hz, which is also a natural frequency of the sensor used. Synchronization at forcing: (a) 0.5 V; (b) 1V; (c) 1.5 V; (d) 2 V; (e) 2.5 V; f) 3 V.

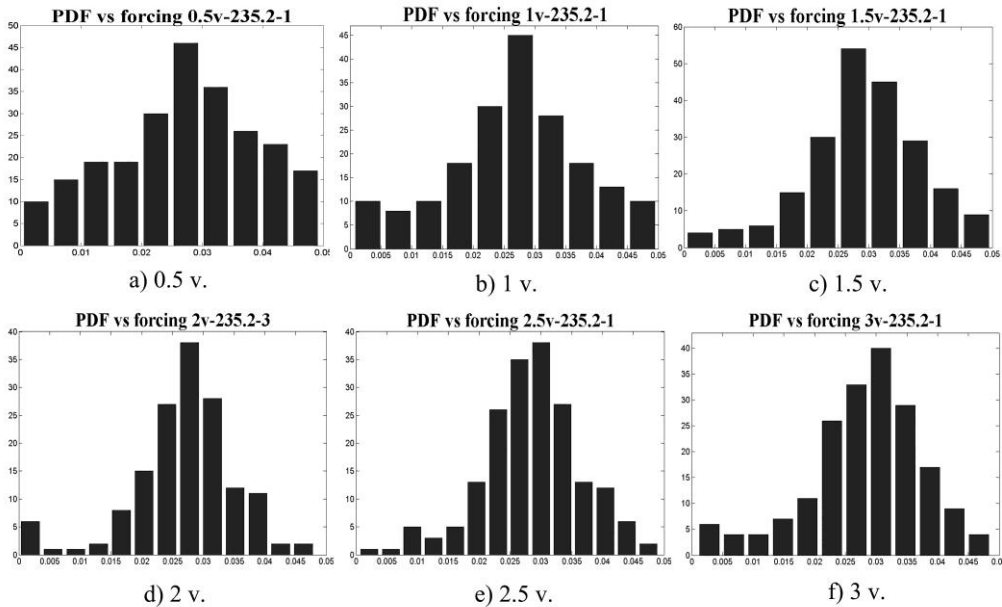


Fig. 7. PDF of number of AE signals at certain phases of forcing (in bins of period) for the stiffness of the spring $K_s = 235.2$ N/m and forcing frequency 20 Hz, which is also a natural frequency of the sensor used. Synchronization at forcing: (a) 0.5 V; (b) 1V; (c) 1.5 V; (d) 2 V; (e) 2.5 V; f) 3 V.

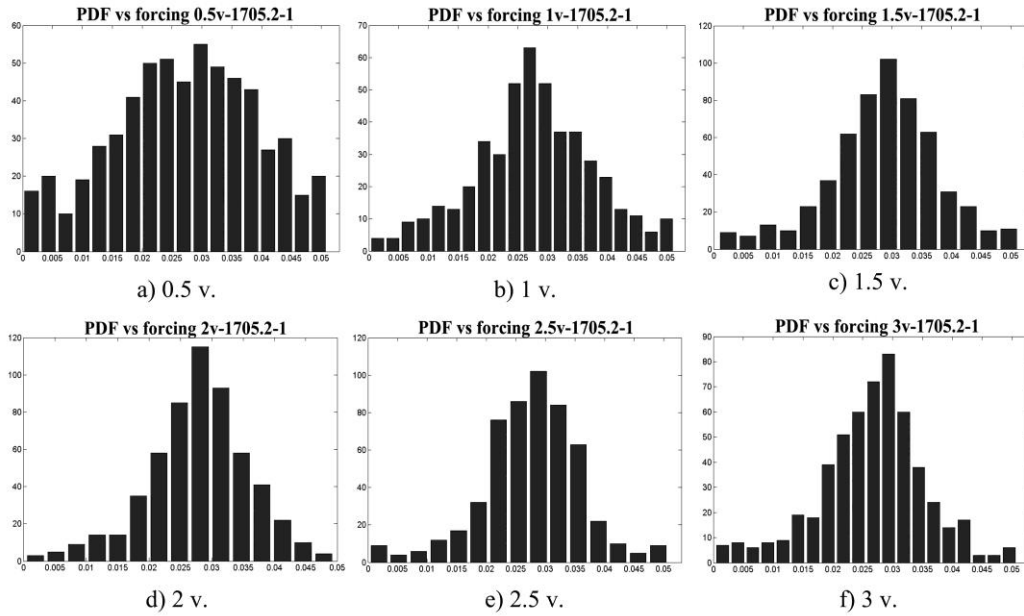


Fig. 8. PDF of number of AE signals at certain phases of forcing (in bins of period) for the stiffness of the spring $K_s = 1705.2$ N/m and forcing frequency 20 Hz, which is also a natural frequency of the sensor used. Synchronization at forcing: (a) 0.5 V; (b) 1V; (c) 1.5 V; (d) 2 V; (e) 2.5 V; f) 3 V.

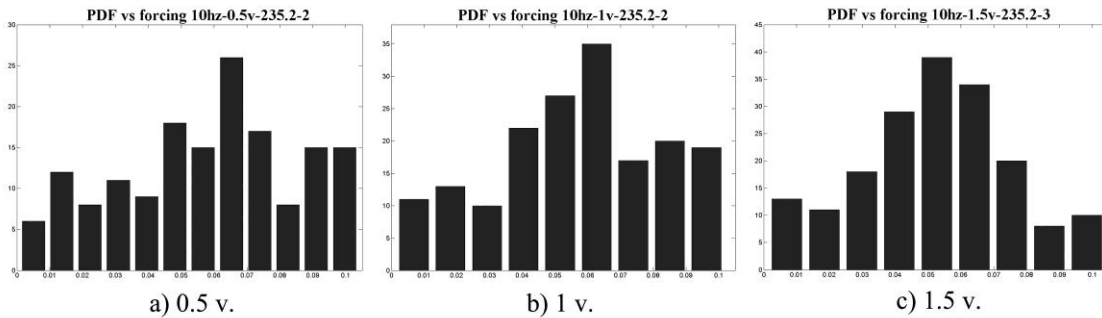


Fig. 9. PDF of number of AE signals at certain phases of forcing (in bins of period) for the stiffness of the spring $K_s = 235.2$ N/m and forcing frequency 10 Hz (natural frequency of sensor 20 Hz). Synchronization at forcing: 0.5 V (a); 1V (b); 1.5 V (c).

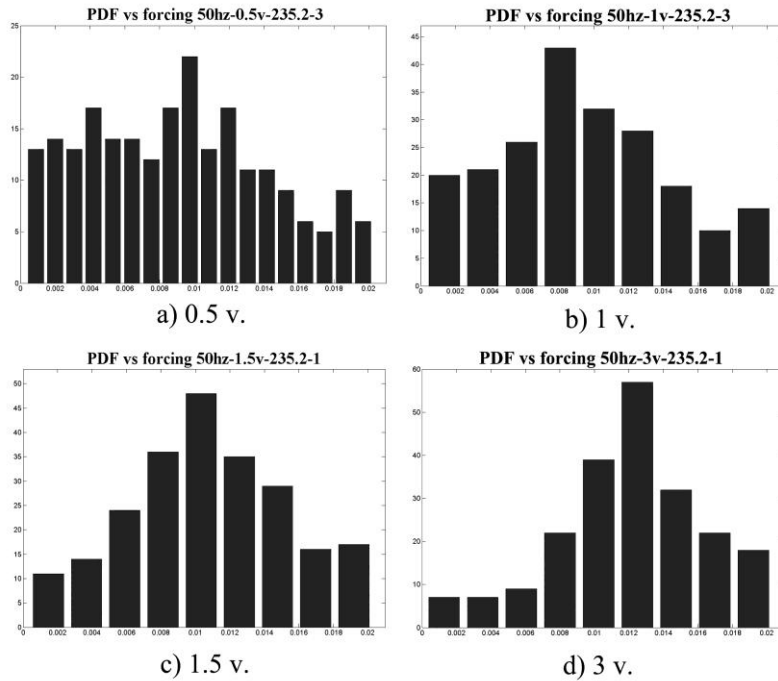


Fig. 10. PDF of number of AE signals at certain phases of forcing (in bins of period) for the stiffness of the spring $K_s = 235.2$ N/m and forcing frequency 50 Hz (natural frequency of sensor 20 Hz). Synchronization at forcing: 0.5 V (a); 1V (b); 1.5 V (c); 3 V (d).

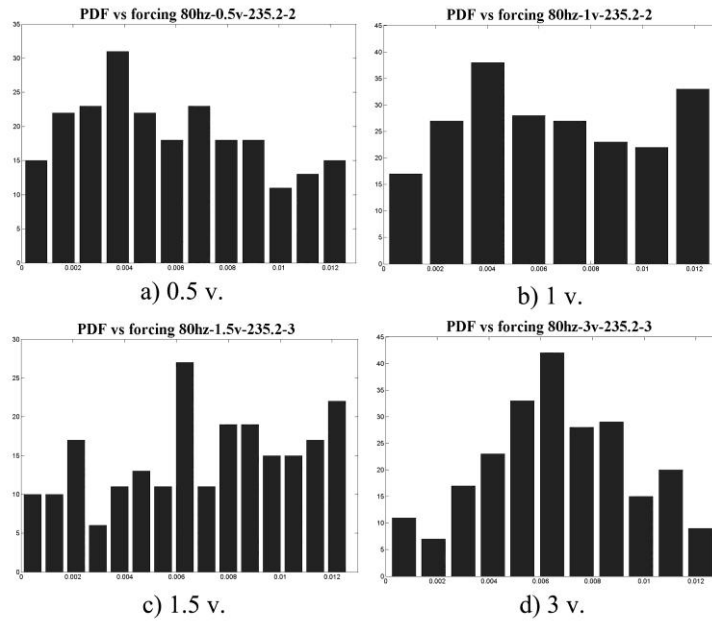


Fig. 11. PDF of number of AE signals at certain phases of forcing (in bins of period) for the stiffness of the spring $K_s = 235.2$ N/m and forcing frequency 80 Hz (natural frequency of sensor 20 Hz). Synchronization at forcing: 0.5 V (a); 1V (b); 1.5 V (c); 3 V (d).

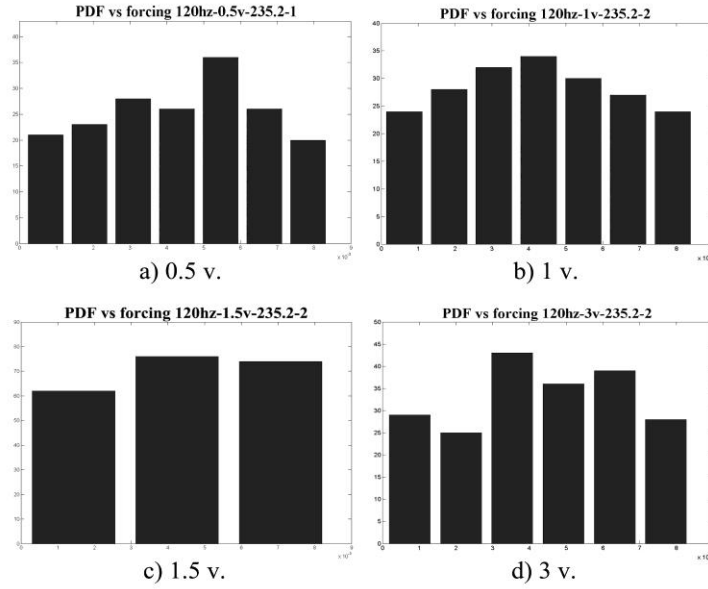


Fig. 12. PDF of number of AE signals at certain phases of forcing (in bins of period) for the stiffness of the spring $K_s = 235.2$ N/m and forcing frequency 120 Hz (natural frequency of sensor 20 Hz). Synchronization at forcing: 0.5 V (a); 1V (b); 1.5 V (c); 3 V (d).

Arnold's tongue for mechanical forcing.

For randomly distributed AE signals such PDF plots are almost flat and for increased strength of synchronization are bell curve like with the half-width ($W/2$) depending on the synchronization strength.

The data obtained allow construction of phase space plot of synchronization strength dependence on intensity and frequency of forcing or Arnold's plot (Fig.13). Here synchronization strength is assessed visually from PDFs in Fig. 7, Figs. 9-12 for spring stiffness $K_s = 235.2$ N/m. Hollow rings mean absence, rings with crosses – moderate and filled rings – good synchronization.

The minimum forcing intensity needed for a strong mechanical synchronization corresponds to the forcing frequencies 40-50 Hz, which is close enough to the optimal forcing frequencies at EM synchronization – 60 Hz (Fig. 4). The filled dots correspond to good synchronization, hollow dots – to absence and dots with crosses – to moderate synchronization.

We guess that the similarity in optimal forcing frequencies can be related to the identity of configuration of sliding and fixed blocks of basalt as well as to closeness of other stick-slip parameters (spring stiffness, drag velocity etc) in both EM and mechanical synchronization experiments.

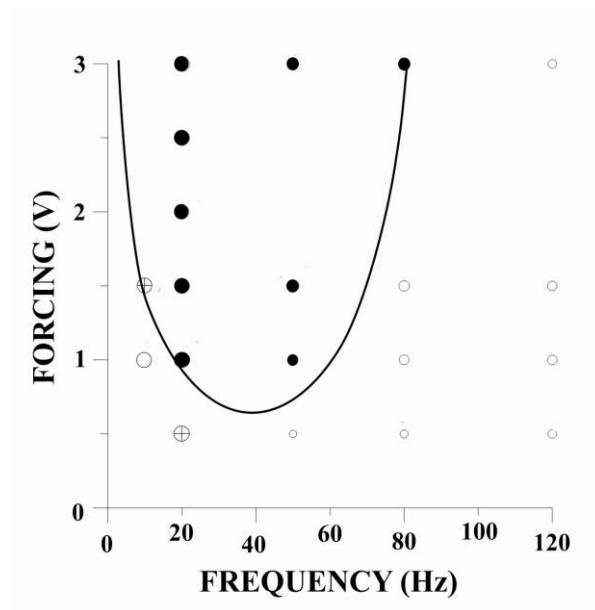


Fig.13. Phase space plot of synchronization strength dependence on intensity and frequency of forcing or Arnold's plot. Synchronization strength was assessed visually from PDFs in Figs.9-12 for the spring stiffness $K_s=235.2$ N/m. Hollow dots mean absence, dots with crosses – moderate and filled dots – good synchronization.

Conclusions

In the paper, the results of laboratory experiments on the mechanical or electromagnetic synchronization of mechanical instability (slip) of a slider-spring system are presented. Slip events were recorded as acoustic emission bursts. The data allow delineating approximately of the synchronization regions (Arnold's tongues) in the plot of forcing intensity versus forcing frequency for both mechanical and electromagnetic synchronization.

The minimum forcing intensity needed for a strong mechanical synchronization is close enough to the optimal forcing frequencies at EM synchronization. We guess that the similarity in optimal forcing frequencies can be related to the identity of configuration of sliding and fixed blocks of basalt as well as to closeness of other stick-slip parameters (spring stiffness, drag velocity etc) in both EM and mechanical synchronization experiments.

Acknowledgements

Authors acknowledge the grant of the Shota Rustaveli National Science Foundation of Georgia (Project 31/31 - "FR/567/9-140/12").

References

1. Chelidze, T., Varamashvili, N., Devidze, M., Tchelidze, Z., Chikhladze, V., Matcharashvili, T., 2002. Laboratory Study of Electromagnetic Initiation of Slip. *Annals of Geophysics*, 45, 587-599.
2. Chelidze, T., Lursmanashvili, O., 2003. Electromagnetic and mechanical control of slip: laboratory experiments with slider system. *Nonlinear Processes in Geophysics*, 20, 1-8.
3. Chelidze T., Matcharashvili, T., Gogiashvili, J., Lursmanashvili, O, Devidze, M., 2005. Phase synchronization of slip in laboratory slider system. *Nonlinear Processes in Geophysics*, 12, 1-8.
4. Chelidze, T., Lursmanashvili, O., Matcharashvili, T., Varamashvili, N., Zhukova, N., Meparidze, E., 2010. High order synchronization of stick-slip process: experiments on spring-slider system. *Nonlinear Dynamics*, DOI 10.1007/s11071-009-9536-6. **a**.
5. [Chelidze, T.](#), [Matcharashvili, T.](#), [Lursmanashvili, O.](#), [Varamashvili, N.](#), and [Zhukova, N.](#), Meparidze, E., 2010. [Triggering and Synchronization of Stick-Slip: Experiments on Spring-Slider System](#). in: *Geoplanet: Earth and Planetary Sciences*, Volume 1, 2010, DOI: 10.1007/978-3-642-12300-9; Synchronization and Triggering: from Fracture to Earthquake Processes. [Eds.V.de Rubeis, Z. Czechowski](#) and [R. Teisseyre](#), pp.123-164. **b**.
6. [Chelidze, T.](#), and [Varamashvili, N.](#), 2010. [Models of Stick-Slip Motion: Impact of Periodic Forcing](#); in: *Geoplanet: Earth and Planetary Sciences*, Volume 1, 2010, DOI: 10.1007/978-3-642-12300-9; Synchronization and Triggering: from Fracture to Earthquake Processes. [Eds.V.de Rubeis, Z. Czechowski](#) and [R. Teisseyre](#), pp. 23-33.
7. Chelidze, T., and Matcharashvili, T., 2013. Triggering and Synchronization of Seismicity: Laboratory and Field Data - a Review. In: *Earthquakes – Triggers, Environmental Impact and Potential Hazards*. (Ed. K. Konstantinou), Nova Science Pub.
8. Kantz, H., Schreiber T., 1997. *Nonlinear time series analysis*. Cambridge University Press, Cambridge.
9. Pikovsky, A., Rosenblum, M. G., Kurths. J., 2003. *Synchronization: Universal Concept in Nonlinear Science*. Cambridge University Press, Cambridge.
10. Prejean, S., Hill, D., 2009. Dynamic triggering of Earthquakes. In: *Encyclopedia of Complexity and Systems Science*, R. A. Meyers (Ed.), Springer, pp. 2600-2621.
11. Rosenblum, M. G., Pikovsky, A., Kurths, J., 1996. Phase synchronization of chaotic oscillators. *Phys. Rev. Lett.*, 76, 1804-1808.
12. Rosenblum, M.G., Pikovsky, A., Kurths. J., 1997. Effect of phase synchronization in driven chaotic oscillators. *IEEE Trans. CAS-I*, 44. 874-881.
13. Zhukova, N., Chelidze, T., Matcharashvili, T., 2013. Automatic onset time picking of acoustic signals. *Journal of Georgian Geophysical Society*, Issue (A), *Physics of Solid Earth*, v.16a, 2013, pp.115-119.

არნოლდის ენები არათანაბარი ხახუნის (Stick-slip) ელექტრომაგნიტური და მექანიკური სინქრონიზაციის დროს

თ. ჭელიძე, ე. მეფარიძე, დ. ტეფნაძე

რეზიუმე

სინქრონიზაციის მოვლენები შეინიშნება სხვადასხვა პროცესებში, როგორცაა მექანიკის, ბიოლოგიური და სოციალური. აქედან გამომდინარე, ბუნებრივია, რომ სინქრონიზაცია აღინიშნება მრავალ გეოფიზიკურ სფეროში, რადგან დედამიწა

განიცდის სხვადასხვა წარმოშობის საკმაოდ ფართო დიაპაზონის სიხშირეების რხევითი (რამდენიმე წამიდან რამდენიმე თვემდე და წლამდე) პროცესების ზემოქმედებას (ე.წ. ფორსინგს). ასეთი მასშტაბური ბუნებრივი პროცესები შეიძლება იყოს მოდელირებადი ლაბორატორიულ პირობებში.

აღნიშნულ ნაშრომში წარმოდგენილია ლაბორატორიული ცდები მექანიკური არამდგრადობის სინქრონიზაცია ელექტრომაგნიტური და მექანიკური პერიოდული ფორსინგის პირობებში. მექანიკური არამდგრადობის მოვლენები ჩაწერილი იქნა აკუსტიკური ემისიის სახით. გრაფიკებზე გამოსახულია სინქრონიზაციის დონის დამოკიდებულება მექანიკური და ელექტრომაგნიტური პერიოდული ფორსინგის ინტენსივობასა და სიხშირეზე (ე.წ. არნოლდის ენები).

Языки Арнольда при электромагнитной и механической синхронизации (Stick-slip)

Т. Челидзе, Е. Мепаридзе, Д. Тепнадзе

Резюме

Явление синхронизации встречается в различных процессах, в механике, биологических и социальных процессах. Таким образом, вполне естественно, что синхронизация наблюдается во многих геофизических сферах, поскольку Земля находится под влиянием колебательных процессов (форсинга) различного происхождения с чрезвычайно широким диапазоном частот, от нескольких секунд до нескольких месяцев и лет. Такие крупномасштабные природные процессы могут быть смоделированы в лабораторных условиях.

В данной работе представлены результаты лабораторных экспериментов при механической и электромагнитной синхронизации неустойчивом трении (стик-слипе) системы. Механические неустойчивости были записаны как всплески акустической эмиссии. Данные позволяют приблизительно ограничивать области синхронизации (языки Арнольда) на графике интенсивность форсинга-частота форсинга при механической и электромагнитной синхронизации.

Preliminary result of stable isotopes monitoring in the Alazani-Iori catchment

¹George Melikadze, ¹Natalia Jukova, ¹Mariam Todadze, ¹Sopio Vepkhvadze, ¹Nino Kpanadze, ¹Alexandre Chankvetadze, ¹Tamar Jimsheladze, ²Ramaz Chitanava

¹Iv. Javakhishvili Tbilisi State University, M. Nodia Institute of Geophysics

²National Environmental Agency of Ministry of Environmental and Natural Resource Protection of Georgia

Abstract

In order to static stable isotopes variation has selected please and organized GNIP and GNIR station on the territory Alazani-Iori catchment. In order to investigate underground water systems in Alazani-Iori catchment, for the first time have been conducted studies based on the hydrochemical and environmental isotope methods. The first step was to organize the monitoring of air temperature, humidity and precipitation on the recharge and discharge areas of aquifer. Also have been organized monitoring of water level and discharge on Alazan and Iori rivers as well as monitoring of underground water level in Lagodekhi and Dedoplistskaro. The results of isotope data analyze clearly shows the seasonal variations. Their composition changes according to the elevation and geographical location of observation stations, which is fully consistent with the regularities of isotope distribution all over the world.

Introduction

Global warming will have negative effect on natural conditions of Georgia. These negative effects could be the most serious in Eastern Georgia, especially in the basin area of the Iori river, which is famous for clearly depicted characteristics of arid-zone and semi-desert. Geomorphologically this is Uplands of Kakheti, which includes: Big and Small Shiraki, Eldari, Taribani, Natbeuri, Naomari, Ole, Jeiran-Choli valleys and their watersheds, as well as majority of Southern slope of Kakheti mountain range, i.e. 3000 km² area of Dedoplistskaro and partially Sagarejo and Gurjaani administrative regions. Preliminary meteorological data show that precipitation has significantly decreased in this region, which caused significant decrease and in some places even drying of surface water flows and depletion of underground water natural springs. Significant decrease of groundwater tables resulted in aeration and exhaustion of soil crust, activation of wind erosion and reduction of areas covered by vegetation (including pastures). Hence, there is a distinct tendency of processes actively leading to desert formation. All these negative ecological events led to deterioration of population's social-economic conditions. It can be expected that the situation will become even worse since the population is already experiencing deficit of potable and irrigation water. As the negative ecological processes become stronger, desert formation can easily turn into irreversible form. Thus, the most promising region for agricultural products, such as crops, cattle-breeding and vine-growing and for developing oil and gas extraction can be left without population.

Understanding the groundwater regime, interactions with surface waters and factors which influence groundwater quantity and quality is therefore of utmost importance to secure water supply for the economy and population.

Besides the traditional methods of hydrogeological survey such as pumping tests, geophysics, geochemistry and groundwater flow modeling, environmental isotopes as water tracers provide useful complementary information on water origin (where does the water come from) and history (which pathways did the water move until it arrived to an aquifer). Chemical and isotopic composition of surface waters and groundwater is determined by the composition of rainfall and modified by the processes in the vadose zone, snow cover, tributaries and aquifers. These modifications are different in various climatic settings and result in different pathways of water from rainfall to runoff and groundwater recharge.

In order to study isotope distribution on the some territory at first is necessary to know its background value in precipitation and surface water. International Atomic Energy Agency IAEA organized regular sampling and analysis of oxygen and hydrogen (^{18}O , ^2H ,) isotopes in surface water-Global Network Isotope in River (GNIR) and precipitation Global Network Isotope in Precipitation (GNIP). This network is becoming common in many countries of World as part of national meteorological, geological and hydrological services. Independent network was organizing in Switzerland or in the USA. This kind of investigation is new and start in the Georgia only now.

In order to definition of hydrogeological, hydrogeochemical and isotope regimes has been planned the organization of multi-disciplinary monitoring in Alazanis-Iori catchment basins in the framework of Rustaveli National Science Foundation Grant.

Field observations

According project goal has selected please and organized GNIP and GNIR station on the territory of Kakhetia. On the first stage, the regime observation of air temperature, humidity, atmospheric pressure and precipitation at the meteorological stations since 2013 had been organized in the recharge areas of aquifers, which are located evenly throughout of all territory of area and characterize the following regions: Tianeti – recharge area of river Iori, Telavmdinare – the upper part of Alazani river, Lagodekhi – the recharge area of left tributaries of Alazani river and Dedoplistskaro – River Iori and the lower part of Alazani river (1).

The parameters were measured daily at the mentioned meteorological stations. Air temperature and humidity were measured by the specialized equipment (HOBO). In addition, the atmospheric precipitation is measured daily and also, in order to determine the stable isotope composition, the sampling takes place once per month. Their Station has been included in network GNIP of IAEA.

In order to determine the water level variations in rivers, the observations has been organized at the groundwater discharge areas, namely on the river Iori in Tianeti and in Alazani river at village Shaqriani (Telavi district). Also, the water sampling has been started for stable isotope analyzes from the mentioned rivers. The stations have been joined to the global network GNIR of IAEA.

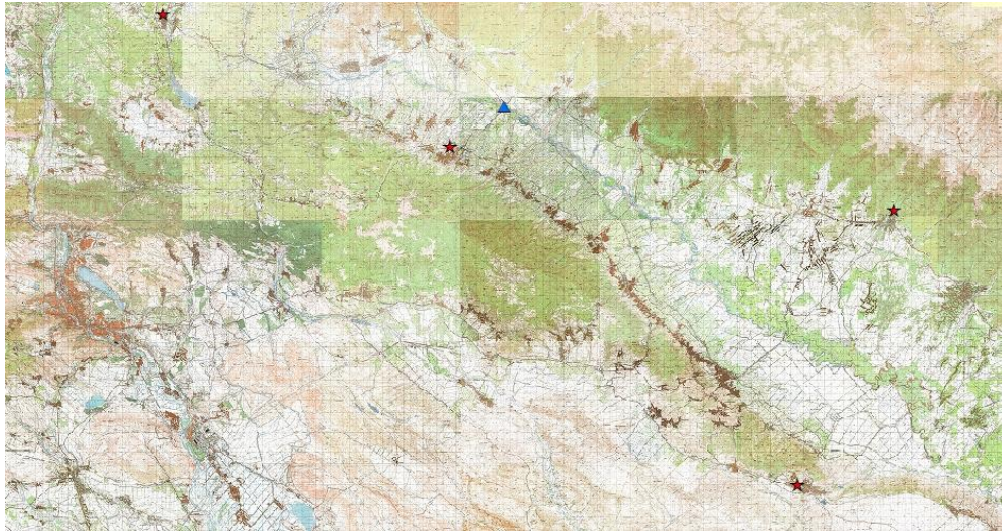


Fig 1. The location of GNIP and GNIR stations

The Isotope and hydrochemical analyze of Water samples have been done with the equipment laser spectrometer “Picarro”, purchased by Agency at the laboratory of Geophysics and Geothermal research Center, Institute of Geophysics.

In order to determine the underground water regime in the main aquifers of Alazani and Iori catchments, the hydrodynamic observations have been organized. The monitoring was started on the borehole, located in Lagodekhi district. The equipment, (produced in the USA) provides the data logging and transfer to the center in Tbilisi by GSM system. Water level in borehole, air temperature and atmospheric pressure is measured in a minute regime.

The observations have also been organized at “Dedoplistskaro” – the “Diver” was installed in the wall. Water level and temperature is measured hourly. Data transfer occurs once per month or two via laptop. It is planned to increase the number of observed parameters in future.

The data is collected at the center by the required frequency. Also, data processing occurs at the center and the influence of seasonal and other factors are analyzed.

Database creation and analysis

In order to fulfill the objectives of the Project, the database was created, which is consistently updated by the meteorological, hydrogeological and hydrological data. Only the primary analysis of Isotope data showed the seasonal variations. In the monthly Precipitation isotope variations are observed from “Telavi” meteorological station. In particular, the Spring fraction is light (-10 ‰ -180; -80 ‰ -2H), which becomes heavier in summer (-4 ‰ 180; -20 ‰ -2H) and in winter period it is reduced again (-15 ‰ -180; -80 ‰; -120H Before). The peak of the “weighting” is marked on almost perfect curve, which is related to the autumn rainy season (fig. 2).

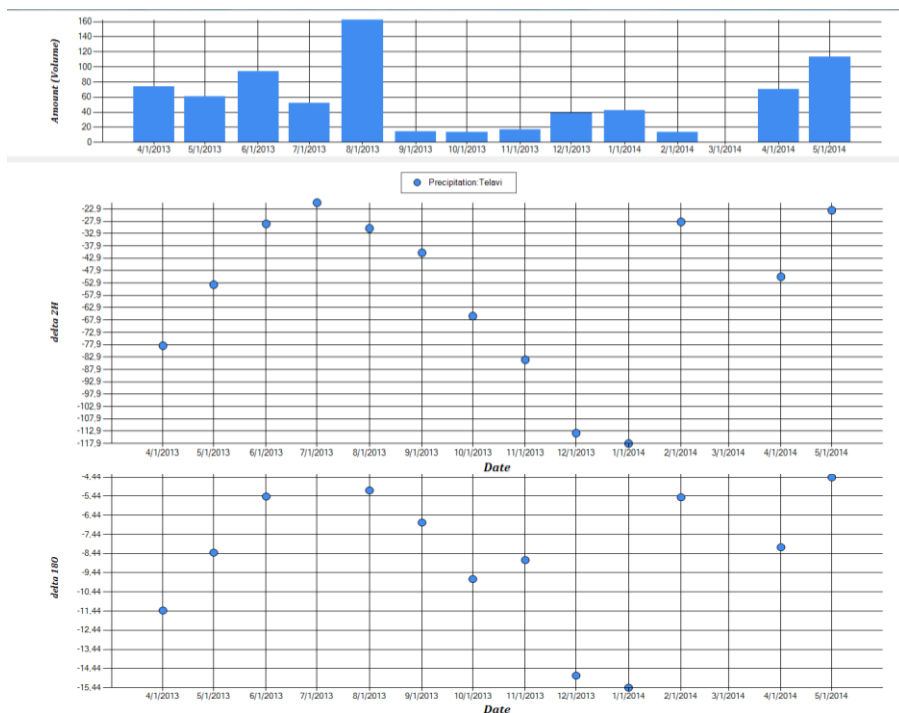


Fig.2 Stable isotope variations in precipitation, “Telavi” station

We get a different picture of the nearby located "Shakriani" Station on the River Alazani" samples (Fig. # 3). The isotopes "Winter" values (-9.2 ‰ - 18O; -60 ‰ -2H) are getting "lighter" in May, which is caused by the mixing of mountain snow melt water into the river (-10 ‰ - 18O; -68 ‰ - 2H), in June-August, the isotopic composition becomes again "heavier", however, it does not fully repeat the Isotope values of atmospheric precipitation curve of nearby located "Telavi" station, because in this case the isotopic composition of river water characterizes the more area from the beginning of Alazani river down to its middle part. The “heavy” peak of rainy season in October and also in January 2014, the peak of getting “lighter” caused by snowfall (10.5 - ‰ - 18O; -72 ‰ - 2H) is observed on the curve.

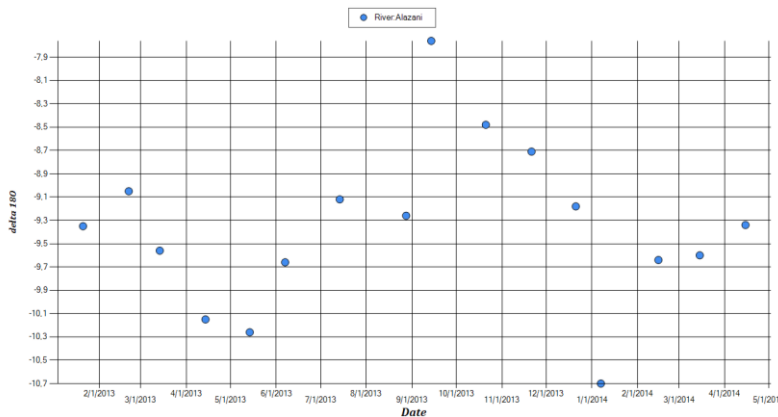


Fig. 3 Stable isotope variation in river Alazani; “Alazani-Shaqriani” station

We have different picture of Isotopic composition in precipitations in samples collected at “Tianeti” meteorological station. Sharply expressed “lightness” of isotope composition (10 - ‰ - 18O; -68 ‰ -2H) in March-April 2013, during the snow melting period (Fig.#4).

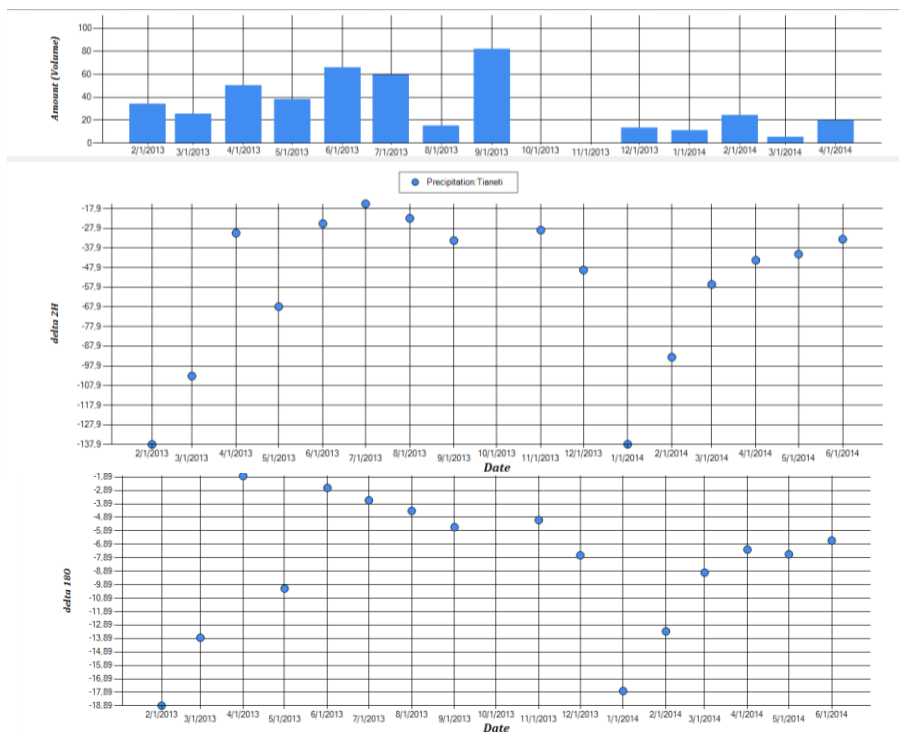


Fig. 4 Stable isotopes Changes in atmospheric precipitation curve; “Tianshi” station

Like previous case, in the precipitation samples from “Dedoplistskaro” station, we observe that isotopes become “lighter” in spring (Figure 5).

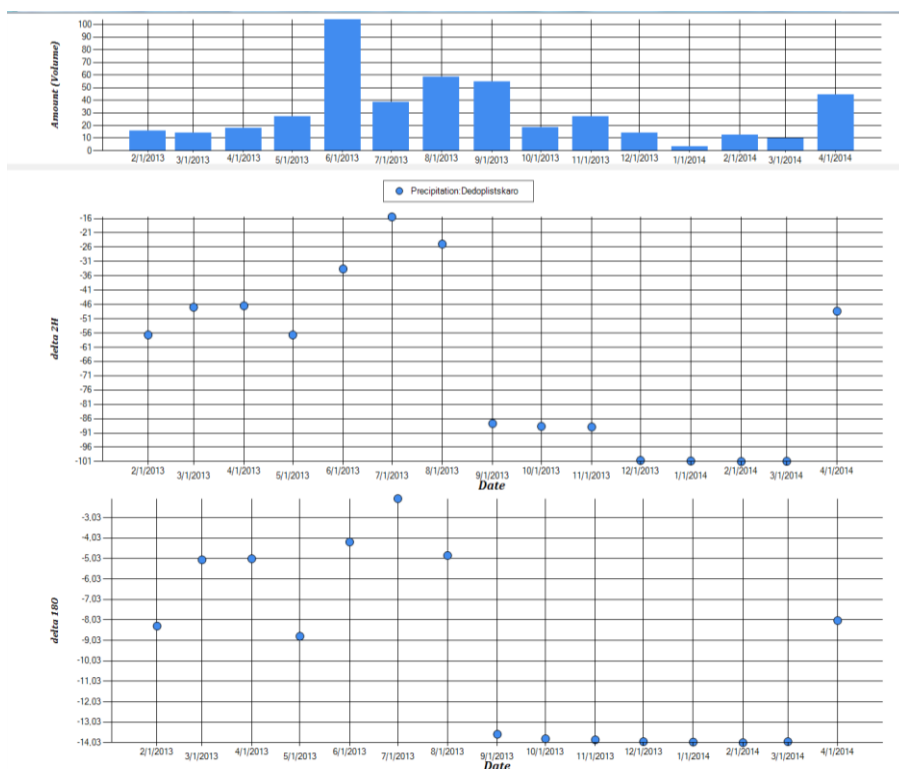


Fig. 5 Stable isotope variation in precipitation curve; “Dedoplistskaro” station

Comparing the Values of isotope composition and character of their variation, the differences between of geographical location and altitude of observation stations should be taken into account. Overall, on "Tianeti" station, the isotope composition variation in "lighter"- less range (-14 - (- 18) ‰ - 18O; -100 - (- 140) ‰ - 2H) has been observed during one year. On the "Telavi" station, which is located southwest and at lower elevation, accordingly we observed "heavier" changes: -11 - (- 16) ‰ - 18O; -80 - (- 120) ‰ - 2H). There are much "heavier" isotope values on "Dedoplistskaro" meteorological station, which is actually located on the semi-desert zone: -5 - (- 8.8) ‰ - 18O; -55 - (- 85) ‰ - 2H)

The isotope composition of river waters is "heavier" then in precipitations. In accordance to the changes of geographical location of observation station, the isotope values of the rivers also changes. In particular, the samples taken from the river "Iori" at "Tianeti" station, isotope composition variation is is -10 - (- 11) ‰ - 18O; -66 - (- 68) ‰ - 2H, which is much "heavier" then values in precipitation at "Tianeti" meteorological station (-14 - (- 18) ‰ - 18O; -100 - (- 140) ‰ - 2H) and at the same time slightly "lighter" than values from "Alazani-Shaqriani" station (-9 - (- 11) ‰ - 18O; -60 - (-70) ‰ - 2H). The Alazani river samples, at "Shaqriani" station, the measured isotope composition is much "heavier" than observed values in precipitation samples at "Telavi" station values (-11 - (- 16) ‰ - 18O; -80 - (- 120) ‰ - 2H).

Conclusions

For the first time on territory of Kakheti have been organized GNIP and GNIR stations in order to study the Stable isotope variations. Fixed up to date revealed regularities, which fully agree with the general regularities of Stable isotope distribution on the World. The continuing of mentioned studies will give us possibility to determine the background value of isotope distribution for this area (global meteoric waterline -GMW L), which is necessary condition for the Hydrological and hydrogeological investigation.

Acknowledgments: The authors thank the Rustaveli National Scientific foundation for financial support of the project #31/27 "Environmental Isotopes Testing in Alazani-Iori Catchments (East Georgia) For Provision of Sustainable Use of Groundwater Resources".

References

1. George Melikadze and all. Assessment aquifer of Alazani-Iori value using stable isotope application, Conference 80 years of the M. Nodia Institute of Geophysics, 2014.

(Received in final form 10 September 2014)

Первичные результаты мониторинга стабильных изотопов в Алазани-Иорском водном бассейне

¹Меликадзе Г.И., Жукова Н. Н., Тодадазе М. Ш., Вефхвадзе С. Г., Капанадзе Н. А., Чанкветадзе А. Ш., ¹Кобзев Г.Н., ¹Джимшеладзе Т.А., Читанава Р. Б.

Тбилисский Государственный Университет им. Ив. Джавахишвили, Институт Геофизики

РЕЗЮМЕ

Для изучения стабильных изотопов были выбраны и организованы GNIP и GNIR станции на территории водосбора Алазани-Иори. Для изучения подземных водных систем водосбора Алазани-Иори были предварительно проведены исследования, основанные на гидрохимических и изотопных методах изучения окружающей среды. Первым шагом стала организация мониторинга температуры воздуха, влажности и осадков в областях питания и разгрузки водоносных горизонтов. Было организовано также наблюдение за уровнем воды и водной разгрузкой на реках Алазани и Иори, а также мониторинг за уровнем подземными вод в Лагодехи и Дедоплисцкаро. Результаты изотопного анализа ясно показали наличие сезонных колебаний. Их состав меняется в зависимости от высоты и географического расположения наблюдательных станций, которые полностью соответствует закономерностям распределения изотопов во всем мире.

ალაზანი-იორის წყალშემკრებ აუზებში სტაბილური იზოტოპების მონიტორინგის პირველადი შედეგები

¹გიორგი მელიქაძე, ¹ნატალია ჟუკოვა, ¹მარიამ თოდაძე, ¹სოფიო ვეფხვაძე, ¹ნინო კაპანაძე, ¹ალექსანდრე ჭანკვეტაძე, ¹თამარ ჯიმშელაძე, ²რამაზ ჭითანავა

ივ. ჯავახიშვილის სახ. თბილისის სახელმწიფო უნივერსიტეტი, მ. ნოდიას გეოფიზიკის ინსტიტუტი

საქართველოს გარემოსა და ბუნებრივი რესურსების დაცვის სამინისტრო, გარემოს ეროვნული სააგენტო

რეზიუმე

ალაზანი-იორის წყალშემკრებ აუზებში, მიწისქვეშა წყლებში სტაბილური იზოტოპების ვარიაციების შესწავლის მიზნით შეიქმნა გნიპ და გნირ სარეჟიმო სადგურები და ორგანიზება გაუკეთდა რეჟიმულ დაკვირვებებს. პირველ ეტაპზე, წყალშემცველი ჰორიზონტების კვების და განტვირთვის არეალებში, ორგანიზება

გაუკეთდა რეჟიმულ დაკვირვებებს ჰაერის ტემპერატურასა, ტენიანობასა და ატმოსფერულ ნალექებზე. მდინარე ალაზანსა და იორზე დაიწყო რეჟიმული დაკვირვებები მდინარის დონესა და ხარჯზე და ასევე მიწისქვეშა წყლების დონეებზე ლაგოდებსა და დედოფლისწყაროში. იზოტოპური მასალის ანალიზმა დააფიქსირა სეზონური ვარიაციები მათ ცვლილებაში და განსხვავებები მათ მნიშვნელობებში, სადგურების გეოგრაფიულ მდებარეობისა და სიმაღლის მიხედვით, რაც სრულად ეთანხმება მსოფლიოში იზოტოპების გავრცელების ზოგად კანონზომიერებებს.

SOME METHODS OF ANALYZE GEODYNAMIC IMPACT ON THE DEEP AQUIFARE

George Melikadze , Genadi Kobzev, Tamar Jimsheladze

Iv. Javakhishvili Tbilisi State University, M. Nodia Institute of Geophysics

Abstract

During hydro-geodynamical observation on the territory of Georgia has fixed various anomalies in water level before earthquakes. Revealing of the mechanism of interrelation between the deformation processes, forestall strong earthquakes, and a hydrodynamic variation of underground waters, would allow to explain such preliminary behavior of hydrodynamic effects and to develop scientifically proved methods of the forecast of earthquakes. For a select of a correct method the comparative analysis of various methods of processing has been carried out in view of all possible working factors. One of methods based on the idea, that aquifer property (porosity and conductivity) is changing during the geodynamic strass. According Results during normal period it change according tidal variation and has “background” value, but during the seismic event changed the porosity, as indicator of tectonic activity.

Introduction

From the end of the last century have developed a special network of hydro-geodynamical (water level, Atmosphere pressure and air temperature) observation on the territory of Georgia. 15 deep boreholes located basically on the main geo-structure and open deep aquifers. These wells as sensitive strain meters recorded all kinds of deformation caused by exogenous (atmospheric pressure, tidal variations and season variation), as well as endogenous processes. Observations were carried out using the specialized equipment, providing measurement of deformation up to 10^{-9} degrees (1-3).

During observation have observed various anomalies in water level before earthquakes, besides in most cases, on enough distant places from an epicenter.

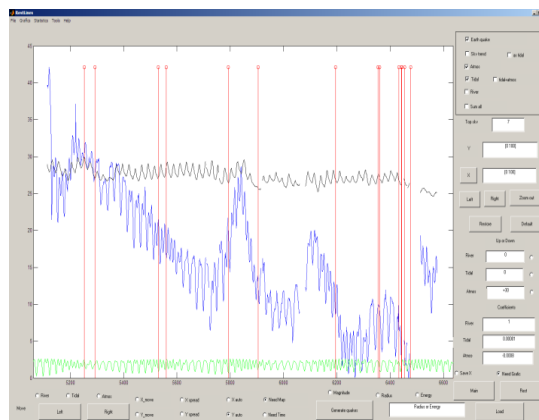


Fig. 1 Graphic of a tidal (the bottom line), an atmospheric pressure (The top line) and the underground water level (an average line) variations in time. Vertical lines show earthquakes having place for this period.

Database creation and analysis

Many scientific works have been dedicated to research of the nature of these anomalies. Despite lacking unequivocal understanding of this process, the hydrodynamic data are admitted as the most informative for the forecast of earthquakes (4-6). Revealing of the mechanism of interrelation between the deformation processes, forestall strong earthquakes, and a hydrodynamic mode of underground waters, would allow to explain such preliminary behavior of hydrodynamic effects and to develop scientifically proved methods of the forecast of earthquakes.

To solve this problem some scientists tried to add here anomalous violation in a hydrodynamic regime with the deformation processes proceeding directly in the epicenter, but could not explain "long-range action" of anomalies (7-9). Others held the opinion, that anomalies are formed directly in aquifer of the borehole and are reaction of water bearing horizon on all kinds of deformation processes, including seismo-generative ones. Therefore in parallel with studying hydrodynamic characteristics of aquifer of the boreholes (porosity, conductivity, etc.), scientists analyzed reaction of water bearing horizon on deformation both endogenous, and the exogenous origins (2-4).

At the analysis of materials, scientists individually selected methods of mathematical statistics, but all of them had one thing in common: after removal of the trend caused by exogenous factors (tidal the variation of the ground and atmospheric pressure), used frequency filters that in our opinion, deforms a required endogenous signal. The residuary values were analyzed for revealing correlation with seismic events.

For a select of a correct method the comparative analysis of various methods of processing has been carried out in view of all possible working factors (1, 2, 3). One of methods based on the idea, that aquifer property (porosity and conductivity) is changing during the geodynamic strass. According investigation of Russian scientists (10) can calculated amount of aquifer porosity by equation:

$$dh = dP / \rho g = \Delta * K_w / (n \rho g)$$

where:

n – porosity;

Δ – amplitude of tidal variation ($3 * 10^{-8}$);

K_w – volume module of elasticity of water ($2.25 * 10^9$ Pa);

ρ – density of water (10^3 kg/m³);

g – acceleration of gravity (9.8 m/s²)

By this equation calculated static value of porosity for Georgian network boreholes. Amount of it are depends from many factors such as depth of a borehole, its design, an originality of a geological and hydro-geological structure water-bearing horizon, value of the gas factor, etc.

Tab. 1 Data of porosity for difference boreholes

Boreholes name	Amplitude of water level reaction on the tidal, cm	Porosity, %
Kobuleti	4	17
Marneuli	7-9	7.6-9.8
Lagodexi	5-7	9.8-13.6
Borjomi70	15-16	4.3-4.5
Borjomi47	12-14	4.9-5.7
Borjomi67	11-12	5.7-6.2
Gori	3	22.9
Nakalakevi	7	9.8

Change of value of porosity will be depends from the strass variation and all geodynamical in fact around aquifer.

In order to fix influence of the tectonic factor on the aquifer, during preparation strong earthquakes, was prepared special program in MatLab area. This program can show porosity amount variation in time. The program gives possibility to show porosity amount variation in time, by comparison of data of tidal and underground water level variations (fig. 2).

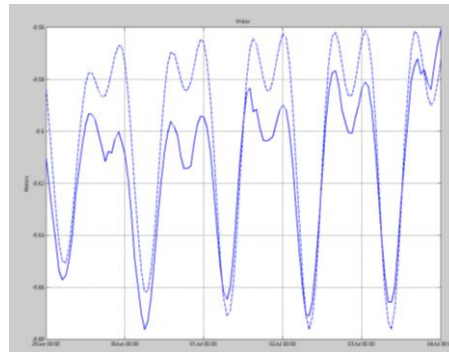


Fig. 2 Tidal (dashed lines) and the underground water level variations on the Marneuli borehole in 2012.

In order calculate value of porosity, has been made the calculation between the water level and the theoretical value of the tidal variations according equation.

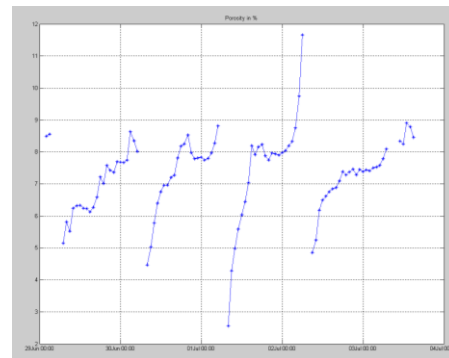
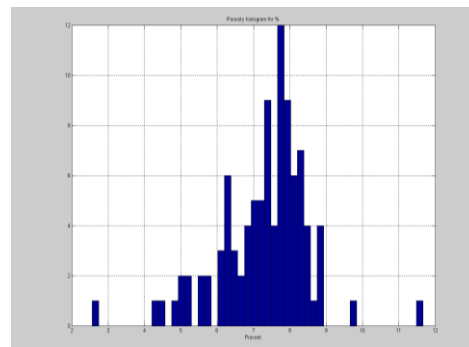


Fig. 3 Variation of Porosity on the borehole Marneuli in 2012.

Porosity value was changed according stress variation caused by tidal influence and has background value. Has been built histogram of variation porosity for this period.



. Fig. 4 Typical histogram of porosity for Marneuli, 2012

Figure show normal distribution of parameter for this period (6-9%).

On the Marneuli boreholes, every minute recorded water level, atmosphere pressure and temperature value. There are observed the significant violation of water level before and during the period of seismic events (fig. 5).

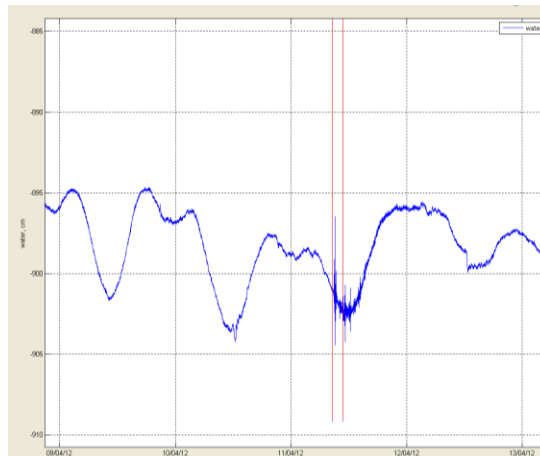


Fig. 5 Variation of water level on the Marneuli boreholes during Sumatra earthquake (11 April 2012)

Period anomalies, porosity value changed compare with background value.

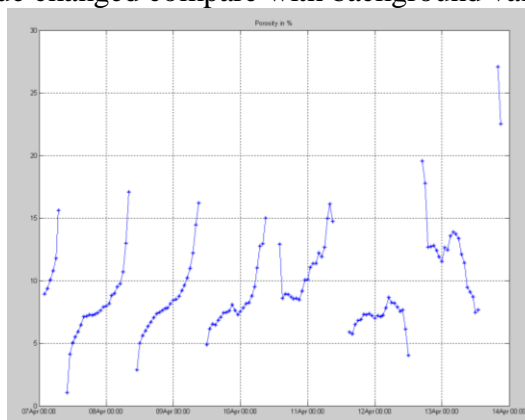


Fig. 6 Variation of porosity value on the Marneuli boreholes during Sumatra earthquake (11 April 2012)

In the Histogram fixed second pick related with anomaly value of porosity. Typical porosity equal 6-9%, after earthquake porosity equal 11-13%

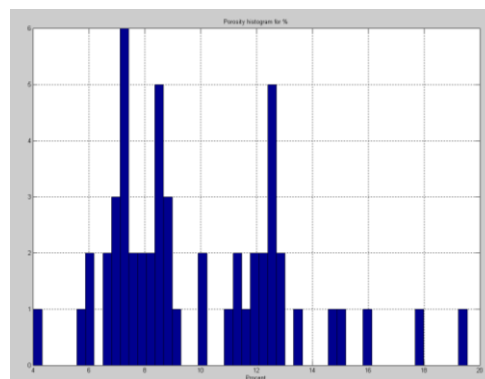


Fig. 7 Histogram of porosity value on the Marneuli boreholes during Sumatra earthquake (11 April 2012)

Conclusions

Results have shown that variation of porosity of aquifer is caused by stress. During normal period it change according tidal variation and has “background” value. Variations during the seismic event demonstrated change of the porosity value above “background” (tidal variation), as indicator of tectonic activity.

Acknowledgments: The authors thank the Rustaveli National Scientific foundation for financial support of the project #156/13 “Spatial and Temporal Variability of Geodynamical Field and Its Influence on the Deep Aquifers and Geomagnetic Field“.

References

1. Bella, Biagi P., Melikadze G. et al. - Anomalies in geophysical and geochemical parameters revealed on the occasion of the Paravani (M=5.6) and Spitak (M=6.9) earthquakes (Caucasus). Amsterdam, Tectonophysics 202 Elsevier Science Publishers B. V.,1992, p.p. 23-41
2. P. A. Hsieh, I. D. Bredehoeft, I. M. Farr. Determination of Aquifer Transmissivity from Earth Tide Analysis. Water resources research. vol. 23. 10. 1987, p.p. 1824-1832.
3. P. A. Hsieh, I. D. Bredehoeft, S. A. Rojstaczer. Response of Well-Aquifer Systems to Earth Tides: Problems Revisited. Water resources Research vol. 24. No. 3. 1988, p.p. 468-472.
4. Melikadze G., Popov E. A technique of Hydro-geological supervision with the purposes of the forecast earthquake on territory of Georgia. A series geology «Gruziinti» N7, 1989.
5. Melikadze G., Adamchuk Y, Todadze M Search informational harbingers of earthquakes on the territory Georgia. A series Geology «Gruziinti» N10, P., 1989
6. Melikadze G., Matcharashvili T., Chelidze T., Ghlonti E. Earthquake related disturbance in stationarity of water level variation. Bulletin of the Academy of sciences of the Georgian, 165 № 1, 2002
7. Melikadze G., Buntebarth G., Chelidze T. Hydrodynamic and microtemperature monitoring in seismic areas. Georgian Engineering News, # 3, 2004 , p.p 12-132
8. Melikadze G., Matcharashvili T., Chelidze T. Nonlinear analysis of dynamics of water level variation in Georgia during increased regional seismic activity. Book – Time-Dependent microtemperature and hydraulic signals associated with tectonic/seismic activity. Printed by Institute of Geophysics; European Center “Geodynamical hazards of high dams ” of open partial agreement on major disasters, council of Europe; Editors: G. Buntebarth, T. Chelidze, Tbilisi, 2005.
9. Rojstaczer S. Intermediate period response of water wells to crustal strain: Sensitivity and noise level, J. Geophys. Res., 93, 13,387-12,402. 1988.
10. Timofeev V. and al. Assessment post-seismic deformation of environment fracture parameters on the base water level variation in the borehole, Physic of Earth, 2012, № 7–8, c. 89–102 i)

Методика оценка геодинамического влияния на водоносные горизонты

Меликадзе Г.И, Кобзев Г.Н., Джимшеладзе Т.А.

Тбилисский Государственный Университет им. Ив. Джавахишвили, Институт Геофизики

Резюме

Во время гидродинамических наблюдений на территории Грузии до землетрясений было зафиксированы различные аномалии уровня воды. Выявление механизма связи между деформационными процессами и гидродинамическими изменениями подземных вод могут позволить объяснить такие гидродинамические эффекты и выработать научно обоснованные методы предсказания будущих землетрясений. Для выбора нужного метода был проведен сравнительный анализ различных методов обработки с учетом различных влияющих факторов. Один из методов основывается на идее, что свойства водоносного слоя (пористость и проводимость) меняются во время геодинамического стресса. Во время спокойного периода они меняются под влиянием гравитационной составляющей и имеют "фоновое" значение, однако во время сейсмической активности меняется пористость, тем самым являясь одним из индикаторов сейсмической активности.

ღრმა წყალშემცველ ჰორიზონტებზე გეოდინამიკური გავლენის შეფასების მეთოდი

მელიქაძე გ., კობზევი გ., ჯიმშელაძე თ.

ივ.ჯახიშვილის სახ.თბილისის სახელმწიფო უნივერსიტეტი, მ.ნოდისა გეოფიზიკის
ინსტიტუტი

რეზიუმე

საქართველოს ტერიტორიაზე განლაგებულ ღრმა ჭაბურღილებზე დაკვირვებებისას დაფიქსირებული იქნა მრავალი ანომალია მიწისძვრის წინ. მიწისძვრის გამომწვევ დეფორმაციულ პროცესებსა და მიწისქვეშა წყლების ჰიდროდინამიკურ რეჟიმს შორის დამაკავშირებელი მექანიზმების დადგენა ხელს შეუწყობდა ამ მოვლენის ახსნას და მიწისძვრების პროგნოზირების მეცნიერულად დასაბუთებული მეთოდის შემუშავებას. კორექტული მეთოდის შერჩევის მიზნით ჩატარდა სხვადასხვა მეთოდების შედარება ყველა შესაძლო ფაქტორის გავლენის დასადგენად. ერთ-ერთი მეთოდი ეფუძნება მოსაზრებას, რომ წყალშემცველი ჰორიზონტის თვისებები (ფილტრაციის კოეფიციენტი, ფორიანობა) იცვლება გეოლოგიური დამაბულობისას. შედეგების მიხედვით ეს თვისებები იცვლება მიმოქცევითი ვარიაციების შესაბამისად და აქვს "ფონური" მნიშვნელობა, ხოლო მიწისძვრის პერიოდში იცვლება და წარმოადგენს ტექტონიკური აქტივობის ინდიკატორს.

Evaluation of recharge origin of groundwater in the Alazani-Iori basins, using hydrochemical and isotope approaches

¹George Melikadze, ¹Natalia Jukova, ¹Mariam Todadze, ¹Sopio Vepkhvadze, ¹Nino Kapanadze,
¹Alexandre Chankvetadze, ¹Tamar Jimsheladze,
²Tomas Vitvar

¹Iv. Javakhishvili Tbilisi State University, M. Nodia Institute of Geophysics
²Czech Technical University in Prague, Faculty of Civil Engineering

Abstract

85 groundwater, stream water and lake water samples were analysed in 2013 for composition of major ions and isotopes ^{18}O , ^2H and ^3H in the Alazani-Iori area, eastern Georgia. Three groups of groundwaters were identified, revealing the dominant evolution in mineralization from Northwest to Southeast, with major increase in the Shiraki syncline area. The geochemical patterns among these groups evolve from $\text{Ca}(\text{Mg})/\text{HCO}_3$ type in the Kvareli aquifer to $\text{Na}/\text{SO}_4(\text{Cl})$ type in the Shiraki syncline. Almost all aquifers in the study area contain admixture of older waters recharged prior to the 1950's or paleowaters with no Tritium and low $\delta^{18}\text{O}$ values between -11 and -13 per mil SMOW. Although most of the artesian boreholes are up to 500m deep, their groundwaters belong to different hydrochemical and isotopic groups and must be considered with respect to local stratigraphy. Whereas the groundwaters in the Alazani valley artesian aquifers are concluded to be of a good quality for drinking, it is recommended to enhance the use of waters from the karstic formations such as the Dedoplistskaro Plain for alternative drinking water sources in the Shiraki –Iori basin.

Introduction

Eastern Georgia encounters, due to its semiarid climate, a big deficit of water for irrigation and domestic use. The aquifers of the Alazani basin are generally abundant in artesian groundwater due to recharge from Cretaceous and Jurassic formations of the southern slope of the Greater Caucasus and the northern slope of the Kakhetian ridge, the growing population and industrial and agricultural activities require new insights into the monitoring, assessment and development of these resources, partly abandoned after the collapse of the Soviet Union. Historically, the Alazani area was not prone to droughts and was not characterized by water shortages. However, runoff predictions for a temperature increase of 1.3 °C and precipitation decrease by 12% in 2011-2040 compared to 1961-1990 data result in average decrease in annual water flow by 12% (1). This may lead to lower groundwater recharge and cause water shortage for crops. Particularly the Shiraki plain encounters serious water quality problems due to limited regional recharge, elevated evapotranspiration-induced salinity and high content of organic sulphates. The communities on the Shiraki plain therefore need a better assessment of their groundwater supply facilities for drinking water purposes.

The groundwater resources of Eastern Georgia were systematically assessed since the 1940's. First boreholes were drilled in the northwestern part of the Alazani basin (Kvareli aquifer). Geophysical and hydrochemical studies were conducted until the 1990's, but their publication has been very sparse. Some geochemical data from the 1950's and 1960's mostly based on the work of Buachidze and Zedginidze (2) were published in the USAID report "Groundwater Resources of the Alazani Basin"(3). Data from the 1970's and 1980's were partly elaborated in Beselia (4), Bagoshvili

(5) and in particular Buachidze and Zedginidze (2). They have revealed the hydrogeological and hydrochemical characteristics of the principal aquifers (Kvareli, Telavi, Gurjaani) of the Alazani basin, demonstrating the main groundwater flow gradient and hydrochemical evolution from Northwest to Southeast. Geochemical evolution from Ca/HCO₃ type to Na/Cl (SO₄) type appears in the Telavi and Gurjaani artesian aquifers, the Lower Alazani series and the Cretaceous-Jurassic formations, whereas the Kvareli artesian aquifer is concentrated around Ca/HCO₃ type. Groundwater in the Quaternary synclines around the Shiraki Plain shows Na/Cl (SO₄) characteristics and in particular remains poorly understood. No tangible publications exist on the water resources on the Shiraki Plain and its surroundings. Because groundwater and surface water resources have been assessed separately from the institutional point of view, little is known on the interactions between streams and aquifers and on the groundwater recharge travel times.

Until the beginning of 1990, about 2000 hydrological and geological boreholes were drilled in the study area, including about 20 % observation wells and the rest production wells (7). Most of them are in a very poor condition and without any documentation or records. A large proportion of these wells are overflow wells, and their construction does not allow them to be sealed and there is therefore a huge loss of groundwater and significant disruption to the piezometric conditions of the hydrogeological structure. Non-artesian wells or wells which have lost their artesian overflow over time have in most cases been destroyed because their wellheads have been stolen and such wells are currently overgrown or buried. This may have a negative impact groundwater flow and cause hydraulic short circuit, unnatural overflowing between watershed layers, decrease of water levels and deterioration of the entire hydrogeological structure (7).

Besides the traditional methods of hydrogeological survey such as geochemistry and groundwater flow modelling, environmental isotopes as water tracers provide useful complementary information on water origin (where does the water come from) and history (which pathways did the water move until it arrived to an aquifer). These methods have been applied in Georgia since the first decade of this century through projects under the auspices of the International Atomic Energy Agency (IAEA). While the first project of this nature has focused on the identification of recharge areas drinking water resources in the Borjomi-Bakuriani region (8 and 9), recent activities cover various parts of Georgia, incl. eastern Georgia.

The Rustaveli National Science Foundation Grant was awarded for assessment of recharge conditions in the principal hydrogeological units of the Alazani-Iori catchment basins including the semi-desert areas, using environmental isotope and hydrochemical approaches. This paper has therefore the following objectives:

- a) Evaluation of recharge conditions in the principal hydrogeological units of the Alazani-Iori area
- b) Evaluation of groundwater travel times and hydrochemical evolution along flowpaths
- c) Identification of zones of increased groundwater vulnerability and possible alternative sources of drinking water.

Geological and hydrogeological settings

The area of the Alazani and Iori basins is located in eastern Georgia. It has an area of approximately 8000 sqkm. It includes the Alazani and Iori artesian aquifers, the adjacent aquifers of the Shiraki Plain synclinale and the Kakheti-range in the West-Northwest. This range and the entire Greater Shiraki Plain are a climatic boundary between the water-abundant Alazani basin and the water-scarce Iori basin.

The geological composition of the study region is complex and contains Jurassic, Cretaceous, Palaeogene, Neogene and Quaternary rocks. Most of the area belongs to the folded system of the Greater Caucasus, and a smaller part on the southeast (Garekaxheti Plateau) belongs to the Transcaucasian Intermountain Area (10).

The major units of the Alazani-Iori water-bearing complex are the Telavi and Gurdjaani water-bearing horizons. The Telavi water-bearing horizon is located from village Kogoto to the village of Sabatlo over 150 km. It contains about six water-bearing layers with the total capacity up to 50 m. The horizon is formed from coarse-grained sand and fine pebbles with the sandy filler. The horizon is deposited at the depth from 90 to 360 m, gradually submerging towards north-east and south-east directions, to the central part of Alazani valley. The Gurdjaani water-bearing horizon belongs to the upper part of the middle section of the Alazani. It submerges at the depth of 125-500 meters and is observed from the Velistsikhe station to the Gumbati village over 140 km. The Gurdjaani horizon is formed by porous gravely sediments with sandy fillers, in about nine water-bearing layers. The maximum number of these layers is observed in Gurdjaani-Kardanakhi region. Almost the whole horizon is covered by the Telavi water-bearing horizon. Eastwards of the Lagodekhi meridian the groundwaters from this water-bearing horizon border with Azerbaijan.

In contrast, the water-bearing horizons of the Iori-Shiraki artesian basin are developed locally within the boundaries of monoclinal and synclinal structures such as Sartichala, Sagaredjo, Mtsvanemindori, Shiraki, Olei and Djeiran-Choli basins.

Methodology

Fieldwork

85 water points (two examples on Fig.1) were sampled during six campaigns from April 2013 until October 2014. They include 5 points on surface waters (rivers and lakes) and 76 on groundwaters (springs, boreholes, dug wells). Major ions, ^{18}O , ^2H and ^3H were measured at each site. Physico-chemical parameters in the field (Temperature, pH, DO, EC) were obtained by the WTW Multi 340i set.

Depth and position of screen in the boreholes were taken from local archives and registers (2),

Additional monthly monitoring of isotopes ^{18}O , ^2H and ^3H in rainwaters and streamwaters was established in the study area in the framework of the Global Network of Isotopes in Precipitation (GNIP) and Global Network of Precipitation in Rivers (GNIR) operated by the IAEA (11). New GNIP (^{18}O , ^2H) stations in the study area include the recharge area in Tianeti (since January 2013), the central area in Telavi (since May 2012), and the discharge area in Dedoplistskaro (since January 2013) and Lagodekhi (since July 2013). While the information on temperature, rainfall amount and air humidity at Telavi is supplied by the adjacent meteorological station, the rain samplers at Tianeti, Dedoplistskaro and Lagodekhi were complemented by air temperature and humidity sensors HOBO. New GNIR (^{18}O , ^2H) stations include Alazani/Shakriani (since May 2012) and Iori/Tianeti (since January 2013), both equipped with HOBO water level sensors. Available meteorological datasets and discharge data from official meteorological and hydrological stations were obtained from the office of Hydro-Meteorological service of Ministry of Environment and Natural Resources Protection in Tbilisi.



Fig. 1 “Tetri-Tsklebi” –Borehole (left) and “Telavi” -Borehole №1 (right)

Laboratory

Stable isotope (^{18}O , ^2H) analyses of water samples were performed in the Laboratory of the Ivane Javakhishvili Tbilisi State University, M. Nodia Institute of Geophysics, by the Picarro Laser Water Isotope Analyzer L2110-I equipment purchased in the framework of the IAEA projects. Major ions were obtained by Flame photometer PFP7 and spectrophotometer DREL2800. Tritium was measured in the radioisotope laboratory Hydrosys, Inc. in Budapest, Hungary. Additional stable isotope and hydrochemical analyses were also carried out in other external laboratories in Hungary, Czech Republic and Morocco.



Fig. 2 laboratory equipment “Picarro” and “Flame photometer”

Interpretation

According on the regional knowledge, obtained field data and information on the geology and existing boreholes, the sampling points were assembled into following groups for further interpretation:

1. AK Kvareli artesian aquifer
2. AT Telavi artesian aquifer
3. AG Gurjaani artesian aquifer
4. AN Lower Alazani series artesian aquifer
5. SCJ Springs in Jurassic and Cretaceous formations
6. CJ Jurassic and Cretaceous formations - boreholes
7. SQS Quaternary formations of the Shiraki syncline –springs
8. QS Quaternary formations of the Shiraki syncline - boreholes
9. R Streamwaters (and lake)

The distribution of the water points according to these categories is given in Fig. 3.

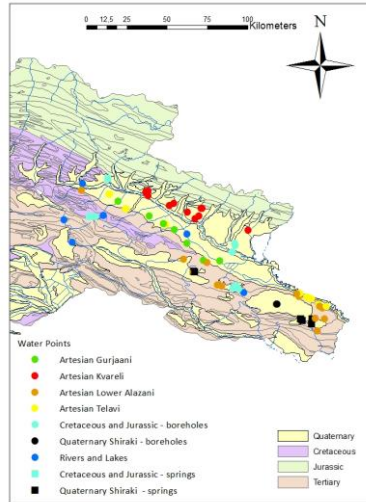


Fig. 3 – Distribution of water points according to hydrogeological groups.

Following techniques were used to visualize and interpret the hydrochemical and isotopic data

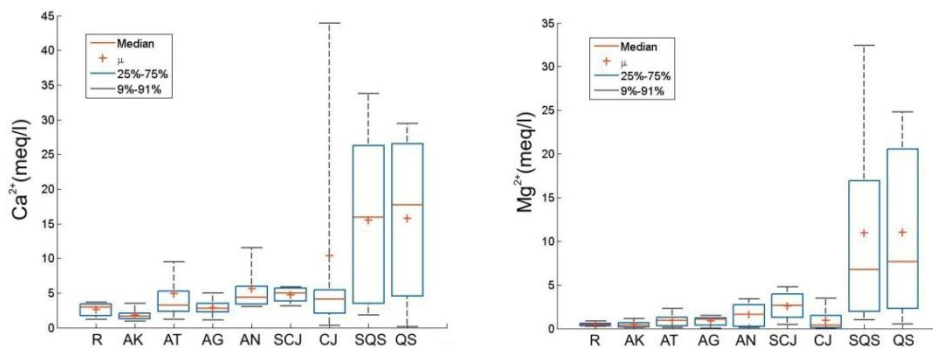
- Bivariate plots and Box-Whisker plots
- Aquachem 5.0 with trivariate plots (Piper-diagrams)

Results

Hydrochemistry

Hydrochemical composition of water samples from different aquifer units was assessed. Patterns of formation of the chemical composition of groundwater were refined with new data and the hydrochemical zonation of groundwater “Alazani-Iori” Artesian Basin was created.

Fig. 4 displays the hydrochemical characteristics of the different hydrogeological groups of water points.



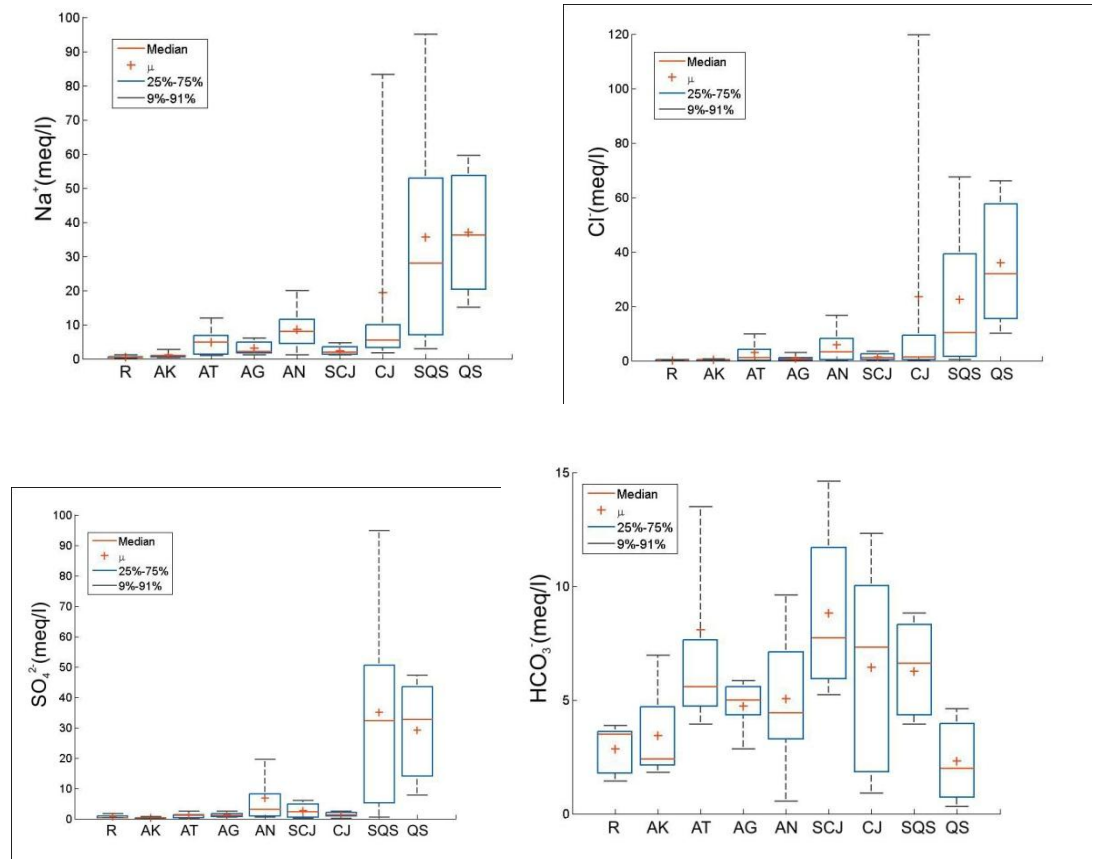


Fig. 4 – Content of major ions in groundwater from the “Alazani-Iori” area according to the main water point groups

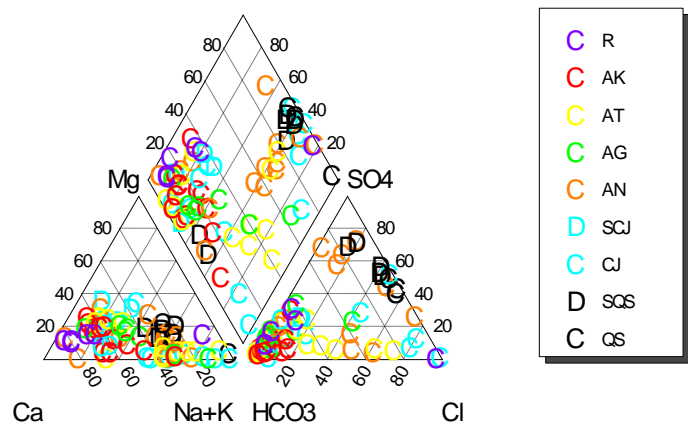


Fig. 5 - Hydrochemical evolution of the groups of water points.

Three types of groundwater were derived from the hydrochemical patterns.

The most mineralized groundwater type covers the territory of the waters of which have total mineralization of more than 2 g/l, temperature 14-19 ° C. By the chemical composition these water are sodium chloride. This type of water are generally located in the Shiraki Plain area (springs QS and boreholes SQS, see Fig. 3). The increased mineralization can be explained by saline sediments of Quaternary age as a result of intense evaporation, with a minimum amount of precipitation. The upper groundwater layer is more mineralized, while the bottom layer which is assessed by the wells, is less mineralized. This can be explained by the fact that the top layer does not have discharge area, being located within a closed syncline under the influence of intense evaporation. There lower-layer pressure horizons discharge as springs, located on the slope north of the Shiraki on the right bank of the Alazani river. They are characterized by a more rapid discharge and relatively good conductivity of the aquifer. These patterns are reflected on the general map of groundwater conductivity (Fig. 6) An upward trend of conductivity is observed along the river Alazani from the North-west to the South-east direction, and on the Shiraki valley from the South-west to the North-east.

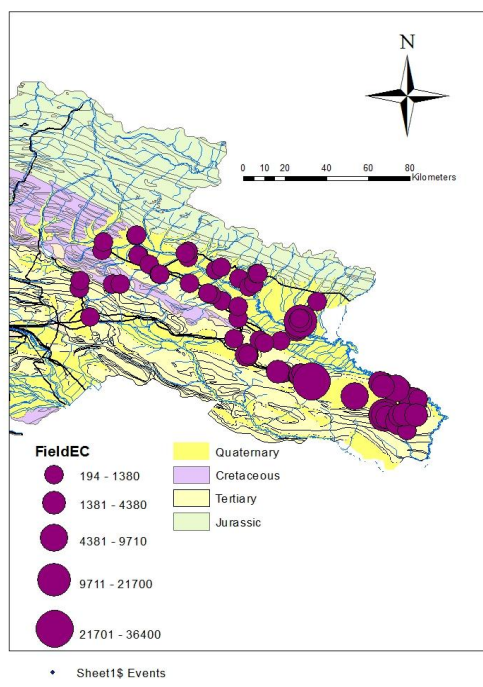


Fig. 6 Spatial distribution of electrical conductivity in the Alazani-Iori area.

Groundwater on the Kakheti ridge (between the Alazani and Iori valleys) has a local distribution due to their confinement to the zones of tectonic faults (Gamardzhveba, Bodbe) in the Lower Alazani series artesian aquifer (AN).

The second type of groundwater has a total mineralization between 1.0 to 2.0 g / l. By chemical composition this water is represented by various compositions of (Na,Mg)/ (Cl,SO4 2-) and temperature between 14 and 19°C. These types of waters are distributed in parts of the Telavi and Kvareli aquifers and in the entire Gurjaani aquifer (AT, AK, AG, see Fig. 3).

The third type of groundwater has a total mineralization up to 1.0 g / l. Water chemistry is represented by various proportions of Ca(Na,Mg)/ HCO3- (SO4 2-) and temperature between 12 and 16°C. This type of groundwater is distributed in the rest of the basin, covering most of the area of distribution Kvareli aquifers and Neogene, Cretaceous and Jurassic sediments.

Pronounced changes in the total mineralization of the artesian water of Telavi, Gurjaani and “methane” aquifers of the Alazani series are observed in the vertical cross section of the boreholes.

Isotopes

Stable isotopes (^{18}O , ^2H) and Tritium (^3H) were analysed in all water samples from the different hydrogeological groups. Fig. 7 reveals that modern recharge with $\delta^{18}\text{O}$ values between -8.5 and -9.9 ‰ V-SMOW is dominant in groundwaters of the Alazani series (AN), Kvareli aquifer (AK), springs (SQS and SCJ) and in the rivers. Aquifers of Telavi (AT) and Gurjaani (AG) artesian structures as well as the Cretaceous and Jurassic formations (CJ) and the Shiraki syncline (QS) contain paleowaters with $\delta^{18}\text{O}$ values between -11 and -13 ‰ V-SMOW. Similarly, the Tritium concentrations (Fig. 7) show a presence of older (recharged prior to 1950's) waters in samples from all groups except for the Quaternary Shiraki springs (SQS) and the rivers (R). The isotopic composition of samples confirms the groundwater hydrochemical patterns explained in 4.1. The first highly mineralized groundwater type has relatively low concentrations of tritium (0.1-1.8 TU), which characterizes old groundwaters recharged prior to the 1950's, including paleowaters. Tritium concentrations increase for the second (3-6 TU) and third group of waters, respectively (7-11 TU). These values indicate waters with modern recharge (after 1950), partly with admixture of old components.

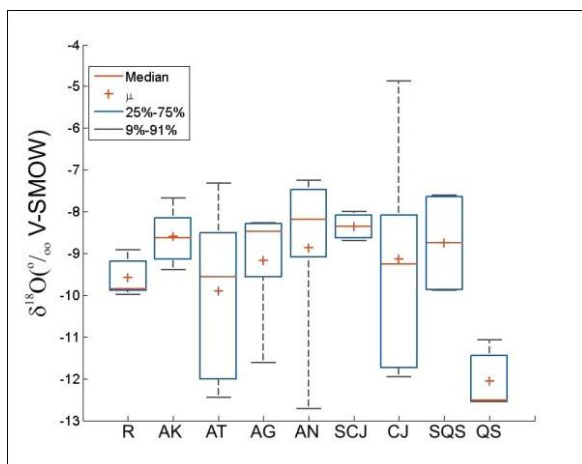


Fig.7– Isotopic characteristics of waters in the Alazani-Iori area. Left: content of ^{18}O ; right : content of ^3H .

Tritium concentration is decreasing from the West direction to East on the territory and smallest is observed on the Shiraki plain (Fig. 8).

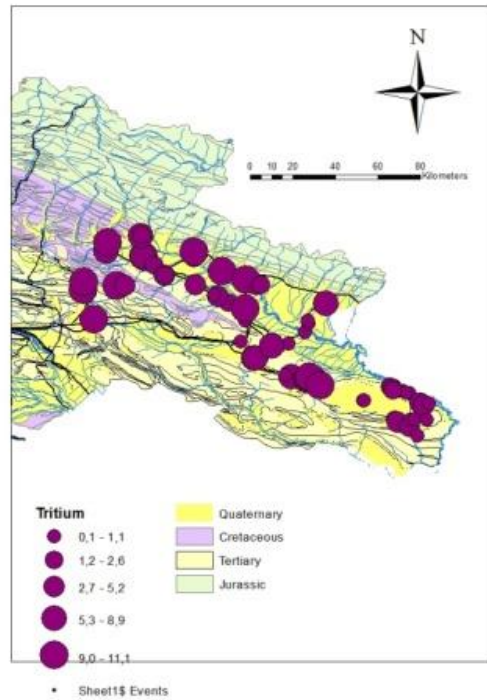


Fig. 8- Spatial distribution of Tritium in the Alazani-Iori area.

Fig. 10 displays the ^{18}O - ^2H relationship. It reveals that waters in almost all samples are located along the global meteoric water line. Values of two samples deviate from the global meteoric water line – the Lake Kechabi on the Shiraki Plain, and the geothermal karst spring Heretitshkali. These deviations are related to evaporation under semiarid climate conditions and to water-rock interactions in geothermal environment.

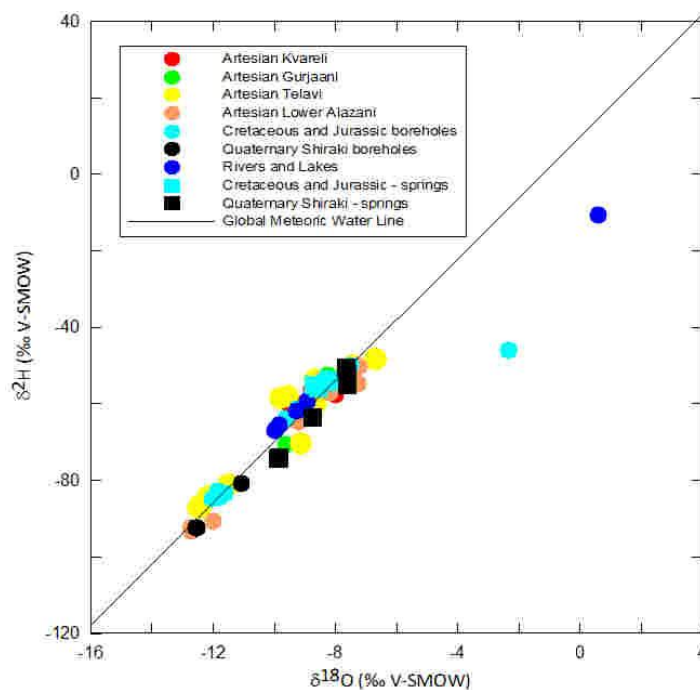


Fig. 10. Plot of ^{18}O - ^2H of waters in the study area.

Conclusions

Complex geological, hydrogeological, hydrogeochemical and isotope investigations were carried out in the Alazani-Iori area. They have confirmed the evolution in mineralization from Northwest to Southeast, with major increase in the Shiraki syncline area. Isotope investigations have confirmed the entirely modern groundwater origin of the Kvareli aquifer and admixture of pre-1950 waters (or paleorecharge in case of $\delta^{18}\text{O}$ values between -11 and -13 per mil SMOW) in all other aquifers. Although most of the artesian boreholes are up to 500m deep, their groundwaters belong to different hydrochemical and isotopic groups and must be considered with respect to local stratigraphy. Waters on the Shiraki plain area are characterized by high content of SO_4 and Cl and therefore lower quality for drinking. It is recommended to enhance the use of waters from the karstic formations such as the Dedoplistskaro Plain for alternative drinking water sources in the Shiraki region. The conjunctive use of hydrochemical and isotopic approaches demonstrates a high potential for future water resources studies in Georgia.

Acknowledgments: The authors thank the Rustaveli National Scientific foundation for financial support of the project #31/27 “Environmental Isotopes Testing in Alazani-Iori Catchments (East Georgia) For Provision of Sustainable Use of Groundwater Resources”.

(Received in final form 3 September 20014)

5. References

1. Shotadze M., Barnovi E. (2011) Integrated Natural Resources Management in Watersheds (INRMW) of Georgia Program. Technical Report, USAID No.CA # AID-114-LA-10-00004, 79 pp.
2. Buachidze, I.M., Zedginidze, S.N. (1985). Hydrogeology and Perspectives of Groundwater Use in the Alazani-Agrichai aquifer. Tbilisi, 335pp. (in Russian).
3. Gaprindashvili, T. (2002). Groundwater Resources of the Alazani Basin. Technical Report. Subcontract No. 3335-105-005 under USAID/DAI Prime contract No. LAG-I-00-00017-00 „Water Management in the South Caucasus Project. “Gorgasali” Joint Stock Company, Tbilisi, Georgia, 14pp.
4. Beselia, B.N. (1988). Preliminary survey on the appearance of groundwaters - Quaternary alluvial-proluvial confined and Upper Jurassic and Lower Cretaceous aquifers between the rivers Chelti and Durudji. Ministry of Geology of USSR, Tbilisi, 3 volumes. (unpublished, in Russian)
5. Bagoshvili, G.N. (1990). Report on hydrogeological survey 1:50000 on the southern slope of the Greater Caucasus. Ministry of Geology of USSR, Tbilisi, 2 volumes, 95 and 163 pp. (unpublished, in Russian)
6. Buachidze, G. (2005). Transboundary Artesian Basin of Georgia. Presentation at the conference EURO-RIOB 2005, Namur, Belgium, 29 Sept-1 Oct 2005. http://www.riob.org/IMG/pdf/Euro-RIOB_29sept2005_Buachidze.pdf
7. Pilot project for re-activation of groundwater level and quality monitoring network of Alazani-Agrichai aquifer, 2013. Technical Report of the Czech Official Development Assistance “Aid for Trade” Program between National Environmental Agency of Georgia and AQUATEST a.s. (J. Sima, ed.) 59p, December 2013.
8. Melikadze G., Chelidze T., Zhukova N., Rozanski K., Dulinski M., Vitvar T. (2009). Using nuclear technology for environmental safety and sustainable development of water resources in Borjomi region (Southern Georgia). Journal of Georgian Geophysical Society, Issue (A), Physics of Solid Earth 13a, 17-25.
9. Melikadze G., Chelidze T., Jukova N., Malik P., Vitvar T. (2011). Using Numerical Modeling for Assessment of Pollution Probability of Drinking Water Resources in Borjomi Region (Southern

- Georgia). In: Climate Change and its Effects on Water Resources, Issues of National and Global Security (Baba A., Tayfur G., Gunduz O., Howard K.W.F., Fridel M.J., Chambel A., eds.), NATO Science Series. Springer. ISBN:978-94-007-1145-7. Chapter 29, 267-275.
14. 10. Gudjabidze, G.E. (2003). Geological Map of Georgia. Scale 1:500.000. Georgian State Department of Geology, Tbilisi.
15. 11. Vitvar, T, Aggarwal, P.K., Herczeg, A.L. (2007). Global Network is launched to monitor isotopes in rivers. EosTrans. AGU 88:325–326.

(Received in final form 3 September 20014)

Оценка происхождения и миграции подземной воды в Алазани –Иорском бассейнах с использованием гидрохимических и изотопных методов

¹Меликадзе Г.И., ¹Жукова Н. О, ¹Тодадазе М. Ш., ¹Вефхвадзе С. Г., ¹Капанадзе Н. А.,
¹Чанкветадзе А. Ш., ¹Кобзев Г.Н., ¹Джимшеладзе Т.А., ²Витвар Т. А.

¹Тбилисский Государственный Университет им. Ив. Джавахишвили, Институт Геофизики
²Технический Университет Праги, Чехия, Факультет Гражданского Строительство

РЕЗЮМЕ

2013 году были проанализированы 85 образцов из подземных, речных и озерных вод для изучения состава основных ионов и изотопов ¹⁸O, ²H и ³H в районе Алазани-Иори в Восточной Грузии. Были определены три группы подземных вод, которые показали доминирующую эволюцию в минерализации с северо-запада на юго-восток, со значительным увеличением в синклинальной области Шираки. Геохимические модели среди этих групп эволюционируют от Ca(Mg)/HCO₃ -типа в Кварельском водоносном горизонте к Na/SO₄(Cl) -типу в синклинали Шираки. Почти все водоносные горизонты в области исследования содержат примесь старые предварительно до-1950 воды или палеоводы без трития и низкие значения δ¹⁸O между -11 и -13 промилле SMOW. Хотя большинство артезианских скважин имеют глубину до 500м, их подземные воды принадлежат к разным гидрохимическим и изотопным группам и должны рассматриваться по отношению к местной стратиграфии. Хотя, как выяснено, в долине Алазани артезианские водоносные горизонты имеют хорошее качество и пригодны для питья, рекомендуется расширить использование вод карстовых образований, таких как в Дедоплисцкаро-равнине для поиска альтернативных источников питьевой воды в бассейне Шираки-Иори.

ჰიდროქიმიური და იზოტოპური მეთოდების გამოყენებით მიწისქვეშა წყლების წარმოშობის და მოძრაობის შესწავლა ალაზანი-იორი აუზებში

გიორგი მელიქაძე, ნატალია ჟუკოვა, მარიამ თოდაძე, სოფიო ვეფხვაძე, ნინო კაპანაძე,
ალექსანდრე ჭანკვეტაძე, თამარ ჯიმშელაძე
1ივ. ჯავახიშვილის სახ. თბილისის სახელმწიფო უნივერსიტეტი, მ. ნოდის გეოფიზიკის
ინსტიტუტი

რეზიუმე

2013 წელს გაანალიზებული იქნა ძირითადი იონური შემადგენლობა და სტაბილური იზოტოპების (^{18}O , 2H და 3H) შემცველობა ალაზანი-იორის აუზის ზედაპირულ და წვიმის წყლებში. დადგენილი იქნა მიწისქვეშა წყლების ძირითადი სამი ჯგუფი, ასევე მინერალიზაციის ზრდა ჩრდილოეთიდან სამხრეთი მიმართულებით, მისი უმაღლესი მნიშვნელობების დაფიქსირებით შირაქის ველზე. გეოქიმიურად აღნიშნულ ჯგუფებში ფიქსირდება ჩა(Mg)/ HCO_3 ტიპის წყლების ცვლილება Na/SO_4 (ჩლ) ტიპით. შირაქის ველზე თითქმის ყველა წყალშემცველი ჰორიზონტი შეიცავს ძველი (1950 წლამდე), განამარხებული ტიპის პალეო-წყლებს, რომლებშიც არ ფიქსირდება ტრიტიუმის შემცველობა, ხოლო ჟანგბადის იზოტოპების (^{18}O) შემცველობა იცვლება -11 დან -13 მდე (პერ მილ $\text{SMO}\text{‰}$). თითქმის ყველა არტეზიული ჭაბურღილის სიღრმე აწარბებს 500 მ. მათ მიერ გახსნილი წყალშემცველი ჰორიზონტები თავისი ქიმიური და იზოტოპური შემადგენლობით მიეკუთვნებიან სხვადასხვა ჯგუფებს და განპირობებული არიან ადგილობრივი სტრატეგრაფიით. იმის გათვალისწინებით, რომ ალაზნის ველის მიწისქვეშა წყლები მიეკუთვნებიან სასმელად კარგი წყლების კატეგორიებს, დამატებით რეკომენდირებულია დედოფლისწყაროს კარსტული წყლების გამოყენება სასმელი წყლის ალტერნატიულ რესურსად.

Linear methods of studying the water level variation related with seismicity

¹Tamar Jimsheladze, ¹George Melikadze, ¹Genadi Kobzev,
²Aleksey Benderev, ³Emil Botev

¹Iv. Javakhishvili Tbilisi State University, M. Nodia Institute of Geophysics;
²Bulgarian Academy of Sciences Geological Institute „Strachimir Dimitrov“;
³National Institute of Geophysics, Geodesy and Geography within Bulgarian Academy of Sciences

Abstract

The article describes the methods of hydrodynamic observations for monitoring tectonic processes in real time and seismic isolation component. The developed methods are used to extract the geodynamic component of observation data to examine patterns of its distribution in space and time over large areas in the process of preparation of strong earthquakes. For data processing, we have developed a new method on MATLAB (program RestDance) to synthesize the theoretical signal and compare it with the real data of the water level. The article also describes the method of speed and its values to visualize the anomalous behavior of water level during strong earthquakes.

Introduction

The correlation between the hydrodynamic anomalies of groundwater and seismic phenomena, caused by tectonic processes, long fixed. Physical meaning of this phenomenon: the lithosphere rocks contain cracks and pores that respond to mechanical stresses. As is known, the water is incompressible medium in the case of open system during compression changes the water extracts from the stress-strain medium and this makes it possible to observe the change of intensity. Identifying the mechanism of the relationship of deformation processes, the strong earthquake and hydrodynamics of groundwater helps to explain this variability hydrodynamic field.

Description of the methods of data processing

To monitor hydrogeodeformation field of the Earth, which allows to fix the rapid changes of deformation-stress state of the medium (1), due to the preparation of the earthquake, in the 80s of the last century, work began on the creation specialized network of water wells. Regime wells were chosen so that they are all characterized by large geological units. Well as bulk strain meters, sensitive to deformation of various kinds, both exogenous and endogenous (2-5). Accuracy of the observations reached 10^{-7} - 10^{-9} values. Has accumulated a long series of observations throughout the Caucasus.

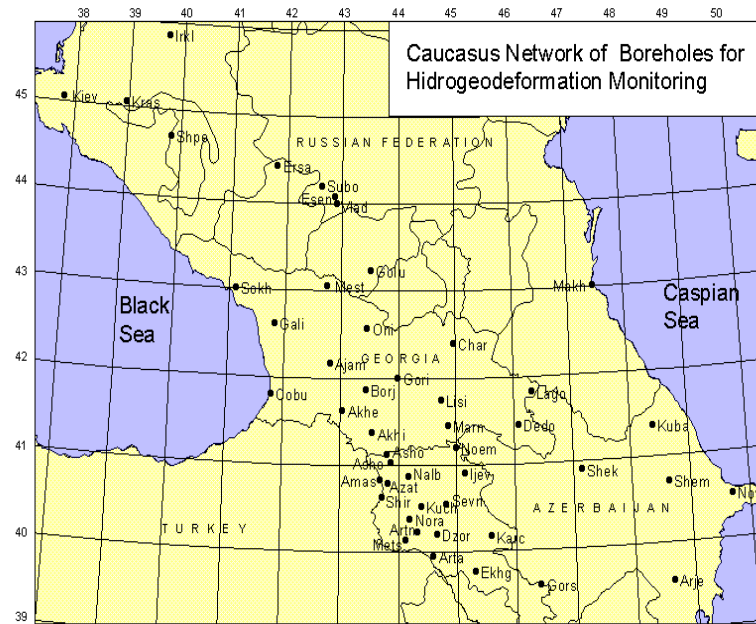


Figure1. Caucasian observation network of Hidrogeodeformational field

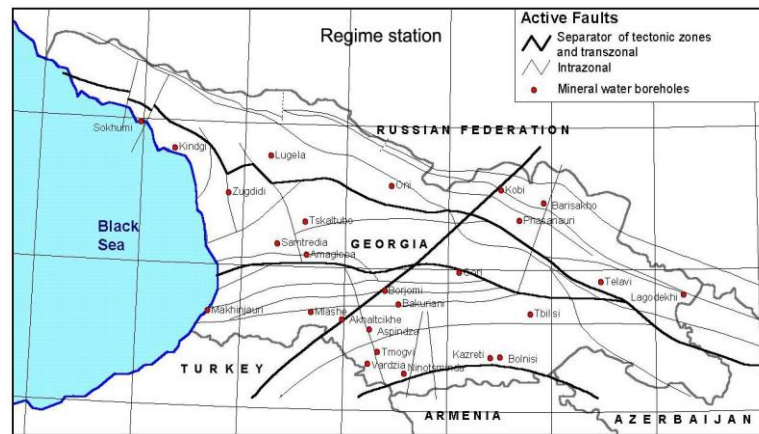


Figure2. Layout observed wells for geological units

Change in water level due to the following factors: atmospheric pressure (AP); precipitation (PR); tidal variation (TI); Tectonics-seismic stress (T/S) and the proportion of errors apparatus (e).

$$\text{Water level} = f(\text{AP}) + f(\text{PR}) + f(\text{TI}) + f(\text{T/S}) + e;$$

To isolate the tectonic components necessary filtering and selection of primary materials netektonicheskikh components. As a good example of the decomposition analysis can point to the analysis of the level of water wells Gaybara (Japan). Akaike et al, 1985 and Tamuta, et al, 1991 developed a special program BAYTAP-G (Bayesian Tidal Analysis Program in a Grouping Method) to filter rainfall and tidal variations. Influence of precipitation on water level by means of regression analysis was evaluated Matsumoto (1992), Matsumoto and Takahashi (1993). It should be noted that Kitagava and Matsumoto (1996) used the Kalman filter to select all netektonicheskikh components of the water level data. They identified tectonic component after

subtracted influence of atmospheric pressure, tidal variations and precipitation. (Matsumoto et al, 2003).

Another example of a consistent approach to the problem is to analyze the data of the water level in the well Lisi, Georgia (Gavrilenko, Melikadze et al, 2000), where the decomposition of the water level was applied a special method. On the basis of real data on the tidal variations, atmospheric pressure and precipitation for the period 1988 - 1992 years. Was promoted synthesis of theoretical reaction variations of the water level in the well Lisi, which was compared with the actual variations in the water level. With this same time period, two strong earthquakes in the Caucasus region - Spitak (7.12.1988, $M = 6,8$, $\Delta = 110$ km) and Raczynski (29.04.1991, $M = 6,9$, $\Delta = 125$ km), here M - is magnitude, and Δ - epicentral distance. Before the earthquakes observed anomaly of water level throughout the region.

For data processing, we have developed a new method on MATLAB (program RestDance) to synthesize the theoretical signal and compare it with the real data of the water level. The program enables counts each exogenous parameter separately and examine their impact on the aquifer.

For example, the article demonstrates variation of parameters during preparation “Racha” earthquakes of 12.08.2009 ($M= 4$) and in 9.09.2009 ($M= 4.6$) in the three boreholes. First of them “Oni” is located in the epicentral areas, the second one, “Adjameti”, is 100 km far to South-West direction and finally “Lagodekhi” is 200 km far to East direction from the epicentre.

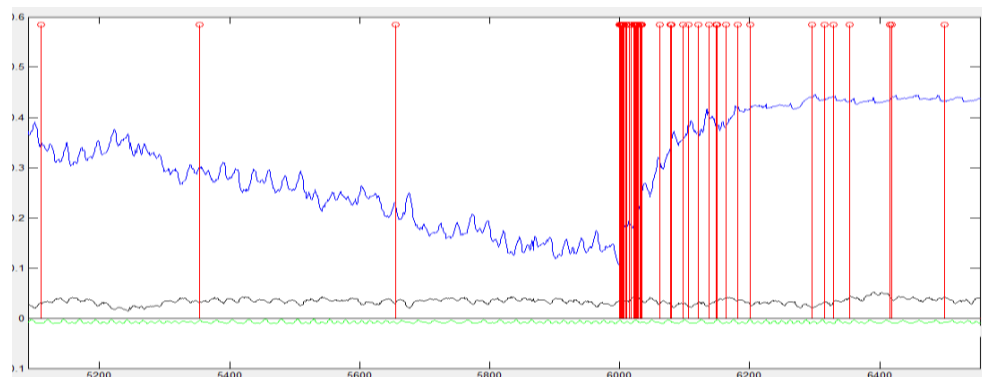


Figure 3. Variation of water level (upper curve), atmosphere pressure (middle curve) and tidal variation (lower curve) at the “Oni” station. The vertical lines mark earthquakes.

The figure shows the violations that occurred at the station Oni at the time of the earthquake in Racha.

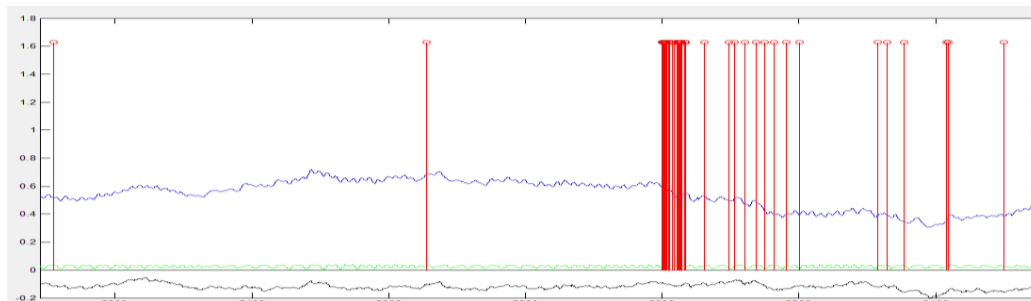


Figure 4. Variation of water level (upper curve), atmosphere pressure (lower curve) and tidal variation (middle curve) on the “Ajameti” station. The vertical lines mark earthquakes.

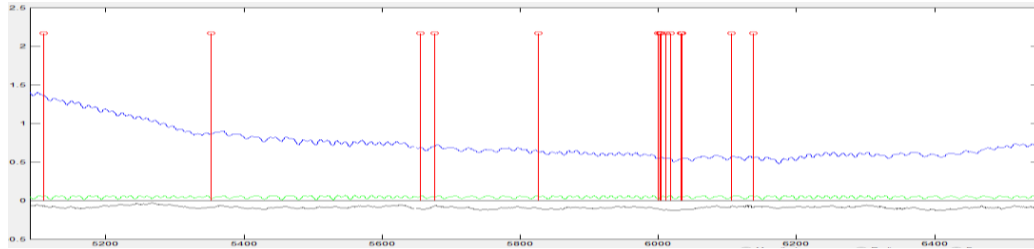


Figure 5. Variation of water level (upper curve), atmosphere pressure (lower curve) and tidal variation (middle curve) on the “Lagodekhi” station. The vertical lines mark earthquake.

The pictures show the variation of different fields on the stations. Water level variation as a multi-signal value contains all exogenous (tidal variation, atmosphere pressure and precipitation) and endogenous (earthquakes) factors' influence. In the seismically passive period the background of variation reflects only exogenous factors, but during earthquake preparation process the character of variation changed (Bella, Biagi P. et al., 1992, Hsieh et al., 1988). In this period are recorded disturbances in the water level variation before and after of earthquakes (Fig. 3-5).

In order to calculate the relationship between changes in the parameters and earthquakes were introduced correlation coefficients with the tidal water level variations - a, with atmospheric pressure changes - b, and the constant- c. To identify the statistical dependence of the change of energy reaching the area well away from the epicenter zone, was written by a special program that allows you to identify "variation" of the coefficients *a*, *b*, *c* and the signal "balance" between earthquakes on the three stations are shown in Fig. (6-11).

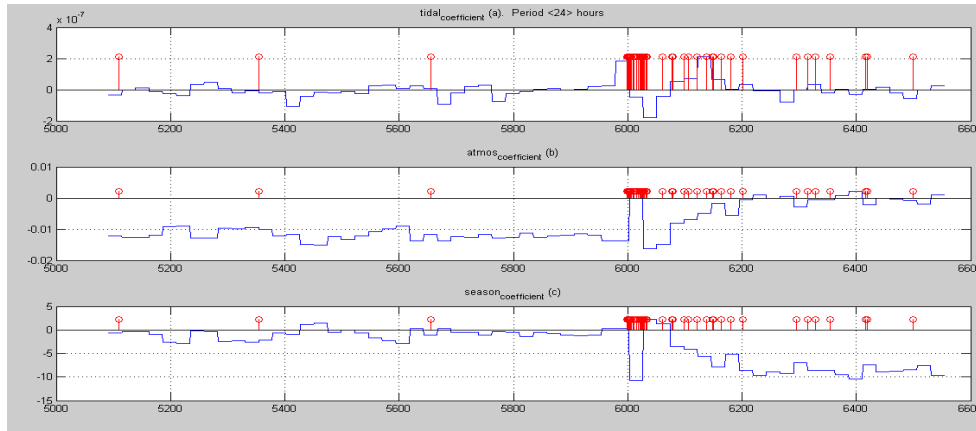


Figure 6. Variation of a, b and c coefficients at the “Oni” station.

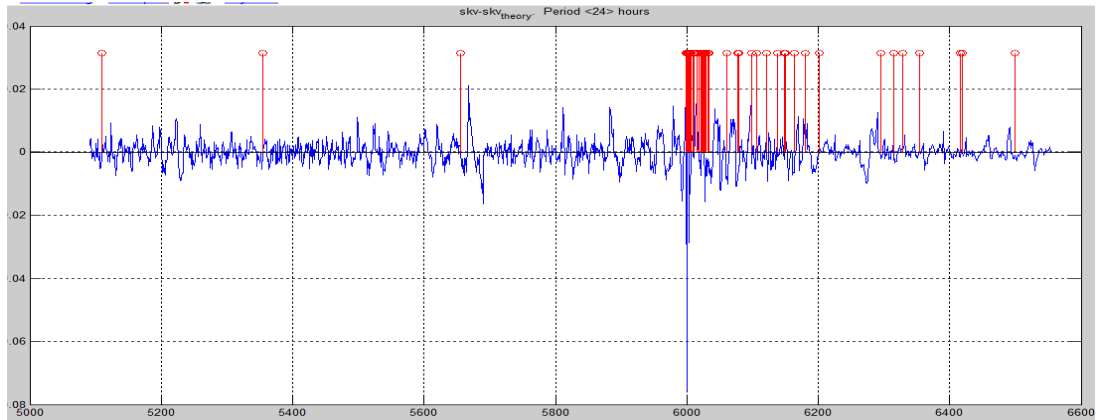


Figure 7. Variation of “residual” signal at the “Oni” station.

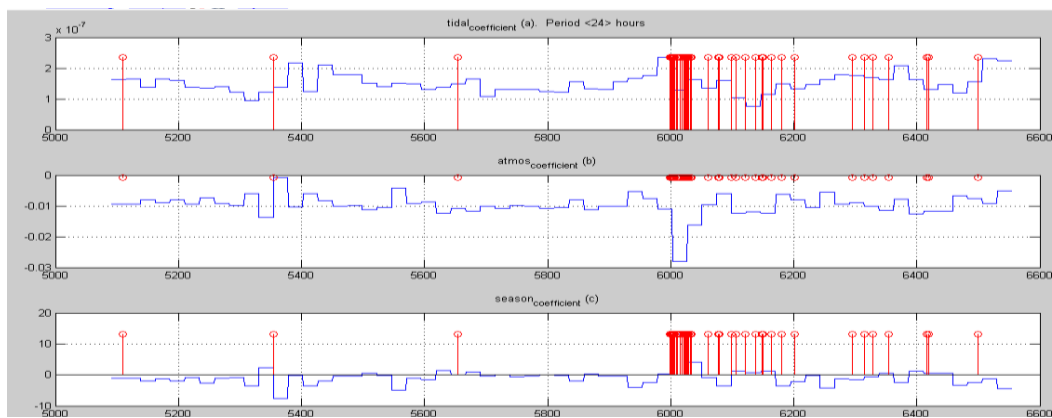


Figure 8. Variation of a, b and c coefficients at the “Adjameti” station.

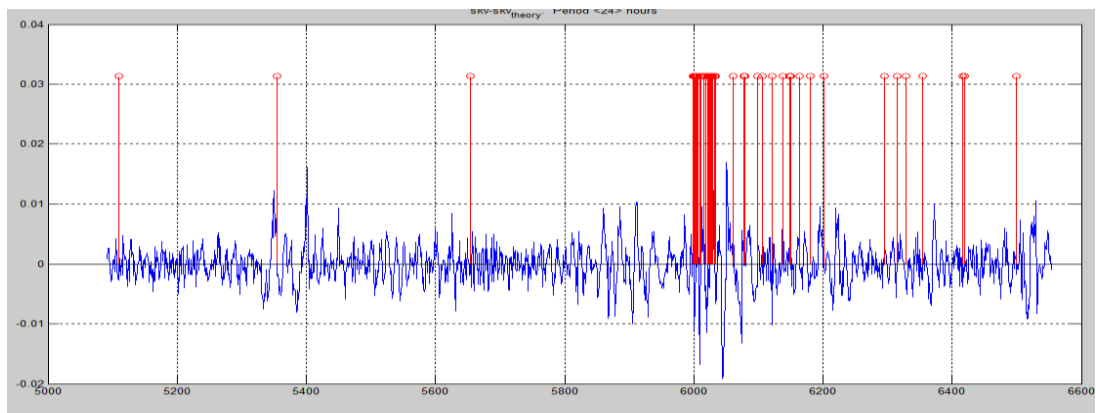


Figure 9. Variation of ”summary” coefficients at the “Adjameti” station.

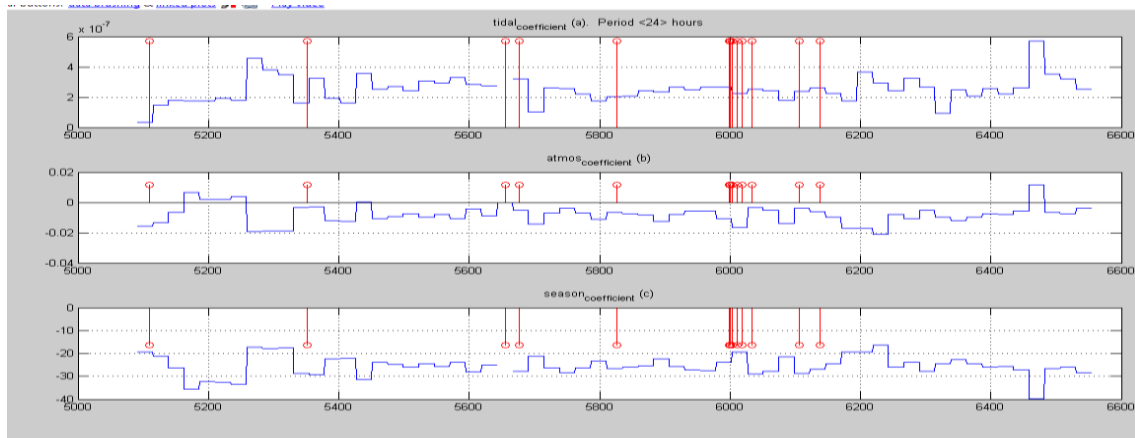


Figure 10. Variation of a, b and c coefficients at the “Lagodekhi” station.

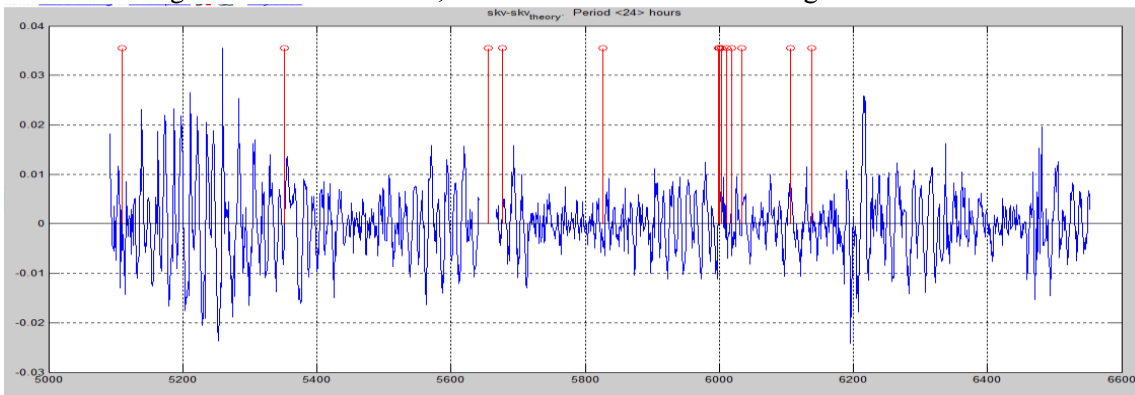


Figure 11. Variation of ”summary” coefficients at the “Lagodekhi” station.

The “background” values of water level variation was changing before and after events (Melikadze et al., 1989). Character of variation of coefficients for each borehole depends on the energy value, which reached boreholes area. “Lagodekhi” borehole is sensitive for local earthquakes then for “Racha” earthquake. At the same time the amplitude of variation before “Racha” earthquake is stronger in the “Adjameti” station. This can be explained by larger strain-sensitivity of “Adjameti” station (Melikadze et al.).

Furthermore, the program calculates variation of “geodynamical” signal -difference between the water level’s theoretical and observed values and “residual” values of high frequency signal in the water level variation. (Fig. 12-14).

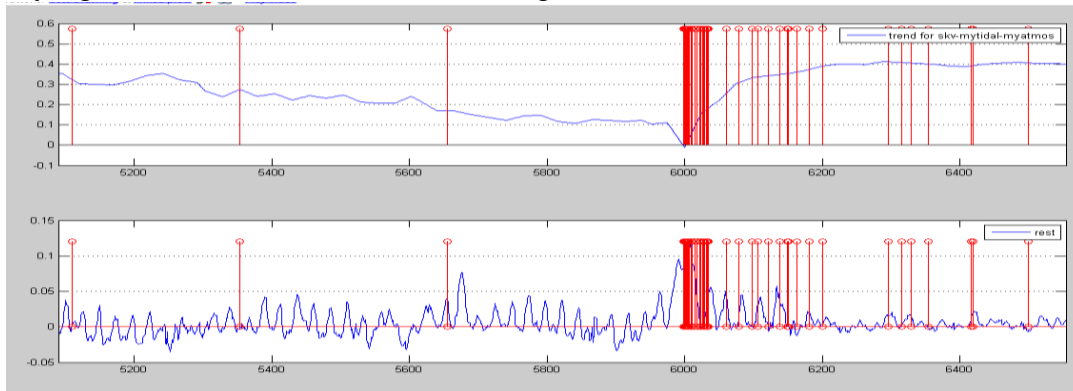


Figure 12. Variation of “trend” value of geodynamical signal (upper curve) and “residual” (lower curve) at “Oni” station.

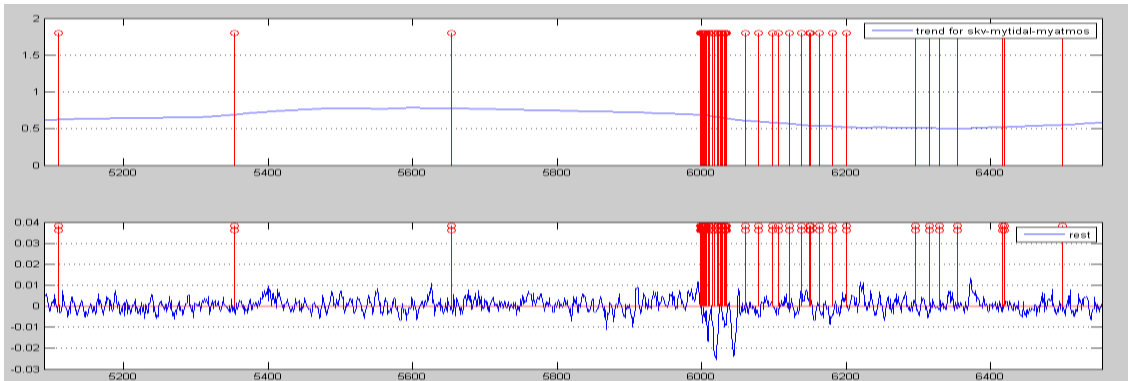


Figure 13. Variation of “trend” value of geodynamical signal (upper curve) and “residual” (lower curve) at “Adjameti” station.

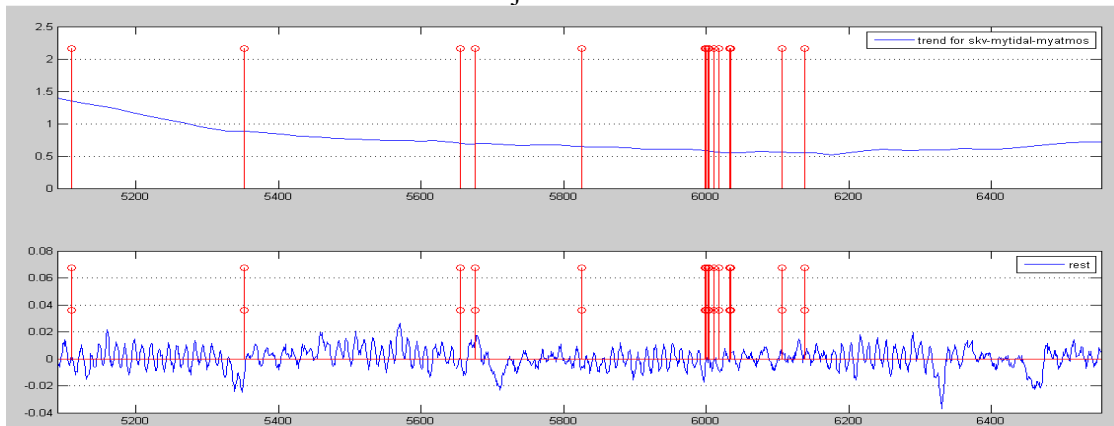


Figure 14. Variation of “trend” value of geodynamical signal (upper curve) and “residual” (lower curve) at “Lagodekhi” station.

The drawdown of water level in the “Oni” and “Lagodekhi” boreholes and increase of the “Adjameti” boreholes are fixed. The first effect is characterizing decompression and the second one - compression of aquifer system before Racha earthquakes. After considered events water level in the “Adjameti” borehole goes down, this characterizes decompression processes. “Oni” station kept compression processes.

Another way to study the anomalous behavior of water level – is the speed method. Seasonal trend, which is usually present in the water level of wells, take a number of problems in monitoring.

Consider the concept of velocity (speed) for the water level.

Definition:

$$\text{Speed } (m + i) = (\text{water } (m + i) - \text{water } (i)) / m, i = 1, 2, 3, \dots$$

Where m is some fixed number of minutes.

In the examples below (Figure 15) the speeds are multiplied on coefficients for visual comparison. We point out that in the speed graph disappears seasonal component.

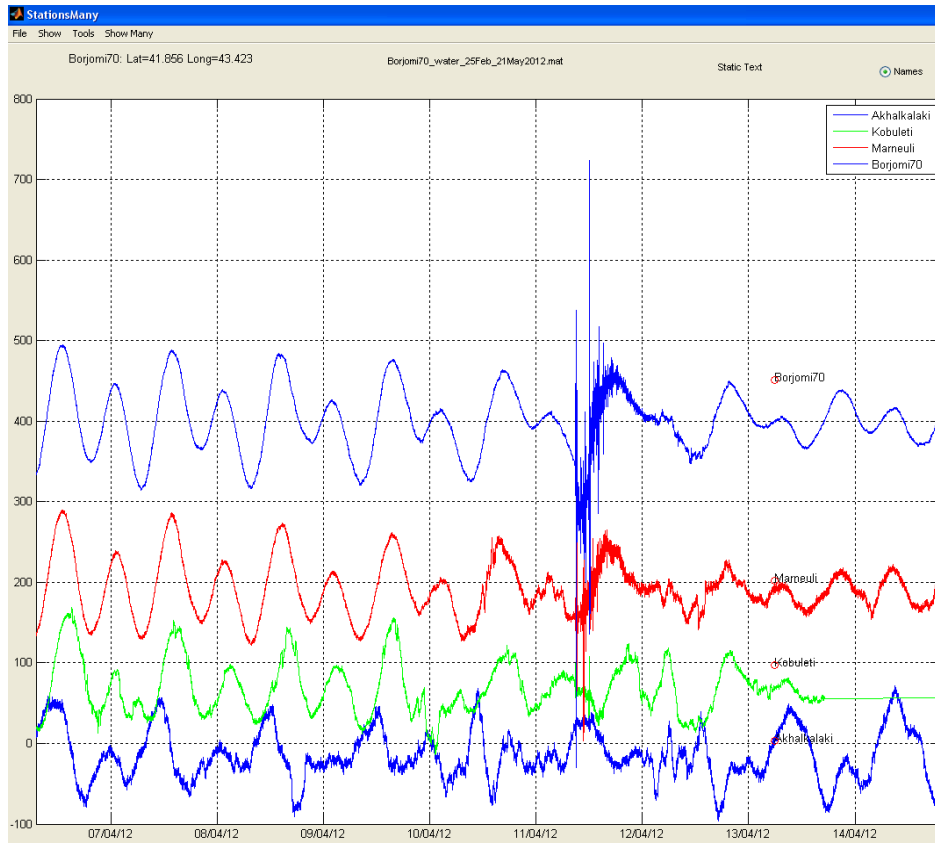


Figure15. Speeds. The reaction to the earthquake in Indonesia (Sumatra)
 From top to bottom: Borjomi70 (top), Marneuli, Kobuleti, Akhalkalaki
 m=180 minutes

The figure shows the velocity violations during an earthquake in Indonesia (Sumatra).

Table 1. shows the values of water level changes that have been committed during the earthquake in Sumatra (Indonesia).

Table1. Earthquake in Sumatra (Indonesia), 11 April 2012, Mag=8.4, distance =6508 km

Borehole	Jump of water (cm)
Kobuleti	4
Marneuli	8
Borjomi70	70

Figure 16. also seen some irregularities that occurred 2-3 days before the earthquake in Turkey (Vani), which occurred October 23, 2011 (Magnitude = 7.2).

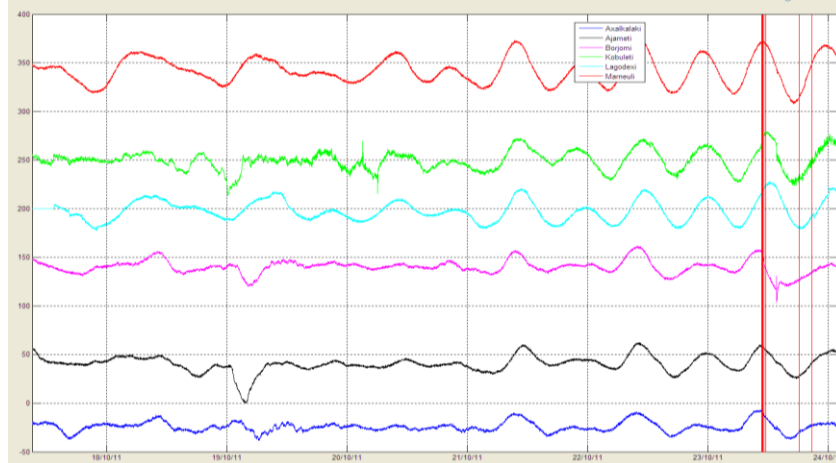


Figure 16. Speeds: $m=180$ minutes interval for boreholes of Georgia, 18-24 October and Turkey (Vani) earthquakes 23 October 2011, Mag=7.2 From top: Marneuli, Kobuleti, Lagodekhi, Borjomi, Ajameti, Akhalkalaki.

Within 2 days, from October 18 to 21, before the earthquake, see the violation, and then there was a leveling off. During an earthquake on October 23 following changes were observed.

- The well Kobuleti, which is located at a distance from the epicenter 369km, there was a drop in water level at 0.5 cm; The well Borjomi, which is located at 339km from the epicenter, there was an increase in water level at 3.5 cm;

- The well Akhalkalaki, which is located at 291km from the epicenter, there was a drop in water level at 0.5 cm.

- Minor violations can be seen at the station Marneuli, which is located at 317km from the epicenter. With help of speed method were also studied water levels for wells of Bulgaria (Irechek, Belgun, Chelopezhene and Vaklino) for 2008-2014 years. In the vicinity of these wells are almost no rivers, as developed karst and surface runoff is absent.

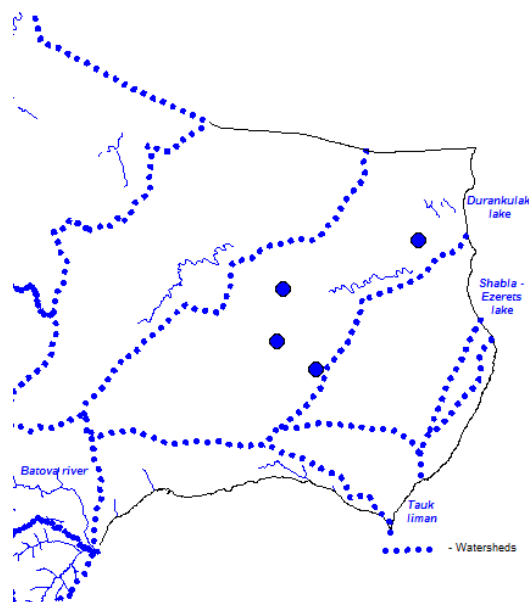


Figure 17. Wells of Bulgaria: Irechek, Belgun, Chelopezhene and Vaklino.

Level temporary rivers near Irechek, Belgun and Chelopechene about 80-100 meters, and near Vaklino - about 15 -20 meters. Two wells are not deep and open the first karst of unconfined aquifer in sarmath (neogen) limestone - Belgun and Vaklino. Wells do not cross the entire thickness of the aquifer. The upper part of the casing strings isolated. Water-bearing intervals Belgun- from 51 to 106 m, and in Vaklino - from 40 to 68 m. Upper limits depend on supply.

The remaining two wells are deep and reach the head waters in the Upper Jurassic-Lower Cretaceous sediments.

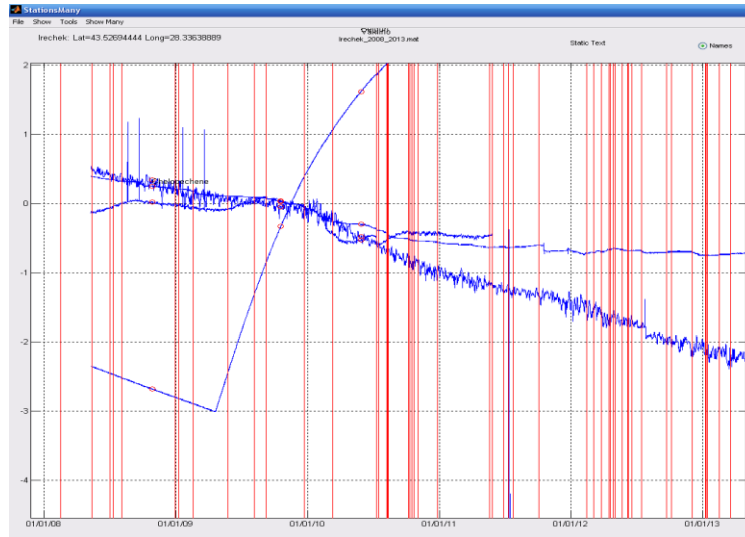


Figure18. Changes in water level in wells located on the territory of Bulgaria. 2008-2014yy. According to the result of the processed data was recorded by the influence of external factors (tidal variations, atmospheric influence, seasonal fluctuations), this they have low information to fix the possible geodynamic factors

Conclusion

The results of data analysis showed deterioration reaction coefficients *a*, *b*, *c* before and during a seismic event. Periods recorded anomalies coincide with periods of strong earthquakes occurrence. Characteristic anomalies (amplitude, period coefficients *a*, *b*, *c*) are correlated with the strength of an earthquake. Speed method showed its suitability for imaging of the anomalous behaviour of water level during strong earthquakes.

Acknowledgments:

The authors thank the Rustaveli National Scientific foundation for financial support of the project #156/13 “Spatial and Temporal Variability of Geodynamical Field and Its Influence on the Deep Aquifers and Geomagnetic Field“.

References

- [1] Вартамян Г.С., Куликов Г.В. Гидрогеодеформационное поле Земли. - Доклад АН СССР, 262, N2, 1982.
- [2] Gavrilenko, P., G. Melikadze, T.Chelidze, D. Gibert & G. Kumsiashvili (2000) Permanent water level drop associated with Spitak Earthquake: Observations at Lisi Borehole (Republic of Georgia) and

- modelling. Geophys. J. Int., 143, 83-98.
- [3] Hsieh, P. A., I. D. Bredehoeft, S. A. Rojstaczer. Response of Well-Aquifer Systems to Earth Ties: Problems Revisited. Water resources Research vol. 24. No. 3. 1988, p.p. 468-472.
- [4] Rojstaczer, S. 1988. Intermediate period response of water wells to crustal strain: Sensitivity and noise level, J. Geophys. Res., 93, 13,387-12,402.
- [5] Melikadze G., Matcharashvili T., Chelidze T., Ghloni E. Earthquake related disturbance in stationarity of water level variation. Bulletin of the Academy of sciences of the Georgian, 165 № 1, 2002

Линейные методы изучения вариации уровня воды в связанных с сейсмичностью

Тамар Джимшеладзе, Георгий Меликадзе, Геннадий Кобзев

Резюме

В статье рассмотрены методы гидродинамических наблюдений для мониторинга тектонических процессов в режиме реального времени и выделения сейсмического компонента. Разработанные методы используются для выделения геодинимической составляющей из данных наблюдений с целью изучения закономерности ее распределения в пространстве и времени на больших площадях в процессе подготовки сильных землетрясений. Для обработки данных был разработан новый метод в среде MATLAB (программа RestDance), позволяющий синтезировать теоретический сигнал и сравнивать его с реальными данными уровня воды. В статье также рассмотрен метод скоростей и его значения для визуализации аномального поведения уровня воды во время сильных землетрясений.

მიწისძვრებთან დაკავშირებული წყლის დონის ვარიაციების შესწავლა წრფივი მეთოდებით

ჯიმშელაძე თამარი, მელიქაძე გიორგი, კობზევი გენადი

რეზიუმე

სტატიაში განხილულია ჰიდროდინამიური დაკვირვების სპეციალური მეთოდები, რომლებიც გამოიყენება რეალურ დროში, ტექტონიკური პროცესების მონიტორინგისა და სეისმური მდგენელების გამოყოფის მიზნით. შემუშავებული მეთოდიკა გამოიყენება დიდ ფართობზე ძლიერი მიწისძვრის მომზადების პროცესში, დაკვირვების მონაცემებიდან გეოდინამიკური მდგენელის გამოყოფისა და მისი დროსა და სივრცეში განაწილების კანონზომიერების დადგენის მიზნით. მონაცემთა დამუშავებისათვის შეიქმნა პროგრამა თ -ის გარემოში (პროგრამა ლესტ ანცე), რომელიც იძლევა საშუალებას მოვახდინოთ თეორიული სიგნალის სინთეზი და შევადაროთ იგი წყლის დონის რეალურ მნიშვნელობას. სტატიაში ასევე განხილულია “სიჩქარეები”-ს მეთოდი და მისი მნიშვნელობა წყლის დონის ანომალური ცვლილების ილუსტრირებისათვის ძლიერი მიწისძვრების დროს.

Hydrogeological and Speleometeorological Dynamics of the Prometheus and Sataplia Show-Caves, Imereti, Georgia

¹Martin Kralik, ² Rudolf Pavuza, ³ George Melikadze

¹ Environment Agency and University of Vienna, Vienna, Austria (Martin Kralik)

² Natural History Museum Vienna, Austria (Rudolf Pavuza)

³ Tbilisi State University, Tbilisi, Georgia (George Melikadze)

Abstract

Prometheus Cave

Water Dynamics

- Rainwater enters the cave relatively quickly at several places therefore guided cave tours should be stopped during strong and long lasting storms
- Water at the lower part of the cave runs as a small brook with a few litres per second (low flow first week of March 2014) up to approximately 1 cubic meter per second during strong floods
- During low water flow in March the microbiological contamination is high and in agreement with traces of artificial sweeteners and corrosion inhibitors indicating inflow of domestic waste water into the cave
- The recharge area of the cave waters should be mapped and waste water treatment of houses and farms in this area should be managed and monitored.

Speleometeorological Dynamics

A general summary of the situation in the Prometheus cave, based on the data already available and on experience from other comparable caves is as follows:

The overall status of the speleometeorological parameters at the given time-interval of investigation (March 2014) can be regarded as quite good with respect to the cave environment and the safety of the visitors. There was no significant enrichment of CO₂, which is mainly due to the natural ventilation, but certainly also due to the early season.

During the summertime CO₂ will increase due to natural causes (increased soil activity plus thermodynamic barrier against the outside air increases the influx of CO₂ into the cave through fissures) as well as due to the increased number of visitors. However, the diminishing, but most likely still existing ventilation will limit it to values that cause no significant threat to the environment and to the visitors. The result of these opposing effects is also documented by a slightly higher content of radon in the Prometheus Cave during the summer months (Vaupotic et al. 2012).

Nevertheless - to remain on the safe side – a modelling of the CO₂ development under changed boundary conditions was performed, with pessimistic boundary conditions and assumptions as well as a more realistic scenario. Taking also research and experiences in other show caves into account, a serious threat to both visitors and the caves is unlikely as long as some simple precautions are taken during the touristic peak season and high outside temperatures.

In our opinion the natural air movement, which could be enhanced by opening doors for two to three hours during the evening hours or during night time (depending on the necessary safety measures) in the summer season, should be sufficient to stay on the safe side.

The inflow of outside air (the relative humidity of which is lower than the cave air) is no threat to the cave atmosphere or the speleothems during the summer season because its relative humidity will increase due to lower water saturation of colder air.

A simple and reliable tool to measure the CO₂ content of the air during the peak season could be DRAEGER diffusion tubes (we used that during our measurements in Marchin addition to direct measurements) for longer measuring periods (> 12 hours) or simple CO₂-monitors for instant measurements. A continuous and much more expensive CO₂-online-measurement equipment is not essential.

Electric cave lighting

In the Prometheus cave sophisticated cave lighting has been installed. Whereas the position of the lighting elements causes no trouble, the lighting colours do, at least in part.

Looking at the wavelengths of optimal lampenflora growth (Fig. 1) – due to the absorption of special wavelength of light – and the spectrum of different LEDs, one can see that especially blue colours and, to a certain degree, red colours should be avoided to reduce at least the growth of mosses and green algae. Blue green algae (being bacteria in fact) cannot be restrained much in that way but cause less trouble than the other kind of lampenflora. White LED is close to the critical wavelengths too, but are acceptable as long as the light intensity close to the lamps is not too high. Simple devices like light shades might be helpful in this case.

We propose especially to avoid blue colours entirely and reduce the red ones to a minimum.

Besides that any reduction of overall lighting times (turning off the lights in sections not visited at the moment would be most effective) would help to reduce the lampenflora, which appears to be a more serious threat to the cave environment and the speleothems than the visitors are.

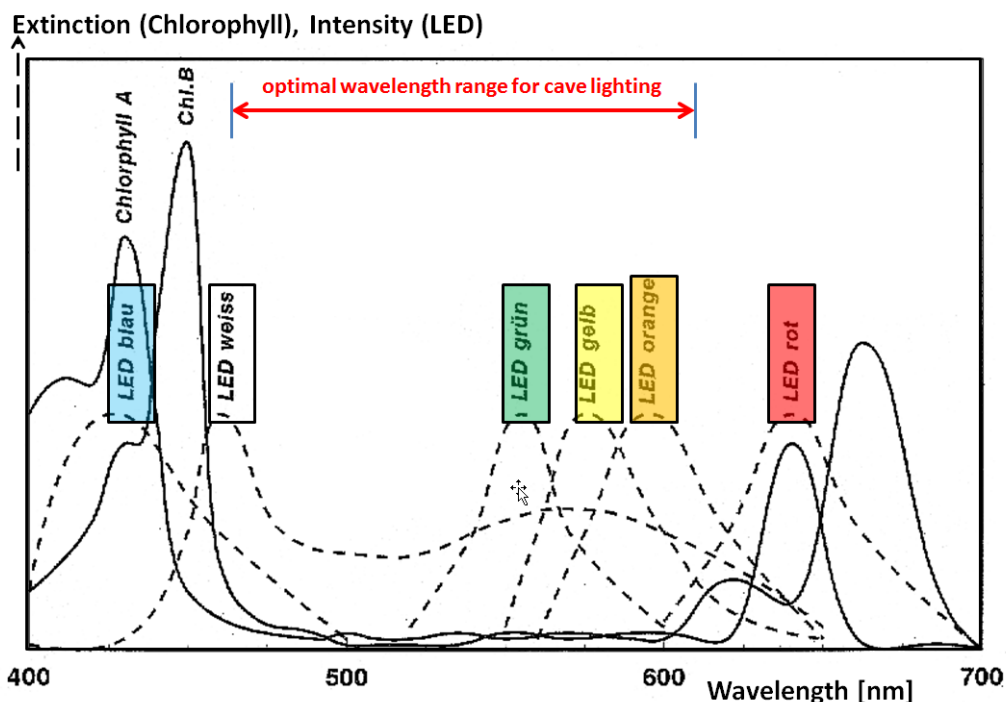


Figure 1 Light spectra of Chlorophyll A and B and spectra of different LED colours. Blue = blau, white = weiss, green = grün, yellow = gelb, orange = orange, red = rot, from Pavuza, Mais&Cech (2002).

Sataplia Cave

Only a reconnaissance investigation was performed on the water flow and the cave climate of the Sataplia Cave. At the director's option no water flow monitoring was installed. Nevertheless, a few preliminary findings are documented here.

Water Dynamics

- Due to the higher altitude and the smaller recharge area the water flow in the cave was significantly cooler (8.5° C) and the flow much lower (1.5 L/s) than in the Prometheus Cave during the first week of March 2014.
- Due to volcanic rocks in addition to karstified carbonate rocks in the recharge area the water composition is less mineralised, but more enriched in magnesium (Mg), sodium (Na), iron (Fe), aluminium (Al) and silica (Si) compared to the one in the Prometheus cave.
- The microbiological contamination was also high in March 2014, but no indicator for domestic waste water could be found. Therefore the microbiological indicators should be monitored over one year to clarify, if the contamination comes from animals living in the recharge area or has other sources.

Speleometeorological Dynamics

Most probably due to the adjacent volcanic rocks, which are also abundant as allochthonous cave sediments in the Sataplia Cave, the gamma-radiation was significantly higher than in the Prometheus Cave (124 against 71 nSv/h – outside values ~ 130 nSv/h). Unfortunately – as all devices had to be used in the Prometheus – we had only the possibility to measure radon daughter products (EEC – Equilibrium Equivalent Concentration = radon-222 progeny concentration) once. The results, being significantly lower than in the Prometheus Cave, point towards a more active ventilation in this cave at least at the time of the measurements.

Introduction

The Imereti Caves Protected Areas include a number of caves in Tskaltubo, Terjola, Tkibuli and Khoni districts. Each of the caves culturally rich, unique and interesting for its characteristics.

Prometheus Cave, located close to the village Kumistavi 20 km north of Kutaisi, in Tskaltubo district (Figure 2), is 20,000 meters in length; however, the tourist pedestrian path is only 1,420 meters. The temperature inside at any time of the year is 14-17°C degrees, the water temperature is 13-14°C and humidity is 97-98%, while the oxygen content in the air is 21%.

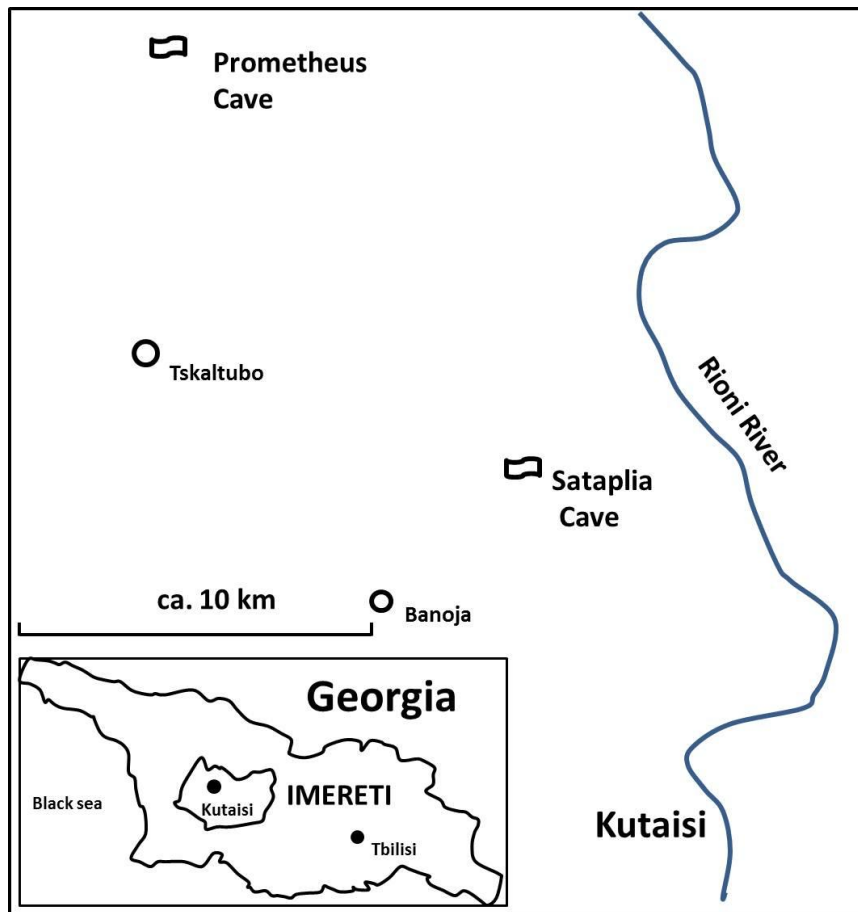


Figure 2 Survey map of the investigated area

Prometheus Cave was discovered in 1983 by the Vakhushti Bagrationi's university team, led by Jumber Jishkariani. In 2011, the cave was visited by 70,331 visitors in total (Georgia today, 2013). Within a short time work was carried out in the 1,060m section of the main cave (Attraction Highway); concrete paths were constructed, bridge-flyovers were built, viewing platforms were prepared and an additional tunnel was cut to facilitate discharge of the cave water flows (Tsikarishvili et al. 2010).

Sataplia Cave is located in Sataplia Nature Reserve, which has a size of 354ha and is located 10km north of Kutaisi (Figure 2). The nature reserves are on the extinct volcano Mt. Sataplia (494m asl). Sataplia Cave was first discovered in 1925. The show path is 309m long; the temperature inside the cave is 12-13°C; the cave receives around 90,000 visitors/per year). A few hundred metres from the cave entrance are footprints of dinosaurs: about 200 footprints have been located, found in two different layers of the Cretaceous limestones (first discovered 1933). The 30cm long footprints of the lower layer belong to an unknown predator; the 48cm long footprints of the upper layer belong to an ornithomimid herbivore (<http://www.showcaves.com/english/ge/showcaves/Sataplia.html>).

The investigations which is the subject of this report were performed in the framework of the EU Twinning project (GE12/ENP-PCA/EN/14) "Strengthening Management of Protected Areas of Georgia". One of the project's tasks is to elaborate a management plan for Imereti Caves Protected Areas. The quantification of the water dynamic and the speleometeorological conditions in Prometheus Cave and Sataplia Cave were selected as special topics for further investigation during a preliminary visit in 2013.

Hydrogeology

Tskhaltubo artesian basin of porous, fracture, fracture -karst and karst waters covers mainly the Lower Imereti plain and its adjacent Samguruli ridge. The mentioned district is

composed by Mesozoic-Cenozoic sediments forming wide folds in a flat part and is uplifting to the north-east on the Samguruli ridge. The Cretaceous, Paleogene and Neogene strata compose Lower Imereti syncline, which is sandwiched between the northern ridges of Adjara-Imereti Range and the southern foot of Samegrelo anticlinal ridge.

Here, as well as in surrounding areas, there is well traced the main artesian horizons: Lower Cretaceous limestones, Upper Cretaceous and Paleogene limestones and Quaternary sand and gravel deposits.

The Lower Cretaceous limestone aquifer contains pressured fracture and fracture-karst groundwater. The biggest deposit of these waters are in Tskhaltubo area, which are weakly radioactive. The outputs of these waters are confined to the gentle anticlinal fold. Here, under the slight layer of Quaternary sands and clays deposited marls of Aptian stage, and under them thick aquifers of Valanginian-Barremian limestones. Chemically Tskhaltubo water is very close to the pressured waters of Lower Cretaceous limestone horizon, developed in the artesian basins in Western Georgia. Their distinguishing features are the radioactivity and the high debit (200-220 l/s). The gas composition is dominated by atmospheric nitrogen.

Climate

Long term data of the Kutaisi meteorological station show a mean temperature of 13.5 °C and an annual precipitation of 1322 mm. The amount of the mean monthly precipitation is lowest in spring and summer months. In January and March 2014 the monthly precipitation was with more than 160mm particular high (Figure 3).

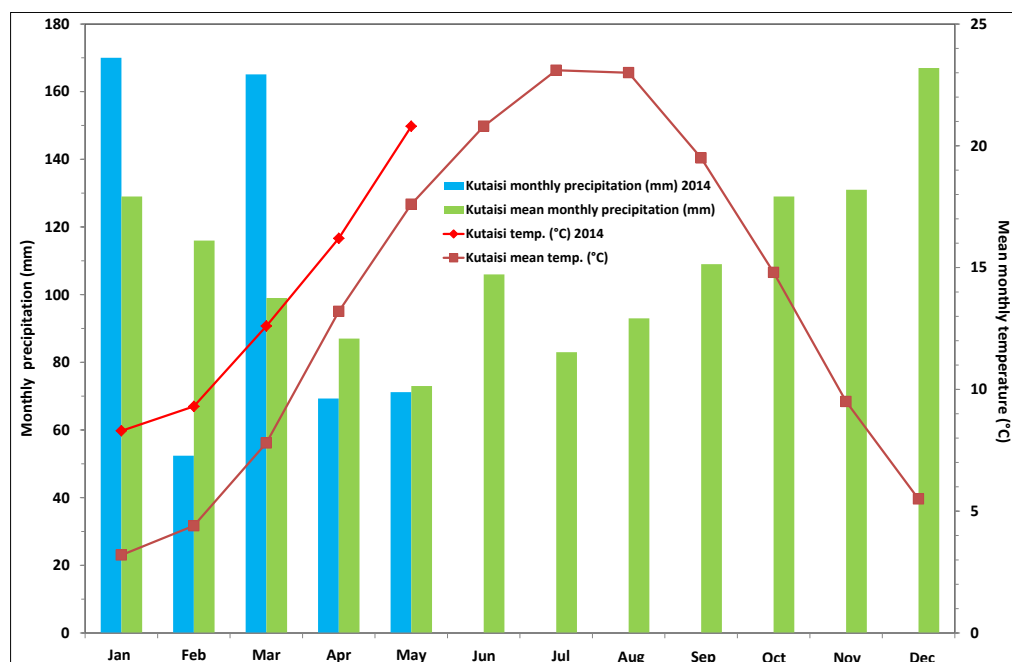


Figure 3 Monthly precipitation sum 2014 compared to mean precipitation (http://en.climate-data.org/location/2079/_140924) compared to mean temperature of the Kutaisi meteorological station (156 m altitude).

Methods

Rain collectors (Palmex Corp.) with minimized evaporation (Gröning et al. 2013) for daily or monthly measurements by means of a measuring cylinder were installed close to the visitor centres of the Prometheus and Sataplia caves in March 2014 (Figure 4).

The discharge of the brooks in the caves was measured in the Prometheus Cave by a combination of a water level gauge board and a capacitance water level recorder (Odyssee Corp.) (Figure 5). The discharge measurements were calibrated by salt dilution measurements

(Hudson & Fraser 2005). Discharge in the Sataplia Cave was measured by a beaker and stop watch.

All stable isotope samples of the precipitation and cave brooks were analysed by laser-spectroscopy (CRDS – System, Types L1102-i Picarro) at the University of Vienna.



Figure 4 Palmex rain collector (2014/2240
GW84: 42.60105°E 42,37688°N 180m) installed
next to the visitor centre of Prometheus Cave
©Foto: M. Kralik



For all the samples water temperature, conductivity and pH (WTW Multiline P4-meter) was measured after calibration in the field. The major ions, the trace elements and the microbiological parameters were measured at the Austrian Institute of Technology.

Dissolved silica was analysed at the Museum of Natural History Vienna (colorimetric, with SQ300 Photometer/Merck). Selected organic tracers as indicators for domestic waste water were measured by the Environmental Agency Austria by a combination of gas-chromatography and mass-spectrometry.

Radon and EEC was measured with Doseman/DosemanPro (Sarad, Dresden), SunNuclear 1028 Continuous Radon Monitor) and Kodalpha Dosimeters (GT-Analytic, Lambesc, France), and CO₂ with Diffusion Tubes (Draeger) and AirCO₂ontrol 3000 (Dostmann), Gamma Radiation by GMZ-dosimeters, temperature by Data-Loggers (Testo174) and calibrated electronic thermometers. Radon (Rn) in water was determined in Vienna (Radim 3-W; SMM Prague) and empirically back calculated to the field value.

Results

Water Dynamics

Discharge measurements

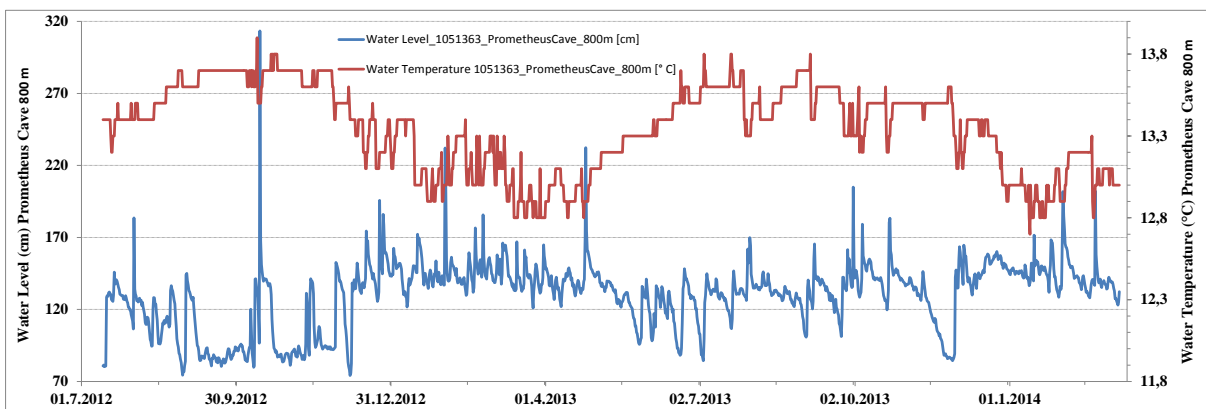
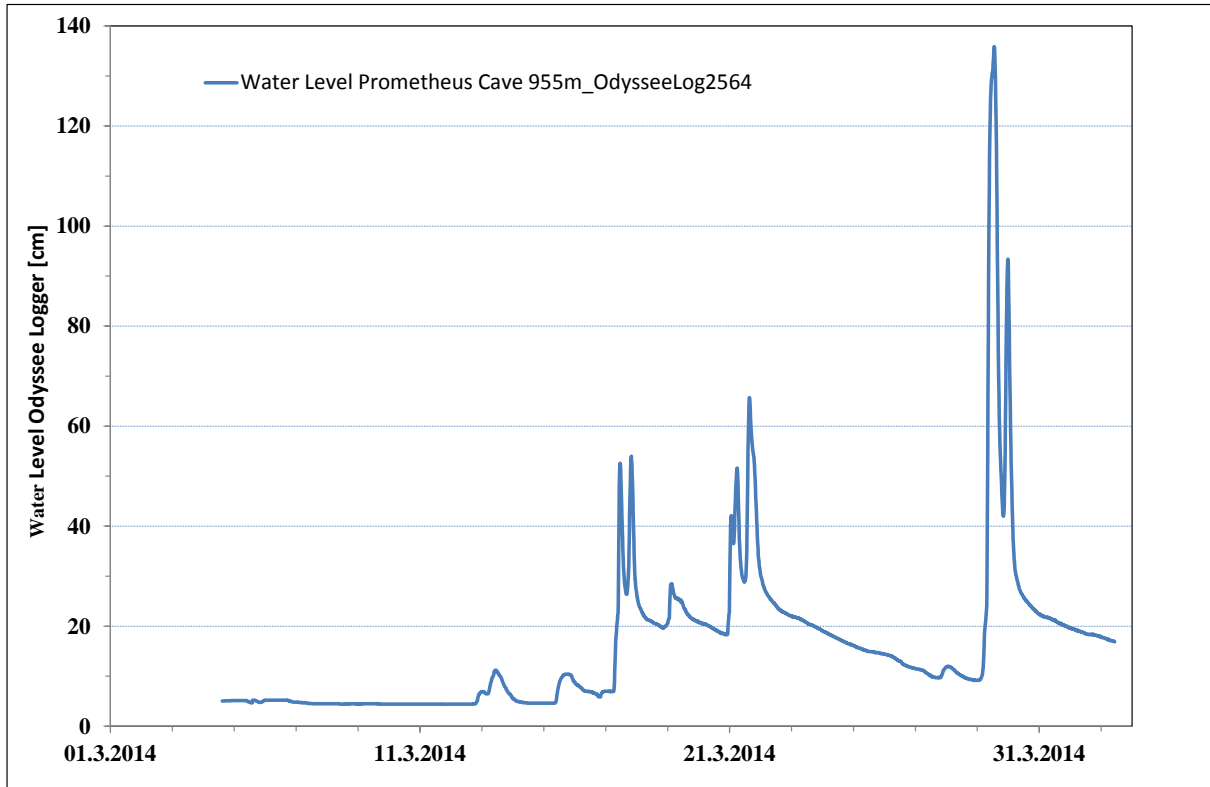
After installation of the water level gauge board and the capacitance water level recorder in the Prometheus Cave (Figure 5) the discharge of the brook were measured in the range of 12 – 138 L/s several times in March and April by the salt dilution method (Table 1).

Table 1 Salt dilution measurements of discharge of the brook in the Prometheus Cave

<i>Sampling site</i>	<i>Date</i>	<i>NaCl l kg</i>	<i>Water Temp. °C</i>	<i>EC¹ μS cm⁻¹</i>	<i>Water Level m</i>	<i>Discharge L s⁻¹</i>	<i>Velocity m/s</i>
Prometheus Cave							
Grove of Aresi bridge at 955 m	4.3.2014 16:15	0.5	13.2	354	4.5	15	0.08
Grove of Aresi bridge at 955 m	5.3.2014 14:00	0.5	13.2	358	3.5	14	0.07
Grove of Aresi bridge at 955 m	7.3.2014 13:30	0.5	13.2	355	3.5	12	0.08
Grove of Aresi bridge at 955 m	2.4.2014 12:00	0.5	13.1	249	19	138	

¹EC: Electric Conductivity;

Water Level recorded in the brook in the Prometheus Cave at 955 m (between sites 8/9 in Figure 6) shows several quick water level changes (up to 1.25 m in ca. 10h) during March 2014 (Figure 7). An earlier installed water level recorder at site 1 (ca. 800 m, Figure 8) shows similar rapid changes in water level from summer 2012 till March 2014. The water temperature varies between winter and summer in the range of 12.9 to 13.7°C. During rapid level changes the water temperature changes about 0.1-0.2°C in winter down to 12.7°C and in summer up to 13.9°C.



The precipitation next to the Prometheus visitor centre, and the waters of the Prometheus, Sataplia and Opichum Cave (small cave close to the Prometheus Cave) were analysed for water temperature, electric conductivity (EC), pH, oxygen-18 and hydrogen-2 composition (Table 2). The water temperature in the Sataplia Cave (ca. 400 m asl) is significantly lower than in the Prometheus (ca. 150 m asl) and Opichum Caves due to the higher altitude. The electrical conductivity of the water in the Sataplia Cave is significantly lower than in the Prometheus Cave due to the mixture of volcanic and carbonate rocks.

Table 2 Oxygen-18 (^{18}O) and deuterium (2H) values in the waters of Prometheus and Sataplia Cave

<i>Sampling site</i>	<i>Date</i>	<i>Discharge $L s^{-1}$</i>	<i>Water Temp. $^{\circ}C$</i>	<i>EC¹ $\mu S cm^{-1}$</i>	<i>pH</i>	<i>$\delta^{18}O$ SMO W ‰</i>	<i>δ^2H SMO W ‰</i>
Prometheus Cave							
Precipitation next to visitor center ²	3.3.2014 14:53- 1.4.2014 12:00					-9.75	-65.8
No.4 Quick dripping sword like stalagmite	3.3.2014 14:00	0.004	15.3	467	8.1 3	-9.77	-64.5
No.1 Siphon with groundwater at 850 m	3.3.2014 14:00	10	13.3	361	7.3 0	-10.15	-65.8
No.1 Siphon with groundwater at 850 m	8.3.2014 09:15	10	13.3	360	7.4 5	-9.98	-65.5
No.8 Grove of Aresi brook 7m away from footpath	3.3.2014 16:30	10	13.3	361	7.4 0	-9.54	-62.5
No.9 Water at the start of boat exit	3.3.2014 16:45		13.3	365	7.5 2	-10.10	-65.9
Well next to Visitor Centre 100 m depth	7.3.2014 16:00		14.3	467	7.5 5	-9.98	-65.4
Sataplia Cave							
Right of footpath just before exit	6.3.2014 14:30	1.5	9.6	256	7.8 6	-10.35	-68.1
Right of footpath just before exit	8.3.2014 10:10	1.5	8.9	265	8.0 3	-10.39	-67.4
Opichum Cave							
Small spring left of cave entrance	5.3.2014 17:00	2.5	14.2	545	7.2 6	-9.86	-65.0

¹EC: Electric Conductivity; ²Palmex rain collector No. 2240 GW84: 42.60105°E 42,37688°N 180m

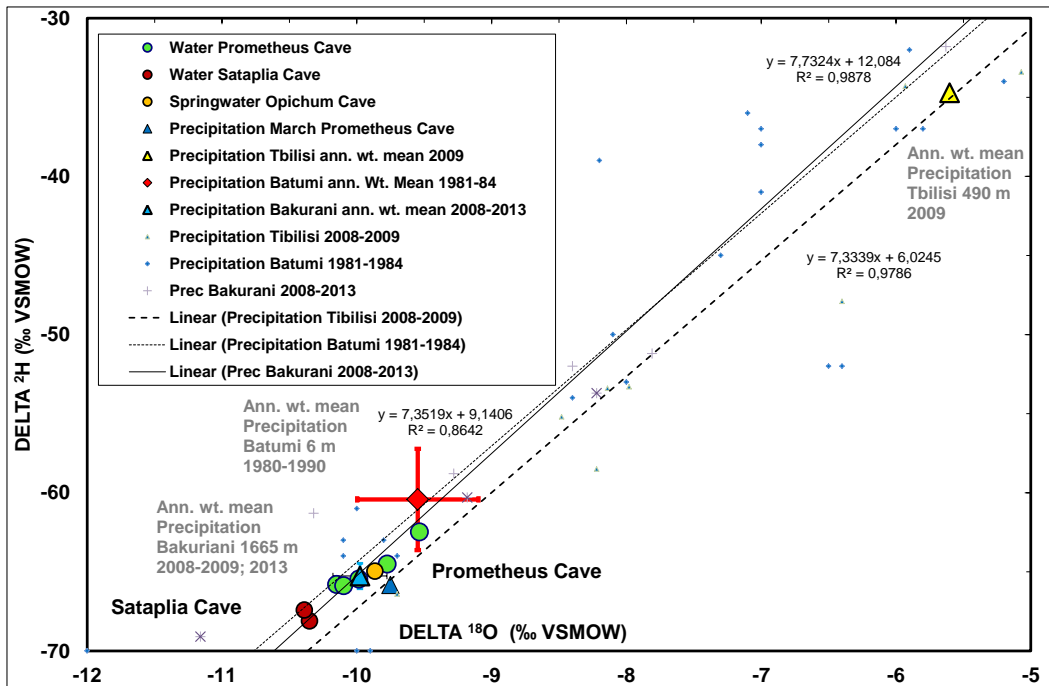


Figure 9 Delta Oxygen-18 vs. hydrogen-2 of the waters of the Prometheus and Sataplia cave compared to the weighted mean precipitation data (GNIP 2014) of the Bakuriani (1665m) Batumi (6 m) and Tbilisi (490 m) station.

The delta oxygen-18 and hydrogen -2 values of the waters of the Prometheus Cave vary between δ -10,2– -9,5 ‰ and -68,1– -62,4 ‰. Significantly, one water sample in the brook in the Grove of Aresi (Table 2 and Figure 9) is different. The mean precipitation of March and the spring water of the Opichum Cave have similar values. The water samples of the Sataplia Cave show lower δ ¹⁸O (-10.39 to -10.34 ‰) and δ ²H (-68.1 to -67.4 ‰) values due to their higher altitude.

Table 3 Chemistry and microbiology of two water samples from the Prometheus and Sataplia Cave

Parameter	Concentrations	Prometheus Cave	Sataplia Cave
No.		No. 1	SC
Sampling site		Siphon with groundwater at 850 m	just right of exit
Sampling date		08.03.14 09:10	08.03.14 10:10
Discharge	(L/s)	12.0	1.5
Color		slightly brown/susp. matter	slightly brown/susp. matter
smell		no	no
Water Temp.	(° C)	13.3	8.9
EC ³ (25°)	(μS/cm)	360	265

pH		7.45	8.03
Ca	(mg/l)	69.2	45.3
Mg	(mg/l)	9.7	10.5
Na	(mg/l)	1.70	4.30
K	(mg/l)	0.50	0.50
HCO ₃	(mg/l)	259.1	190.3
SO ₄	(mg/l)	4.2	4.9
Cl	(mg/l)	1.4	1.6
NO ₃	(mg/l)	4.4	4.4
Sum	(mg/l)	350.2	261.8
Cations	mmol (eq)/l	4.337	3.323
Anions	mmol (eq)/l	4.447	3.339
Cation.-Anion.	[%]	-2.5	-0.5
Ca/Mg		7.13	4.31
Na/Cl		1.21	2.69
Na/K		3.40	8.60
SiO ₂ ²	(mg/l)	4.0	11.3
PO ₄	(mg/l)	<0.5	<0.5
Fe	(mg/l)	0.05	0.11
Mn	(mg/l)	<0.001	0,001
Zn	(µg/l)	<50	<50
Cu	(µg/l)	<10	<10
Al	(mg/l)	0.08	0.14
F	(mg/l)	<0.5	<0.5
Cd	(µg/L)	<1	<1
Cr	(µg/L)	<5	<5
Li	(µg/L)	<5	<5
Mo	(µg/L)	<5	<5
Ni	(µg/L)	<5	<5
Pb	(µg/L)	<2	<2
KBE 22°C	Anz./1 ml	880	1600
KBE 37°C	Anz./1 ml	220	120
Escherichia coli	Anz./100 ml	100	44
coliforme Bakterien	Anz./100 ml	100	108
Entero-kokken	Anz./100 ml	50	45
Pseudomonas aeruginosa	Anz./100 ml	2	0

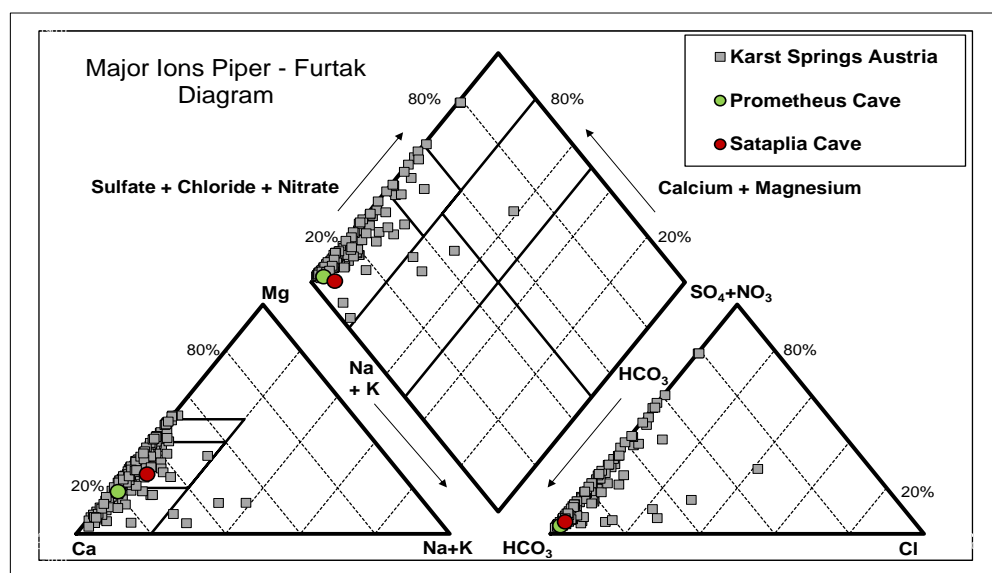
¹ Analyst: Aqua Test, Austrian Institute of Technology; ² Analyst: R. Pavuza; ³ EC: Electric Conductivity.

The main ion composition of the water samples of the brooks in the Prometheus and Sataplia Cave is very similar to common karst water composition (e.g. the mean of Austrian karst springs).

The water of the Sataplia Cave is significantly lower in the ion sum but higher in magnesium (Mg), sodium (Na), iron (Fe), aluminium (Al) and silica (Si) (Table 3 and Figure 10).

Both water samples show a high concentration of specific cultivatable bacteria (e.g. Escherichia coli) indicating impacts of excretion mammals or human beings.

From the same brooks analyses were made of a set of waste water indicators which frequently occur in waste water of modern households (Table 4): Artificial sugars (acesulfam, sucralose), corrosion inhibitors (1H-benzotriazole and tolyltriazole) and pharmaceuticals (e.g. carbamazepine, sotalol, metoprolol). Acesulfam and 1H-benzotriazole were detected in the brook water of the Prometheus Cave, whereas in the brook waters of the Sataplia Cave all these indicators



are below detection limits.

Table 4 Waste water indicator test of brook waters in the caves

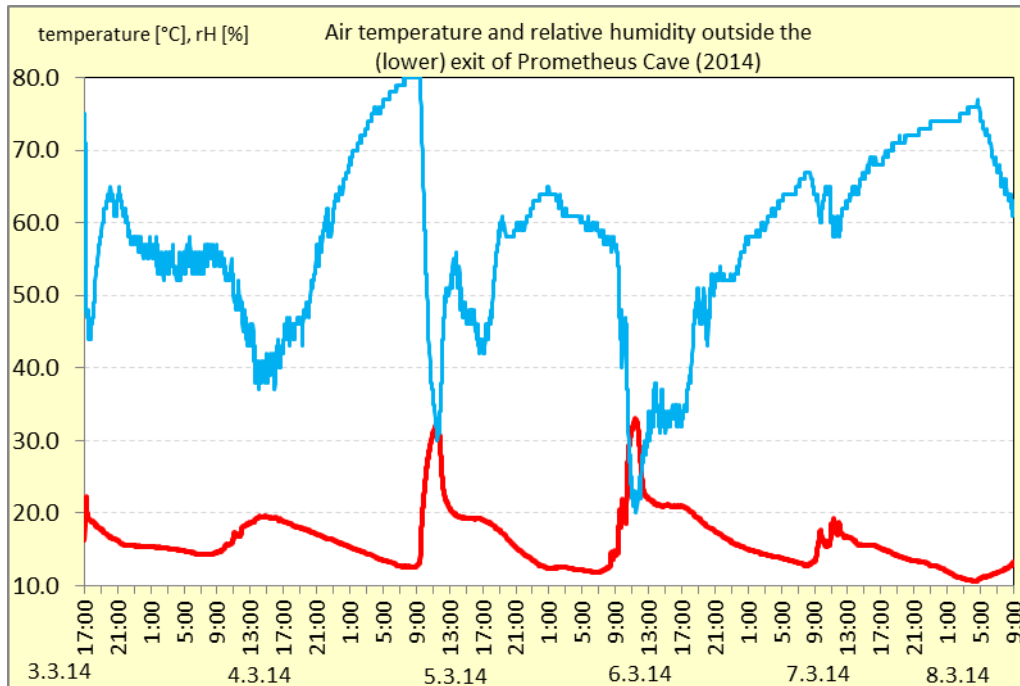
Sampling site	Date	Ace-sulfa m ng/L	Sucr a- lose ng/L	Tolyl- triazol e ng/L	Carba ma- zepine ng/L	1H- Benzo - triazol e ng/L	Sota - lol ng/L	Met o- Prol ol ng/L	CBZ - DiO H ng/L
Prometheus	8 3 2014	20	<5	<5	<0.5	180	<2	<2.5	<2
Satanlia Exit	8 3 2014	<2.5	<5	<5	<0.5	<5	<2	<2.5	<2
Detection		2.5	5	5	0.5	5	2	2.5	2
Limit of		5	10	10	1	10	4	5	4

Analyst: Kulcsar & Schuster, Environment Agency Austria

Measurements of speleometeorological parameters

Between March 3rd and 8th 2014 single and continuous measurements of temperature, radon, radon daughter products (EEC), gamma-radioactivity, CO₂, relative humidity, air pressure and air velocity were conducted at different sites in the Prometheus Cave (see Figure 6).

The outside temperature and humidity (Figure 11) was primarily measured to check whether lower night temperatures do have an influence on the air movement in the cave. It turned out that during



the night hours the outside temperature dropped below the cave temperature and a reverse air movement (from the boat exit into the cave) developed, characterised by sharp drops of air temperatures at the very sensitive measuring device in the Amphitheatre Hall, adjacent to the boat exit (Figure 12).

This night-time inflow of comparatively cold and therefore more humid air (relative humidity 60-80 %) into the cave became more saturated (most probably up to ~ 100 %) by passing over the water body in the boat passage. Therefore, this does not have any effect on the relative humidity (which is usually close to 100 %) in the cave.

It further turned out that in the Amphitheatre Hall the air movement – and therefore the influence of

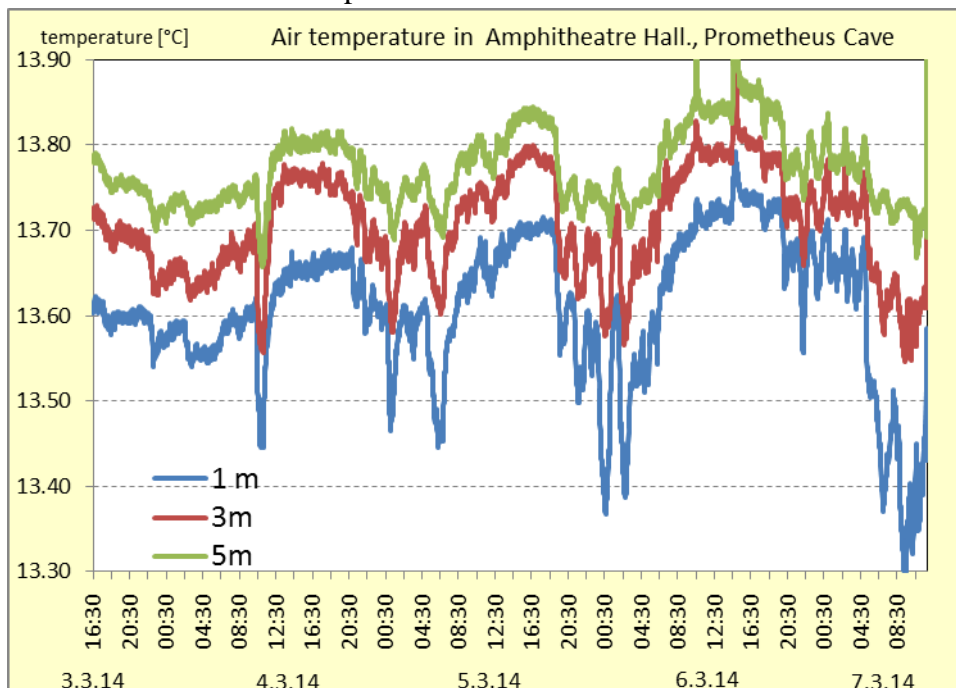


Figure 12 High precision measurement of air temperature at different heights in the Prometheus Cave

the inflowing air during the night – was higher in the lower part of this big chamber. The average temperature increased in the upper part, but stayed more constant (the standard deviation decreases, see Figure 12). As the correlation is nearly linear, a slow and non-turbulent air flow is most likely.

Investigating the average temperatures of the period March 3rd to 7th 2014 of different points within the cave a striking decrease near the emergence (“spring”) of the cave brook (between points 7 and 8, see Figure 6) can be observed (Figure 13). The lower temperature of the brook water (ca. 1 degree lower than the air temperature at the higher parts of the cave) yields a significantly cooling of the cave air. The stratification of air within the cave complex (colder air below warmer air in the cave and much warmer air outside) results in a stronger air flow during the day. The pedestrian exit

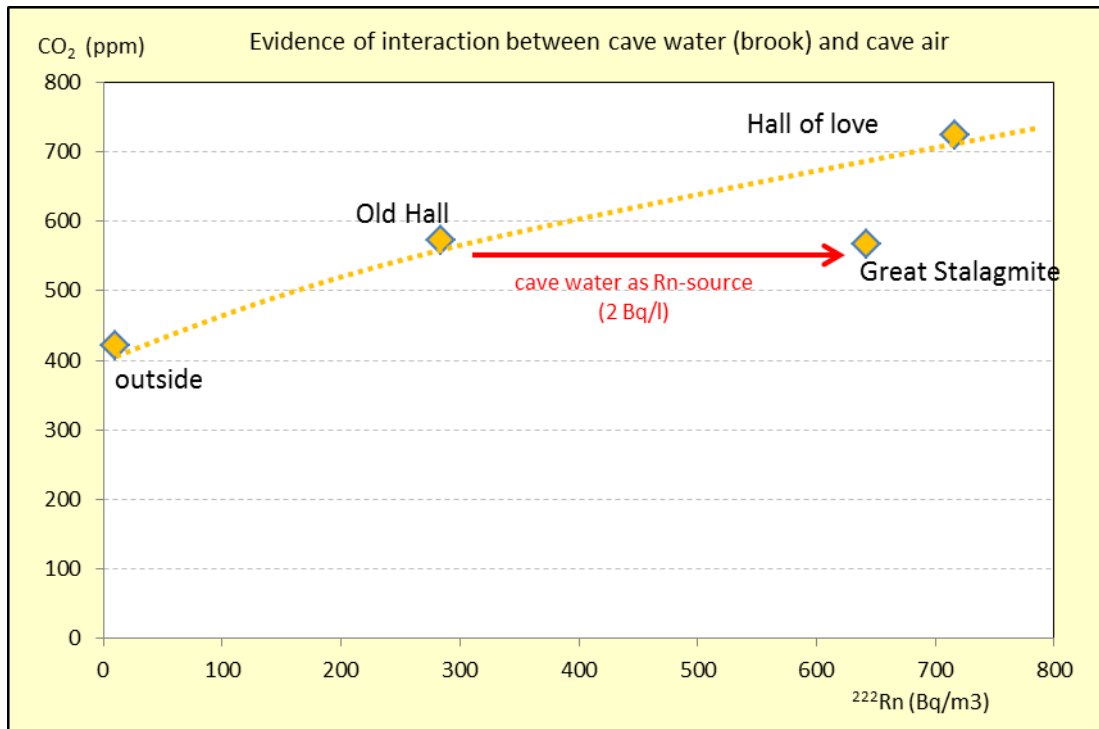


Figure 13 Average radon activity and CO₂ contents in the Prometheus Cave (March 2014)

tunnel on the other hand – entirely isolated from the cooler cave brook and lake – shows a similar temperature average as the higher parts of the cave.

Taking average CO₂ values (ppm) as well as ^{222}Rn activities (Bq/m³) into account (Figure 14), one can see an increase of both parameters along the path from the upper entrance to the lower exit. This relation is disturbed again – like the air temperature, see above – close to the inflow of the brook water (“spring”) into the cave. This water yields 2 Bq/m³ (which is slightly radon-oversaturated with respect to the cave air), leading to an abrupt increase of ^{222}Rn in the cave air at this point and implying that in the remaining part of the cave the cave brook dominates the behaviour of ^{222}Rn in air.

This is most significant near the beginning of the boat exit, where a radon-datalogger has been placed during the measuring period (Figure 15).

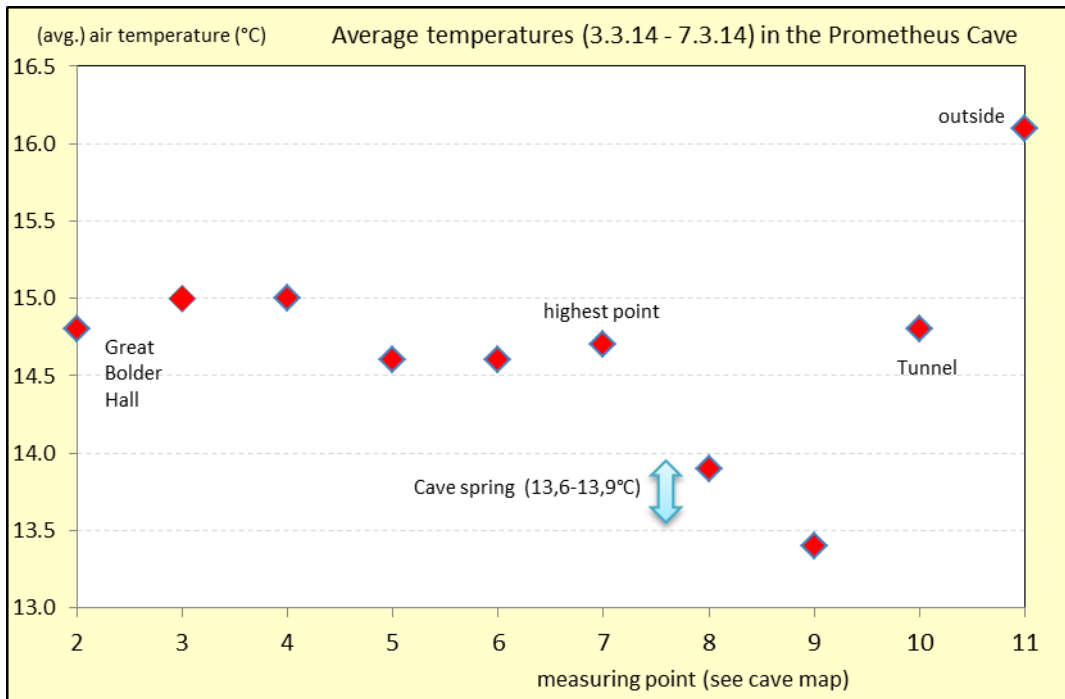
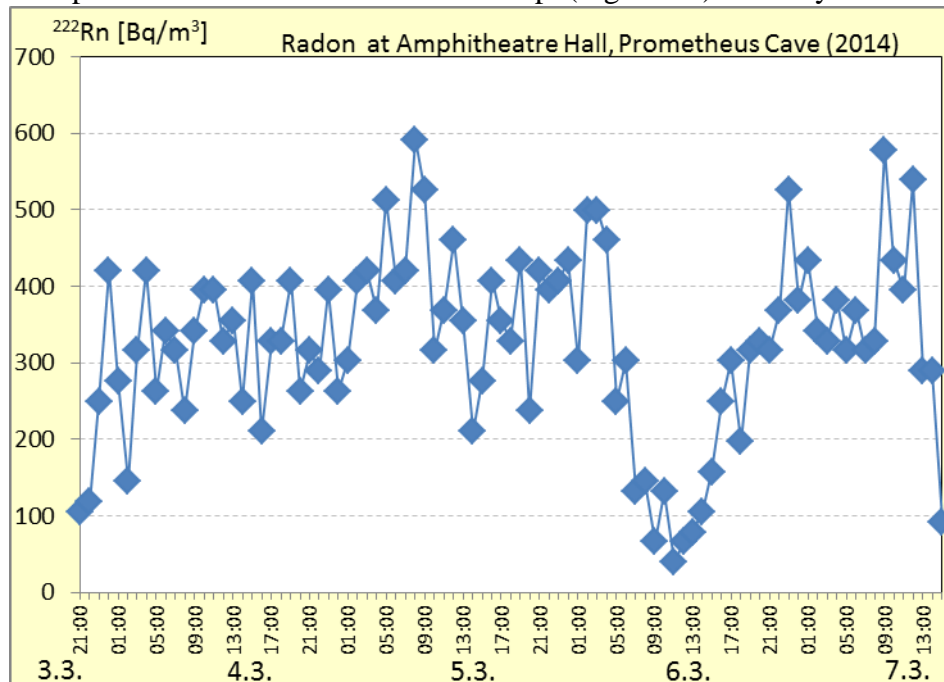


Figure 14 Average values of air temperatures at different sites in the Prometheus Cave



In contrast to the temperature, radon did not generally indicate the inflow of air during the night hours in the Amphitheatre Hall near the boat ramp (Figure 16): usually radon is much more



sensitive to air movements than the air temperature and low values of ²²²Rn should arise therefore during the night hours.

This is not the case in this part of the Prometheus Cave, leading to the conclusion that the ²²²Rn activity in the cave air is almost entirely influenced by the radon - degassing of the lake as the cave brook – feeding the lake – showed a slightly elevated radon-222 activity with respect to the cave air. The distinct decrease of radon, starting in the morning hours of March 6th (Figure 16), on the other hand, shows the limits of the degassing process: during that particular night the inflow of air was more significant than in the previous nights (Figure 11), the increased volume of inflowing air more than offset the effect of radon-degassing – which diminishes along the flow path anyway.

No fast air pressure variations – which usually lead to abrupt alterations of Rn-values - could be observed during the measurement period (Figure 17), indicating that the variation of outside temperatures was the driving force for air movements and variations of temperature and radon in the Prometheus Cave.

Discussion

Water Dynamics and Water Quality of the Prometheus Cave

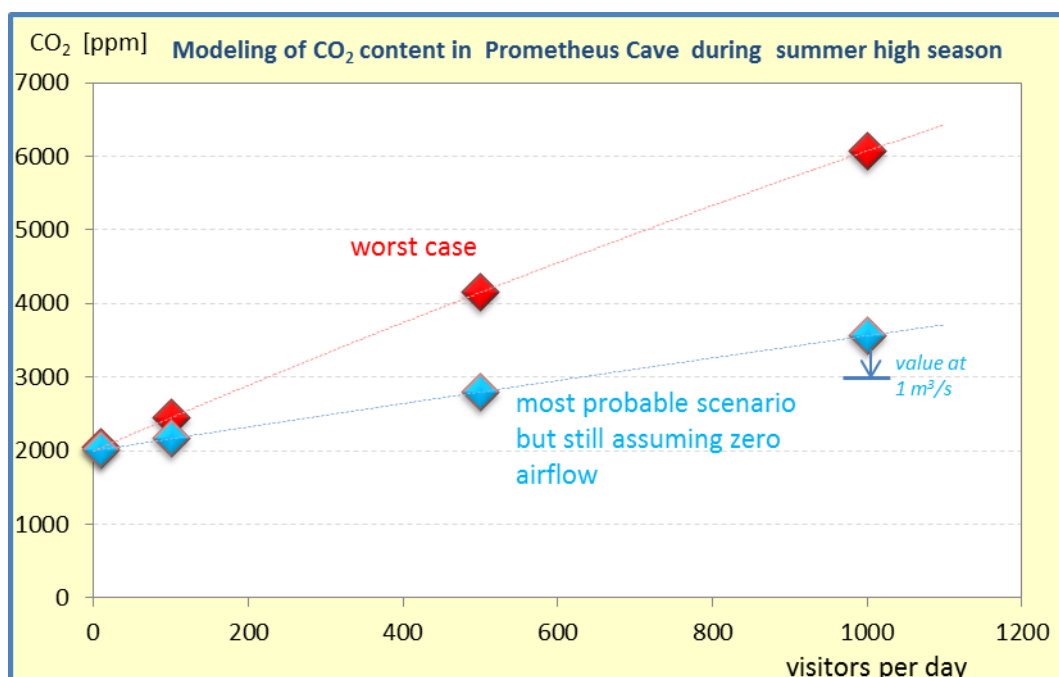
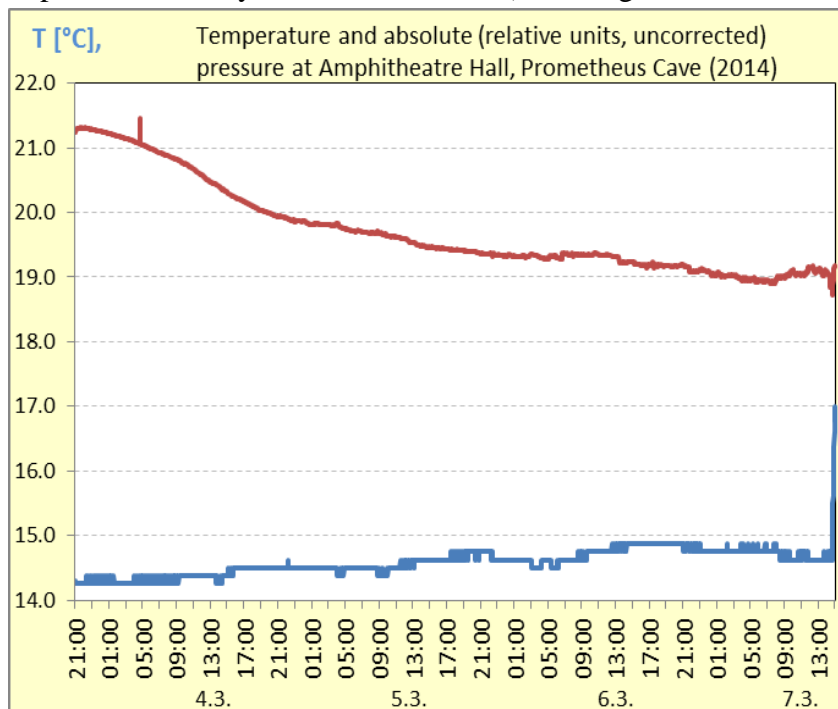
Water enters in the upper part of the cave (until up to 800 m, site 1 Figure 6) at a very small rates as dripping stalagmites. At the site 1 (800m) water flows via a siphon at dry periods at a rate of several litres per second. During strong and longer rain storms the water discharge rate in the brook seems to rise over the period of hours up to several hundreds of litres per second (Table 1; Figure 7-8).

The similar $\delta^{18}\text{O}$ values of the precipitation of March and the brook water in the cave indicate that both are from precipitation of the winter half-year (Oct. – Mar.) and lower than the weighted yearly mean of Batumi (Figure 9). However, the water sample in the brook in the Grove of Aresi with a $\delta^{18}\text{O}$ values of -9.54‰ is significantly different to the rest of the brook water samples (-9.98‰ – -10.15‰) indicating at least two major infiltration areas of the brook water.

The major ion composition is characteristic for karst water in contact with a dolomitic limestone with no obvious contamination. However, the microbiological analyses indicate a certain contamination by humans or mammals. The artificial sweetener acesulfam and the corrosion inhibitor 1H-benzotriazole support the assumption that some domestic waste water enters the Prometheus cave. Microbiological contamination and waste water may have a negative effect on the stalagmites and the ecological habitat of the cave. Due to the low flow (12-14L/s) during sampling the concentrations may be higher than normal, but during summer time the concentration could be influenced by a large number of visitors as well.

Air Dynamics of the Prometheus Cave

Prometheus Cave is a moderately ventilated cave, showing increased CO₂ and Rn with respect to the outside air and slightly elevated radon daughter products (EEC; Equilibrium factor > 0.5). These values are comparable to many other show caves (including some in Austria). At the time of the



investigation (March) the air movement was certainly higher than it usually is during the summer months due to lower outside temperatures in spring time. Therefore an increase of both parameters (CO₂ and Rn) is likely. However earlier measurements as well as modelling tests indicate that the values still stay in ranges that are not dangerous to visitors, staff and the cave environment. The radon content seems to be influenced by the ventilation and the degassing of the brook water in the cave. Additional measurements at times of very high and very low outside temperatures might enhance the validity of these conclusions.

Modelling approach for summer high-season CO₂ in the Prometheus Cave air

In order to evaluate the influence of visitors to the CO₂ content of the Prometheus Cave some measurements, published and unpublished data and – in general – very pessimistic assumptions (“worst case scenario”) were used for a modelling procedure:

Air volume of the cave: length 1000 m, average cross section 50 m² > minimum cave air volume 50 000 m³

Air flow (summer high season): none (4/2014: 1 – 2 m³/h near the upper entrance)

Average CO₂ content of exhaled respiratory air: 40 000 ppm (wikipedia)

Average CO₂ content of cave air before opening: 2 000 ppm 4/2014 max. 750 ppm

5/2013 avg. 1100 ppm (unpubl. Czech data)

6/2013 avg. 1600 ppm (unpubl. Czech data)

11/2013 avg. 800 ppm (unpubl. Czech data)

Respiratory volume per visitor (strong breathing): 6 m³/hour
(www.msporting.com/planung/4_2_2%20Athem.htm)

Length of stay per visitor: 1 hour

A second modelling was done with a “most probable scenario” data (cave air volume 70 000 m³, respiratory volume per visitor 3 m³/h, but still assuming no airflow within the cave.

Finally a single point modelling for an airflow value of 1 m³/s, taking 8 hours of guided tours into account was done too (Figure 18).

This brief modelling with some pessimistic assumptions yields maximum CO₂ contents of some 5,000 ppm assuming that there is no airflow even with doors open, which is not likely. The measured airflow during springtime of 1-2 m³ per second (even with closed doors) would enable an air exchange to a large extent e.g. during the late evening. Anyway, 5,000 ppm would not cause a danger to visitors (5,000 ppm is the maximum CO₂ concentration for working space in Austria and Germany – for an average 8 hours working day).

In some Austrian show caves – like Eisensteinhöhle (Lower Austria) and Grasslhöhle (Styria) - these values are exceeded during the summer season. In show caves in Western Australia CO₂ values are getting sometimes much higher and visitors may have some breathing problems. This will not happen even at pessimistic 5,000 ppm in the Prometheus Cave.

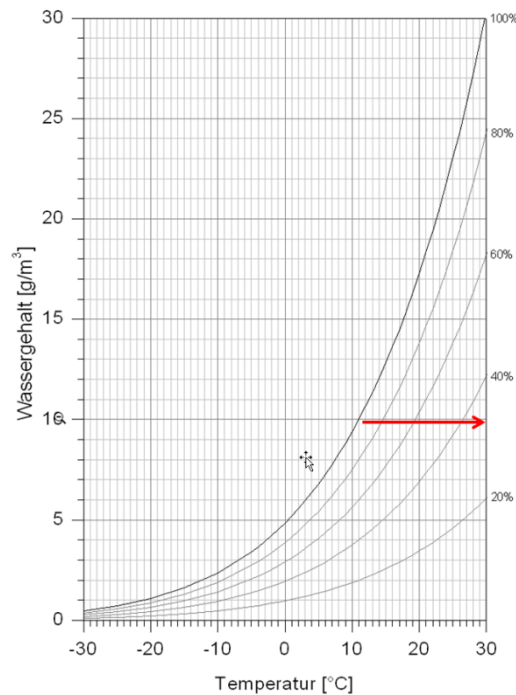
Concerning the potential corrosion of speleothems there is barely any data available apart from empirical observations at the Austrian caves mentioned above, where no significant corrosion could be observed even at rates well above 5,000 ppm. Nevertheless Dragovic&Grose (1990) used a “limestone corrosion threshold” of 2,400 ppm for their evaluations in the Jenolan Caves (Australia). For the example of Prometheus cave – using the pessimistic assumptions again – this would mean that the threshold would be reached at a level of already 100 visitors per day. Taking into account that the visitors do not show up in one large group and that values drop during the night when no tours are conducted, this value will be reached only at higher visitor rates – still assuming that there is no air movement at all. The “most probable scenario” however would enable at least 300 persons per day to reach that value of 2,400 ppm, still assuming no airflow (which would decrease the CO₂ value).

Furthermore, as the solubility of CO₂ in H₂O decreases with temperature (in the order of 5 % per degree centigrade) , speleothems in colder caves with an elevated amount of CO₂ (e.g. at higher

altitudes in alpine environments) are more endangered than those in temperate caves like Prometheus.

In our opinion the natural air movement, which could be enhanced by opening doors for two to three hours during the evening hours or during night time (depending on the necessary safety measures) in the summer season, should be sufficient to stay on the safe side. The inflow of outside air (the relative humidity of which is lower than the cave air) is no threat to the cave atmosphere or the speleothems during the summer season because its relative humidity will increase due to lower water saturation of colder air.

Figure 19 shows that the cave air (e.g. 12°C with rH close to 100 % corresponds with an outside air of 30° C and a rH of ~ 35 % - both bearing the same amount of water vapour (~ 10 g/m³)



A simple and reliable tool to measure the CO₂ content of the air during the peak season could be DRAEGER diffusion tubes (we used this instrument during our measurements in March additionally to direct measurements) for longer measuring periods (> 12 hours) or simple CO₂-monitors. A continuous and expensive CO₂ online-measurement equipment is not necessary from our point of view.

Water Dynamics and Water Quality of the Sataplia Cave

A small brook enters the cave just north of the exit and only small amounts of water in form of few dripping stalagmites is added. The small discharge of about 1.5 L/s below the entrance of the cave was about the same as that entering the cave next to the exit. The dynamic of the discharge during the rest of the year is unknown and not recorded.

The $\delta^{18}\text{O}$ values of the brook water are about 0.37 ‰ lower than in the Prometheus cave. Due to the altitude difference of about 200 m a decrease of about 0.19 ‰ per 100 m altitude increase is in the range of international reported values.

The lower electric conductivity and ion sum as well as the higher concentrations in magnesium (Mg), sodium (Na), iron (Fe), aluminium (Al) and silica (Si) are the result of the occurrence of volcanic rocks in large parts of the recharge area.

The major ion composition of the brook water shows no sign of contamination and all indicators of domestic waste water (Table 4) are below detection limits, but the microbiological

analysis shows high concentration of cultivatable bacteria. The source of these high values is unknown and should be studied in more detail.

Acknowledgment

We thank Zaal Kvantaliani (Director), Temur Muhkudiani, Mogeli Chogovadze and Nino Giorgadze(ICPA Administration) for general support. Tamaz Kopaleishvili and KukuriTsikarishvili introduced us to the caves. We also thank Nino Janiashvili for linguistic support and Mike Garforth for help in administration and for improving the English text.

References

- Dragovic, D. &Grose, J. (1990): Impact of tourists on carbon dioxide levels at Jenolan Caves, Australia: an examination of microclimatic constraints on tourist cave management.-Geoforum, 21(1):111-120.
- Georgia today (1913): Prometheus Cave – explore the myths of the Argonauts and Prometheus. (http://www.-georgiatoday.ge/article_details.php?id=11225_140731).
- Hudson, R. & Fraser, J. (2005): Introduction to Salt Dilution Gauging for Streamflow Measurement Part IV: The Mass Balance (or Dry injection) Method. Streamline Watershed Management Bulletin, 9, 6-12.
- Pavuz, R., Mais, K. &Cech, P. (2002): ErsteUntersuchungenzurLampenflora in der AllanderTropfsteinhöhle (Niederösterreich) / Preliminary investigations of the “Lampenflora” in the show cave of Alland (Austria).- Proc. Int.Conf. Cavelighting (Nov.2000, Budapest):117-122, Magyar Karszt- ésBarlangkutatóTársulat, Budapest.
- Tatashidze, Z K, Tsikarishvili, K, Jishkariani, J, Jamrishvili, A, Geladze, G and Lominadze G. 2009b.The Tskaltubo cave system. [Tbilisi: “Petiti” Publishing House.] 72pp. [in Georgian.].
- Tsikarishvili, K., Barjadze, S., Kvavadze, E., Bolashvili, N., Djanashvili, R. &Martkoplshvili, I. (2010): Speleology of Georgia: aspects of its current situation and perspectives. Cave and Karst Science, 37, 73-78, Transactions of the British Cave Research Association.
- Vaupotic, J., Bezek, M., Kapanadze, N., Melikadze, G., Makharadze, T., Machaidze, Z. &Todadze,M.(2012): Radon and Thoron Measurements in West Georgia.- Journal Geog.Geophys.Soc., Iss.(A) Phys. Solid Earth, v15a, 2011-2012: 108-117.
- Webgate Europa (2013): Strengthening Management of Protected Areas of Georgia. Programme: ENPI 2010 Annual Action Programme Twinning number:GE12/ENP-PCA/EN/14. (<https://webgate.ec.europa.eu/.../index.cfm?>).

Appendix

Compilation of single air parameter measurements in the Prometheus Cave

Lokallität	"meters"	date	Air - T °C	Air - T (avg.) °C	Water - T °C	Air Velocity m/s	rel. Hum. %	CO ₂ (direct) ppm	CO ₂ (avg) ppm	²²² Rn avg Bg/m ³	²²² Rn H2O Bg/l	EEC	Remark
2 Great Bolder Hall	90	03.03.2014 3.3.-7.3.		14,8		1,5		463					air velocity within doorframe; 2 m3/s, inbound
3 Kolchida Hall	140	03.03.2014 3.3.-7.3.		15,0				668					
4 NE Old Hall	255	03.03.2014 07.03.2014 3.3.-7.3.		15,0		0,25		486 659					358 air velocity in gallery, 1m3/s, outbound (S->N)
5 Medea Hall	440	03.03.2014 07.03.2014 3.3.-7.3.		14,6				619 670	390	284			
6 Golden Waterfall	610	03.03.2014 3.3.-7.3.		14,6				674					
7 Hall of Love	645	03.03.2014 07.03.2014 3.3.-7.3.		14,7				729 719					
1 "Cave Spring"	790	03.03.2014 04.03.2014 05.03.2014 08.03.2014			13,6 13,9			728					
8 E Great Stalagmite	880	03.03.2014 04.03.2014 05.03.2014 07.03.2014 3.3.-7.3.		13,9 14,6	13,3		99,9	549 522 631	479	642		289 478	2
9 Amphitheatre Hall	"1020"	03.03.2014 07.03.2014 3.3.-7.3.		13,4			>99,9	623 492					air movement inbound (S->N)
10 Tunnel	1200	03.03.2014 07.03.2014 3.3.-7.3.		14,8				638					air movement inbound, when opening door
11 Outside Exit	1233	03.03.2014 3.3.-7.3.		16,1				421					

ჰიდროგეოლოგიური და სპელეომეტეოროლოგიური დინამიკა სათაფლისა და პრომეთეს მღვიმეებში, იმერეთი, საქართველო

¹მარტინ კრალიკი, ²რუდოლფ პავუზა, ³გიორგი მელიქაძე

1 გარემოს სააგენტო და ვენის უნივერსიტეტი, ვენა, ავსტრია (მარტინ კრალიკი)

2 ბუნების ისტორიის მუზეუმი, ვენა, ავსტრია (რუდოლფ პავუზა)

3 ივანე ჯავახიშვილის სახელობის თბილისის სახელმწიფო უნივერსიტეტი, თბილისი, საქართველო (გიორგი მელიქაძე)

რეზიუმე

წყლის დინამიკა

- მღვიმეში წვიმის წყალი რამოდენიმე ადგილას შეედინება შედარებით სწრაფად, რის გამოც, ძლიერი და ხანგრძლივი წვიმების დროს უნდა შეწყდეს მღვიმეში ვიზიტორთა მიღება.
- მღვიმის დაბალ ნაწილებში წყალი მიედინება მცირე ნაკადულის სახით რამოდენიმე ლიტრი/წამში ნაკადით (დაბალი ნაკადი 2014 წლის მარტის პირველი კვირა) ძლიერი წყალდიდობების დროს ნაკადი აღწევს $1\text{მ}^3/\text{წმ}$.
- მარტში წყლის დაბალი ნაკადის დროს მაღალია მიკრობიოლოგიური დაბინძურება, მღვიმის წყლებში აღმოჩენილი ხელოვნური დამატკობლებისა და კოროზიის ინჰიბიტორების კვალი მიუთითებს მღვიმეში საყოფაცხოვრებო წყლების შედინებაზე.
- უნდა აიგეგმოს მღვიმის წყლების კვების არე და უნდა მოხდეს საცხოვრებელი სახლებიდან და ფერმებიდან გამომავალი საყოფაცხოვრებო ნარჩენი წყლების გაწმენდა და გაგრძელდეს შემდგომი მონიტორინგი.

სპელეომეტეოროლოგიური დინამიკა

უკვე არსებულ მონაცემებსა და სხვა მსგავს მღვიმეებში მიღებულ გამოცდილებაზე დაყრდნობით, პრომეთეს მღვიმეში სიტუაცია შესაძლებელია შეფასდეს შემდეგნაირად:

აღნიშნულ დროის მონაკვეთში (მარტი, 2014) ჩატარებული კვლევების სპელეომეტეოროლოგიური მონაცემები მღვიმის გარემოსა და მის ვიზიტორთა უსაფრთხოებასთან მიმართებაში შეიძლება ჩაითვალოს საკმაოდ კარგად. არ დაფიქსირებულა ნახშირორჟანგის კონცენტრაციის მნიშვნელოვანი ზრდა, რომელიც ძირითადად ბუნებრივი ვენტილაციითაა გამოწვეული, თუმცა გასათვალისწინებელია ის ფაქტიც, რომ გაზომვები ჩატარდა ადრეულ სეზონზე.

ზაფხულის განმავლობაში გაიზრდება CO_2 -ის კონცენტრაცია ბუნებრივი პირობების ცვლილებისა და (ნიადაგის გაზრდილი აქტივობა და მას დამატებული ნაპრალებში CO_2 -ის გაზრდილი შემოდინება, რაც გამოწვეულია გარედან შემომავალი ჰაერისთვის თერმოდინამიკური ბარიერის გაჩენით) ასევე ვიზიტორების გაზრდილი რაოდენობის გამო. თუმცა შემცირებული, მაგრამ როგორც ჩანს, მაინც არსებული ვენტილაციის გამო მისი მნიშვნელობა არ იზრდება იმ დონემდე, რაც საფრთხისშემცველი იქნებოდა მღვიმის გარემოსა და ვიზიტორებისათვის. ამ

ურთიერთსაპირისპირო ფაქტების შედეგები დაფიქსირებულია ზაფხულის თვეებში პრომეთეს მღვიმეში რადონის შემცველობის მცირედ გაზრდილი კონცენტრაციით (Vaupotic et al. 2012).

იმისათვის, რომ თავიდან იქნას აცილებული მღვიმეებში ნახშირორჟანგის სახიფათო კონცენტრაციები, ჩატარდა მისი ცვლილების მოდელირება მოვლენების განვითარების როგორც ყველაზე პესიმისტური, ასევე რეალური სცენარის მიხედვით. სხვა მღვიმეებში ჩატარებული კვლევების შედეგებისა და გამოცდილების გათვალისწინებით, ტურისტული სეზონის პიკისა და გარე ჰაერის მაღალი ტემპერატურის პირობებში, თუკი მიღებული იქნება რამოდენიმე მარტივი ზომა, ნაკლებ სავარაუდოა ნახშირორჟანგის კონცენტრაციის მღვიმის გარემოსა და ვიზიტორთათვის სახიფათო ნიშნულამდე აწევა.

ჩვენის აზრით, ზაფხულის სეზონის დროს ჰაერის ბუნებრივი მოძრაობა შესაძლებელია გაუმჯობესდეს შესასვლელი და გამოსასვლელი კარებების რამოდენიმე საათით გაღებით საღამოს ან ღამის განმავლობაში (დამოკიდებულია უსაფრთხოების საჭირო ზომებზე). გარე ჰაერის მღვიმეში შეღინება (რომლის ფარდობითი ტენიანობა დაბალია მღვიმის ჰაერის ტენიანობაზე) არ წარმოადგენს არანაირ საფრთხეს არც მღვიმის ატმოსფეროსა და არც მასში წარმოქმნილი ფორმაციებისათვის, რადგან გაიზრდება მისი ფარდობითი ტენიანობა მისი დაბალი წყლით გაჯერებულობის გამო.

პიკურ სეზონებში ჰაერში CO₂-ის შემცველობის გასაზომად შედარებით გრძელი პერიოდისათვის (> 12 სთ) შესაძლებელია გამოყენებული იქნას მარტივი და საიმედო ხელსაწყო დიფუზიურ-ვენტილაციური მილი (რაც გამოყენებული იქნა ჩვენს მიერ მარტში პირდაპირ გაზომვებთან ერთად) ან სწრაფი გაზომვისათვის - CO₂- მონიტორი. ხანგრძლივი და უფრო ძვირადღირებული CO₂- ონლაინ გამზომი ხელსაწყო არ არის აუცილებელი.

მღვიმეების ელექტრო განათება

პრომეთეს მღვიმეში დაინსტალირებული იქნა თანამედროვე განათების სისტემები. მიუხედავად იმისა, რომ განათების ელემენტების მდებარეობა არ ქმნის არანაირ პრობლემას, განათების ფერები მაინც ნაწილობრივ პრობლემატურია.

იმის გამო, რომ მღვიმეებში ფლორა (lampenflora) შთანთქმავს სინათლის კონკრეტული ტალღის სიგრძეს და ასევე, ნათურების გააჩნია განსხვავებული სპექტრი, ჩვენ ვხედავთ, რომ ლურჯის და ნაწილობრივ წითელი ფერის ნათურების გამოყენება უნდა იქნას თავიდან აცილებული, რათა არ მოხდეს ხავსისა და მწვანე წყალმცენარეების ზრდის პროვოცირება. ამ გზით ლურჯ-მწვანე წყალმცენარეების (რომელიც ფაქტიურად ბაქტერიაა) ზრდა მნიშვნელოვნად არ იზღუდება, მაგრამ წარმოადგენს ნაკლებ პრობლემას, ვიდრე სხვა სახის ფლორა. თეთრი ნათურები ასევე ახლოსაა კრიტიკულ ტალღის სიგრძესთან, მაგრამ მაინც მისაღებია, რადგან სინათლის ინტენსიურობა ნათურებთან ახლოს არ არის ძალიან მაღალი. ამ შემთხვევაში ეფექტურია ისეთი მარტივი მიწყობილობის გამოყენება, როგორცაა საჩრდილობლები.

ჩვენ გთავაზობთ, თავიდან ავიცილოთ განსაკუთრებით ლურჯი ფერის განათების გამოყენება საერთოდ და წითელი ფერის გამოყენება დაყვანილი იქნას მინიმუმამდე.

ამის გარდა, ფლორის შესამცირებლად, სასარგებლო იქნებოდა განათების დროის შემცირება (ყველაზე ეფექტური იქნებოდა განათების გათიშვა იმ სექტორებში, სადაც ვიზიტორები არ არიან) რაც, როგორც ჩანს უფრო მეტად სერიოზული პრობლემაა მღვიმეების გარემოს შესანარჩუნებლად, ვიდრე ვიზიტორთა სიმრავლე.

სათაფლიას მღვიმე

სათაფლიას მღვიმეში წყლის ნაკადისა და კლიმატის მხოლოდ წინასწარი გაზომვები ჩატარდა. მღვიმის დირექციის გადაწყვეტილების გამო არ მოხდა წყლის დონის მონიტორინგის ხელსაწყო დაინსტალირება. მიუხედავად ამისა, რამოდენიმე წინასწარი შედეგი იქნა დოკუმენტირებული:

წყლის დინამიკა

- უფრო მაღალი აბსოლუტური სიმაღლისა და ნაკლები ფართობის კვების არის გამო, სათაფლიას მღვიმეში წყალი იყო უფრო მნიშვნელოვნად ცივი (8.5°C) და ნაკადიც მცირე (1.5 ლ/წმ), ვიდრე პრომეთეს მღვიმეში მარტის პირველი კვირის განმავლობაში (2014).
- კვების არეში განლაგებული ვულკანური და ამასთან ერთად გამოკარტსებული კარბონატული ქანების არსებობის გამო, წყლის შემადგენლობა ნაკლებად მინერალიზებულია, მაგრამ უფრო მდიდარია მაგნიუმით (Mg), ნატრიუმით (Na), რკინით (Fe), ალუმინითა (Al) და სილიციუმით (Si), ვიდრე წყალი პრომეთეს მღვიმეში.
- 2014 წლის მარტში ასევე უფრო მაღალი იყო მიკრობიოლოგიური დაბინძურება, მაგრამ არ იქნა აღმოჩენილი საყოფაცხოვრებო ნარჩენი წყლის კვალი. ამის გამო, იმისათვის, რომ დადგინდეს, თუ რა არის დაბინძურების წყარო (კვების არეში მცხოვრები ცხოველები თუ სხვა წყარო) მიკრობიოლოგიური ინდიკატორების მონიტორინგი უნდა გაგრძელდეს ერთი წლის განმავლობაში მაინც.

სპელეომეტეოროლოგიური დინამიკა

სათაფლიას მღვიმეში გამა გამოსხივება მნიშვნელოვნად უფრო მაღალია, ვიდრე პრომეთეს მღვიმეში ($124\text{--}71\text{ nSv/h}$ –გარეთა ფონთან შედარებით $\sim 130\text{ nSv/h}$), რაც დიდი ალბათობით გამოწვეულია ვულკანური ქანების სიმრავლით, რომელიც მრავლადაა წარმოდგენილი ასევე მღვიმეში ალოქთონური ნალექების სახით.

სამწუხაროდ, - პრომეთეს მღვიმეში გამოყენებული ხელსაწყოებიდან სათაფლიას მღვიმეში ჩვენ გვქონდა მხოლოდ ხელსაწყო, რომელიც ზომავს მხოლოდ რადონის შვილობილ პროდუქტებს (radon-222 გაწონასწორებული მდგომარეობისთვის). შედეგები, რომლებიც მნიშვნელოვნად დაბალია, ვიდრე პრომეთეს მღვიმეში, გამოწვეული უნდა იყოს სათაფლიას მღვიმის უფრო აქტიური ვენტილაციით, ყოველ შემთხვევაში გაზომვების დროს მაინც.

Гидрогеологическая и спелеометеорологическая динамика в прометоиских и сатафлиских пещерах Имеретии, Грузия

¹Мартин Кларик, ²Рудолф Равуза, ³გიორგი Меликадзе

¹Природоохранное Агентство и Венский Университет, Австрия

²Музей Истории Природы, Вена, Австрия

³Тбилисский Государственный Университет, Тбилиси, Грузия

Резюме

Пещера Прометея

Динамика воды

- Дождевая вода входит в пещеру относительно быстро в нескольких местах, поэтому экскурсии в пещеру должны быть остановлены во время сильных и продолжительных штормов.
- В нижней части пещеры небольшой ручей с расходом нескольких литров в секунду (низкий расход в первую неделю марта 2014 г.) до примерно 1 кубический метр в секунду во время сильных наводнений.
- Во время малого расхода воды в марте микробиологическое загрязнение является высоким и согласуется со следами искусственных подсластителей и ингибиторов коррозии, указывающих на приток бытовых сточных вод в пещеру.
- Область питания пещерных вод должны быть заснята съемкой. Должна осуществляться и контролироваться очистка сточных вод из жилых домов и ферм в этой области.

Спелеометеорологическая динамика

Ситуация в пещере Прометея, на основе имеющихся данных и опираясь на опыте других аналогичных пещер, выглядит следующим образом:

Общий статус спелеометеорологических параметров на данном временном интервале исследования (март 2014 года) можно рассматривать как неплохой по отношению к окружающей среде пещеры и к безопасности посетителей. Там не было никакого существенного обогащения CO₂, что в основном связано с естественной вентиляцией и с началом сезона.

В летнее время содержание CO₂ увеличивается в силу естественных причин (повышение активности почвы плюс термодинамический барьер против наружного воздуха увеличивает приток CO₂ в пещеру через трещины), а также в связи с увеличением числа посетителей. Тем не менее, скорее всего до сих пор существующая вентиляция будет ограничивать их значение до величин, которые не вызывают серьезной угрозы для окружающей среды пещеры и ее посетителей. Результатом этих эффектов является фиксирование немного повышенного содержания радона во время летних месяцев (Vaupotic et al. 2012).

Тем не менее, для целей безопасности, было выполнено моделирование изменения CO₂ при изменении граничных условий как при пессимистичных сценариях, а также при более реалистичных условиях. Учитывая эти исследования и опыт других пещер, отсутствуют серьезные угрозы для посетителей и для пещеры, если будут приняты некоторые простые меры предосторожности во время пика туристического сезона и при высоких температурах наружного воздуха.

На наш взгляд, естественное движение воздуха можно было бы повысить путем открытия двери на два-три часа в вечерние часы или в ночное время (в зависимости от необходимых мер безопасности) в летний сезон, и это должно быть достаточно, чтобы обеспечить безопасность. Приток наружного воздуха (относительная влажность которого ниже, чем у воздуха пещеры) не создаст угрозы для атмосферы пещеры или спелеобразований во время летнего сезона, поскольку его относительная влажность будет увеличиваться за счет более низкой водонасыщенности холодного воздуха.

Простым и надежным инструментом для измерения содержания CO₂ в воздухе во время пикового сезона могут быть Draeger диффузионные трубки (мы их использовали, как дополнение к прямым измерениям, во время наших измерений в марте) для измерений на долгий период (>12 часов) или простые CO₂-измерительные устройства для немедленных замеров. Непрерывная и более дорогая онлайн CO₂-измерительная аппаратура не является необходимой.

Электрическое освещение пещеры

В пещере Прометея была установлена сложная система освещения. В то время как положение световых элементов не вызывает никаких вопросов, то цвета освещения можно изменить, по крайней мере частично.

Из-за поглощения волн света определенной длины, глядя на спектр излучения разных светодиодов, надо учесть, что синие (особенно) и красные (частично) цвета надо избегать, чтобы уменьшить рост мхов и зеленых водорослей. Сине-зеленые водоросли (на самом деле, бактерии) нельзя ограничить таким способом, однако они вызывают беспокойства меньше. Белые светодиоды имеют тоже близкую к критической длину волны света, однако допустимы, если их интенсивность не слишком близка к лампам. Простые устройства светлых оттенков могут быть полезны в этих случаях.

Мы предлагаем полностью избегать синие цвета и уменьшить красные до минимума.

Кроме того, что любое сокращение общего времени освещения (выключая свет в непосещаемый момент) будет наиболее эффективным и будет способствовать снижению т.к. называемой флоры ламп, которая представляет собой более серьезную угрозу для окружающей среды пещеры, чем посетители.

Пещера Сатаплиа

Только предварительное исследование было проведено об изменении воды и климата в пещере Сатаплиа. По желанию директора, не было проведен мониторинг движения воды. Однако некоторые предварительные итоги здесь приведены.

Динамика воды

- В связи с большей высотой и меньшей площадью области питания поток воды в пещере был значительно холоднее (8.5°C) и поток намного меньше (1.5 л / с), чем в пещере Прометей в течение первой недели марта 2014 года.
- В связи с наличием вулканических пород и карстованностью карбонатных пород в зоне подпитки состав вода менее минерализован, но более обогащен магнием (Mg), натрием (Na), железом (Fe), алюминием (Al) и диоксидом кремния (Si) по сравнению с пещерой Прометея.
- Микробиологическое загрязнение также была высоким в марте 2014, но ни один из индикаторов бытовых сточных вод не был найден. Поэтому микробиологические показатели должны контролироваться в течение одного года, чтобы уточнить, происходит ли загрязнение от животных, живущих в районе подпитки или имеет другие источники.

Спелеометеорологическая динамика

Повидимому, в связи с соседними вулканическими породами, которые там в изобилии, а также аллохтонных пещерных отложений в в пещере Сатаплиа, гамма-излучение было значительно выше, чем в пещере Прометея (124 против 71 nSv/h – наружный фон $\sim 130\text{ nSv/h}$). К сожалению, поскольку все устройства были использованы в пещере Прометея, мы имели возможность только дочерние продукты радона (ЕЕС – равновсное значение радон-222) лишь однажды. Результаты, будучи значительно ниже, чем в пещере Прометея, указывают на более активную вентиляцию в этой пещере, по крайней мере на момент измерений.

Result of numerical modelling of groundwater resource in the Shiraki catchment

¹George Melikadze, ¹Natalia Jukova, ¹Mariam Todadze, ¹Sopio Vepkhvadze
²Tomas Vitvar

¹Iv. Javakhishvili Tbilisi State University, M. Nodia Institute of Geophysics
²Czech Technical University in Prague, Faculty of Civil Engineering

Abstract

In order to assessment water resource, a numerical model of groundwater was elaborated for Shiraki area. It is consists of 3 layers. Each layer represents a porous material with different infiltration properties. The model was calibrated in transient transport mode to tritium concentration measured in boreholes and springs located in Shiraki area. Tritium was assigned as a single mobile species, not reacting with chemical elements and concentrated in water, what allowed determining the residence time of groundwater flow. The model estimated discharge and recharge zones, groundwater flow directions and velocities as well as groundwater age for Shiraki area. It is recommended to enhance the use of waters from the karstic formations as alternative drinking water sources.

Introduction

Eastern Georgia encounters, due to its semiarid climate, a big deficit of 1040 million cubic meters of water for irrigation and domestic use. One of the most important examples is the agricultural area of Shiraki Plain, which occupies over 80.000 km² on a large, partly artesian aquifer of the Alazani basin and on the upland synclines between the rivers Alazani and Iori (1). In order to assessment water resource, numerical model of groundwater hydrodynamics was elaborated for this area based on the conceptual model, which based on the provisional data (geological, geophysical, hydrogeological, hydrological, etc). Model of the aquifer have been processed by special software Visual Modflow Package.

Geological and hydrogeological settings

In geo-tectonic point of view the region is part of the tectonic zone of the river Mtkvari (2), and forms slanting and wide (up to 20km) syncline of considerable extension (up to 50km). The core and wings of the crease lie in the form of sediments of Krasnokolodski suite with the power of 1000m, which belongs to the akchagil-Apsheronian layer. Lythologically this uniform width of the crumby drift-pebbly layers belong to argillaceous sands, also loamy sands containing pressure waters (3,4). On the whole area of the Shiraki Plain basic rocks are covered with proluvial -deluvial and lake gypsiferous argil sands with sub-layers of loamy sands and gravel. The fourth cover is, on the whole, characterized with great diversity of the lythogenic composition of the soil of different genetic types and variable power, ranging from 5-10 to 40-50.

The dynamics of the ground waters are greatly affected with the peculiar composition of Shiraki Massif, which is the component of the Iori Plateau dividing the basins of the rivers Iori

and Alazani in the lower current. To the north the Shiraki Massif is distinctly divided from the Alazani valley with the eroded tectonic batter of 400m of height. Within the plain the modern relief is characterized with considerable sloping towards the axial part. Besides, bending can be observed along the axis of the syncline as well, thus, in spite of the general regional sloping in the south- east direction, the plain is contoured as a locked depression.

In conditions of the entire lack of the hydrographic network in the area the ground water supply takes place at the expense of atmospheric precipitation, which is proved by the given regime observations. Besides we suppose the possibility of some injection of the ground waters from below by the downstream waters. The horizon of the ground waters is dated for the fourth sediments and is mapped quite sharply by the given measurements of the boreholes. The horizon is, on the whole, weakly aquifer and is characterized by the low filtration values. The average value of the filtration quotient equals $K=0,1-1,2$ m per 24 hours. On the map hydroisogyps the picture of water movement from the relatively raised peripheral parts of depression towards the lower and locked central part where ground waters are closer to the ground surface is quite distinctly depicted (6m at the middle sedimentary depth of 25m) and on the whole are spent on evapotranspiration. A great width of the crumby continental layers krasnokolodski suite (Akchagil- afsheron), lain in a large syncline, is a main aquifer, and contains pressure ground waters. Part of the boreholes situated on the south-western rim of the Shiraki Syncline and opening the pressure horizons within the intervals of 400-600m of depth, gives a well-spring with the maximal debit of 1,7litres per second. The rest of the wells are sub-artesian but having negative water level close to the ground surface. Besides we can observe increase in productivity of the falls of the aquifer deep horizons. Aquifer is contain paleowaters with $\delta^{18}O$ values between -11 and -13‰ V-SMOW and relatively low concentrations of tritium (0.1-1.8 TU).

The issue of the hydraulic interconnection among the pressure and ground waters of the Shiraki Plain and the possibility of surface water reserves extraction for drinking and irrigation purposes is very interesting.

Database creation and analysis

Conceptual 3D model consists of 3 layers (Q,N,J). Each layer represents a porous material with different infiltration properties. Data from geological profiles and maps where used to recreate layers. 2 layers (Q and N) are designed as unconfined.

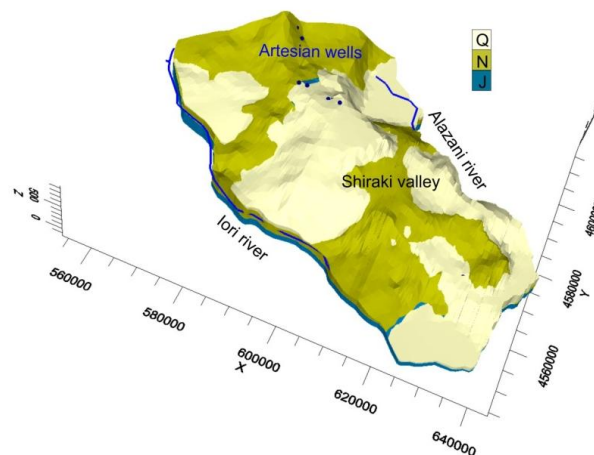


Fig. 1 (Conceptual model) Conceptual and numerical model were developed in Visual Modflow Flex 2012 and Visual Modflow Classic 2011 programs.

Each layer, as single hydro stratigraphic unit, was determined by hydraulic conductivity, specific storage, and effective porosity:

Layers	Hydraulic conductivity (m/s)	Specific storage (m ⁻¹)	Effective porosity
Q	7.6042×10^{-5}	3×10^{-6}	0.05
N	1.6204×10^{-6}	5×10^{-5}	0.03
J	1.8519×10^{-6}	9×10^{-4}	0.07

Rivers were used as boundaries of the model area. They were assigned as specific flow boundary conditions.

River	Riverbed thickness (m)	River width (m)	Riverbed conductivity (m/day)
Alazani	5	50	20
Iori	3	30	10

Visual Modflow Flex supports the standard Drain Boundary Package; we used it to simulate the boreholes under artesian conditions. 20 drain boundary conditions were added to the model. Next table shows parameters which were assigned to drains. Debit rate depends on the position of well screen.

Artesian boreholes screen geology	Debit rate (L/sec)
Q	Up to 165
N	Up to 60
J	Up to 10

Recharge boundary condition (800 mm/year) was assigned to upper right zone of model. Conceptual model were converted to numerical one and further development. Debits rate of artesian wells where used for to calibrate model in steady-state mode.

The model was also calibrated in transient transport mode to tritium concentration in springs and boreholes located at the Shiraki area. Tritium was specified as a single species with first-order decay of 12.32 yr. The longitudinal dispersivity was selected to be 10 m. Initial concentration was set to 10 T.U. The simulated tritium concentration for the Shiraki model is shown in the Fig. 2.

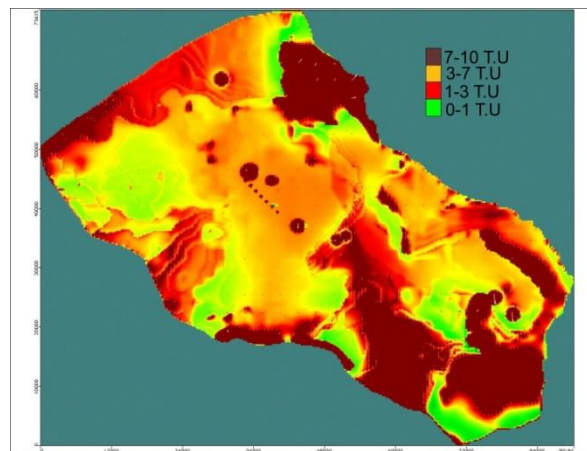


Fig. 2 Distribution of tritium concentration

Simulated water table is shown on Fig. 3

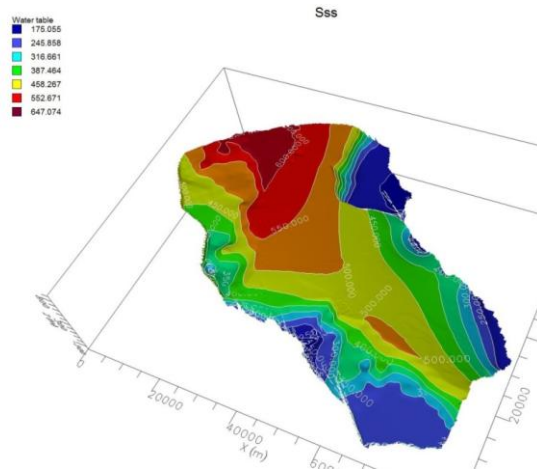


Fig. 3 Water table

In the model was fixed water level in absolute elevation (Fix 3) and was simulated Flow velocities for Shiraki area (Fig. 4).

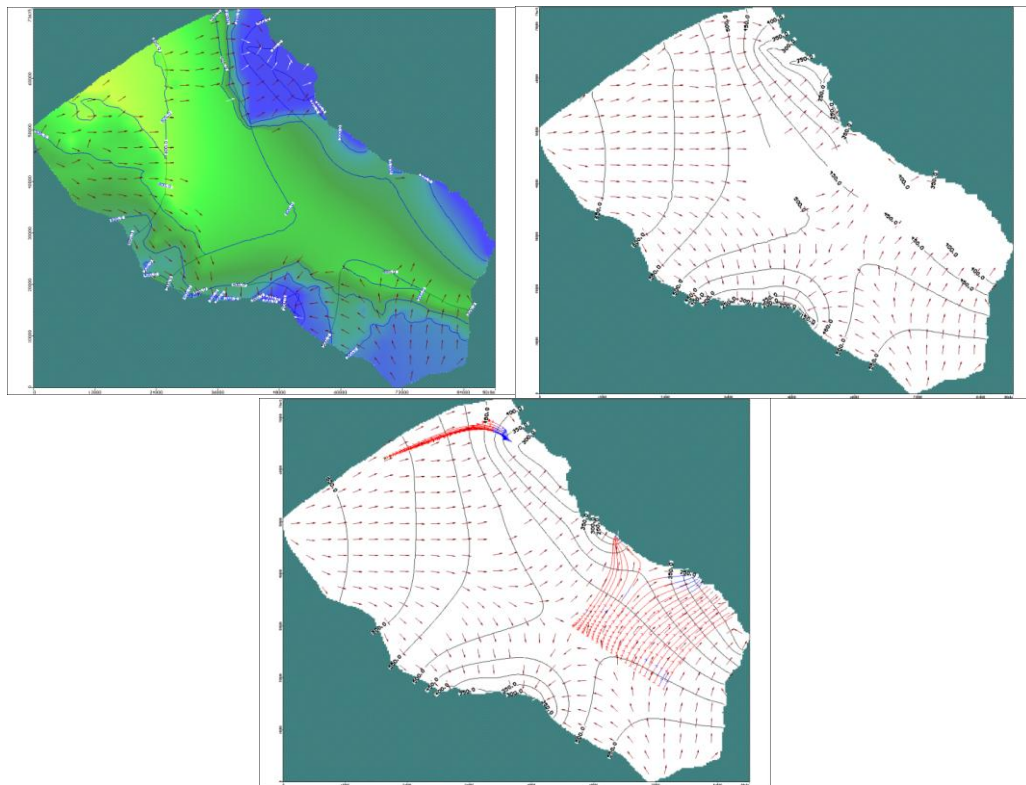


Fig. 4 Flow velocities of a) 1st layer; b) 2nd layer; c) 3rd layer

Fig. 4 shows us flow velocities intensity and direction of simulated water system. As we can see water does not enter the system in upper horizon. 1st horizon is weakly water-bearing and does not infiltrate water down. In the middle zone water is discharged in the rivers. Middle horizon is recharged by groundwater flows. Intense of flow is increasing in the 3rd layer.

From the tritium-calibrated MT3DMS model, the groundwater age was assigned as a single mobile species that allowed determining the residence time of groundwater flows. From the Shiraki valley groundwater moves to the Azalani site, average water age between 2 locations is about 35 years. From the Shiraki hills water moves to Iori site's artesian wells (Kasritskali and others), water age between 2 locations is about 9 years (Fig.5).

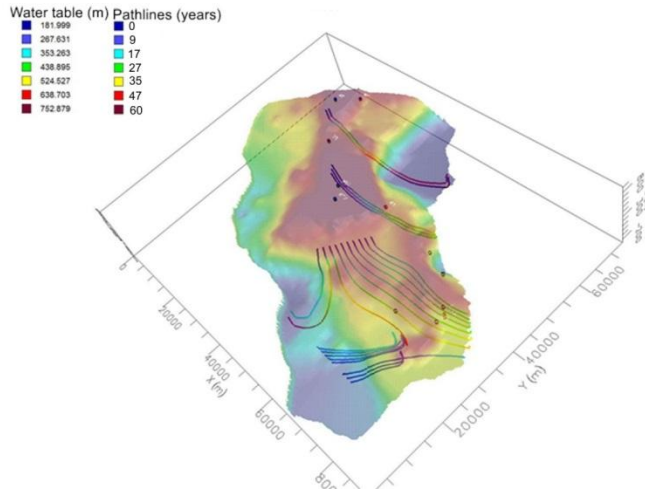


Fig. 5 Groundwater flow pathlines and residence time

We specified two zones to investigate flow budget in the model. Zones are marked by dark regions in the Fig. 6.

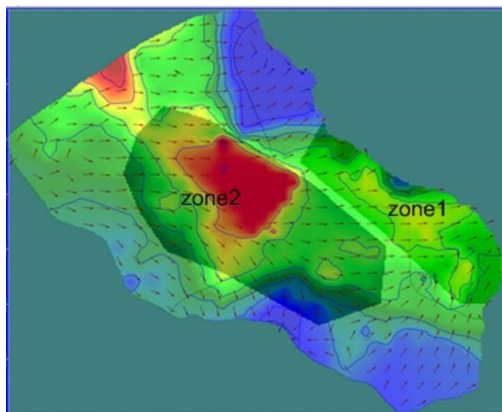


Fig. 6 Water table depth and specified zones

Fig.6 shows us total flow budget of the model. As we can see, zone1 is recharged more intense than zone#2, but water discharged in general in the zone#1. Drains in the Fig.7 represent artesian wells. Groundwater discharge of drains is rather slight compared to rivers.

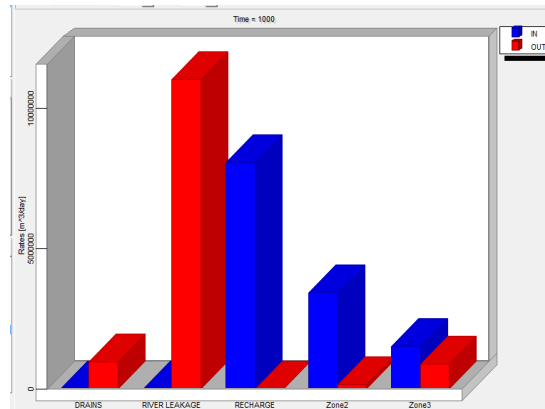


Fig. 7 (Flow Budget), Blue is discharge, Red is recharge

Conclusions

Complex geological, hydrogeological, hydrogeochemical and isotope investigations were carried out and created the numerical model of the Shiraki Artesian Basin.

Groundwater belongs to different hydrochemical and isotopic groups and must be considered with respect to local stratigraphy. Groundwater has confirmed the evolution in mineralization from Northwest to Southeast, with major increase in the Shiraki syncline area. Therefore, are observed changes of total mineralization in the vertical cross section of the boreholes.

Model fixed water path lines. From the tritium-calibrated model, the groundwater age was assigned as a single mobile species that allowed determining the residence time of groundwater flows from the Shiraki valley groundwater moves to the Azalani site, average water age between 2 locations is about 35 years.

It is recommended to enhance the use of waters from the karstic formations such as the Dedoplistskaro Plain for alternative drinking water sources in the Shiraki region.

References

1. Bagoshvili, G.N. (1990). Report on hydrogeological survey 1:50000 on the southern slope of the Greater Caucasus. Ministry of Geology of USSR, Tbilisi, 2 volumes, 95 and 163 pp. (unpublished, in Russian)
2. Beselia, B.N. (1988). Preliminary survey on the appearance of groundwaters Quaternary alluvial-proluvial confined and Upper Jurassic and Lower Cretaceous aquifers between the rivers Chelti and Durudji. Ministry of Geology of USSR, Tbilisi, 3 volumes. (unpublished, in Russian)
3. Buachidze, G. 2005. Transboundary Artesian Basin of Georgia. Presentation at the conference EURO-RIOB 2005, Namur, Belgium, 29 Sept-1 Oct 2005. http://www.riob.org/IMG/pdf/Euro-RIOB_29sept2005_Buachidze.pdf
4. Buachidze, I.M., and Zedginidze, S.N. 1985. Hydrogeology and Perspectives of Groundwater Use in the Alazani-Agrichai aquifer. Tbilisi, 335pp. (in Russian).

Acknowledgments

The authors thank the Rustaveli National Scientific foundation for financial support of the project #31/27 “Environmental Isotopes Testing in Alazani-Iori Catchments (East Georgia) For Provision of Sustainable Use of Groundwater Resources”.

შირაქის წყალშემკრების ციფრული მოდელირების შედეგები

¹გიორგი მელიქაძე, ¹ნატალია ჟუკოვა, ¹მარიამ თოდაძე, ¹სოფიო ვეფხვაძე
²ტომას ვიტვარ

¹ივ. ჯავახიშვილის სახ. თბილისის სახელმწიფო უნივერსიტეტი, მ. ნოდისა
გეოფიზიკის ინსტიტუტი
²პრადის ტექნიკური უნივერსიტეტი, ჩეხეთი, სამოქალაქო მშენებლობის ფაკულტეტი

რეზიუმე

მიწისქვეშა წყლების რესურსების შეფასების მიზნით შემუშავდა შირაქის წყალშემკრების რეგიონის ციფრული მოდელი. ის შედგება ფენისგან. თითოეული ფენა შედგება სხვადასხვა გამტარებლობის ფოროვალის გარემოსაგან. მოდელში გადაადგილების ნაწილი დაკალიბრებული იქნა ტრიტიუმის მნიშვნელობებით, რომელიც გაზომილი იქნა წყალპუნქტებში. მოდელში განსაზღვრული იქნა კვებისა და განტვირთვის არელები. ასევე დაფიქსირდა წყლის გადაადგილების გზები, სიჩქარე და მიწისქვეშ მოძრაობის პერიოდი. გაცემული იქნა რეკომენდაციები კარსტული წყლების გამოყენებისთვის როგორც სასმელი წყლის ალტერნატიული წყაროსი შირაქის რეგიონისთვის.

Результаты цифрового моделирования ресурсов подземных вод Ширакского водосбора

¹Меликадзе Г. И., ¹Жукова Н. О., ¹Тодадзе М. Ш., ¹Вепхвадзе С. Г., ²Витвар Т. А.

РЕЗЮМЕ

¹Тбилисский Государственный Университет им. Ив. Джавахишвили, Институт Геофизики

²Технический Университет Праги, Чехия, Факультет Гражданского Строительство

С целью оценки ресурсов подземных вод численная модель грунтовой воды была разработана для области Шираки. Модель состоит из 3 слоев. Слои представляют собой

геологические породы с различными фильтрационными свойствами. Модель была откалибрована в переходной режиме по значениям трития, который мерился в скважинах и источниках Шираки. Тритий был использован в модели как независимое вещество, которое не вступает в реакции, но концентрируется в воде. Модель определила области питания и разгрузки грунтовых вод, пути и скорость движения подземных вод, а также время задержки воды под землей. Рекомендуется увеличить использование вод в карстовых формированиях как альтернативный источник питьевой воды.

Identification of the possible criteria for prognostication of earthquakes on the ground of the data of the observed deformographic processes and triggered micro-earthquakes

K. Kartvelishvili, D. Gamkrelidze, S. Ghonghadze, G. Kartvelishvili, M. Nikolaishvili, O. Yavolovskaya.

M. Nodia Institute of Geophysics of Ivane Javakhishvili Tbilisi State University

Abstract

Here we consider some latent process of deformation caused by the forces in the Earth's crust or/and cosmic, latent as well, ones. These processes represent a certain regularities in the nature where, as we know, all physical events are caused by other events and in their turn produce some other ones. To such events belong naturally crust deformations. These events are in organic cause-effect relation with earthquakes and cosmic tidal processes. Many signs and criteria are related to the period of preparation of earthquakes, and it is necessary to attempt to predict to some extent their (earthquakes') parameters (time, place, strength...) on this ground.

The Earth is characterized by multi-geophysical processes. The problems of studying their nature and their control represent some of the main subjects of scientific investigation. There are some processes which are easy to identify. To their class belong, among others, strong earthquakes. However, it is impossible to control them. The only possible thing to do here is taking some preventive measures, such as, for instance, are reinforcement of buildings and constructions, in order to avoid or alleviate the catastrophic consequences. Unfortunately this will not give us absolute guarantee, for there are still many factors of which we have very little knowledge.

There are also processes which are weakly manifested though they accompany and promote the development of strong processes. To such processes belong: change of inclination of the Earth's surface, deformation in the Earth's crust, triggered earthquakes and other. The present article is dedicated to the study of such processes, namely, of the connection of the nature of earthquakes and the structure of the Earth's crust.

An earthquake is perhaps the most destructive phenomenon for human society (either for human lives or material objects) among all the natural ones that threaten it. Its hardness increases due to the unexpectedness of its occurrence. However it is impossible yet to calculate even approximately where and when it will occur and of what strength it will be. These questions are of a particularly importance for seismoactive regions, such as are the Caucasus and Georgia, as its integral part. It is well known, what disaster brought the Spitak Earthquake of $M=6.9$, 1988 (Armenia), Racha-Ossetian, $M=7.1$, 1991, Baris Akho, $M=6.3$, 2003 (Georgia).

The picture given in Fig. 1 gives some idea of seismic activity of the Caucasus.

Considering what was said above, it is not necessary to look for the additional arguments for stressing the urgent necessity for the Caucasus (Georgia) to carry out the works which

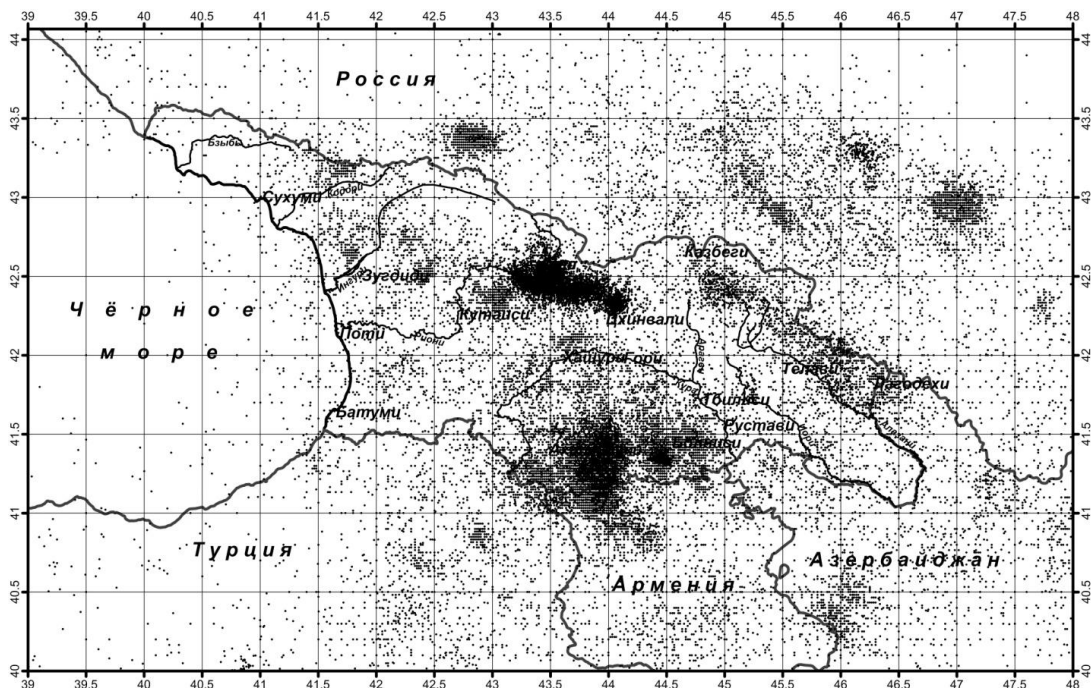


Fig. 1 The scheme of distribution of the instrumentally recorded earthquakes which took place in Georgia and its adjacent territories in 1900-2008.

could help us to advance on our way to the achievement of the above stated goal – prediction of the possible earthquake’s place, time and magnitude. In Fig. 2 a seismic zoning of the territory in relation to intensive earthquakes ($M > 3.5$) is presented. And we have all the grounds to expect the similar picture of seismic activity in the future.

So, any attempt to any scope in this direction is undoubtedly justified. Particularly when there are parametric data of absolutely new physical essence connected with earthquake processes, recording them from the moment of their formation and to the end of the event.

It is acknowledged that tiltometric and extenzometric (deformographic) measurements of the Earth’s crust as well as these of micro-earthquakes provoked by dynamic triggering represent at present stage one of the most important and perspective means for the study of tidal processes in the Earth’s crust, mechanisms of tectonic deformation and seismicity.

The study of the tidal processes in the Earth’s crust in Tbilisi has started since 1960 by gravimetric observation of the tidal variations of gravitation force.

From 1963 an underground observatory of 102 m length with horizontal tunnel at 60 m depth from the surface with 0.005°C variation of temperature was founded, where the following scientific-research equipment was installed:

1. Askania Werker, two fixed gravimetric recorders of tidal variations of gravitation force of $\text{Gal} \cdot 10^{-7}/\text{mm}$ sensitiveness.
2. Deformation recording ternary linear quartz deformograph:
 - a) Base 42 m, horizontal, azimuth $\text{N } 66,5^{\circ}$, E sensitiveness $0.22 \cdot 10^{-9}/\text{mm}$.
 - b) Base 14.5 m, horizontal, azimuth $\text{N } 30^{\circ}$, W, sensitiveness $0.7 \cdot 10^{-9}/\text{mm}$.
 - c) Base 6.45 m, vertical, sensitiveness $0.15 \cdot 10^{-9}/\text{mm}$.
3. Eight photo-electric tiltmeters, which were placed on two independent basalt platforms, four on each one and oriented by pairs in N-S ($\text{N}^{\circ}45$, $\text{N}^{\circ}87$) and E-W ($\text{N}^{\circ}33$, $\text{N}^{\circ}85$) azimuths, with sensitiveness $0.01 \text{ m sec}/\text{mm}$.

The research works in dynamic triggering of seismicity was started in Tbilisi by uninterrupted acceleration observations in November 2010.

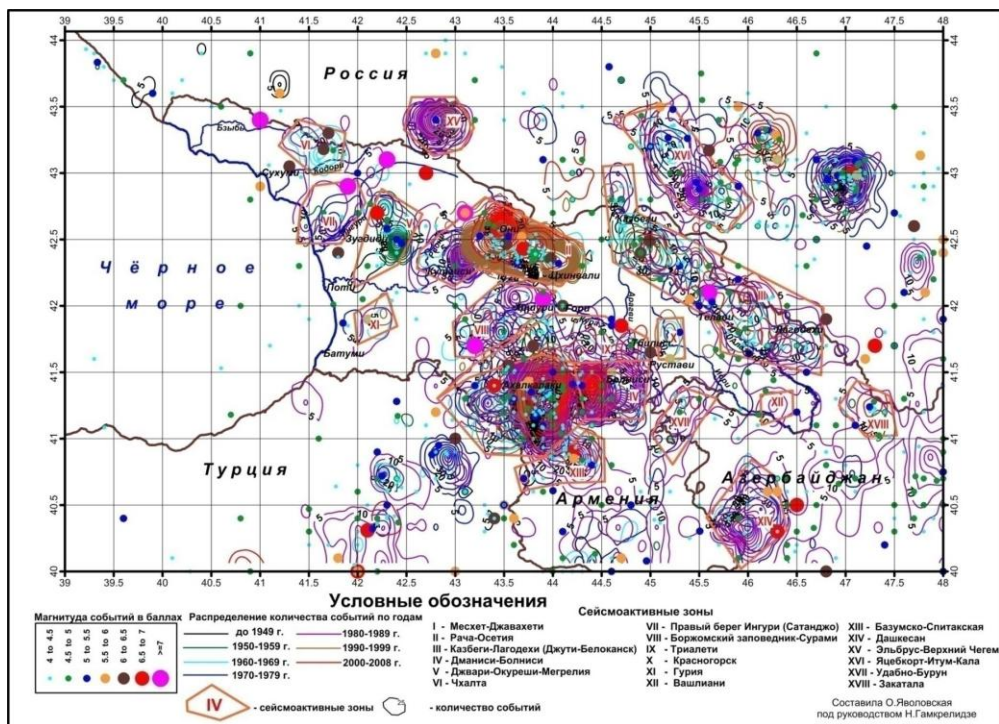


Fig. 2 The general scheme of seismicity and seismic regularities of Georgia and its adjacent territories for the period of 1900-2008

In both cases and particularly in the first one (a half of the century of observation) a unique experimental material has been accumulated which needs theoretical and practical processing with consequent generalization: study of the genesis, of the mechanisms of working, the role of the structure of the environment, and other aspects.

a) The noted parameters are recorded with frequent significant anomalous divergences from the background values which (divergences) according to express-interpretation data are connected with the forces caused by cosmic bodies and the processes that take place in Earth's crust (earthquakes etc.).

The drawing on Fig. 3 needs study by spectral analysis. Intuitively it may be said that there takes place a drift in time-interval in the north-western direction with a tendency of increasing inclination and uneven gradient, in which a periodicity of 5 years interval is observable. This fact is of much interest, and namely, how is it connected with other geophysical facts.

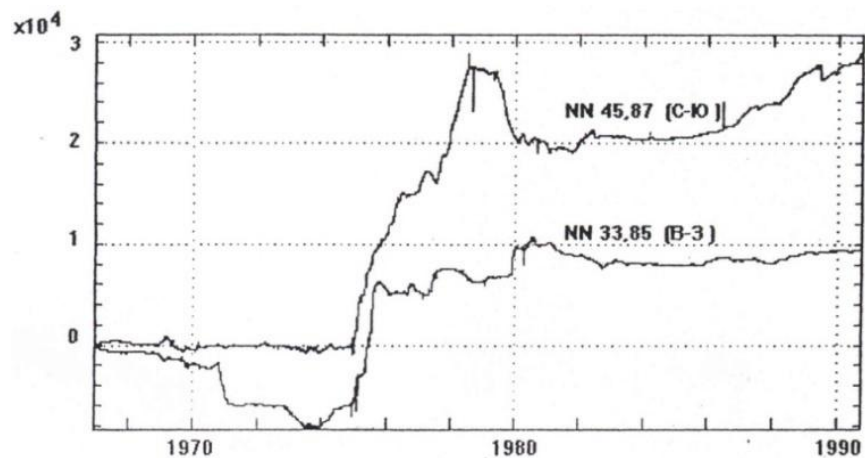


Fig. 3 Averaged drifts of tiltmeters on the Earth's surface in Tbilisi 1967-1991

The summary move of the inclinations is given on Fig. 4 in the shape of a vector diagram. Such presentation of inclinations is often rather convenient, because it gives an opportunity to define for any moment the value of the inclination as well as its direction. The summary

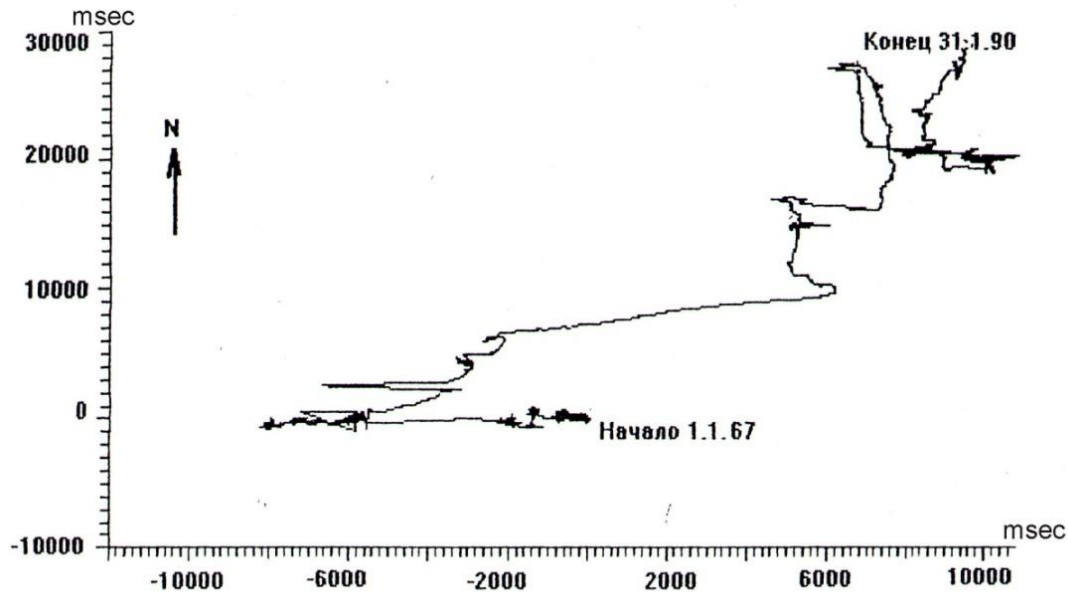


Fig. 4 The vector diagram of inclinations of the Earth's surface in Tbilisi in 1967-1991

inclination during 24 years of observation made up 27",0 in northern direction and 9",2 in eastern. The module of the summary inclination made approximately 28",5, which gives us 1",2 yearly or 0",003 for a day, which points to stability of the point of observation. At moments, the change of inclination shows itself here more sharply than on Fig. 3, due, it seems, to the processes that take place in the crust.

b) Non-tidal inclinations in Tbilisi during the Spitak and Racha earthquakes. According to modern theories, genesis of earthquakes is ascribed to tectonic processes. These processes produce in the beginning cracks which gradually broaden up to large complex fracturing, which causes change in the volumes and properties of rocks, and produce defects in them.

On the basis of measurement and calculation it is noted [2] that a tension of 1000 N/cm² may be accumulated in a hearth, which is caused by deformation of the rocks of which the value may reach 10⁻⁵-10⁻⁴. Such accumulations should mainly be connected with the block structure of the Earth's crust. The blocks differ from each other in size as well as physical-mechanical properties. There takes place a distribution of the additional energy they receive among them and the change in their energetic condition takes place. In certain conditions the system may become instable, one of the possible results of which may be an earthquake. Immediately before the earthquake the character of deformation changes which causes variation of different background geophysical fields and produces some so called earthquake's preconditions, which are characterized by an interval of formation and the radius of possible spread.

The radius of earthquake's precursors ρ_ε (km) is defined by the following ratio between relative deformation ε and the magnitude M of the earthquake (Kasakhara, 1985)
$$\rho_\varepsilon = \frac{10^{0.433M - 2.73}}{\varepsilon^{\frac{1}{3}}}$$

Other Japan scientists propose the following linear relation between magnitude M and τ at the time of earthquake's preparatory period: $\lg \tau = 0.79M - 1.88$, where τ is measured in 24 hours. The connection between magnitude M and seismic energy E (erg) is calculated: $\lg E = 1.5 M - 11.8$

There in the records of tiltmeters some anomalies were noted of which the origin according to express-interpretation should be connected only with strong earthquakes.

The summary moves of inclination of the Earth's surface at Spitak and Racha earthquakes at the periods before and after the occurrences are shown on Fig. 5 in the shape of vector diagrams. It must be noted, in the first place, that the diagrams deeply differ formally from each other, changing with different gradients and in different direction. The Racha Earthquake is characterized by several 2-3 abrupt changes of inclination, while in the Spitak Earthquake diagram such thing is hardly observable and/or may be noted only once. Studying the resemblance and difference of their diagrams, several factors must be taken into consideration: first, these objects are situated on different sides from Tbilisi, correspondingly in southern and in northern; and they are in different geological and seismological conditions. In what ones, and why? These questions must be answered by investigation.

In addition, it may be said in regard of the Spitak diagram, that starting from January 1988 the Earth's surface in Tbilisi had been inclining with constant speed and in northern direction, where the angle of inclination during 6 months was $2.2''$ (second), and in eastern direction $-0.4''$. During 5 months after the earthquake the inclinations changed direction from east to west. It may be seen on the diagram that two months before the earthquake the direction of the vector of inclination coincided with the direction towards the epicenter.

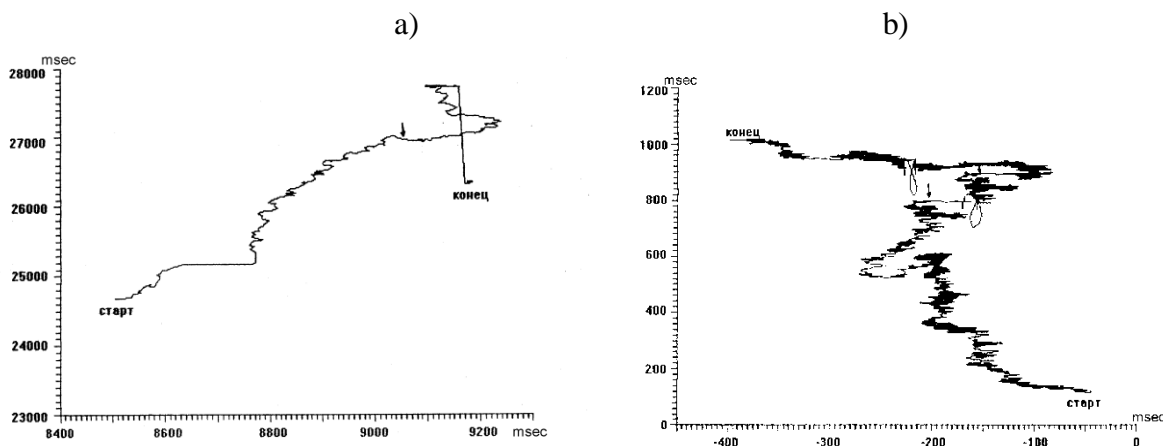


Fig. 5 Vertical diagrams of the inclinations of the Earth's surface in Tbilisi during the Spitak 1988 (a) and Racha 1991 (b) earthquakes, at the anterior and posterior periods of their occurrences.

On the vector diagram of inclination for 11.10.1990-5.9.1991 of the Earth's surface during Racha earthquake, two earthquake occurrences may be noticed; one the properly Racha 29.04.1991, $K=15.5$, $\Delta_{Tb}= 140$ km and Java - 15.06.1991, $K=11.5$, $\Delta_{Tb}= 115$ km. The arrows point to some moments of the earthquake. In both cases the direction of the vector coincides with the line connecting epicenter of the earthquake and the recording equipment.

Physical grounds of anomalous inclinations in the period of preparation and the preceding period of an earthquake are considered in different theoretical models, where it is shown that the variations of the velocity of deformation in the zone of seismic focus should have a bay-like character. It may be supposed that outside the focus zone the variations of deformation must have the same character. Here it must be noted that the existence of the anomalous tectonic regime in the zone of earthquake's preparation arouses a great interest of scientists not only because it can be observed long before the earthquake. This circumstance is particularly important because it gives us the opportunity of localizing future earthquake's epicenter with the help of integral investigations.

With the help of the above given empirical relations we estimated the radius of manifestation of the earthquake's precursors ρ_ε for the Spitak (7.12.1988) and Racha (29.4.1991) earthquakes. The time of manifestation of anomalous symptoms corresponding to the precursors τ has also been estimated. For the value of the anomalous precursor we take the inclination of the Earth's surface in Tbilisi, which exceeds 20 msec (20 msec represents the summary tidal inclination for Tbilisi as well as the zone of Enguri Power Station in E-W direction). The Table 1 shows the corresponding values.

Table 1

##	The time of the earthquake	Magnitude M	Distance from the epicenter, km	ρ_ε , km	T, year
1	Spitak 7.12.1988	6.9	105, Tbilisi 300, Enguri	380	8.0
2	Racha 29.4.1991	7.1	140, Tbilisi	470	11.4

As can be seen from this evaluation, the radius of manifestation of the precursors ρ_ε is different for the noted earthquakes, the time of manifestation of the deformational precursors τ is also substantially different. Here it must be noted: if for the given ρ_ε , and τ and different earthquake's epicenters their formation takes place at the same time, it is possible that their precursors superimpose each other and anomalous disturbances have a complex form, which can, of course, impede their identification.

The noted empirical examples allow us to suppose with the sufficient confidence that they are perhaps the precursors of earthquakes and there are other similar deformational-mechanical and geophysical precursors which are necessary to study with the deepest possible scientific earnestness. And this in our firm opinion will quite certainly take place in the nearest future.

It must be said that the equipment for registration of tidal processes gives us an opportunity to make registration of long-period seismic waves, which is impossible for classic seismic equipment. On one of such recordings in Tbilisi observatory have been received some distant $\Delta > 100^\circ$ many times going round the globe Rayleigh $R_1, R_2 \dots R_{10}$ and Love $L_1, L_2 \dots L_{10}$ waves caused by an earthquake, according to which the $S_1, S_2 \dots S_{10}$ and $T_1, T_2 \dots T_{10}$ specters of free oscillation of the Earth were determined. The earthquake that took place in the south of Tonga Island on June 22, 1977 ($M=7.9$; $\Delta=141.2^\circ$; $h=65$ km) with deformometer component N 66.5° E, recorded in Tbilisi

It is known that the tension which exists inside the Earth is produced and changes under the influence of the forces acting inside it. At particular places and in particular conditions some accumulation of energy takes place; then upon reaching the limits of durability of solid bodies the latter snap. Accumulation of elastic energy, which is unleashed during the earthquake, needs certain time, for which reason an earthquake is preceded by a certain period of preparation. We can connect earthquake's precursors with these processes which are reflected on the change of the conditions of tension as well as on different characteristic parameters of geophysical fields. Having this circumstances in view, we tried to calculate tidal inclinations of the Earth's surface registered in Tbilisi in connection with the two last and most intensive earthquakes in the Caucasus (Spitak, 1988 and Racha, 1991), the so called tiltmeter γ -factor (γ is the ratio of the tidal inclination angle and the theoretic angle of the place) by the method of harmonic analysis of main tidal 12-hour wave M_2 by means of 60 day long time series. Then the central moment of the series was replaces by two days and the diagram of γ -function was drawn. To determine this factor only M_2 wave was used, correspondingly, for N-S and E-W azimuths. Theoretical amplitudes for these azimuths at Tbilisi latitude are $A_{N-S}=7.85$ msec; $A_{E-W}=11.79$ msec.

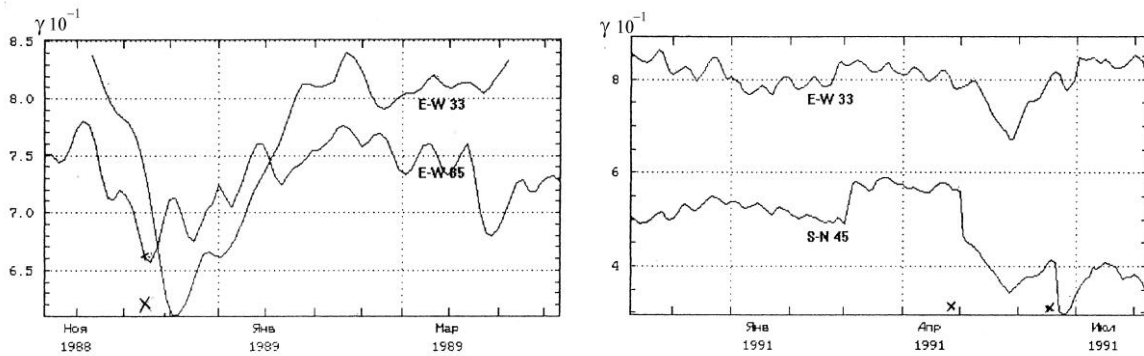


Fig. 6 The change of γ -function during Spitak 1988 (a) and Racha 1991 (b) earthquakes

It turned out that before both events – the earthquakes in Tbilisi and in Enguri – the reduction of the value of γ took place. Fig. 6 shows the diagram of change of γ -factor at Spitak and Racha earthquakes. In the noted time the interval value of γ in Spitak was systematically reducing and reached its minimum on November 12, 26 days before the earthquake. Then the growth began and reached its maximal value by the end of December. The whole change made 15% of the average value of γ , $\gamma_{av}=0.64$.

After that it was interesting to study the specters of tidal waves. In order to find out how the spectral densities of tidal waves changed for the above mentioned two earthquakes we built spectral time diagrams for corresponding periods with the help of the periodogram analysis. The results obtained show that during the earthquakes a sharp reduction of amplitudes of 12-hour and 24-hour waves took place, and in some cases even the whole disappearance of 24-hour waves (Fig. 7).

It is assumed that earthquakes are the results of abrupt shift of the masses of tectonic dislocation, which is characterized by a period of preparation – continuous physical changes.

In order to observe the precursors of these changes it possible to use any physical quantity which reflects tension in the rocks as well as its change. It may be change of seismic regime of the region reflected in different properties of geophysical fields. The changes of the parameters which are connected with the change of the physical properties of the rocks.

The materials of tidal inclinations with mechanical properties were processed for the Spitak and Racha earthquakes, the change in time of which may have caused the changes of inclinations and deformations of the Earth's surface around them and as a result the change of amplitudes of tidal waves. So, for instance, shrinking of the Earth's surface may cause consolidation of the rocks in the zone of dislocation, while stretching can cause the opposite effect. In the first case, the amplitude of tidal wave inside the zone would diminish and grow again outside it. Such is the apriori conception proposed in literature, let us see how it will work in regard of Spitak and Racha earthquakes' materials and in the differing seismic and geological conditions of Javakheti.

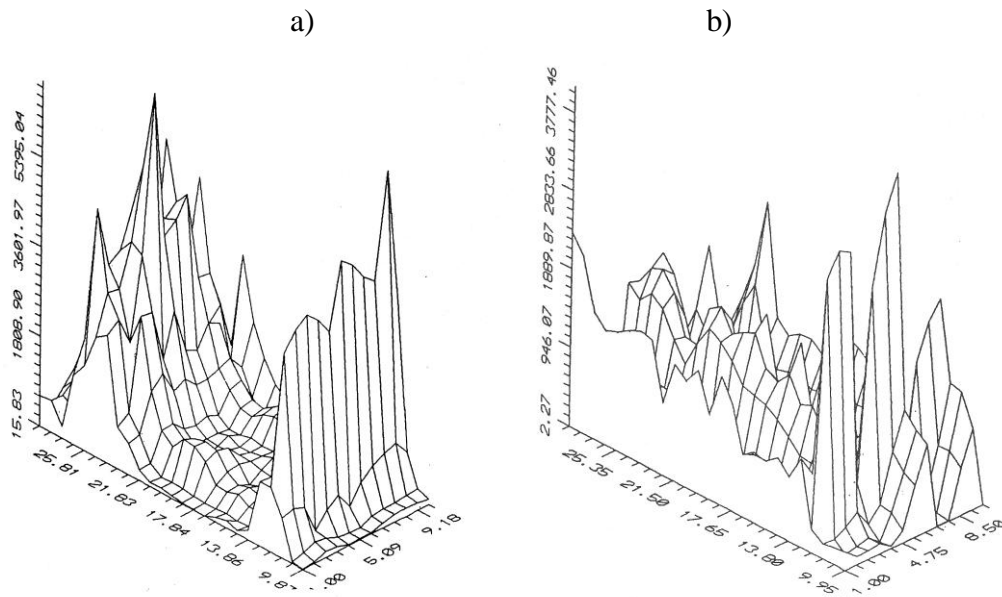


Fig. 7 Change of spectral density of tidal waves during Spitak 1988 (a) and Racha 1991 (b) earthquakes

A physics of earthquakes uses the theory of dislocation. However, the scope of dislocation investigations was substantially broadened and enriched after development of the Volterra theory. For determination of the residual shift we have to integrate the following (Volterra-Vaingartner) equation:

$$U_m(Q) = \iint_{\Sigma} \Delta U_k(P) W_{kl}^m(P, Q) v_l(P) d\Sigma$$

where Σ -is the surface of the dislocation, W_{kl}^m – the kl component of Green tensor for homogenous half-space caused by elementary force of M direction applied to a point; $\Delta U_k(P)$ - the shift on the surface of dislocation; $\Delta U_k(Q)$ – the shift in the observation point; γ_e – normal in p -point to the dislocation surface;

$\Delta U_k(P) = U_k^+ - U_k^-$ - represents shift on the dislocation surface in P -point; and U_k – the shift of right and left surfaces relative to initial location.

In general, it is impossible to integrate this equation. For its solution it is necessary to make a simplified model of dislocation. Here the rectangular vertical dislocation was considered to be of $2L$ length, and immersion of the lower boundary – D , immersion of the upper boundary – d .

The calculations may be made for two cases:

1. The shift on dislocation is made along the fall of the dislocation in horizontal direction (Straight-Slip)
2. The shift on dislocation is made along the fall of the dislocation in vertical direction (Deep-Slip)

For these cases the shift components u_1, u_2, u_3 are found out.

In this way, the materials obtained in Tbilisi with the help of the old Reber-Elest horizontal three-component pendulum in 1899-1916 as well as more recent – photo-electric tiltmeters, three-component quartz extezometer, fixed plotter with gravimeters Askania Werke, will be processed.

Such investigations will give us the opportunity to calculate also the deformational energy of the Earth which is discharged during strong earthquakes.

As it was noted, the events of triggering and synchronization can be observed in many geophysical processes, because the Earth generates a broad specter of oscillations and itself takes part in these processes. To strong geophysical forces often correspond more unobvious forces, of which the periodicity varies in wide range, from seconds up to years. Their influence on other weak or powerful

geophysical processes is not easy to estimate and they may even have catastrophic effects. It is often underlined in scientific literature the far-reaching influence of weak outside forces in connection with the change of intensity of seismic regime, which is explained by nonlinear nature of seismic processes, inadequacy of cause-effect factors. To such events belong micro-seismic oscillations caused by triggering of strong earthquakes. Of great interest in this respect is the monitoring and analysis of local micro-seismicity triggered by distant strong earthquakes, which may turn out to be an effective means of controlling the existing tension in the Earth's crust and a criteria for indentifying seismicity. This approach is new and perspective in seismology of earthquakes. In the conditions of present dense seismo-metric net and high-frequency wide-diapason seismic equipment it is possible to record dynamically triggered processes and connect them with strong earthquakes, on the one side, and with the local structure of the Earth's crust and the processes in it, on the other.

Many examples can be brought from the literature, though we will mention here just a few ones: dynamic triggering processes of Lander (1992), Denal (2002), Hector mine (1999), Sumatra (2004) and other earthquakes caused increased seismicity at different distances. Particular raise of seismicity was observed in the areas of active volcanic regimes and geothermal tension [4].

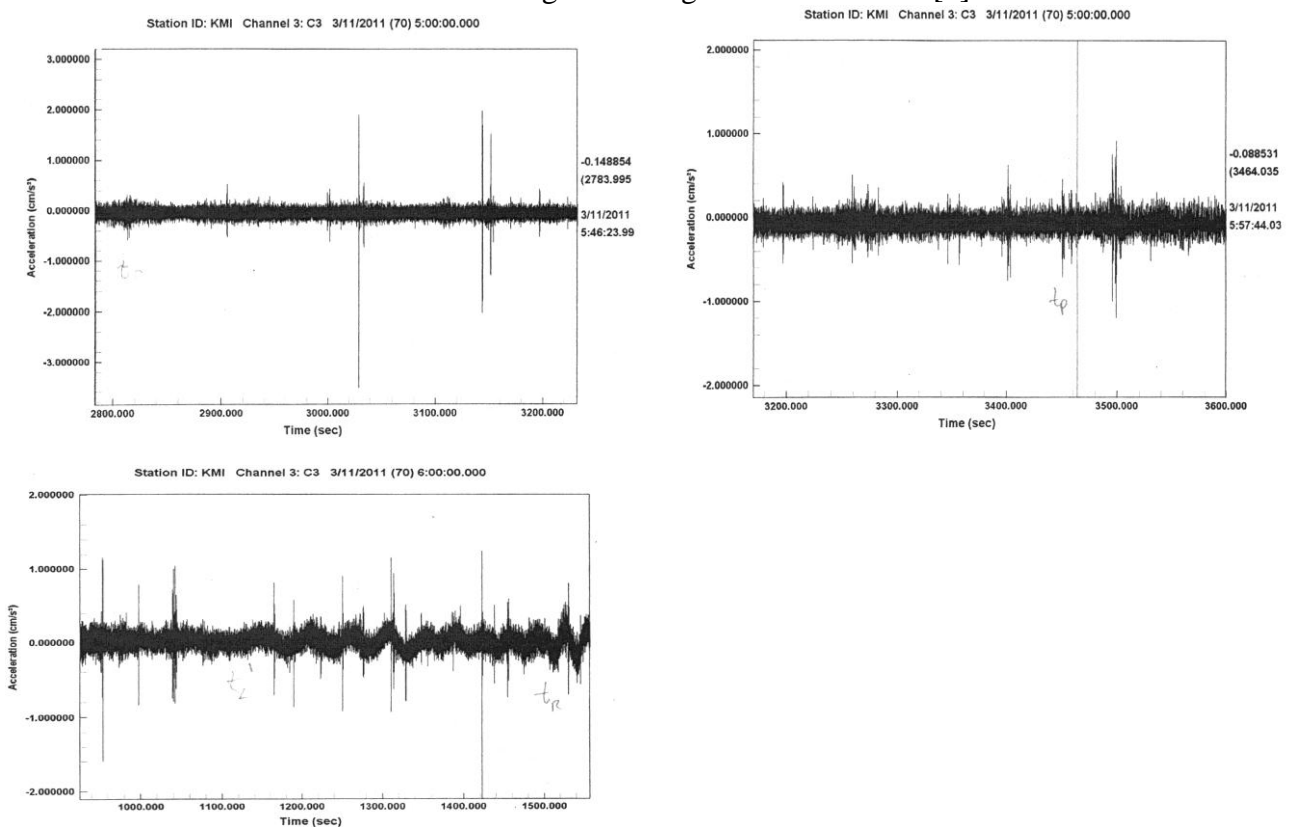


Fig. 8 The fragments of the record of triggering oscillations in Tbilisi by an accelerometer a) before the arrival of background waves b) at the time of arrival P-waves c) at the moment of arrival surface waves

As it was noted, triggering processes in our country are recorded by accelerometers. An important informational empirical material has been accumulated. To analyze and generalize the results it is necessary to compare it with the records of highly sensitive wide-frequency range equipment of seismic stations,.

The Fig. 8 shows the oscillations caused by strong Japan-Tohoku earthquake (11.03.2011), M=9, $\Delta \approx 7800$ km recorded in Tbilisi: the corresponding parameters are given in Table 2.

Table 2

N	Earthquakes	Components	$ \max + \min $ cm/sec ²	$ A2D $ cm/s ec ²	$ A2D $ sm/s ec ²
	11.02.2011 (Japan) T=06 ^h 1615 ^s	Ch1(z) Ch2(N550.5) Ch3(N340.5)	8.20 4.95 7.20	8.74	12.0

In order to establish the nature of triggered micro-seismic processes, the records in Tbilisi of two distant earthquakes had been chosen for express-interpretation: 1. New Zealand of 21.02.2011 M=6.3, $\Delta \approx 17000$ km and 2. Japan-Tohoku 11.03,2011 M=9, $\Delta \approx 78000$ km. The values of acceleration of ground for their maximal tremors (micro-seisms) in plane and space have been determined. Here the azimuth of the vector of acceleration is directed from the point of observation to the epicenter of the observed occurrence. It must be mentioned that on the seismogram a clear arrival of Love and Rayleigh surface waves with velocity dispersion can be noticed.

The object of investigation is the concept that seismic response of the lithosphere with a certain probability represents one of the most important means of determination of the epicenter mechanisms or, in particular, of evaluation of the environmental durability in relation to its critical condition.

One more theoretic consideration: the tensions which seismic waves transport over tele-distance are 10^5 times less than corresponding tensions in depth where the generation of seismic waves takes place. In spite of such ratio, according to the theory of synchronization, even weak forces can have great influence on the resonance rhythms of oscillating systems, the results of which are sometimes catastrophic! Resonance process, in particular, should be connected with the arrival of surface waves, triggered oscillations are also connected with the arrival of these waves.

c) The role of the Earth's tides as starting mechanism for earthquakes

Here, too, the considerations are hypothetical, grounded on the fact that the tension and deformations in the Earth's crust are not even in space and permanent in time. In some areas, and particularly there where the intensive tectonic processes are observed even the small changes in tension and deformation cause all kinds of dislocations, including faults of tension, and manifest themselves through earthquakes. There are different manifestations of nonlinear properties of geological environment, among which we note:

1. Seismic emission belongs to the class of nonlinear seismic events which shows itself in the fact that comparatively weak long-periodic oscillations can cause high-frequency oscillations of the environment (dynamic triggering).

2. Strong response to weak impact – is neatly manifested and frequently observed effect. It is apparent in the cases when the tension of the environment reaches a certain critical limit and at that moment some additional force (for instance, tides caused by the Moon or the Sun) affects it. It is noted in literature that such influence can cause earthquakes (static triggering).

As an experiment we tried to check the role of the tidal tension in inducing earthquakes, according to the seismic and tidal data on the Caucasus 1960-1979. For this the most seismically active Javakheti region was selected, which is located at $\Delta \sim 150$ km distance on the average from the epicenters of strong ($M \geq 5$) earthquakes. This choice was motivated by the following circumstances:

1. Javakheti region, having $\varphi = 40^\circ 8' \div 41^\circ 3'$; $\lambda = 43^\circ 3' \div 44^\circ 3'$ coordinates, is situated in a particularly seismically active zone and is characterized by a complex seismological-geological structure. In the noted period here occurred 65% of all the earthquakes of the Caucasus, among which $K \leq 7$; =80%; $K = 8$; =40%; $K = 9 \div 11$; =10%; not one of them with $K > 13$;

2. Close to Javakheti Plateau (in 150 km on the Turkish side) several epicenters of strong earthquakes ($M=6.1<65$) are located of which the influence on the seismicity of the region has not been noted. On the other hand, the tidal maximum in the noted period often correlates with the earthquake occurrences of $M<3$.

The seismic response represents an urgent problem for study and must characterize many important details of tectonic structure of the place, such as durability and stability moment.

If dynamical triggering causes the discharge of the static environmental tension it must be considered a positive event, and it may be noted: if that is so whether it is not possible to cause gradual discharging in the seismically tense areas? Such thing could be perceived as a preventive measure. Though if the artificial dynamic cause comes in resonance with static tension it may trigger a strong earthquake which can have a devastating effect on the environment. These problems deserve certainly the closest attention on the part of the scientific society.

References

1. Melchior P. – The Tides of the Planet Earth. Pergamon Press, 1978
2. Касахара К. – Механика землетрясений, Н. Мир, 1985
3. Балавадзе Б. К., Картвелишвили К.З. – Приливы в твердом теле Земли, Тбилиси, «Мецниереба», 1984
4. Kartvelishvili K. Z., Kartvelishvili N. K. – Tidal Triggering of Earthquakes, Journal of Georgian Geophysical Society, V2A, pp 81-86, Tbilisi, 1996
5. Kartvelishvili K. Z., Chelidze T. L. – Particular Ground Tilting Accompanying Some Near Large Earthquakes, Journal of Georgian Geophysical Society, V4A, pp 59-65, Tbilisi, 1999
6. Картвелишвили К. З., Картвелишвили Д.К. – Деформационная энергия земной коры, высвобождаемая при сильных землетрясениях, Тр. Института Геофизики АН ГССР Т.LVIII, стр. 3-6, Тбилиси, 2004
7. Картвелишвили К. З., Картвелишвили Д.К. – Остаточные наклоны поверхности Земли при некоторых близких землетрясениях, Тр. Института Геофизики АН ГССР Т.LVIII, стр. 7-11, Тбилиси, 2004
8. Картвелишвили К. З., Картвелишвили Д.К. – Остаточные смещения деформации и наклоны поверхности Земли, связанные с сильными землетрясениями, Тр. Института Геофизики АН ГССР TLVIII, стр. 12-20, Тбилиси, 2004

**გეოდერმოგრაფიულ და ტრიგერირებულ სეისმურ მონაცემთა
ზოგიერთი შედეგები მიწისძვრების პროგნოზირების შესაძლო
კრიტერიუმების დადგენის მიზნით**

კ. ქართველიშვილი, დ. გამყრელიძე, ს. ღონღაძე, გ. ქართველიშვილი,
მ. ნიკოლაიშვილი, ო. იავოლოვსკაია

რეზიუმე

განიხილება მიწის ქერქში მიმდინარე ფარული დეფორმაციული პროცესები, გამოწვეული შიდა ქერქშივე არსებული ან/და კოსმოსური ასევე ფარული ძალებით. ეს პროცესები ნაწილია ბუნების კანონზომიერებისა, სადაც წარმოიქმნება ფიზიკურ მოვლენათა სიმრავლე და თვითონ წარმოქმნიან რაღაც მოვლენებს. ასეთ მოვლენებს განეკუთვნება ქერქის დეფორმაციები. ეს მოვლენები ორგანულ მიზეზ-შედეგობრივ კავშირშია მიწისძვრებთან და კოსმიურ მიმოქცევებთან. მიწისძვრების მომზადების პერიოდს უკავშირდება ქერქის დეფორმაციის მრავალი ნიშანი და კრიტერიუმი, რის საფუძველზედაც შესაძლებელია გაკეთდეს რაიმე დონეზე მათი წარმოქმნის ადგილის, ინტენსივობის და დროის პროგნოზირება.

**Некоторые результаты геодермографических и триггерированных
сейсмических данных с целью установления возможных
прогностических критерий землетрясений.**

*К. Картвелишвили , Д. Гамкрелидзе , С. Гонгадзе , Г. Картвелишвили,
М. Николайшвили , О. Яволовская.*

Резюме

Рассматриваются происходящие в земной коре скрытые деформационные процессы, вызванные действующими внутри нее или внешними космическими силами. Эти процессы представляют часть природных закономерностей, где возникает все разнообразие физических явлений и, в свою очередь, вызывают какие-то явления. К таким явлениям относятся также коровые деформации. Эти явления находятся в причинно-следственной связи с землетрясениями и космическими приливными явлениями. С подготовительным периодом землетрясений связано множество признаков критериев деформации коры, на основании которых возможно строить определенного уровня прогнозирование места, интенсивности и времени землетрясений.

Simulation of point explosion's seismic energy by means of the frequency spectrum of body waves

Z. kereselidze, N. Tsereteli

M. Nodia Institute of Geophysics at I.Javakhishvili Tbilisi State University,
1 Akeksidze str., 0193 Tbilisi, Georgia nino_tsereteli@tsu.ge or
nino66_ts@yahoo.com

Abstract

Solve the inverse problem, which is aimed at modeling a discrete frequency spectrum of seismic body waves generated by artificially weak point explosion or a natural earthquake ($M \leq 4$). Proposed a spherical model of the hollow area of the point explosion and used a well-known analytical method for modeling the hydro-mechanical oscillations of a liquid drop. Innovation in the applied work is the use of a complete solution of the radial Euler equation. Such a modification of the classical scheme, which uses only an internal solution is mathematically quite correct, because it means virtuality of seismic source's elastic oscillation. As a result, with the help of the discrete spectrum of seismic body waves can be determined the linear parameters and total energy of point explosion (weak earthquake) that is approximated as a hollow body with spherical shape.

Keywords: weak earthquake, hollow area, elastic oscillation, fundamental frequency.

Introduction. Despite the similarity of effects that accompany earthquakes and explosions, these phenomena have a different nature. Primarily, the point source of explosion can be located anywhere while hypocenter of earthquake is always in seismically active zone and significant tectonic stresses area. The energy released during an earthquake and a point explosion in the focal zone is distributed according to the same pattern from a mechanical point of view: a significant portion of this energy expended in irreversible changes in the sources area, the rest part of its generates the body and surface seismic waves. The point explosion's energy comparable with the weak earthquakes ($M \leq 4$) (perhaps with the exception of particularly powerful nuclear explosions), during which most of the energy of elastic deformation is consumed to generate the seismic body waves. There are differences in the method of measuring the total energy released during moderate and strong earthquakes and point explosions. However, before the era of underground nuclear explosions was assumed that in case of lack of dispersion, the amplitude of the elastic body waves of point explosion should be proportional to the square root of the oscillations energy density (as for earthquake). However, analysis of the underground nuclear explosions's series data in 1958, that in fact are analogous to the point explosions, this is not confirmed. The relationship between the explosion's energy and the amplitude was linear, so new model of explosion source have been proposed [1]. According to this model, the area of any explosion source is a special, so-called zone violation, in which energy is transferred and absorbed by nonlinear laws. It is believed that the radius of the zone is proportional to the cube root of the energy of the explosion. Further, beyond the violations zone, disturbance is linearly elastic in the medium. It is assumed that propagating compression wave here are not subjected to the dispersion. In this case, the individual harmonics of the body waves can propagate independently. Obviously, such a situation is ideal and is expected wave propagation without any obstacles, which is possible only in a completely homogeneous medium. In fact, analysis of seismic waves propagation can be quite complex in the elastic medium, not only because of the heterogeneity of the environment and the absorption of waves,

but also the existence of a free boundary, for example: the earth's surface and the fault. Therefore, it was suggested that the medium is uniform in a sufficiently large area, the radius of which substantially exceeds the radius of the explosion energy release, in other words, the zone of nonlinear transformations. In some studies, factually the model in [1] has been used to simulate the change of the radial stress at the interface of the inelastic and elastic region [2].

Model of a point explosion. The purpose of work [1] was an analytical justification of the relationship between soil displacement and the explosion energy carried out by body seismic waves. Obviously, such a task is straightforward because suggests a correlation between the known parameters: given energy of the explosion and the observed value of soil displacement. However, besides displacements soil informative are also themselves seismic wave frequency spectrum, which is also dependent on the energy of the explosion. If we consider that the heterogeneity of the medium influenced less significant effect on seismic waves, in particular, on their frequency, an attempt to study the relationship between the explosion energy and body waves can be considered as a perspective task. It should be noted that assuming no dispersion of body waves, in contrast to [1], it is possible to solve the inverse problem, i.e. determine the explosion energy by body waves frequency spectrum. An attempt to solve such a problem has been undertaken in the work [3]. Physical conditions of the work actually coincide with the statement of the problem in [1] as it also assumes that the point explosion is followed by an avalanche-like release of energy resulting in the generation of shock waves and plastic deformations. So there should be a zone of non-linearity. On the border of this zone must establish a balance between the pressure force and the elastic force of the environment. It is evident that the balance of forces arise only if the energy density of the explosion will be commensurate with the energy density of the elastic deformation. The front propagation of disturbances caused by a point explosion is supposed to be radial in a homogeneous incompressible medium. Spherical symmetry is violated with increasing distance in an inhomogeneous medium. However, in any case, the deviation from sphericity is unlikely to be so significant that the boundary of the plastic deformation of the explosion could not be approximated by a spherical, or more complex, by the surface of the rotation ellipsoid. The same form can be assumed also for the outer boundary of linear elasticity area, if we neglect the inhomogeneity of the medium and to postulate the absence of free boundaries. In this case, in work [3] was proposed hypothesis that body seismic waves are the result of self mechanical oscillations of the body, which is an spatial abstraction of the linearity zone around the point explosion source. Obviously, these oscillations induced by the elastic force and should have a discrete frequency spectrum. In the simplest case, discussed body may have the shape of a hollow sphere, the inner radius equal to the radius of the zone violation. The next step is to approximate the area of a point explosion by hollow rotation ellipsoid. This figure has a lower degree of symmetry comparable with the sphere. Due to this the degenerate oscillations will take place. Therefore effects of shear deformation can be neglected at a point explosion, unlike earthquakes. This is essential since simulation of the vibrational spectrum, generated by a strong earthquake is very challenging. During the earthquake, as a rule, there are considered as body waves, so surface seismic waves. Analytical solution of this problem is obtained only in the case of spherical symmetry by presenting the shear modulus as a sum of normal modes of vibrations [4].

Statement of the problem. The problem of accurate determination of the total energy released by an earthquake, is the main task of seismology. It is known that some of the total energy, the so-called seismic energy, is consumed to generate the body and surface seismic waves. Unlike natural earthquakes, the total energy is known in advance during point explosion. Furthermore, for an underground nuclear explosions has been determined that the approximately 5-8% of the total energy passes to the elastic seismic waves [5,6]. Therefore, if the total energy of the explosion is known, there is no need to determine the seismic energy by seismic data. However, estimation of total energy, during the earthquake, is a problem. It is obvious that the direct transfer of the result, which is valid for explosions, to an earthquake is incorrect. It is known that seismic energy is dependent on the source

volume [7]. In the case of moderate and strong earthquakes this area is difficult to determine because of the considerable scatter of aftershocks in time and space. Therefore, proportion of seismic energy in the total energy can very substantially changed with increasing earthquake magnitude. However, for small earthquakes, like an nuclear and tecnical explosions, almost all the seismic energy transfer in body waves. Therefore, the relationship between seismic energy and the total energy of the earthquake in both cases varies in the same range. It is obvious that, like explosions, for small earthquakes seismic source zone is a violation within the meaning of [1].

Assessment of the explosion volume, and consequently, the seismic energy, when we know its total energy, it is not difficult. During the earthquake the total energy is unknown that could be estimated by seismic data. Therefore, any attempt that simplifies the tedious process of seismic source volume determination can be considered relevant. In particular, it appears that the volume of weak earthquakes source can be quite easy define following [3], the essence of which is given below.

Scheme of mathematical modeling. The physical analogy with hydromechanical natural oscillations of a liquid incompressible drop of spherical configuration has been used as the basis of the model proposed in [3]. It is known that small perturbations of its surface is able to maintain the shape of a drop due to the action of capillary forces [8]. If it is assume that the generation of body waves associated with perturbations of the boundary of a hollow elastic body, we can use the mathematical scheme of self hydro-mechanical oscillations of a spherical drop. As it was shown in [8] this scheme can be generalized to the case where the drop has shape of elongated rotation spheroid. Obviously, for the area of a point explosion such shape is more appropriate than a sphere. Though, to estimate the volume of seismic source is enough to use the result, which corresponds to the most simple spherical symmetry. According to [8], a mathematical model is correct if the amplitude of the oscillation or radial displacement of the boundary of the hollow body modeling area of point explosion considerably small compared with the characteristic linear dimension of the body. Additionally, the oscillation speed of the hollow body surface should be substantially less than the velocity of shock waves generated in the nonlinear transformation zone or in seismic source area. It is obvious that both of these requirements are performed that is the necessary condition for small perturbations causing the linear elasticity, and generating self mechanical oscillation of the body, identified with the area of the point explosion. It is believed that regardless of the site condition, this area despite a small radial displacement of its borders is incompressible and homogeneous, both before and after an explosion (or a weak earthquake). Consequently, the oscillation motion of the hollow body obeys the Laplace equation

$$\Delta\psi = 0, \quad (1)$$

where ψ is potential, oscillation speed - $\vec{V} = grad\psi$.

In a spherical coordinate system, the condition of equilibrium boundary of the hollow body, modeling area of a point explosion, is given with the Laplace formula for a liquid drop

$$P_1 - P_2 = KL \left(\frac{1}{R_1} + \frac{1}{R_2} \right), \quad (2)$$

where P_1 and P_2 are the pressures respectively inside and outside the sphere, R_1 and R_2 are the principal curvature radii of the oscillating surface. The coefficient of capillary surface tension giving the elasticity effect is replaced by the product of the uniform compression modulus K by the characteristic linear dimension of the sphere boundary L

$$K = \frac{E}{3(1-2\sigma)}, \quad (3)$$

where E is the tension modulus (Young's modulus) and σ - the Poisson coefficient.

Therefore the difference between the pressures can be defined by means of the expression [8]

$$\Delta P = P_1 - P_2 = -\rho g u - \rho \frac{d\psi}{dt}, \quad (4)$$

where u is the radial displacement producing the oscillation of the spherical surface, ρ - density of the medium, g - gravity force acceleration. In the Spherical system, the displacement velocity is related with the motion potential by the expression

$$\frac{\partial u}{\partial t} = \frac{\partial \psi}{\partial r}. \quad (5)$$

Since the gravity force does not influence the elastic deformation effect without loss of generality in (4), we can neglect the first term on the right-hand side, i.e. in the sequel it will be assumed that

$$\Delta P = -\rho \frac{\partial \psi}{\partial t}, \text{ which coincides in form with the first motion integral [8].}$$

This condition and also analytical expression for the parameter $\frac{1}{R_1} + \frac{1}{R_2}$ defined by variation surface used in the expression (4), from which we obtain the boundary condition for ψ

$$\left. \frac{\partial^2 \psi}{\partial t^2} \right|_r - \frac{K \cdot L}{\rho r^3} \left\{ 2 \frac{\partial \psi}{\partial r} + \frac{\partial}{\partial r} \left[\frac{1}{\sin \theta} \frac{\partial}{\partial r} \left(\sin \theta \frac{\partial \psi}{\partial \theta} \right) + \frac{1}{\sin^2 \theta} \frac{\partial^2 \psi}{\partial \varphi^2} \right] \right\} = 0. \quad (6)$$

Condition (6) is valid if the potential will have the form of a standing wave

$$\psi = A \cdot F(r, \theta, \varphi) e^{i\omega t}, \quad A = const, \quad (7)$$

where the function $F(r, \theta, \varphi)$ satisfies the Laplace equation (1). As is well known, any solution of this equation can be represented as a linear combination of volumetric spherical functions:

$F(r, \theta, \varphi) = X(r)Y(\theta)Z(\varphi)$ where $X(r)$ - radial function, $Y(\theta) = P_n^m(\cos\theta)$, - the Legendre function, $Z(\varphi) = e^{im\varphi}$. In the work [3] is used the function: $X = A_n r^n + B_n r^{-(n+1)}$, that is **full** solution of the Euler radial equation. This is different fundamentally from the solution in [8], where the potential in (7) represented only by the inner part of the radial function $\sim r^n$. As a result, after standard transformations, the discrete spectrum of **natural** frequencies of a hollow sphere can be obtained

$$\omega_n^2 = \frac{KL}{\rho r^3} \left[(n-1)(n+2) \frac{nA_n r^{n-1} - (n+1)B_n r^{-(n+2)}}{A_n r^{n-1} + B_n r^{-(n+2)}} \right], \quad (8)$$

where $n \geq 2$ ($n = 0$ corresponds to a state at rest, $n = 1$ to translational motion).

Expression (8) differs from the formula defining oscillations of a solid spherical drop. First, in (8) is presented as a multiplier value of compression modulus and density of the medium, which is the square of the velocity of body waves [3]. Addition, solution for a solid sphere must be valid everywhere, including the focal point. So in classical scheme only the inner solution of the Euler equation is used as a solution of the form: $r^{-(n+1)}$ at point $r = 0$ is divergent. For a hollow body this problem does not exist and therefore we can use a general solution. As a result, as is seen from (8), the frequency should not be real, it may be has an imaginary value **too**. Such a situation is quite favourable when modelling the point explosion region whose inner surface must bound the volume in which shock waves propagate and plastic deformations take place. An example of a relatively simple formula for a

hollow sphere of finite thickness clearly shows that it is only by means of a general solution of the Euler equation that we can define the size of the region where elastic forces may generate seismic waves. For this purpose, it is necessary to determine the constants of a complete radial function by introducing a radius of the boundary between the linear and nonlinear zones. On this surface, according to the model, the frequency of elastic waves should be zero. Thus, from (8) we have

$$nA_n R^{n-1} = (n+1)B_n R^{-(n+2)}, \quad (9)$$

which implies

$$B_n = \frac{n}{n+1} A_n \cdot R^{2n+1}$$

Consequently, because of the relation (9) constants in the formula (8) should be excluded. After the introduction of the parameter R , the characteristic linear dimension of the hollow body also be defined: $L = (r - R)$. Finally the following expression for discrete frequency spectrum has been obtained

$$\omega_n^2 = \frac{\alpha V_m^2}{r^2} \left[(n-1)(n+2) \frac{\left(\frac{r}{R}\right)^{n-1} - \left(\frac{R}{r}\right)^{n+2}}{\frac{1}{n}\left(\frac{r}{R}\right)^{n-1} + \frac{1}{n+1}\left(\frac{R}{r}\right)^{n+2}} \right], \quad (9)$$

were $\alpha = (1-R/r)$, $V_m = \left(\frac{K}{\rho}\right)^{\frac{1}{2}}$ - velocity of longitudinal body wave without taking into account the

shear deformation. Velocity of primary seismic wave: $V_p = \left[\frac{E}{3\rho(1-2\sigma)} + \frac{2E}{3\rho(1+\sigma)} \right]^{\frac{1}{2}}$. It almost

exceeds the speed of secondary shear wave $V_s = \left(\frac{G}{\rho}\right)^{\frac{1}{2}}$ average by a factor 1.7 in any environment

($G = \frac{E}{2(1+\sigma)}$ - transverse shear modulus). So velocity $V_m \approx 0.8V_p$.

Discussion of the inverse problem. The aim of this work is to show the way for a relatively simple solution of the inverse problem for the hollow sphere approximation, when two linear parameter of a point explosion were defined: the radii of the plasticity and linear elasticity zones. Besides the physical parameters of the considered medium it is assume that the spectrum of point explosion frequencies is also the given one, then we can define the unknowns R and r . In fact, the problem is in the knowledge of the fundamental frequency ω_2 ($n=2$), as in a homogeneous medium $\frac{\omega_3}{\omega_2} \approx 2$.

Therefore, the spectral analysis of point explosion is necessary to solve the inverse problem, which should give the value of the fundamental frequency of seismic body waves. The desired radius can be determined by the first two equations (9) corresponding frequencies ω_2 and ω_3 .

A distinctive feature of this work is to neglect of the effect of shear deformation and use the modulus for compression as a parameter of the elastic properties of the Earth's environment. This assumption is justified in the case where the power of a point explosion is not higher than the power of weak earthquakes ($M \leq 4$). According to [2], for sufficiently powerful underground nuclear explosions, when the transverse seismic waves became visible, their fundamental frequency is given by equation

$$\omega_0 = \frac{2V_s}{R}, \quad (10)$$

where R is the radius of the surface elastic wave generation. Obviously, in the case of the expression (9) yields the fundamental frequency of the same order as that of the expression (10).

It is notable that one solution of task is known to determine the frequency spectrum of the radial natural oscillations of an elastic sphere. Physically, it is obvious that realization such oscillations is possible only when the speed of displacement changes is directed along a radius and depends only on coordinate r [8,10]. According to the boundary condition on the surface of the sphere, the radial component of the strain tensor is equal zero. The problem of periodic oscillations in time reduces to the general wave equation for the potential movement. The solution of this equation, which is valid throughout the volume of a sphere, including its centre, has the form

$$\varphi = A \frac{\sin kR}{R} e^{-i\omega t} \quad (11)$$

Due to equation (11) and the boundary conditions resulting from the Hooke's condition on the surface $R = r$, the transcendental equation was obtained for kr

$$\frac{tgkr}{kr} = \frac{1}{1 - 0.25[(V_p/V_s)kr]^2}, \quad (12),$$

$k \sim \frac{1}{r}$ - is the wave number. The roots of this transcendental equation (the exact analytical solution of which is impossible) determine the frequency of natural oscillations of an elastic sphere. However it is possible approximate analytical or numerical solution, after which the fundamental frequency of the radial oscillations of an elastic sphere is determined by the velocity of the longitudinal wave: $\omega_k = V_p k$.

Thus, using the formulas (9) and (10), as well as the numerical solution of equation (12) when the velocity ratio is 1.7, it is possibility to compare different models of elastic oscillation of point explosion. The radius value of linear zone should be considered as the core defined by the expression (9). The underground nuclear explosions represent the most convenient case as all parameters are known for comparative analysis. It is suitable, for example, the very first underground nuclear explosion conducted in Nevada in 1957 [11]. The wave effects of this explosion were well studied. That is necessary to test the effectiveness of our model and the comparison with the parameters obtained from other models. Power of the explosion in Nevada was 1.7 Kt trotyl (equivalent $M \approx 4$), that is corresponding to an energy $E = 7,4 \cdot 10^{12} \text{ J}$.

Now it should be defined the fundamental frequency, which is being main parameter in the formula (9). It is believed that in the case where the magnitude is known, it is possible not to use a spectral analysis and use the empirical relationship between the period and magnitude. However, in the range $M = / 3-5 /$ such a relation is not defined. There is the equation that is considered fair for small magnitudes [12]

$$\lg T = 0.47M - 1.79. \quad (13)$$

According to this equation, the main (peak) frequency should be $\approx 2.4 \text{ Hz}$ when $M \approx 3$. Obviously, for $M \approx 4$, it will be even less. In fact, for the explosion in the Nevada, main frequency was significantly greater, because fixed frequency were in the ranged $/ 6-40 / \text{ Hz}$. Consequently, the fundamental frequency of this interval should be considered as 6 Hz . However, it should be noted that during the arrival of the first head wave there were two peaks of frequency 3 Hz and 7.5 Hz at the same time. Then, after considerable delay, there were two peaks at 10 Hz and 5 Hz . This is not a very significant difference from the frequency of the first registered interval. This may have been caused by heterogeneity of the medium, as well as by the records error. The observations were made at a distance

of about 600 km from the explosion site. Due to mention above appropriateness of the formula (13) seems doubtful.

Thus, the frequencies: $\omega_2 = 6$ $\omega_3 = 12$ Hz were used to determine the characteristic radii of the Nevada explosion from formula (9). At the same time, the most probable value of the velocity should be used, which, according to our model, can be assumed equal the velocity rate of body waves 6.1 km/s [11]. Consequently, since $V_m \approx 0.8V_p$, we will have $V_p = 7.6$ km/s. As a result, the specific values have been obtained for fundamental and first harmonic from the two equations (9) characterizing the area of underground nuclear explosions $r = 1.84$ km (the radius of the surface of the generation of body waves) and $R = 1$ km (radius of the seismic source).

For comparison the well-known empirical formula for seismic source radius (in kilometers) and the magnitude can be used [13]

$$\lg R = -1.67 + 0.42M \quad (14)$$

According to this formula $R \approx 1$ km, that is identical to the value obtained by our model for $M \approx$

4. Using R we can determine the volume of the seismic source $V_c = \frac{4}{3}\pi R^3$ and seismic energy $E_c = eV_c$, where e is the density of the elastic strain energy. According to [5,6,12], this parameter is $e \approx 10^{-4}$ J. Seismic energy is approximately 5-8% of the total energy of the explosion, so its value will be $(5 \div 8,4) \cdot 10^{12}$ J, which correspond to the nuclear explosions with power in the range of /2-1.2/ kt trotyl. Thus, in this case a good agreement have been established between the known value and corresponding interval of the modelled value of the total energy of an underground nuclear explosion in by the formula (9). Obviously, it is necessary to evaluate the quantitative effect of classical mathematical scheme's modification, which is the basis of our model. For this should be compared the result obtained for the hollow body with the result corresponding to a continuous area for the same value of the fundamental frequency. In this case, in the formula (9) must be regarded as $R = 0$, the following expression will be obtained from which we can determine the radius of the body, approximating the area of a point explosion

$$\omega_n^2 = \frac{\alpha V_m^2}{r^2} [(n-1)(n+2)n] \quad (15)$$

From the equation (15) for $\omega_2 = 6$ Hz we obtain: $r \approx 1,95$ km. If this magnitude is considered as the radius of the source, then the total energy of a point explosion will have a range that is much greater than the energy of the explosion in Nevada: $E = (3.5 \div 5.8) \cdot 10^{13}$ J. Thus, if this range is compared with a range derived above for the hollow body, the efficiency of our model giving real value of the energy is quite apparent.

For comparative analysis, the main frequency can be identified, which is given by equation (12) and formula (10). For this we use the radius of the area of the point explosion: $r \approx 1,85$ km, because according to the formula (9) it corresponding to the frequency $\omega_2 = 6$ Hz. In particular, the first root of the numerical solution transcendental equation (12) is $kr = 0.5$. Since $\omega_k = V_p k$, for $k = 1/r$, and $V_p \approx 7.6$ km/s, we obtain: $\omega_k \approx 2$ Hz. Further, in formula (10) is presented the velocity of shear wave. Its value when $V_p \approx 7.6$ km/s, is equal to: $V_s \approx 0.6V_p \approx 4.6$ km/s. Therefore, according to this model, the fundamental frequency $\omega_0 = 5$ Hz. Based on these estimates, it can be concluded that in most cases there are small difference between the results of the formula (9), equation (12) and (10). But it is apparent

disagreement with the empirical relation (13). These facts serve as a clear demonstration of the effectiveness of our own model for mechanical vibrations of the point explosion. In particular, it is the only one using only the velocity of seismic body waves, as well as their fundamental frequency and the first harmonic explicitly defines the volume of the point explosion and its total energy.

For clarity of the formula (9), figure 1 illustrates the dependence of the radii r and R on the fundamental frequency ω_2 when the ratio $\frac{\omega_3}{\omega_2} \approx 2$. Here a seismic body wave velocity is $V_m \approx 6.1 \text{ km/s}$.

It should be noted that the assumption of the harmonic nature of the seismic waves is quite rude. This requirement becomes very hard when data are recorded on a great distance from the explosion or the weak earthquake. Obviously, in the real environment, due to its heterogeneity, the ratio between the fundamental frequency and the first harmonic will change. During the solution of the inverse problem, this ratio should be determined only by the harmonic analysis of the data.

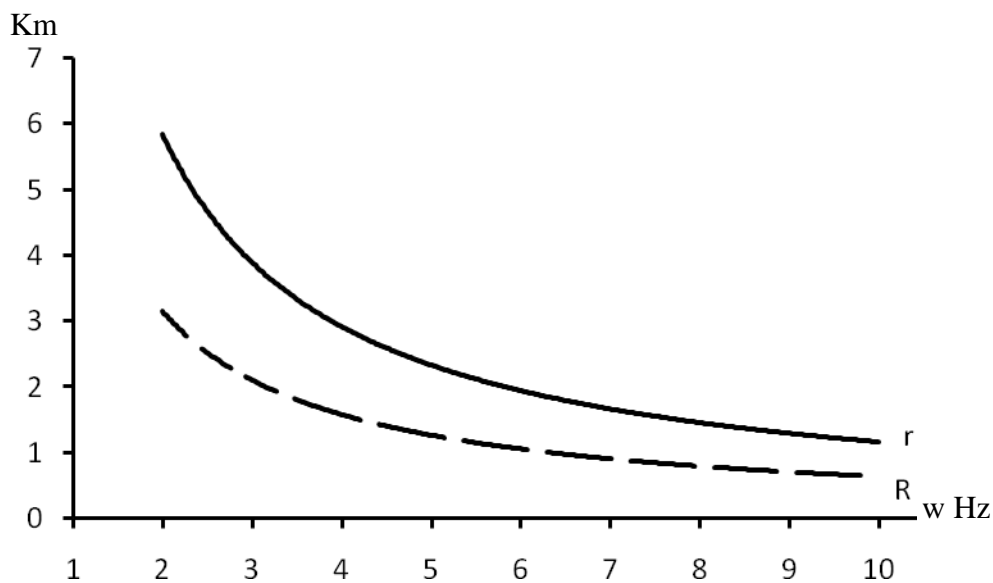


Figure 1. The dependence of the radii r (solid line) and R (dash line) on the fundamental frequency

References:

- [1] Latter, A.L., Martinally, E.A., Teller E. Seismic scaling law for underground explosions. Phys. Fluids, Vol.2, pp.280-82, 1959;
- [2] Rodin, G. Seismology of nuclear explosion. Moscow. MIR, p. 190, 1974, (In Russian) ;
- [3] Kereselidze, Z., Gegechkori, T., Tsereteli, N. Modeling of elastic waves generated by a point explosion. Georgian International Journal of Science and Technology ISSN 1939-5825. Nova Science Publishers, USA, vol. 2, issue 2, pp.155 – 166, 2010.
https://www.novapublishers.com/catalog/product_info.php?products_id=14264 ;
- [4] Aki, K. and P.G. Richards. Quantitative Seismology, Theory and Methods, Vol. I and II, W.H. Freeman, San Francisco, 1980;
- [5] Sadovski M. A, Kedrov O.K., Pasechik I, P. About Seismic energy and volume of foci of crustal earthquakes and underground explosions. DAN SSSR, V.283, №5, pp.1153- 56, 1985;
- [6] Sadovski M. A. Complex investigation in the Physics of Earth. M. Nauka, pp. 203-214, 1989, (In Russian);

- [7] Krowley B.K., Germain L.S. Energy released in the Benham aftershocks. Bull. Seismol. Soc. Amer., Vol. 61, №5, pp.1293-1301, 1971;
- [8] Landau, L., Lifshitz, E. M. Continuum Mechanics. M., Publishing House Tech. Teor. Lit, P. 795, 1954 (In Russian);
- [9] Gvelesiani, A., Kereselidze, Z., Khantadze, A. About the spectrum of the natural frequencies of the Earth's magnetosphere. Tbilisi, Ed. TSU, pp.36-49, 1983 (In Russian);
- [10] Landau, L., Lifshitz, E. M. Theory of Elasticity. M. Nauka, P. 202, 1965 (In Russian);
- [11] Grosling, B. F. Seismic waves from underground nuclear explosion in Nevada. Bull. Seismol. Soc. of Amer., Vol.49, №1, pp.11-30, 1959;
- [12] K. Kasaxara. Earthquake Mechanics. Cambridge Univ. Press, 1981;
- [13] Riznichenko, Y. B. Problem of Seismology. M. Nauka, p. 407, 1985, (In Russian);

წერტილოვანი აფეთქების სეისმური ენერჯის მოდელირება მოცულობითი ტალღების სიხშირული სპექტრის საშუალებით

ზ.კერესელიძე, ნ.წერეთელი

რეზიუმე

ამოხსნილია შებრუნებული ამოცანა, რომლის მიზანს წარმოადგენს იმ მოცულობითი სეისმური ტალღების დისკრეტული სიხშირული სპექტრის მოდელირება, რომელთა გენერაციის მიზეზს წარმოადგენს ხელოვნური წერტილოვანი აფეთქება ან სუსტი ბუნებრივი მიწისძვრა (M). გამოყენებულია სითხის წვეთის საკუთარი ჰიდრომექანიკური რხევების მოდელირების ცნობილი ანალიზური მეთოდი და შემოთავაზებულია სიცარიელის მქონე წერტილოვანი აფეთქების არის სფერული მოდელი. ნაშრომის სიახლეს წარმოადგენს ვილერის რადიალური განტოლების სრული ამონახსნის გამოყენება. კლასიკური სქემის, რომელშიც გამოიყენებოდა მხოლოდ შინაგანი ამონახსნი, ასეთი მოდიფიკაცია მათემატიკურად საკმაოდ კორექტულია, რადგანაც გულისხმობს სეისმური კერის რხევის ვირტუალობას. ამრიგად, მოცულობითი სეისმური ტალღების სიხშირეთა დისკრეტული სპექტრის საშუალებით, შესაძლებელი ხდება სიცარიელის მქონე სფერული სხეულით აპროქსიმირებული წერტილოვანი აფეთქების (სუსტი მიწისძვრის) პარამეტრების განსაზღვრა. ასეთი მახასიათებლებია: სეისმური კერის (პლასტიკურობის ზონა) რადიუსი და წრფივი დრეკადობის არის რადიუსი. ამის შემდეგ შესაძლებელია წერტილოვანი აფეთქების ან სუსტი მიწისძვრის სეისმური და სრული ენერჯის სიდიდის საკმაოდ მარტივად შეფასება.

Моделирование сейсмической энергии точечного взрыва при помощи спектра частот объемных волн

З. Кереселидзе, Н. Церетели

Резюме

Решается обратная задача, цель которой заключается в моделировании дискретного спектра частот объемных сейсмических волн, генерированных искусственным точечным взрывом или слабым естественным землетрясением (M). Предлагается сферическая

модель полый области точечного взрыва и используется известный аналитический метод для моделирования собственных гидромеханических колебаний жидкой капли. Новшеством, примененным в работе, является использование полного решения радиального уравнения Эйлера. Такая модификация классической схемы, в которой применялось лишь внутреннее решение, является математически достаточно корректной, т.к. подразумевает виртуальность упругих колебаний сейсмического очага. В результате, при помощи дискретного спектра частот объемных сейсмических волн, можно определить линейные параметры области точечного взрыва (слабого землетрясения), аппроксимируемой полым телом сферической формы. Такими линейными характеристиками являются радиус сейсмического очага (зона пластичности) и радиус зоны линейной упругости. После этого можно достаточно просто оценить сейсмическую и полную энергию точечного взрыва либо слабого землетрясения.

Additional experiments on the study of peculiarities of clear water, H_2O , and both water sugar, $C_{12}H_{22}O_{11}$, and edible salt, $NaCl$, solutions of maximal densities by means of original fluids bubble boiling method

Anzor Gvelesiani, Nodar Chiabrishvili

*Iv. Javakishvili Tbilisi State University, M. Nodia Institute of Geophysics
1, Alexidze Str., 0171 Tbilisi, Georgia,
e-mail: <anzor_gvelesiani@yahoo.com>*

Abstract

There are considered results of the laboratory works which continue the modeling of vertical convective motions in different geophysical fluids (theoretically) and (experimentally) – in artificial and natural water solutions – by means of suggested before original fluids bubble boiling method (FBBM)[1, 2]. Using the edible salt and sugar water solutions, peculiarities of their temperature-density, $T(\rho)$, temperature-time, $T(t)$, entropy-temperature, $\Delta S(T)$, and heat intensity-time, $Q'(t)$, functional dependences were investigated experimentally, in detail. Three characteristic values of temperature of the bubble boiling regime change, $T(H_2O) = T(C_{12}H_{22}O_{11}) = 40^{\circ}C, 80^{\circ}C, 100^{\circ}C$ and $T(NaCl) = 40^{\circ}C, 80^{\circ}C, 108^{\circ}C$, were found, respectively. These values were obtained on the base of detail experiments for accessible intervals of densities (minimal-maximal) equal, respectively: $\Delta\rho(NaCl) = (1.01-1.2) g\ cm^{-3}$ u $\Delta\rho(C_{12}H_{22}O_{11}) = (1.04 -1.47) g\ cm^{-3}$. Experimental curves $T(\rho)$, $T(t)$ and $\Delta S(T)$, as a rule, in the temperature interval $\Delta T = 40^{\circ}C - 80^{\circ}C$ undergo the discontinuity of the second kind. They allowed us to establish the law of appearance of the points of the second kind discontinuities. Obtained $T(\rho)$, $T(t)$ and $\Delta S(T)$ experimental curves (Figs. 1-6) have universal character, are independent on the substrate's nature and initial temperature of the researched solutions. They give sufficiently full information about new results of provided experiments, which may have not only applied meaning. It is necessary to emphasize an importance of obtained experimental dependences, ($T(\rho)$, $T(t)$, $\Delta S(T)$, and $Q'(t)$) from the point of view of opening perspectives of development and deepening of suggested method both to avoid superfluous technical efforts quickly and without error, find main characteristics of investigated fluids.

I. Introduction.

In this report, new results of experimental research of vertical one-dimensional two-phase flow, modeling natural convective processes according to the original fluids bubble boiling method (FBBM) suggested by us in works [1, 2]. These laboratory modeling experiments are further continuation of above mentioned investigations of fluids vertical convective motions.

The character values of studying thermodynamic system, such as dependences: temperature-heating time, $T(t)$; entropy-temperature, $\Delta S(T)$; hysteresis curves, $T^+(t)-T(t)$, (“+” and “-“ signs correspond to heating and cooling of fluids, respectively), are represented in Figs. 1-6 and Table 1. Each of Figs. 1-5, both for convenience of analysis and limitation of place, simultaneously contains two by two graphs: upper – constrained by means of net experimentally measured data, $T(t)$; lower – on the

base of calculated characteristics of system, $\Delta S(T)$. It is necessary to note, that analogical laboratory modeling vertical one-dimensional geophysical convective flows in literature practically are absent ([6, 7, 1, 2], see also refs in [1]).

II. Method and results of the experiments.

Both graphs, $T(t)$ and $\Delta S(T)$, in Fig.1 for clear water have a second kind of discontinuity at temperature $T_1 = 80^\circ\text{C}$, connected with bubble boiling point [1, 2]. The temperature is achieved (in conditions of our experiments, at intensity of heating about 15 cal/min flux) after the lapse of 25 min from the initial temperature of $T_0 = 10^\circ\text{C}$. Experiments provided on investigated water solutions of different materials showed that on the background of the curves of $T(t)$ and $\Delta S(T)$ appear a new additional point of the second kind of discontinuity at more low temperatures. The entropy curve, $\Delta S(T)$, of NaCl maximal density water solution ($\rho_{\text{max}} = 1.2 \text{ g cm}^{-3}$ (see Fig. 5, where the entropy curve has two points of the second kind of discontinuity at $T_1 = 80^\circ\text{C}$ and $T_2 = 40^\circ\text{C}$, respectively) exactly just so behaves, as $T(t)$ one. In common with the results of our previous works [1, 2], and by the present ones it was experimentally established, that any substance water solutions curves, $T(t)$ and $\Delta S(T)$, have two points of the second kind discontinuity ($T_1 = 80^\circ\text{C}$ and $40^\circ\text{C} < T_2 < 80^\circ\text{C}$) – for solution densities ($\rho_{\text{max}} > \rho_s > 1.0 \text{ g cm}^{-3}$) (see Figs. 1-5).

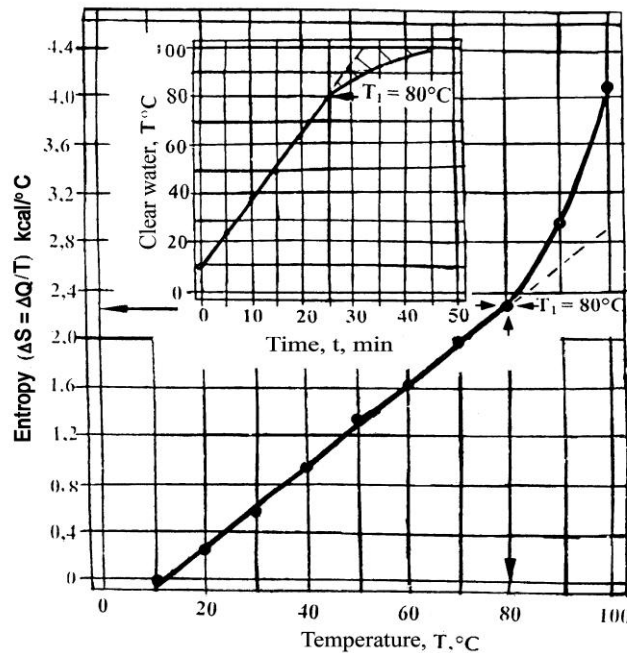


Fig. 1. Above – temperature-time dependence, $T(t)$; lower – entropy-temperature dependence, $\Delta S(T)$, of clear water of density, $\rho = 1.0 \text{ g cm}^{-3}$, heating from 10°C up to 100°C .

Fig. 2 illustrates results of experiments on the sugar, $\text{C}_{12}\text{H}_{22}\text{O}_{11}$, water solutions of density $\rho = 1.08 \text{ g cm}^{-3}$. As is seen, both curves, $T(t)$ and $\Delta S(T)$, have two by two points of the second kind

discontinuities at temperatures $T_1 = 80^{\circ}\text{C}$ and $T_2 = 60^{\circ}\text{C}$, respectively. It is interesting to note that the NaCl water solution of the same density, $\rho = 1.07 \text{ g cm}^{-3}$, has analogical readings (see Fig. 5).

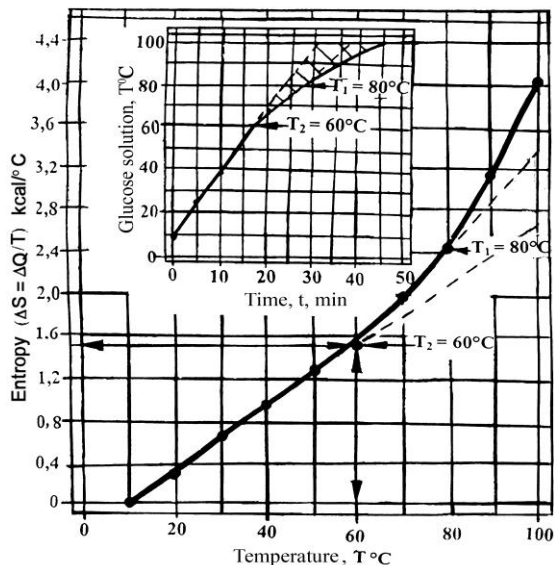


Fig. 2. Above – temperature-time dependence, $T(t)$; lower – entropy-temperature dependence, $\Delta S(T)$, of sugar, $\text{C}_{12}\text{H}_{22}\text{O}_{11}$, water solution ($\rho = 1.08 \text{ g cm}^{-3}$), heating from 10°C up to 100°C .

Fig. 3 corresponds to the the maximal density ($\rho = 1.47 \text{ g cm}^{-3}$) sugar, $\text{C}_{12}\text{H}_{22}\text{O}_{11}$, water solution, heating from below at initial temperature $T_0 = 10^{\circ}\text{C}$. After 6 min (see Table 1 in [2]), it is achieved the sugar solution bubble boiling temperature $T_2 = 40^{\circ}\text{C}$, and then, after 24 min, – the sugar solution intensive bubble boiling temperature invariably equals to $T_1 = 80^{\circ}\text{C}$. The entropy, as a rule, undergoes both discontinuities at $T_2 = 40^{\circ}\text{C}$ and $T_1 = 80^{\circ}\text{C}$, too.

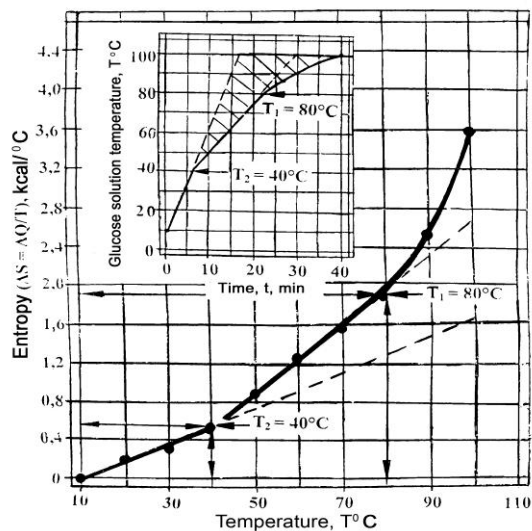


Fig. 3. Above – temperature-time dependence, $T(t)$; lower – entropy-temperature dependence, $\Delta S(T)$, of sugar, $\text{C}_{12}\text{H}_{22}\text{O}_{11}$, water solution ($\rho = 1.47 \text{ g cm}^{-3}$), heating from 10°C up to 100°C .

Fig. 4 shows the curves of $T(t)$ and $\Delta S(T)$ for light NaCl water solution ($\rho = 1.07 \text{ g cm}^{-3}$). Here, saying figuratively, the same past the baton of two points of the second kind discontinuities ($T_1 = 80^\circ\text{C}$ and $T_2 = 60^\circ\text{C}$) to NaCl and other substances (see, present Figs. 1-3, and [1, 2]).

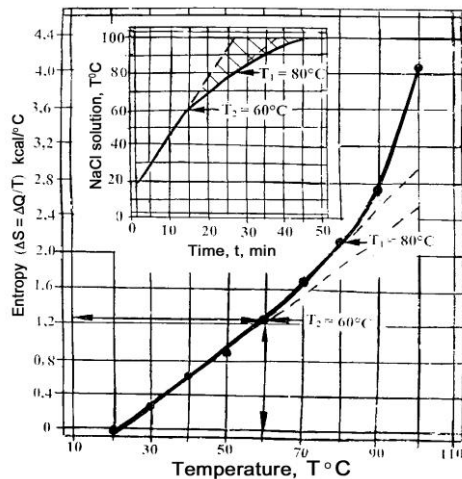


Fig. 4. Above – temperature-time dependence, $T(t)$; lower – entropy-temperature dependence, $\Delta S(T)$, of NaCl water solution ($\rho = 1.07 \text{ g cm}^{-3}$), heating from 20°C up to 100°C .

In Fig. 5, it is recurred the same very interesting property – availability of two points of the second kind discontinuity on the curves $T(t)$ и $\Delta S(T)$. Here it was used the same NaCl water solution, but of the maximal density ($\rho = 1.2 \text{ g cm}^{-3}$), having two limit values of solution bubble boiling points $T_1 = 80^\circ\text{C}$ и $T_2 = 40^\circ\text{C}$ (!), as in the case of the sugar water solution of maximal density (see above and [1, 2]).

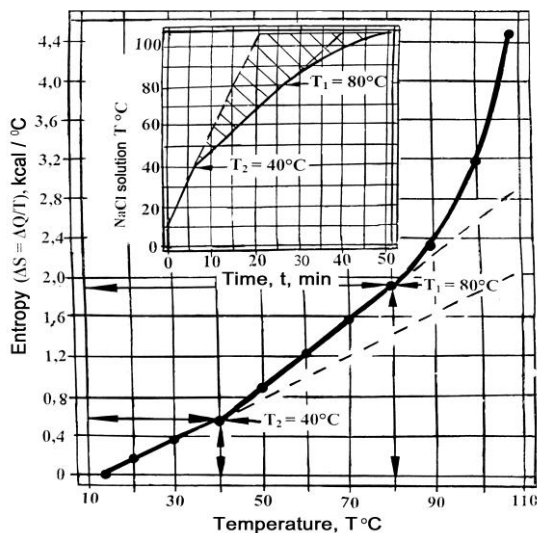


Fig. 5. Above – temperature-time dependence, $T(t)$; lower – entropy-temperature dependence, $\Delta S(T)$, of NaCl water solution ($\rho = 1.2 \text{ g cm}^{-3}$), heating from 10°C up to 100°C .

Fig.6 shows results of detail measuring during heating to the bubble boiling and then reverse motion of both curves (H_2O and $\text{C}_{12}\text{H}_{22}\text{O}_{11}$ solution of maximal density, $\rho = 1.47\text{g cm}^{-3}$). There are two points of crossing curves at temperature $T_3 = 100^\circ\text{C}$ (Figs. 6a, 6b) and lower at $T_2 \approx 62^\circ\text{C}$ (Fig. 6a). In case of clear water, H_2O , time of heating from 20°C to 100°C equals to 45 min; coordinates of the second kind discontinuity are following $T_1(80^\circ\text{C}, 25 \text{ min})$; coordinates of point of boiling are – $T_3(100^\circ\text{C}, 45 \text{ min})$. In case of sugar, $\text{C}_{12}\text{H}_{22}\text{O}_{11}$, time of heating from 20°C to 100°C equals to 40 min; coordinates of the second kind discontinuity are following $T_2(40^\circ\text{C}, 5 \text{ min})$; coordinates of point of boiling are – $T_3(100^\circ\text{C}, 40 \text{ min})$.

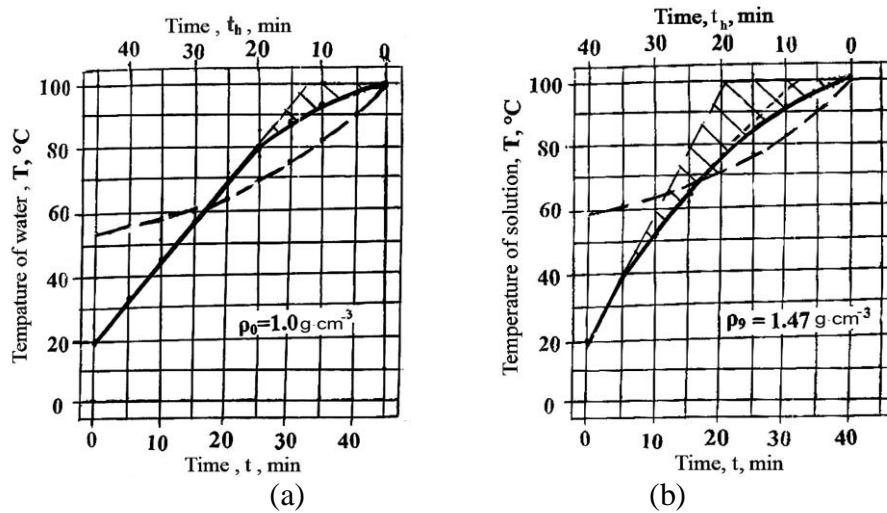


Fig. 6. The clear water (a) and sugar solution (b) bubble boiling (solid lines, time scale – below) and hysteresis (dashed lines, time scale – above) curves. Heat flux, $Q'(t) \approx 15 \text{ cal s}^{-1}$.

Unlike the water solution of NaCl (with maximal density $\rho = 1.2 \text{ g cm}^{-3}$, and temperature of boiling $T_3 \approx 108^\circ\text{C}$), in case of sugar water solution ($\text{C}_{12}\text{P}_{22}\text{O}_{11}$), a rise of boiling temperature doesn't occur, and its boiling temperature $T_3 = 100^\circ\text{C}$. In case of sugar water solution of maximal density ($\rho = 1.47 \text{ g cm}^{-3}$), the hysteresis square (ΔD_h) between solid line and dashed one, directed in the opposite direction (of low cooling process of the solution from the point of boiling $T_3 = 100^\circ\text{C}$) before their crossing with each other equals to, respectively: (a) for clear water ($\rho = 1.0 \text{ g cm}^{-3}$) hysteresis square $\Delta D_h(\text{H}_2\text{O}) \approx 3.5 \text{ sq. un.}$, coordinates of this point are following (see Fig. 6a): $T_h \approx 62^\circ\text{C}$, and corresponding time of cooling, $t_h = 28 \text{ min}$; (b) for sugar solution of maximal density $\rho = 1.47 \text{ g cm}^{-3}$, $\Delta D_h(\text{C}_{12}\text{P}_{22}\text{O}_{11}) \approx 2 \text{ un. sq.}$; coordinates of this point are following (see Fig. 6b): $T_h = 68^\circ\text{C}$, and corresponding time of cooling, $t_h = 23 \text{ min}$; ratio between hysteresis squares of sugar and clear water $\Delta D_h(\text{C}_{12}\text{P}_{22}\text{O}_{11}) : \Delta D_h(\text{H}_2\text{O}) \approx 4:7$.

III. Analysis and discussion.

It is necessary to note, at once, that the results of measuring of character parameters of considered solutions in the most complete form represent in Fig. 6 a,b (during of heating: $T_1, T_2, T_3; \Delta S_1, \Delta S_2, \Delta S_3; t_1, t_2, t_3$; during cooling – hysteresis parameters: $\Delta D_h, T_h, t_h$).

On the derivation of initial linear parts of $T(t)$ -curves at achievement of the points of the second kind of discontinuities – to the side of decrease along elliptical curve (when a heat is spent during a bubble boiling process); in case of the $\Delta S(T)$ -curves the initial linear character of growth of the curve, after the points of the second kind of discontinuity, is continued in the form of growing parabolic curve. In the solutions, such picture is repeated twice because of appearance the second analogical

point of discontinuity. Increasing of the entropy curves growth temp is accounted for its inverse proportionality to the temperature of solution. Here it is also necessary to take into consideration that we have dealings with associated fluids (in particular, the water belongs to them, too), at heating of which, except of formation of bubbles of vapour, a part of the heat is spent in addition for dissociation of molecules, and, as a result, – the second kind of discontinuities in all curves $T(t)$ and $\Delta S(T)$ (Fig. 1-6).

The vapours bubbles, generating into the fluids during boiling, are under hydrostatic pressure of column of water, surface of water curvature, and atmospheric pressure. To not to be crushed, the bubble must contain sufficiently high value of saturated vapour pressure in order to resist of whole external pressure. But, as is known, inside of the bubble, because of concave surface, the pressure of saturated vapour is less, than over a plate surface, and the smaller than the smaller of bubbles radius, too. Because the bubble boiling process begins from generation of very small size bubbles ($r = 10^{-7}$ cm), then this insufficiency of the pressure inside of the bubble reaches considerable value, and the bubble of air fast becomes flat and disappears. In the volume of heating fluids, huge accumulation of the smallest bubbles slowly moves vertically upwards, under action of Archimedes force. The boiling does not begin, although from the outside of the liquid the conditions of the boiling are available. When temperature of liquid at the bottom of the vessel is increased, the vapour bubbles of size $r \sim 10^{-4}$ cm suddenly quickly growth at the temperatures (T_1 and T_2) of the second kind discontinuity. In case of clear water $T_1 = 80^\circ\text{C}$, and in case of different substance solutions the temperature of discontinuities is between $T_2 = 40^\circ\text{C}$ and 80°C , and following growth of liquids temperature and completing very intensive bubble boiling temperature $T_3 = 100^\circ\text{C}$ (for clear water, H_2O , and for the water solution of sugar, $\text{H}_{12}\text{C}_{22}\text{O}_{11}$, of maximal density $\rho = 1,47 \text{ g/cm}^3$) и $T_3 = 108^\circ\text{C}$ (for NaCl water solution of maximal density, $\rho = 1,2 \text{ g/cm}^3$), intensive boiling in form of stable vertical columns of lengthened bubbles, which maybe named “hose” – boiling.

IV. Conclusion.

Thus, obtained experimental curves $T(\rho)$, $T(t)$ and $\Delta S(T)$ (Figs. 1-6) (or the bubble boiling method):

(1) – have universal character are independent on the substrate’s nature and initial temperature of the researched solutions; (2) – allow one to establish the law of appearance of the points of the second kind discontinuities; (3) – give sufficiently full information about new results of provided experiments; (4) – may have independent and not only applied meaning; (5) – are significant from the point of view of opening perspectives of development and deepening of suggested method; (6) –the method allows also to avoid superfluous technical efforts, quickly and without error, find main thermodynamic parameters of investigated solutions.

References

- [1] Gvelesiani A.. J. On the one-dimensional two-phase/many-component convective flows in different geophysical mediums: laboratory method of modeling of fluids bubble boiling. Georgian Geophys. Soc., 2013, v.16B, pp. 119-128.
- [2] Gvelesiani A., Chiabrishvili N. Laboratory modeling of thermals generation in geophysical environments by means of fluid bubble boiling method. J. Georgian Geophys. Soc., 2013, v.16B, pp. 129-137.
- [3] Gvelesiani A. Open thermodynamic systems: some new aspects of convection processes modeling by fluids bubble boiling laboratory method. J. Georgian Geophys. Soc., 2014, v.17B, pp. .
- [4] Bunn Ch. Crystals. The role in nature and in science. Academic Press. New York – London,

- 1964 (Чарлз Банн. Кристаллы. Их роль в природе и науке. М.: Мир, 1970, 312 с.)
- [5] Pavlov V. I. Mechanics. Molecular Physics. M.: GTTL, 1955, pp. (265-266), 356. (in Russian)
- [6] Jellinek A. M., Manga M. Links between long-lived hot spots, mantle plumes, D", and plate tectonics. Reviews of Geophysics, 2004, v. 42, RG3002, pp. 1-35.
- [7] Golitsyn G. S. Study of convection with geophysical application and analogues. L.: Gidrometeoizdat, 1981.

(Received in final form 30 August 2014)

**სუფთა წყლის, H_2O , და სხვადასხვა სიმკვრივის
მქონე შაქრის, $C_{12}H_{22}O_{11}$, და სუფრის მარილის, $NaCl$,
წყლის ხსნარების ბუშტისებრი დუღილის თავისებურებათა კვლევის
დამატებითი ექსპერიმენტების შესახებ**

ანზორ გველესიანი, ნოდარ ჭიაბრიშვილი

რეზიუმე

წინამდებარე სტატიაში განიხილება დამატებითი ლაბორატორიული ცდების შედეგები, რომლებიც წარმოადგენენ კონვექციური პროცესების მოდელირების კვლევების შემდგომ განვითარებას. შემოთავაზებული სითხის ბუშტისებრი დუღილის ლაბორატორიული მეთოდის გამოყენებით [1, 2]. მარილის და შაქრის წყალხსნარების მაგალითზე $T(t)$ და $\Delta S(T)$ დამოკიდებულება საკმაოდ დეტალურადაა შესწავლილი. გამოსაკვლევი ხსნარების მოცულობითი დუღილის პროცესისათვის ნაჩვენებია სამი მახასიათებელი სიდიდის – ხსნარის დუღილის ტემპერატურის, ენტროპიის და მიწოდებული სითხის ინტენსივობის ($T(\rho)$, $T(t)$, $\Delta S(T)$ და $Q'(t)$) – არსებობა. ისინი წარმოადგენენ ბუშტისებრი დუღილის პროცესის რეპერულ წერტილებს: $T(H_2O) = T(C_{12}H_{22}O_{11}) = 40^\circ C, 80^\circ C, 100^\circ C$ და $T(NaCl) = 40^\circ C, 80^\circ C, 108^\circ C$. კვლევის შედეგად დადგენილია, რომ სუფთა წყლის ($\rho=1,0\text{გ/სმ}^3$) და მარილის და შაქრის წყალხსნარების შემთხვევაში სიმკვრივეების ინტერვალებში (დაშვებული მინიმალურიდან მაქსიმალურამდე), სათანადოდ: $\Delta\rho(NaCl) = (1,01-1,2)$ გ/სმ³ და $\Delta\rho(C_{12}H_{22}O_{11}) = (1,04-1,47)$ გ/სმ³. ამასთან უნდა აღინიშნოს, რომ მიღებული უნივერსალური ექსპერიმენტული მრუდები – $T(\rho)$, $T(t)$, $\Delta S(T)$, $Q'(t)$ – იძლევა უწყვეტობის მეორე გვარის წყვეტის ორ-ორ წერტილს, რომლებიც იმყოფიან ($40^\circ C-80^\circ C$) ინტერვალში. ფიგ. 1-6-ზე წარმოდგენილი მრუდები შეიცავენ საკმაოდ სრულ ინფორმაციას მიღებულ ახალ მეცნიერულ შედეგებზე და აქვთ არა მხოლოდ გამოყენებითი მნიშვნელობა. შემოთავაზებული მეთოდი ზედმეტი ტექნიკური დანახარჯების გარეშე საშუალებას იძლევა პირველ მიახლოებაში სწრაფად და უშეცდომოდ განისაზღვროს გამოსაკვლევი ხსნარის ძირითადი თერმოდინამიკური რეპერული მახასიათებლები.

Дополнительные эксперименты по исследованию особенностей пузырькового кипения чистой воды, водных растворов сахарозы, $C_{12}H_{22}O_{11}$, и поваренной соли, $NaCl$, различных плотностей

Анзор Гвелесиани, Нодар Чиабришвили

Резюме

В настоящей статье рассматриваются результаты лабораторных работ, являющихся дальнейшим продолжением исследований конвективных процессов, по оригинальному лабораторному методу моделирования процесса пузырькового кипения растворов различных плотностей [1, 2]. На примере водных растворов поваренной соли и сахара тщательно изучены особенности временного хода температуры растворов и зависимости энтропии от температуры. Показано наличие трёх характерных значений температуры, энтропии и интенсивности подаваемого тепла ($T(\rho)$, $T(t)$, $\Delta S(T)$ и $Q'(t)$) в процессе объёмного кипения изучаемых растворов, являющихся реперными точками смены режима пузырькового кипения: $T(H_2O) = T(C_{12}H_{22}O_{11}) = 40^{\circ}C, 80^{\circ}C, 100^{\circ}C$ and $T(NaCl) = 40^{\circ}C, 80^{\circ}C, 108^{\circ}C$. При этом обнаружено, что для чистой воды ($\rho = 1,0 \text{ г см}^{-3}$) и водных растворов поваренной соли и сахарозы в интервалах плотностей (допустимых минимальных- максимальных значений), соответственно: $\Delta\rho(NaCl) = (1,01-1,2) \text{ г см}^{-3}$ и $\Delta\rho(C_{12}H_{22}O_{11}) = (1,04-1,47) \text{ г см}^{-3}$. Полученные графики зависимости между точками разрывов непрерывности второго рода – $T(\rho)$, $T(t)$, $\Delta S(T)$, $Q'(t)$ – имеют универсальный характер, независимы от природы растворимого в воде вещества и начального значения температуры раствора. Представленные экспериментальные графики (Фиг. 1-6) содержат достаточно полную информацию о поведенческих результатах, которые могут иметь не только прикладное значение. Предлагаемый метод позволяет, без лишних технических затрат и времени, в первом приближении быстро и безошибочно определить основные (реперные) термодинамические характеристики изучаемых растворов.

The Modified Version of t_0 Method

Davit Kitovani

Abstract

The article refers to the modified variant of the well known method of t_0 . It is shown that if there exists one complete hodograph and oncoming hodograph is not complete, but with its help the apparent speed can be calculated. In this case it is possible to build the refractive border with adequate accuracy and to determine its parameters.

The study of deep structure of the Earth is an important goal during the prospecting on oil, gas, ore, hydrological or regional researches. During these researches the Physical characters of various borders are studied, the contacts, tectonic disturbances, ore bodies are revealed, also the depths of deposition of existing borders and the strength of the zone of weathering is determined.

Following seismic methods are used for solution of this objectives: the Method of Reflective Waves (MRW), the Method of General Deep Point (MGDP), the Correlative Method of Refractive Waves (CMRW), the Method of Exchanging Progressing Waves (MEPW), and the Deep Seismic Zondage (DSZ).

In some cases, because of the character of the border, the most detailed and accurate methods - MRW and MGDP do not allow reliable prospecting of the reflective border. Even in the case of reliable registration of reflective waves only the geometry of borders are researched. DSZ allows to research deep layers and the speed with very low accuracy, which is caused by the usage of low frequencies and small detail of the monitoring systems.

The method which gives the most accurate determination of refractive borders and the speed of the distribution of waves in these borders is CMRW, but it cannot settle all objectives listed above, also it does not work with the enough accuracy everywhere. This is caused by: 1. inadequate readiness of physical basis of the method; 2. Sometimes the complex relief hampers to receive the high level field information.

There are various level difficulty and accuracy techniques of building of refractive borders. One of the ways for determination of refractive borders is the method t_0 . This method allows to define the refractive borders with enough high accuracy and reliably and to calculate the speed of the distribution of waves. For this method both branches of the hodograph (straight and reverse) are needed which are connected by the reciprocal spot T.

In this article we want to show that the refractive border can be defined with enough accuracy and reliably, if we have only one complete hodograph and the other one is not complete but it can calculate the apparent speed.

Supposedly we have a two-layer environment. Lets specify the speed of spreading of resilient waves in the upper layer with V_1 and in the lower one V_2 . The angle of inclining of the border is specified by $I \varphi$ and straight and reverse hodographs with t^+ and t^- and the apparent speeds which are defined by them accordingly will be V^+ and V^- . h and h_x are deep beddings refractive border under the points of explosions O and O_1 . With the help of these values lets calculate t_{01} , t_{02} and t_0 .

$$t_{01} = 2h \cos i / V_1$$

$$h_x = h + x \sin \varphi; \quad V^+ = V_1 / \sin (i + \varphi); \quad V^- = V_1 / \sin (i - \varphi);$$

$$t_{02} = 2(h + x \sin \varphi) \cos i / V_1 = 2h \cos i / V_1 + 2x \cos i \sin \varphi / V_1 = t_{01} + x / V_1 (2 \cos i \sin \varphi) =$$

$$= t_{01} + x/V_1 [\sin(i + \varphi) - \sin(i - \varphi)] = t_{01} + x/V^+ - x/V^- = t - x/V^-$$

$$\text{Analogously - } t_{01} = t - x/V^+$$

And now let's calculate t_0

$$t_0 = t - x/V_2 = t_{01} + x/V^+ - x/V_2 = 2h \cos i / V_1 + x \sin(1 + \varphi) / V_1 - x(V^+ + V) / (V^+ \cdot V) = 2h \cos i / V_1 + x \sin(1 + \varphi) / V_1 - x \sin i \cos \varphi / V_1 = 2h \cos i / V_1 + x \sin \varphi \cos i / V_1$$

Accordingly:

$$t_0 = 2h \cos i / V_1 + x \sin \varphi \cos i / V_1 = (t_{01} + t_{02}) / 2$$

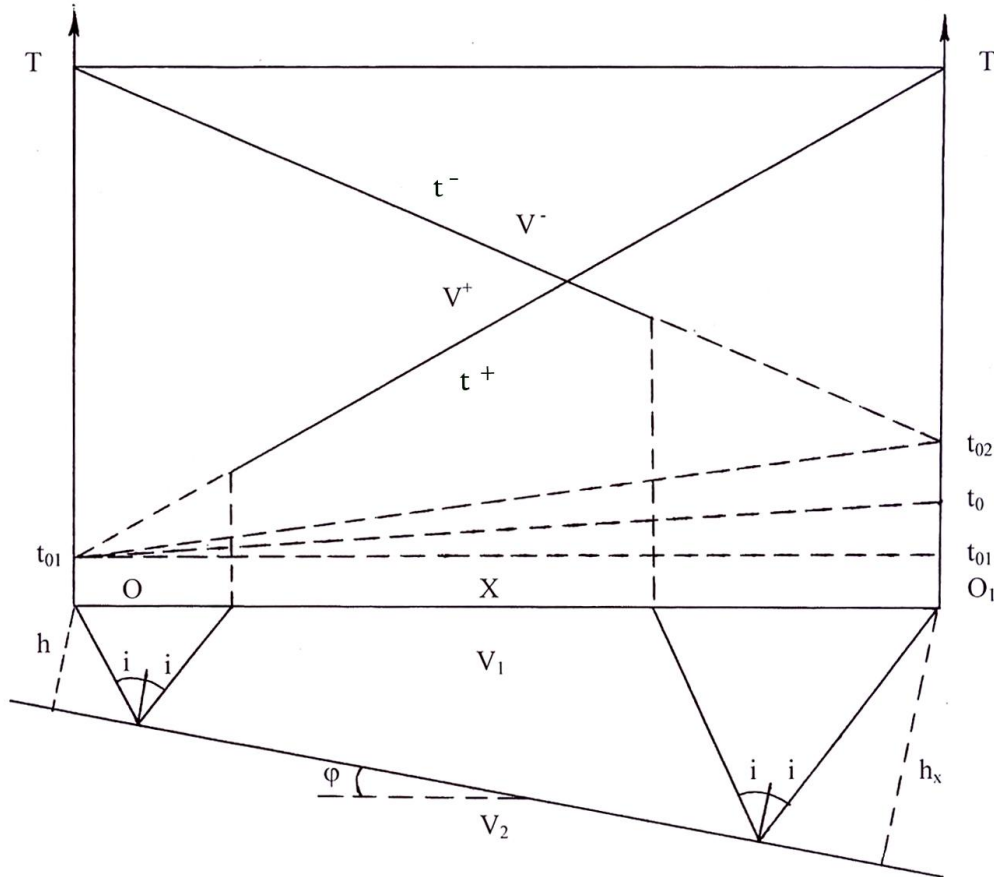


Fig. 1

The result is following: if we have full hodographs (straight and reverse), for finding the spot t_0 the straight hodograph (t^+) is processed by apparent speed which is calculated by the reverse (t^-) hodograph (speed V), and on the contrary - the reverse hodograph is processed by speed V^+ , which is calculated by the straight hodograph. t_0 is received from the averaging of the value t_{01} and t_{02} , accordingly - $t_0 = (t_{01} + t_{02}) / 2$.

If we have only one hodograph and the finding of the apparent speed is possible with the help of another (not complete) one, in this case the separation of refractive border and the calculation of the apparent speed in the border layer is also possible.

This result is important for the country like Georgia, which is characterized by the complex relief and high agrarian field compactness, what as usual does not support the process of receiving of good field results.

References:

1. Епинатьева А.М. Физические основы сейсмических методов разведки М.изд –во МГУ, 1970.
2. Гурвич И.И. Боганик Г.Н. Сейсмическая методов разведка М.изд –во Недр.1980.
3. Гамбурцев Г.А. Основы сейсморазведки М. Гостоптехиздат.1962.

t_0 -ის მოდიფიცირებული მეთოდი

დავით კიტოვანი

სტატიაში განხილულია ცნობილი მეთოდის t_0 -ის მოდიფიცირებული ვარიანტი. ნაჩვენებია, რომ თუ გვაქვს ერთი სრული ჰოლოგრაფი, ხოლო მისი შემხვედრი ჰოლოგრაფი არასრულია, მაგრამ მისი საშუალებით შესაძლებელია მოჩვენებითი სიჩქარის გამოთვლა, მაშინ გვეძლევა საშუალება საკმაო სიზუსტით დავადგინოთ გარდამტეხი ზედაპირის ჩაწოლის სიღრმე და განვსაზღვროთ მისი პარამეტრები.

Модифицированный метод t_0

Давид Китовани

В статье рассматривается модифицированный вариант известного метода t_0 . Показано, что если имеется один полный годограф, а встречный годограф неполный, но с его помощью можно вычислить кажущуюся скорость, то в этом случае возможно с достаточной точностью построить преломляющую границу и определить ее параметры.

ABOUT THE MECHANISM OF IMPACT OF EARTHQUAKES ON HUMAN HEALTH

Sakvarelidze E., Sharadze Z., Mirianashvili K.

Iv. Javakhishvili Tbilisi State University, Tbilisi 0179, Georgia

Abstract

It is known, that when preparing for an earthquake, at the time of the earthquake and in the period following the earthquake in the epicenter area generated infra-low frequency (0.001-10 Hz) weak electromagnetic fields that are registered in areas far from the epicenter. Generated by an earthquake infra-low frequency fields superimposed on electromagnetic fields of Schumann resonance frequencies, causing changes in the biosphere, the low frequency electromagnetic situation. Values of the Schumann resonance frequency can also be changed by propagation generated by earthquake acoustic-gravity waves (AGW). The amplitude of ionospheric perturbations caused by earthquakes, peaks at a height of Alven resonator (layer F). AGW generated by earthquake and associated propagation of disturbances in the Schumann and Alven resonators alters background ultralow frequency electromagnetic situation of the biosphere and related with this changing biological effect.

Natural geomagnetic fields create conditions for synchronous work of numerous rhythms existing in a human body and its normal functioning. Change of parameters of natural fields in the biosphere during their disturbances causes violent reorganization of an organism according to a new situation, that rather without serious consequences occurs for a healthy, mature human body. In organisms in which ability to adaptation is weakened or being in process of formation (sick, elderly, embryos, children) adaptation proceeds difficult or defectively. Therefore synchronous connection between exogenous "leading" natural rhythms and endogenous biorhythms is broken, that causes desynchronization of endogenous rhythms, and, results in health deterioration. Reaction of biological objects to geomagnetic disturbances represent adaptive stress reaction [1]

In days of magnetic storms infra-low frequency weak natural electromagnetic fields are observed. During these days impact on live organisms is carried out by means of the information mechanism when the bioeffect of influence is measured not by energy of an electromagnetic signal and its frequency, i.e. the information which contains a signal. Information influence is especially effective at so-called resonant frequencies, i.e. at influence of such fields frequencies which coincide or owe close to frequencies of different parts of a human body and own frequencies of biological systems. Such resonant frequencies arise in Schumann resonators (the resonator Earth – ionosphere) and Alven resonators, occupying space between a wall ionosphere of the Schumann resonator and a maximum of electric ionospheric concentration ($h \leq 800$ km). Theoretical values of frequencies of Schuman resonator are: 8 Hz, 14 Hz, 20 Hz, 26 Hz and 32 Hz. The first three frequencies from them are expressed most clearly. Source of excitement of this resonator is atmospheric discharge (lightning) during a thunderstorm.

Thunderstorm is quite frequent phenomenon on Earth therefore the Earth- ionosphere resonator always is in the excited state. Resonance frequencies of the Alven resonator less than 6 Hz and sources of his excitement are in the atmosphere and a magnetosphere.

Values of resonant frequencies of natural resonators depend on a condition of an ionosphere which, in turn, depends on activity of the Sun, geographic latitude of observation point, a season and an interval of day time.

Coincidence of values of frequencies of the main infra-low components of the electromagnetic fields generated by separate systems of a human body with values of resonant frequencies of natural of Schumann and Alven resonators and the short periodical magnetic disturbances became the basis to explain negative influence of magnetic storms on an organism with resonance or information influence of infra-low frequencies weak natural fields

Change of an infra-low frequency electromagnetic state in the biosphere can be provoked by a earthquakes which number also correlates with activity of the Sun, and often strong magnetic storms can occur against strong and weak earthquakes [2]. Those years when the number of spots grows on the Sun, a strengthening of seismic activity is observed on Earth. It is established that by preparation for an earthquake, at the time of an earthquake and during the period following an earthquake in the epicenter area weak electromagnetic fields of ultra-low-frequencies (0,001-10 Hz) are generated, which are registered in the areas remote from epicenter [3,4]. During earthquake preparation the ultra-lowfrequency electromagnetic waves generated in the epicenter are considered as earthquake harbingers, they are perceived by live organisms. Human mortality (generally from cardiac heart attacks and cerebral hemorrhages) in the areas remote from epicenter where there were no destructions, is related to the waves caused by an earthquake generated in the specified frequency range at the time of an earthquake and the subsequent period.

On the infra-low frequencies electromagnetic fields, generated by an earthquake resonant Schumann frequencies are imposed, causing change of an electromagnetic low- frequency situation in the biosphere that affects on human health. Values of Schuman resonant frequencies and, respectively, an electromagnetic situation of the biosphere can be changed also at quasiperiodic ($T = 3 - 40$ sec.) changes of an ionospheric wall's height of the resonator and distribution of the acoustic-gravitational waves (AGW), generated by an earthquake. There are two mechanisms of generation of AGV [5]: 1) at the time of an earthquake AGV are generated in epicenter under the influence of a strong "piston" push on the atmosphere, which are registered for hundreds and thousands kilometers from epicenter; 2) superficial seismic waves, which are generated in epicenter and extend in all the directions. On the way of propagation weak surface fluctuations of Earth also generate AGV in the atmosphere.

It is known [6] that amplitude of atmospheric acoustic-gravitational waves grows depending on height, and in high layers of the atmosphere (at ionosphere heights) is shown in the form of quasiperiodic ($T \sim 5-90$ sec.) variations of parameters of an ionosphere, so-called mobile disturbances of an ionosphere. The disturbances amplitude of ionosphere caused by earthquakes, reaches the maximum values (10-15%, sometimes more) at the height of F layer of ionosphere, where Alven resonator is located. It is possible to expect that AGV generated by an earthquake and the related distribution of disturbance of an ionosphere in Schumann and Alven resonators create prerequisites for intensive quasiperiodic ($T \sim 5-90$ sec.) changes of values of their resonant frequencies and corresponding to these frequencies electromagnetic waves, that surely causes change of a background ultra-low frequency electromagnetic condition of the biosphere and related biological effect with this change. Change of an electromagnetic situation of the biosphere can happen and at AGV transformation in electromagnetic waves.

At the present time at an assessment of negative influence of magnetic storms on human health change of frequency-energetically parameters of background of infralow frequency range electromagnetic fields in the biosphere, caused by close or far earthquakes isn't taken into account, though presumably, the role of earthquakes in the above-noted changes, especially in seismoactive areas, is considerable. Therefore geomagnetic storms, even weak, occurring on low latitudes during strong close earthquakes in seismically active areas, can have bigger biological effect, than on high latitudes, though strong magnetic storms there are observed.

References

1. Е.А. Сакварелидзе, **Шарадзе З.С.** О механизме воздействия электромагнитной погоды на здоровье человека. Актуальные вопросы патологии, терапии и мед. Реабилитации. Тбилиси-Москва: ТБК-РАМ-ТН, 2014, ст.111-118
2. Сытинский Д.Д. О связи землетрясений с солнечной активностью Изв. АН СССР, Физика Земли, 1989, №2, с. 13-30.
3. Kopytenko Yu. A., Matiashvili T.G., Voronov P.M., Kopytenko E.A., Molchanov O.A. Detection of ultralow-frequency emissions connected with the Spitak earthquake and it's after- shok activity, based on geomagnetic pulsations data at Dusheti and Vardzia observatories. Physics of the Earth and Planetary Interiors, 1993, 77, p. 85-95
4. Шарадзе З.С., Джапаридзе Г.А., Жвания З.К., Квавадзе Н.Д., Киквилашвили Г.Б., Лиадзе З.Л., Матиашвили Т.Г., Мосашвили И.В., Николаишвили Н.Ш. Возмущения в ионосфере и геомагнитном поле, связанные со спитакским землетрясением. Изв. АН СССР, Физика Земли, 1991, №11, с. 106-116.
5. Шарадзе З.С., Джапаридзе Г.А., Матиашвили Т.Г., Мосашвили Н.В. Сильные землетрясения и связанные с ними возмущения в ионосфере и магнитном поле.~ Изв. АН СССР, Физика Земли, 1989, №1, с. 20-32.
6. Hines C.O. Internal atmospheric gravity waves at ionospheric heights. Canada J. Phys. 1960, 38, 11, p. 1441-1481

აღამიანის ჯანმრთელობაზე მიწისძვრების ზემოქმედების მქანის შესახებ

ე. საყვარელიძე, **ზ.შარაძე**, კ. მირიანაშვილი

რეზიუმე

დადგენილია, რომ მიწისძვრის მომზადების დროს, მიწისძვრის მომენტში და მიწისძვრის შემდგომ პერიოდში მიწისძვრის რეგიონში ხდება ინფრადაბალსისშირული სუსტი ელექტრომაგნიტური ველების გენერირება, რომლებიც რეგისტრირდებიან ეპიცენტრისაგან მოშორებულ რაიონებში. ეს ველები ზედ ედება შუმანის რეზონანსული სიხშირეების ელექტრომაგნიტურ ველებს და იწვევენ ბიოსფეროში დაბალსისშირული ელექტრომაგნიტური სიტუაციის ცვლილებას. შუმანის რეზონანსული სიხშირეების მნიშვნელობები შეიძლება იცვლებოდეს აგრეთვე მიწისძვრებით გენერირებული აკუსტიკურ-გრავიტაციული ტალღების (აგვ) გავრცელებით. მიწისძვრებით გამოწვეული იონოსფერული შემფოთებების ამპლიტუდა აღწევს მაქსიმალურ მნიშვნელობებს ალვენის რეზონატორის სიმაღლეზე (Fფენა). აკუსტიკურ-გრავიტაციული ტალღები და მათთან დაკავშირებული შუმანისა და ალვენის რეზონატორებში შემფოთებების გავრცელება იწვევს ბიოსფეროს ფონური ინფრადაბალსისშირული ელექტრომაგნიტური სურათის ცვლილებას და ამასთან დაკავშირებულ ბიოეფექტს.

О МЕХАНИЗМЕ ВОЗДЕЙСТВИЯ ЗЕМЛЕТРЯСЕНИЙ НА ЗДОРОВЬЕ ЧЕЛОВЕКА

Сакварелидзе Е.А., Шарадзе З.С., Мирианашвили К.Ю

Резюме

Установлено, что при подготовке к землетрясению, в момент землетрясения и в период, следующий за землетрясением, в регионе эпицентра генерируются инфранизкочастотные слабые электромагнитные поля, которые регистрируются и в районах, удаленных от эпицентра. Генерируемые землетрясением инфранизкочастотные поля накладываются на электромагнитные поля резонансных частот Шумана, вызывая в биосфере изменения электромагнитной низкочастотной обстановки. Значения резонансных частот Шумана могут изменяться также распространением генерируемых землетрясением акустико-гравитационных волн (АГВ). Амплитуда возмущений ионосферы вызванных землетрясениями, достигает максимальных значений на высоте резонатора Алвена (слой F). Генерируемые землетрясением АГВ и связанное с ними распространение возмущений в резонаторах Шумана и Алвена вызывает изменение фонового инфранизкочастотного электромагнитного состояния биосферы и связанный с этим изменением биоэффект.

About Matter and Space

O. Lomaia

M. Nodia Institute of Geophysics

Abstract

For further development of physics it is necessary to reexamine its fundamental notions, as the concept about matter and space existing nowadays.

It is applicable and correct: to divide material objects into three forms or levels: (primary, secondary and tertiary); belonging more delicate objects compared with primary matter to differentiated type of matters. The author thinks that it is necessary the matter space to return the status of absoluteness, provided by I. Newton. To be accepted that forming of the space preceded formation of solid material objects. Space is discrete, non-homogenous, electrically neutral, motionless (doesn't move), has the ability to vibrate. It consists of special, most delicate types of matter. The solid massive bodies consisting of tertiary matter include great pores and they can't curve the space. Space is their important component.

Matter and space present the fundamental notions of physics. Every important step made for the development of science required explorers to review and broaden the knowledge about these foundations. Matter is the base, substratum, substance for every real object and system existing in the universe. All known different types of states of substance belong to matter: plasma, gas, liquid, solid. Some scientists refer them to cosmic rays, neutrino and other massless proportions and fields. The forms (levels) of matter, their qualitative base differences are various and each of them has specific character, structure, unity of stable connections. It is known that while existing character type differences of these connections you may talk about the state of defined matter. Modern physics recognizes the following types of the state of matter: elementary particles and fields, atoms, molecules, microscopic bodies, planets, stars, inner galactic systems, galaxies, galactic systems. There are also its completely unnatural forms in such astronomic objects as neutron stars, black holes and others. After developing of quantum theory, the process of cognition in physics changed and the attention was attracted on more delicate forms of matter. There is the opinion, that studying of elementary particles helps us to learn deeper laws of the universe.

Modern physicist tries to know the origin of the mass of quarks, electrons and other elementary particles and how the particles with electric charge are created. The scientists have already reached the resolution to this question [1].

It is clear that substance is made from energy. And the latter is the constant component of the universe. Many modern physicists think that the continuous process of creation new substances takes place in the universe, agrees with the ideas of W. Heisenberg and K. Paul that the particles and forces present the exposure of deeper quantum fields of reality. Particles are combined energy of different fields [1].

There is the concept that the electron is born along with spreading of the light by participation of particles created in space microstructures, in the points where light beam crosses its wavy part scheme [2]. By piling radial and wavy energies there is formed such energy quantity that is enough to transform the virtual electron into real electron. There may be the idea that newly born free electron, which

moves in high speed with light wave in the space will meet nucleus which will attract it and make it as its companion. So is made the first atom-hydrogen. It is clear that the processes of appearing, disappearing and intertransmitting of virtual and elementary particles and also other particles that are included in the matter are constantly running in the universe [1]. The knowledge about matter existing in scientific literature doesn't give us the base to believe that definition of the forms of matter made by physicists is appropriately approved and is close to reality [3.4].

We think it is right to divide all material objects into three forms: primary, secondary and tertiary ones. Such division corresponds to the interaction of three varieties – nuclear, electromagnetic and gravitational. Besides mentioned forms there are also the most delicate types of matter, fields of different energy, light, warmth and others. Statements on this kind of classification is referred in modern literature, but leading physicists has no paid attention on this issue yet. Among the forms of matter the most delicate form of matter is the primary matter. All virtual particles – protoelements are included to it. They are made from energetic field when its energy reaches special importance. The secondary matter is more solid. All elementary particles belong to it. It is made from the energetic field of the primary matter when its concentration exceeds the special limit. From the secondary matter is made plasma; it is also the component part of the space existing around the stars. The tertiary matter is the most solid one. They are atomic particles. It is made from energetic field of the secondary matter, when the latter reaches the special limit and exceeds it. All the solid physical surrounding, subject, body and object are included in the list of the tertiary matter.

The concept that the process of creation and development of matter is directed from the most delicate objects to solid forms and not vice-versa is close to reality. The idea, that forming of space precedes the process of formation of matter and substance in space should be true and the latter is made form the most delicate creations – special varieties of matter.

In the past in atomic theory of Democritus and in cosmology space wasn't discussed as void. According to his supposition, there are native elements distributed in the space. It is non-homogenous and has defined structure [5]. According to I. Newton space is objective and doesn't depend on concrete movements of the body. Attention should be attracted to the supposition of I. Newton that there are ethereal, unusually flexible substance are spread having the ability to contract and expand [6]. He wrote: "I think that ether that fills up the universe consists of particles that differ from each other in delicacy [6]. In XX century physicists noted that the ether mentioned by Newton which fills up the universe is very close to the space mentioned by Descartes and his "hierarchy of delicacy – is related to hierarchy of particles mentioned by Descartes [5]. I. Newton thought that general skeleton of nature is nothing but the net of different ethereal creations. Following to his concept we can't conclude that the space is void". I. Newton refers ether the ability of oscillation. According to his conception real absolute space existed before creation of subjects [6]. According to the theory of I. Newton there is absolute motion existing (along with the relativity of motion of bodies) in relation with absolute space that is three dimensional and immovable.

At the end of XIX century H. Hertz and H. Lorentz made theories based on the concept that space is filled up with "ether of the world". According to the theory of H. Lorentz ether is motionless. It doesn't participate in the motion of material systems. This was the base for the existence of reference systems connected with motionless ether the same or the space. E. Mach criticized the supporters of the notions of absolute space: he thought that the mentioned concept was against general manual of classical science – the interaction of bodies as the reason for all happening in the universe. There is a question: was this "manual" really untouchable and true? From the standpoint of E. Mach the gravitational field is fully defined by the masses of the bodies and stars make the space [5]. The concepts of A. Einstein coincide with the principles of E. Mach. He thought that the construction of space exists as there are its creator stars, planets and other material bodies and systems. The first postulate of A. Einstein starts with the followings: "none of physical experiments held in laboratories (reference system) gives ability to know if this laboratory is in motionless state or moves equally and

rectilinearly, that's why the absolute motion isn't revealed and the absolute space of Newton is such a fiction as its material substrate – ether". In connection with this postulate there appears the natural question: is the impossibility of proving something by experiment under the condition of given knowledge and the level of technical development the hard evidence of its non-existence?

A. Einstein argued that space was non-homogenous and its geometrical structure is depended on distribution of masses, substance and the field. He took four-dimensional space-time notion and concept that in surrounding of great material bodies the structure of the bodies is non-euclidean so the space is curved. Here dominates geometry made by B. Riemann.

Physicists faced the following acute question: does space exist independently or is it made from substance? The majority of scientists thought that the characteristic features of space aren't depended on moving bodies existing in it, though many of them believed that local curving of space is formed by bodies.

The special theory of relativity by Al. Einstein overthrew ether and changed it by void space-surrounding carrying the impulses of elector-magnetic fields. His theories demoted space and granted it with general characteristic features of physical universe that are changed due to motion or gravitation [1].

It becomes clearer for modern physicists that the universe has special orderly structure and space is its level system. It is impossible to describe it by general mathematical methods that are used during examination of macro processes and natural phenomenon. The structure of space can be described only partially yet by the laws of modern science. The part of physicists argues that space is isotropic and all directions in it are equivalent. It is more probable that the complex structure of space is non-homogenous and non-isotropic. According to Mach micro space has grain type structure, so it is interrupted. The analogue opinion is expressed by Van-Danzig when he speaks about space quantum and the fact that the processes between them aren't subject to observe [7]. I. Tamm also supposes that in microscopic scales it is possible the space to be discrete [8]. At the end of fifties of XX century it was experimentally stated that under the events of weak influence the law of keeping evenness is violated. Besides, there was created the necessity of reexamination of outlooks about characteristic features of the universe.

Modern physicists often talk about absoluteness of the space and relativity of such notions as homogeneity in space and isotropy. As deep and universal characteristic features of space there is acknowledged its objectivity and specificity as unity of matter form and type, unity of interruption and continuity and etc.

Logical discussion of the knowledge about space existing in science at the present time and private vision of its essence became the base for the conclusion below made by the author:

1) Space doesn't present only set proportions brought by scientists expressing coordination of coexisting objects – distance and orientation between them, their size and location in relation with each other as it was confirmed by some leading physicists.

2) The statement that absolute space doesn't exist made by scientists was a great mistake. The concept about existing of absolute space provided by I. Newton is true. Absolute space exists in realty and it is the source and base of material universe.

3) Forming of space preceded formation on material objects in it. It isn't made with stars.

4) From composition standpoint it is material type – it consists of special type of delicate matter, is discrete, small graining type, electrically neutral. Space grains are curved that plays important role in the events passing in space. Corns are distributed separately; the structure of space is similar to the surface of corn cob (Fig.).



Fig.1 Approximate scheme of microstructure of space surface

5) Hard massive bodies existing in space, that are composed by the matter of tertiary form, don't curve it as they have great pores between atoms and molecules (in atoms emptiness takes huge place) and the space (that is resilient) fully exposures these bodies and is its important part. So, the concept that space due to the objects inside it, is curved doesn't correspond to reality.

6) Space is motionless from the standpoint that it doesn't move, but it has ability to vibrate and other very important characteristic features, creation of virtual particles, their development and etc. Space is formed from emptiness (where there are many things, but there aren't matter and scientists called it as vacuum), inside it and combined in it, as its indivisible and important part - the base of grandiose and multiform material world, the initial source of evolution processes going there.

References:

- [1] Steven Weinberg Dreams of a final theory: editorial URSS: Moscow; 2004 (in Russian)
- [2] O. Lomaia Concerning Issue of Substance Radiation. Journal of the Georgian geophysical society. Vol.14A 2010, pp. 104-109
- [3] G. Feinberg Nature of Matter. Moscow, Mir, 1984 (in Russian)
- [4] T. Erdey-Gruz, The foundations of Structure of Matter. Mir, Moscow, 1976 (in Russian)
- [5] V.N. Svidersky Space and Matter. Gospolitizdat, Moscow, 1958 (in Russian)
- [6] S. I. Vavilov Isaac Newton, addition. AN USSR, Moscow, 1961 (in Russian)
- [7] D. Dantzig. Some Possibilities of the Future Development of the Nation and Time. Erkenntnis, B. 7, H, 3, 1938, p. 146.
- [8] I. E. Tamm A. Einstein and Modern Physics. "Advances in Physical Sciences". T. LIX, publishers 1, May, 1956, pg. 9 (in Russian).

მატერიისა და სივრცის შესახებ

ო. ლომაია

რეზიუმე

ფიზიკის შემდგომი განვითარებისთვის აუცილებელია მისი ფუნდამენტური ცნებების, კერძოდ - მატერიისა და სივრცის შესახებ ამჟამად არსებული შეხედულებების გადასინჯვა.

მიზანშეწონილად და სწორად არის მიჩნეული: მატერიალური ობიექტების სამ ფორმად ან დონედ დაყოფა (პირველადი, მეორადი და მესამეული); პირველად მატერიაზე უფრო ნატიფი ობიექტების მატერიის განსხვავებული სახეობებისადმი მიკუთვნება. ავტორი ფიქრობს, რომ საჭიროა სივრცეს მყარად დაუბრუნდეს აბსოლუტურობის სტატუსი, რომელიც მას ი. ნიუტონმა მიანიჭა. აღიარებულ იქნას, რომ სივრცის წარმოშობა წინ უსწრებს მასში მყარი მატერიალური ობიექტების წარმოქმნას.

სივრცე დისკრეტულია, არაერთგვაროვანი, ელექტრულად ნეიტრალური, უძრავი (არ გადაადგილდება), ფლობს ვიბრირების უნარს. შედგება მატერიის განსაკუთრებული უნატიფესი სახეობისგან. მესამეული მატერიისაგან შემდგარი მკვრივი მასიური სხეულები შეიცავს დიდ ფორებს და მათ არ ძალუძთ სივრცის გამრუდება. სივრცე მათ განსჭვალავს და არის მათი მნიშვნელოვანი შემადგენელი ნაწილი.

К вопросу материи и пространства

О. Ломаия

Резюме

Для дальнейшего развития физики необходимо пересмотреть и уточнить взгляды на некоторые фундаментальные основы физики, в частности - на материю и пространство.

Представляется обоснованным и целесообразным: принять деление всего многообразия материальных объектов на три формы (уровни) - первичную, вторичную и третичную; объекты более тонкие, чем первичная материя, отнести к различным видам материи.

Автор считает, что пространству надо вернуть статус абсолютности, предложенный И. Ньютоном, и признать, что образование пространства предшествует формированию в нём материальных объектов. Пространство дискретно, неоднородно, электрически нейтрально, неподвижно (не перемещается), обладает свойством вибрировать. Состоит из особого вида тончайшей материи. Плотные массивные тела из третичной материи, имеющие большие поры, не могут изгибать пространство, которое пронизывает все материальные объекты и составляет их важнейшую часть.

Remote Sensing and Geological/Geophysical Data Integration for Oil and Gas Prospecting

Sergey A. Stankevich, Olga V. Titarenko

Scientific Centre for Aerospace Research of the Earth, Kiev, Ukraine

Abstract

Model for remote sensing and geological/geophysical data integration based on Bayesian probabilistic inference is described. The proposed model has been tested on example of the Khukhra oil and gas condensate field territory in Ukraine. The results of testing are accorded well with previous geological forecasts.

Key words: oil and gas prospectively, geospatial data integration, Bayesian probabilistic inference, Khukhra oil and gas condensate field.

Introduction

Oil and gas fields forecasting and exploration is a complex and knowledge-intensive problem. Effective solution to this problem requires all available data consideration using new geoinformation technologies for geospatial analysis.

Direct methods for oil and gas prospecting, such as drilling and seismic measurements, require considerable expenses. Therefore, the modern satellite technologies for the new hydrocarbon deposits detection and mapping can reduce cost and time of exploration.

The main goal of exploration is to improve the accuracy and reliability of oil and gas fields forecasting. Satellite-based geological research is conducted to assess tentatively the oil and gas potential of study area before exploratory boring. At the moment, significant amount of various necessary information (remote sensing imagery, geological maps, geophysical data, etc.) are involved to implement such assessment in shorter time and with the least financial costs. However, large amount of data from different information sources, on the one hand, complement each other, and, on the other – require adaptive and flexible scientific and methodological tool for integration and joint processing.

State of the art

A number of studies are addressed to data integration problem. The simplest approach to integration and joint processing of data from different information sources is a summation of data of the same physical nature [1]. In other cases the development of effective model for data fusion is a great challenge. Models for statistical-based and ontology-based data integration are considered in [2-4]. Such models are quite efficient; they are implemented in existing software.

Modern technology of remote sensing application in geological prospecting is based on the integration of remote sensing data with other geospatial data – cartographic, geological, geophysical, geochemical and other available ones [5, 6]. This approach dampens a subjectivity, inherent the visual interpretation of satellite imagery. Integration of remote sensing and other geoscience spatial data computerizes the study area evaluation and calculates its similarity to a reference sites (deposits) [7]. Classification of remote sensing and geological/geophysical data hypercube maps the probability of oil and gas occurrence inside study sites and ranks them by its prospectivity.

Method

In this paper the model of integration of remote sensing and geological/geophysical data based on Bayesian probabilistic inference is proposed.

The Bayesian probabilistic inference in oil and gas prospecting involves a priori and conditional probability estimates of data hypercube dots membership in positive or negative reference patterns to calculate the posterior probability of each dot membership in positive one.

The posterior probability of a positive reference pattern $P^+(x)$ for the current dot $x \in X$ of data hypercube X is estimated by the Bayesian rule:

$$P^+(x) = \frac{P^+ \cdot P(x | X^+)}{P^+ \cdot P(x | X^+) + P^- \cdot P(x | X^-)} \quad (1)$$

where P^+ , P^- are a priori probabilities of positive and negative reference patterns, $P(x/x^+)$, $P(x/x^-)$ are conditional probabilities of x membership in positive X^+ and negative X^- reference patterns of data hypercube [8].

The information divergence $D(x/y)$ between normalized values of hypercube vectors is used to estimate conditional probabilities $P(x/x^+)$ и $P(x/x^-)$ in oil and gas prospecting using remote sensing and geological/geophysical data [9]:

$$D(x/y) = \int_{u \in U} f[x(u)] \cdot \log_2 \frac{f[x(u)]}{f[y(u)]} du \quad (2)$$

where $f[\cdot]$ is a probability density distribution of values in hypercube vector, U is the range of possible values.

Probability density distributions of vectors values both of hypercube single dots $f(x)$ and positive $f(X^+)$ or negative $f(X^-)$ reference patterns can be estimated by matching histograms of data hypercube [10]. Information divergence (2) is uniquely associated with a counterpart conditional probability [11]:

$$P(x/x^+) \cong 1 - 2^{-n^+ \cdot D(x/x^+)} \quad (3)$$

where n^+ is a statistical sampling size of corresponding reference pattern.

A posteriori probability (3) of positive reference pattern mapping over hypercube as a matter implements the remote sensing and geological/geophysical data integration in oil and gas prospecting.

Data

The proposed model for remote sensing and geological/geophysical data integration based on Bayesian probabilistic inference was tested over the Khukhra oil and gas condensate field territory, which is located in the Akhtyrka district within the Sumy region of Ukraine. The field is characterized as complex geological media. It consists of layers of Paleozoic, Mesozoic and Cenozoic sedimentary rocks that overlie the crystalline rocks of Precambrian basement. There are multiple stratigraphic discordances inside the sedimentary cover.

In tectonic terms, the south-western part of the field lies within the northern cutoff edge of the Dnieper graben while the north-eastern part lies within the northern edge of Dnieper-Donetsk depression. They are separated by marginal disruption zone. The basement topography of northern edge and northern cutoff edge are significantly different [12, 13]. Productivity of Mesozoic and Devonian petroleum systems is proved for this territory. Deposits are layered, tectonically and lithologically screened. They form a multilayer field with different combination of gas-bearing and oil-bearing stratum at depths over 5000 m [14].

Available heterogeneous geospatial data have been incorporated into the integrated geological model of Khukhra oil and gas field (Fig.1): bore-wells (both productive and non-productive) positions; map of provincial and regional faults; lineament zones and lineaments; maps of lineaments density in different directions; map of the residual gravity; field outline according seismography; thermal anomalies within the territory; neotectonic (depression and ridge) blocks; geochemical anomalies; optical anomalies; routes of soils and vegetation ground spectrometry; structural horizon B₂₁ isohypses; maps of sedimentary strata; digital terrain elevation data; surfaces of terrain vertical and horizontal dissection.

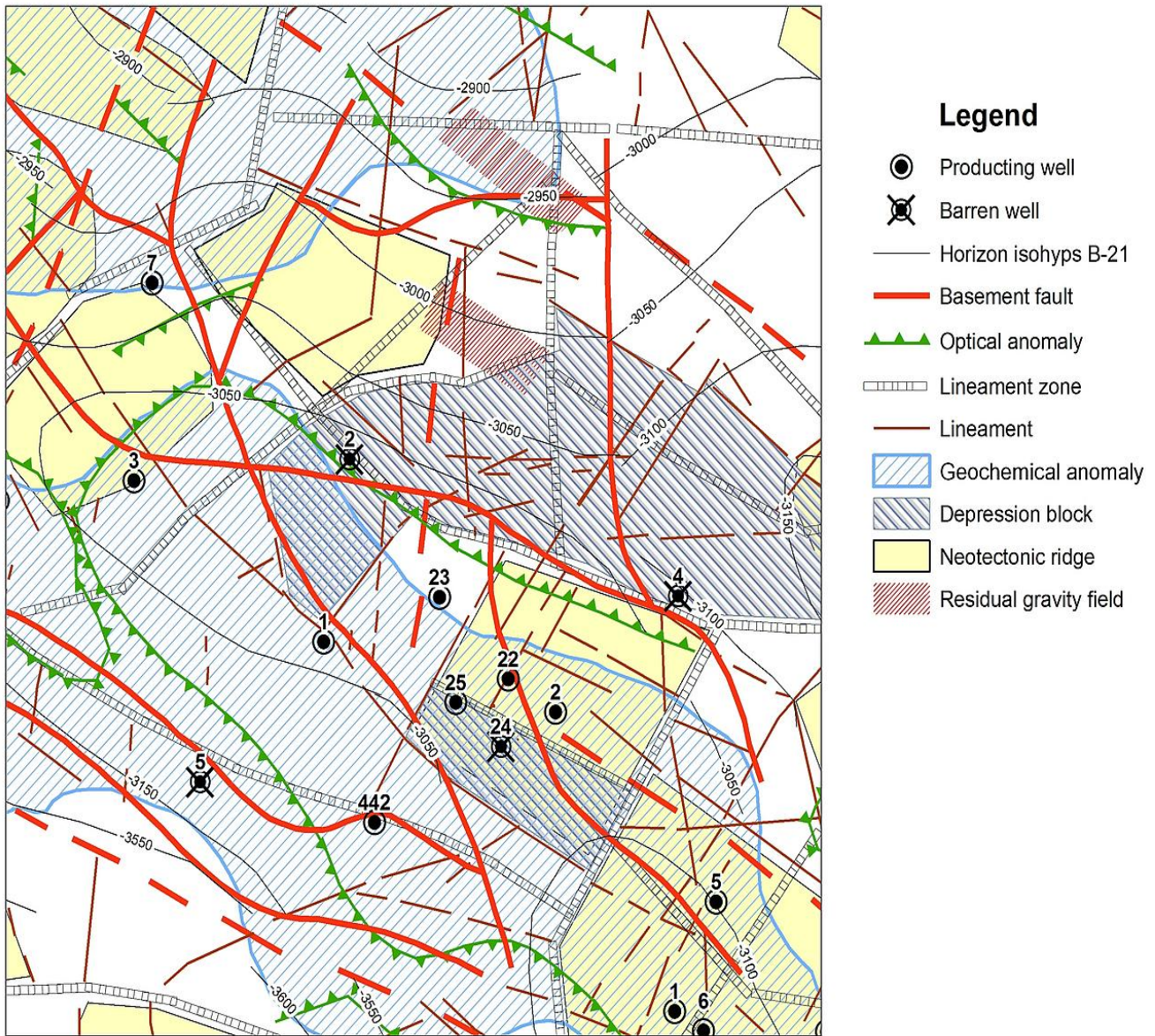


Fig.1. Geospatial database for the Khukhra oil and gas condensate field territory (Ukraine)

All geospatial data were georeferenced, rasterized and converted to 30 m spatial resolution for the further stacking into hypercube.

Result and discussion

As a result of performed remote sensing and geological/geophysical data integration the spatial distribution of a posteriori probability is obtained (Fig.2a), which can be interpreted as an integral rating of oil and gas prospectivity inside the study area.

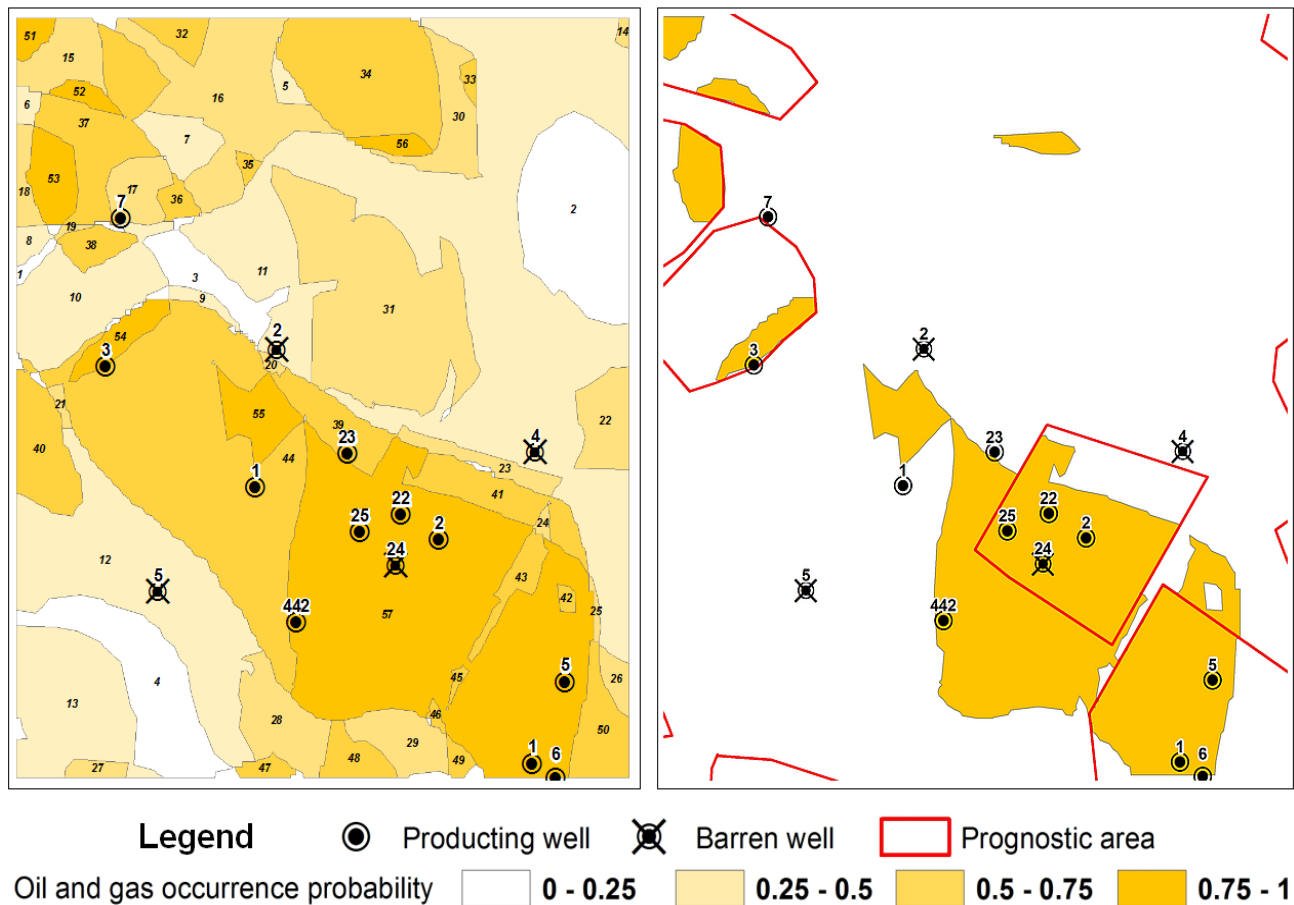


Fig.2. Probability distribution of oil and gas occurrence by result of geospatial data integration

There are several medium and small sites (plots 51, 52, 53, 56) with a high probability of oil and gas occurrence were detected in the northern area of Khukhra field. In addition, plots 32, 33, 34, 35, 36 can be recommended for further detailed exploration. This result correlates well with the previous geological forecasts and available structural and geomorphological data interpretations (Fig.2b); also it provides a subsequent area reduction of sites, which are recommended for drilling.

The occurrence or lack of hydrocarbon deposit in the forecast point was determined by the results of exploration drilling. Because reliable quantitative specifications of hydrocarbon reservoirs are not available yet, the rank correlation between the distribution of a posteriori probability and the location of productive/non-productive bore-wells was estimated. The Spearman's rank correlation coefficient, according to 13 exploration bore-wells data is equal to 0.786. This fact demonstrates a reasonable efficiency of carried out data integration [15].

Conclusion

Thus, the remote sensing and geological/geophysical data integration is an efficient and descriptive tool for overall assessment of oil and gas prospectivity within the territory of interest. Approach to data integration based on Bayesian probabilistic inference provides mapping of spatial distribution of similarity to known similarity to a reference oil and gas bearing sites. Such maps are very important for decision-making information support on detailed exploration strategy.

References

- [1] Genesereth M. Data Integration: The Relational Logic Approach. Stanford, Morgan and Claypool Publishers, 2010, 110 p.
- [2] Challa S., Koks D. Bayesian and Dempster-Shafer Fusion. *Sadhana*, vol. 29, part 2, 2004, pp.145–176.
- [3] Stathaki T. Image Fusion: Algorithms and Applications. L., Academic Press, 2008, 500 p.
- [4] Wache H., Vögele T., Visser T., Stuckenschmidt H., Schuster H., Neumann G., Hübner S. Ontology-Based Integration of Information – a Survey of Existing Approaches. Proc. the IJCAI-01 Workshop on Ontologies and Information Sharing. Seattle, American Association for Artificial Intelligence, 2001, pp.108-117.
- [5] Petovsky A.P., Gazhenko N.S., Krupsky B.L., Gladun V.V., Cherpil P.M., Tsyoha O.G., Bodlak P.M., Oblekov G.I., Polyn I.I. New Possibilities for Oil and Gas Fields Geology Aspects Studying and Prospectivity Evaluation Using Integrated Interpretation of Geological/Geophysical Data. *Geoinformatics*, No 3, 2005, pp. 24-26, (in Russian).
- [6] Stankevich S.A., Titarenko O.V. Remote Sensing and Geophysical Data Fusion Technique for Oil and Gas Prospecting. *Scientific Notes of Taurida V. Vernadsky National University*, vol. 22(61), No1, 2009, pp.105-113, (in Ukrainian).
- [7] Schallehn E., Sattler K.-U., Saake G. Efficient Similarity-Based Operations for Data Integration. *Data & Knowledge Engineering*, vol.48, No 3, 2004, pp.361-387.
- [8] Stankevich S.A., Bunina A.J., Chepurnoy V.S. Operability Evaluation of the Geological/Geophysical and Remote Sensing Data Integration for Land ore Prospectivity Mapping. *Technogenic Environmental Safety and Civil Defence*, No 6, 2014, pp. 53-59,(in Ukrainian).
- [9] Stankevich S.A., Titarenko O.V. Technique for Mapping of Hydrocarbon Deposit Boundaries Using Remote Sensing Data. *Aerospace Monitoring of Oil and Gas Facilities*. / Ed. by V.G. Bondur/, Scientific World, M., 2012, pp. 425-430, (in Russian)
- [10] Popov M.A., Stankevich S.A., Markov S.J., Zaytsev A.V., Kudashev E.B. Heterogeneous Spatial Data Integration in Gas and Oil Prospecting. *Russian Digital Libraries Journal*, vol.16, No 2, 2013, <http://www.elbib.ru/eng/journal/2013/part2/PSMZK>. (in Russian).
- [11] Kullback S. Information Theory and Statistics. N.Y. Dover Publications, 1997, 432 p.
- [12] Solovyov V.O., Borisovets I.I., Vasilyev A.N., Pavlov S.D., Suyarko V.G., Tereschenko V.A., Fyk I.M., Scherbina V.G.. *Geology and Petroleum Potential of Ukraine*. Kharkov, Cursor, 2014, 294 p., (in Russian).
- [13] Gladun V.V. Prospects for the Oil-Gas-Bearing Capacity of the Dnieper-Donets region. *Reports of the NAS of Ukraine*, No 8, 2011, pp.91-96.
- [14] Lukin A.E., Dovzhok E.M., Knishman A.Sh., Goncharenko V.I., Dzubenko O.I. Helium Anomaly in Petroliferous Visean Carbonate Reservoirs of the Dnieper-Donets Depression. *Reports of the NAS of Ukraine*, No 7, 2012, pp. 97-104, (in Russian).
- [15] Song P. X.-K. *Correlated Data Analysis: Modeling, Analytics, and Applications*. N.Y.: Springer, 2007, 346 p.

დისტანციური და გეოლოგიურ–გეოფიზიკური მონაცემების ინტეგრირება ტერიტორიების ნავთობგაზპერსპექტიულობის შეფასებისას

ს. სტანკევიჩი, ო. ტიტარენკო

რეზიუმე

აღწერილია დისტანციური და გეოლოგიურ–გეოფიზიკური მონაცემების ინტეგრაცია ბეიესის ალბათური დასკვნის საფუძველზე. შემოთავაზებული მოდელი აპრობირებულია უკრაინის ტერიტორიაზე არსებული ნავთობგაზკონდენსატის საბადოს მაგალითზე. აპრობაციის შედეგები კარგ თანხვედრაშია ადრეარსებულ გეოლოგიურ პროგნოზებთან.

Интегрирование дистанционных и геолого-геофизических данных при оценивании нефтегазоперспективности территорий

С.А. Станкевич, О.В. Титаренко

Резюме

Описана модель интеграции дистанционных и геолого-геофизических данных на основе байесовского вероятностного вывода. Предложенная модель апробирована на примере нефтегазоконденсатного месторождения на территории Украины. Результаты апробации хорошо согласуются с предшествующими геологическими прогнозами.

Information for contributors

Papers intended for the Journal should be submitted in two copies to the Editor-in-Chief. Papers from countries that have a member on the Editorial Board should normally be submitted through that member. The address will be found on the inside front cover.

1. Papers should be written in the concise form. Occasionally long papers, particularly those of a review nature (not exceeding 16 printed pages), will be accepted. Short reports should be written in the most concise form not exceeding 6 printed pages. It is desirable to submit a copy of paper on a diskette.
2. A brief, concise abstract in English is required at the beginning of all papers in Russian and in Georgian at the end of them.
3. Line drawings should include all relevant details. All lettering, graph lines and points on graphs should be sufficiently large and bold to permit reproduction when the diagram has been reduced to a size suitable for inclusion in the Journal.
4. Each figure must be provided with an adequate caption.
5. Figure Captions and table headings should be provided on a separate sheet.
6. Page should be 20 x 28 cm. Large or long tables should be typed on continuing sheets.
7. References should be given in the standard form to be found in this Journal.
8. All copy (including tables, references and figure captions) must be double spaced with wide margins, and all pages must be numbered consecutively.
9. Both System of units in GGS and SI are permitted in manuscript
10. Each manuscript should include the components, which should be presented in the order following as follows:
Title, name, affiliation and complete postal address of each author and dateline.
The text should be divided into sections, each with a separate heading or numbered consecutively.
Acknowledgements. Appendix. Reference.
11. The editors will supply the date of receipt of the manuscript.

CONTENTS

T. Chelidze, I. Shengelia, N. Zhukova, T. Matcharashvili, G. Melikadze, G. Kobzev M9 Tohoku earthquake response in Georgia – possible local tremors and hydroseismic effects	3
<i>Nodar Varamashvili, Tamaz Chelidze, Zurab Chelidze</i> Acoustic pulses detecting methods in granular media	20
<i>T. Chelidze, E. Mepharidze, D. Tephnadze</i> Arnold’s tongues at electromagnetic and mechanical synchronization of stick-slip	28
<i>George Melikadze, Natalia Jukova, Mariam Todadze, Sopio Vepkhvadze, Nino Kpanadze, Alexandre Chankvetadze, Tamar Jimsheladze, Ramaz Chitanava</i> Preliminary result of stable isotopes monitoring in the Alazani-Iori catchment	39
<i>George Melikadze, Genadi Kobzev, Tamar Jimsheladze</i> SOME METHODS OF ANALYZE GEODYNAMIC IMPACT ON THE DEEP AQUIFERS	47
<i>George Melikadze, Natalia Jukova, Mariam Todadze, Sopio Vepkhvadze, Nino Kapanadze, Alexandre Chankvetadze, Tamar Jimsheladze, Tomas Vitvar</i> Evaluation of recharge origin of groundwater in the Alazani-Iori basins, using hydrochemical and isotope approaches	53
<i>Tamar Jimsheladze, George Melikadze, Genadi Kobzev, Aleksey Benderev, Emil Botev</i> Linear methods of studying the water level variation related with seismicity	65
<i>Martin Kralik, Rudolf Pavuza, George Melikadze</i> Hydrogeological and Speleometeorological Dynamics of the Prometheus and Sataplia Show-Caves, Imereti, Georgia.	76
<i>George Melikadze, Natalia Jukova, Mariam Todadze, Sopio Vepkhvadze, Tomas Vitvar</i> Result of numerical modelling of groundwater resource in the Shiraki catchment	102
<i>K. Kartvelishvili, D. Gamkrelidze, S. Ghonghadze, G. Kartvelishvili, M. Nikolaishvili, O. Yavolovskaya.</i> Identification of the possible criteria for prognostication of earthquakes on the ground of the data of the observed deformographic processes and triggered micro-earthquakes . . .	110
<i>Z. Kereselidze, N. Tsereteli</i> Simulation of point explosion’s seismic energy by means of the frequency spectrum of body waves	122
<i>Anzor Gvelesiani, Nodar Chiabrishvili</i> Additional experiments on the study of peculiarities of clear water, H ₂ O, and both water sugar, C ₁₂ H ₂₂ O ₁₁ , and edible salt, NaCl, solutions of maximal densities by means of original fluids bubble boiling method	132
.	
<i>Davit Kitovani</i> The Modified Version of t ₀ Method	140
<i>Sakvarelidze E., Sharadze Z., Mirianashvili K.</i> ABOUT THE MECHANISM OF IMPACT OF EARTHQUAKES ON HUMAN HEALTH.	143

<i>O. Lomaia</i>	
About Matter and Space.	147
<i>Sergey A. Stankevich, Olga V. Titarenko</i>	
Remote Sensing and Geological/Geophysical Data Integration for Oil and Gas Prospecting.	152
Information for contributors.	158

სარჩევი

<i>თამაზ ჭელიძე, ია შენგელია, ნატალია ჟუკოვა, თემურ მაჭარაშვილი, გიორგი მელიქაძე, გენადი კობზევი</i> დიდი ტოპოკუს მიწისძვრის (M9) გამოძახილი საქართველოში - ლოკალური ტრემორები და ჰიდროფოსისმური ეფექტები	3
<i>ნოდარ ვარამაშვილი, თამაზ ჭელიძე, ზურაბ ჭელიძე</i> მარცვლოვან გარემოში აკუსტიკური იმპულსების დეტექტირების მეთოდები .	20
<i>თ. ჭელიძე, ე. მეფარიძე, დ. ტეფნაძე</i> არნოლდის ენები არათანაბარი ხახუნის (Stick-slip) ელექტრომაგნიტური და მექანიკური სინქრონიზაციის დროს	28
<i>გიორგი მელიქაძე, ნატალია ჟუკოვა, მარიამ თოდაძე, სოფიო ვეფხვაძე, ნინო კაპანაძე, ალექსანდრე ჭანკვეტაძე, თამარ ჯიმშელაძე, რამაზ ჭითანავა</i> ალაზანი-იორის წყალშემკვრებ აუზებში სტაბილური იზოტოპების მონიტორინგის პირველადი შედეგები	39
<i>მელიქაძე გ., კობზევი გ., ჯიმშელაძე თ.</i> ღრმა წყალშემცველ ჰორიზონტებზე გეოდინამიკური გავლენის შეფასების მეთოდი	47
<i>გიორგი მელიქაძე, ნატალია ჟუკოვა, მარიამ თოდაძე, სოფიო ვეფხვაძე, ნინო კაპანაძე, ალექსანდრე ჭანკვეტაძე, თამარ ჯიმშელაძე</i> ჰიდროქიმიური და იზოტოპური მეთოდების გამოყენებით მიწისქვეშა წყლების წარმოშობის და მოძრაობის შესწავლა ალაზანი-იორი აუზებში	53
<i>ჯიმშელაძე თამარი, მელიქაძე გიორგი, კობზევი გენადი</i> მიწისძვრებთან დაკავშირებული წყლის დონის ვარიაციების შესწავლა წრფივი მეთოდებით	65
<i>მარტინ კრალიკი, რუდოლფ პავუზა, გიორგი მელიქაძე</i> ჰიდროგეოლოგიური და სპელეომეტეოროლოგიური დინამიკა სათაფლიისა და პრომეთეს მღვიმეებში, იმერეთი, საქართველო	76
<i>გიორგი მელიქაძე, ნატალია ჟუკოვა, მარიამ თოდაძე, სოფიო ვეფხვაძე, ტომას ვიტვარ</i> შირაქის წყალშემკვრების ციფრული მოდელირების შედეგები	102
<i>კ. ქართველიშვილი, დ. გამყრელიძე, ს. ღონღაძე, გ. ქართველიშვილი, მ. ნიკოლაიშვილი, ო. იავოლოვსკაია</i> გეოდეფორმოგრაფიულ და ტრიგერირებულ სეისმურ მონაცემთა ზოგიერთი შედეგები მიწისძვრების პროგნოზირების შესაძლო კრიტერიუმების დადგენის მიზნით	110

<i>ზ.კერესელიძე, ნ.წერეთელი</i> წერტილოვანი აფეთქების სეისმური ენერჯის მოდელირება მოცულობითი ტალღების სიხშირული სპექტრის საშუალებით	122
<i>ანზორ გველესიანი, ნოდარ ჭიაბრიშვილი</i> სუფთა წყლის, H ₂ O, და სხვადასხვა სიმკვრივის მქონე შაქრის, C ₁₂ H ₂₂ O ₁₁ , და სუფრის მარილის, NaCl, წყლის ხსნარების ბუშტისებრი დუღილის თავისებურებათა კვლევის დამატებითი ექსპერიმენტების შესახებ	132
<i>დავით კიტოვანი</i> t ₀ -ის მოდიფიცირებული მეთოდი	140
<i>ე. საყვარელიძე, ზ.შარაძე, ქ. მირიანაშვილი</i> ალამიანის ჯანმრთელობაზე მიწისძვრების ზემოქმედების მქანის შესახებ	143
<i>ო. ლომია</i> მატერიისა და სივრცის შესახებ	147
<i>ს. სტანკევიჩი, ო. ტიტარენკო</i> დისტანციური და გეოლოგიურ-გეოფიზიკური მონაცემების ინტეგრირება ტერიტორიების ნავთობგაზპერსპექტიულობის შეფასებისას	152
ავტორთა საყურადღებოდ	158

საქართველოს გეოფიზიკური საზოგადოების
ჟურნალი

სერია ა. დედამიწის ფიზიკა

ჟურნალი იბეჭდება საქართველოს გეოფიზიკური საზოგადოების პრეზიდიუმის
დადგენილების საფუძველზე

ტირაჟი 200 ცალი

ЖУРНАЛ ГРУЗИНСКОГО ГЕОФИЗИЧЕСКОГО ОБЩЕСТВА

Серия А. Физика твердой Земли

Журнал печатается по постановлению президиума Грузинского геофизического общества

Тираж 200 экз

JOURNAL OF THE GEORGIAN GEOPHYSICAL SOCIETY

Issue A. Physics of Solid Earth

Printed by the decision of the Georgian Geophysical Society Board

Circulation 200 copies